Tomás Augusto Barreiros Pais de Azevedo

An evo-devo approach to vertebral body development: going back to progenitors

UAlg FMCB
UNIVERSIDADE DO ALGARVE
FACULDADE DE MEDICINA E CIÊNCIAS BIOMÉDICAS

Faculdade de Medicina e Ciências Biomédicas

2022

Tomás Augusto Barreiros Pais de Azevedo

An evo-devo approach to vertebral body development: going back to progenitors

PhD Program in Biomedical Sciences

Work under the supervision of:

Professora Doutora Isabel Palmeirim

And co-supervised by

Professor Doctor Paul Eckhard Witten

Professora Doutora Raquel P. Andrade

UAlg FMCB

UNIVERSIDADE DO ALGARVE

FACULDADE DE MEDICINA E CIÊNCIAS BIOMÉDICAS

Faculdade de Medicina e Ciências Biomédicas

2022

This page is intentionally left blank

An evo-devo approach to vertebral body development: going back to progenitors

Declaração de autoria de trabalho

Declaro ser o autor deste trabalho, que é inédito e original. Autores e trabalhos consultados estão devidamente citados no texto e constam da listagem de referências incluída.

.

This work was supported by National Portuguese funding through FCT – Fundação para a Ciência e Tecnologia, scholarship SFRH/BD/84825 /2012

This page is intentionally left blank

An evo-devo approach to vertebral body development: going back to progenitors

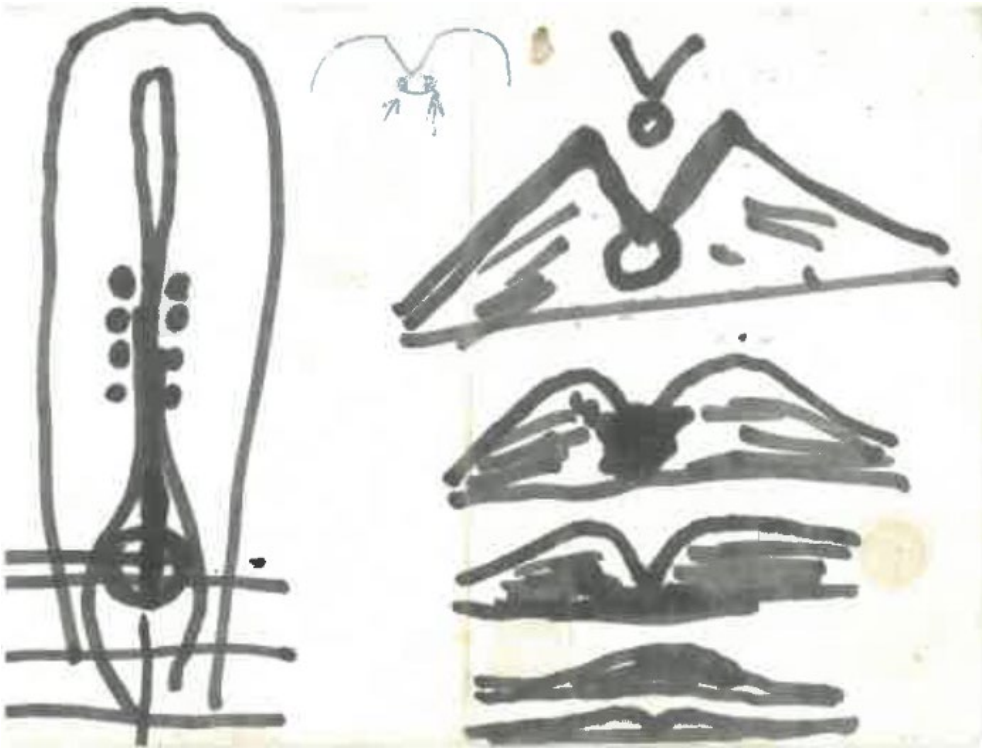

Arise, arise, Riders of Théoden! Spears shall be shaken ! Shields shall be splintered ! A sword-day, a red day, ere the sun rises! (King Theoden)

In *Lord of the Rings: The return of the King (2003)*

This page is intentionally left blank

Acknowledgments

Theoden King stands alone (Gandalf the Gray)

Not alone.! (Eomer)

In *Lord of the Rings: The return of the King (2002)*

Em todas as grandes aventuras se conseguem fazer feitos incríveis, ultrapassar obstáculos intransponíveis e atingir metas inalcançáveis. No entanto só o conseguem fazer porque têm a ajuda de mentores ou companheiros de viagem que os apoiam, que os corrigem, que os ajudam, que os desafiam e que os fazem crescer e tornar-se versões melhores de si mesmos.

Também esta tese foi uma grande aventura. Felizmente, durante os vários anos que durou aventura tive a sorte de ter comigo alguns deles e é a estes que quero agradecer neste momento.

Em primeiro lugar, como não poderia deixar de ser, à minha mentora, , a um dos meus modelos de vida pela sua energia inesgotável e força imparável. Obrigado por me receberes e acreditares em mim, por me ensinares e me ajudares a melhorar as minhas falhas e por valorizares o que tenho de bom. É um prazer poder partilhar o teu entusiasmo pela Ciência e ter a tua inspiração e é uma honra ter a tua amizade. És uma pessoa fora-de-série e obrigado por todos estes anos de partilha e cumplicidade, profissional e pessoal.

To my co-supervisors from Gent, Eckhard and Anne. Thank you so much for receiving me with such kindness in your lab. Thank you for the wonderful conversations and good moments. A very special thanks to you Eckhard for supporting my enthusiasm through our scientific discussions that led to the creation and production of this project. A very strong thank you for all the members of the group, especially for the fries lunches and dinners at the ribs !

E para finalizar (com chave de ouro) o agradecimento aos meus co-orientadores, muito obrigado Raquel. Obrigado pelos teus conselhos e pelas nossas conversas tão enriquecedoras. E obrigado pelo teu carinho, a tua disponibilidade e generosidade e as tuas palavras sempre amigas tornaram esta viagem muito mais fácil e fizeram com que ela chegasse a um muito bom porto. E obrigado ainda por toda a ajuda tanto no laboratório como no computador com as nossas colaborações.

À minha irmã mais velha científica Lisa. Obrigado por me deres dado a tua amizade e companheirismo no laboratório, por tudo o que me foste ensinando e aconselhando e por tão

bem me receberes na tua família. Obrigado por me teres aberto a tua casa de forma tão carinhosa e por partilharmos dias de trabalho, noites de jantares e serões de séries.

E por falar em colegas de laboratório, um agradecimento a todos os membros do grupo da Raquel, passados e presentes. Obrigado por me fazerem sentir parte do vosso grupo. Em especial à Cristina, por toda ajuda que me deste com a tua visão de persistência e inteligência. E ao Gil, meu grande companheiro de armas, obrigado por partilhares o que ias descobrindo, e pelo esforço de equipa que conseguimos ter e que nos solucionou tantos problemas que sozinho não conseguiria resolver da mesma forma.

À minha Maninha Patrícia, por toda a tua amizade e por toda a cumplicidade que partilhámos nestes tempos e por seres das poucas pessoas que me fazia rir a qualquer altura: Nhá nhá nhá ! Só tenho uma coisa a dizer: (Mourinho e o seu gesto)

À Rita pelas nossas noitadas a falar de assuntos tão variados como a batata na notocorda ou a geopolítica da Terra Média, enquanto me levas a passear de carro por Lisboa a fora. Terei todo o prazer em ser o teu copiloto a qualquer altura !

Aos meus alunos de MEE Inês Santos e João Santos pelo vosso entusiasmo, vontade de aprender e dedicação que tiveram nos vossos projectos.

Ao Alexandre Rodrigues pelo teu trabalho incrível em fazer o construct do CNOT2, essencial para os resultados principais deste trabalho e pela companhia e boa disposição que trouxeste ao laboratório.

À Maurícia pelos espetaculares cortes histológicos que fizeste e que foram tão importantes para esta tese.

Ao André pela companhia de tanto tempo aqui no Algarve, em jogos de padel, jantares de pizza ou discussões futebolísticas na citometria.

Ao Rui pelos conselhos todos que me deste e pela calma e sabedoria que sempre me conseguiste transmitir. E obrigado pela tua metáfora do presente.

Ao Paulo Gavaia por todas as dúvidas que me foste tirando, sobretudo no mundo dos peixes e por conversas científicas que muito ajudaram a moldar este projecto. E por falar em moldar o projecto, um agradecimento muito especial à Anabela Bensimon-Brito, já que foste a primeira pessoa que nos mostrou que a notocorda dos peixes era “mais inteligente” e que me apresentou ao Eckhard.

À Ana Marreiros pela tua ajuda providencial na estatística e por partilhares a tua enorme alegria e entusiasmo constantes.

À Professora Leonor Cancela, não só por todo o trabalho por trás da direcção do Programa Doutoral, mas também pela paciência infinita com que esperou até que eu entregasse finalmente esta tese.

À Conceição José, muito obrigado por toda a disponibilidade e simpatia com que sempre me ajudou com a informação certa e simplificar, em todo o tempo da tese, mas em especial, nestes últimos meses antes da entrega.

À Leonor e à Sólveig pelos conselhos e força que me foram dando durante todo este tempo. Em especial pelos conselhos que me deram no meeting de Madrid que me fizeram, não só ter as imagens espetaculares da fissura de Von Ebner com DAPI, como também começar a virar uma página em todo este período.

Ao Gabriel por teres sido o meu primeiro mentor e me teres passado o teu entusiasmo tanto pela ciência, como pela microscopia.

Fora da Academia foram também muitos os amigos que me ajudaram de uma forma ou de outra neste caminho.

Um agradecimento muito especial a um grupo de pessoas excepcionais, sem as quais nada disto seria possível a todos os níveis. À Isabel Duarte, por todo o apoio que me deste ao longo deste tempo, em especial por não teres desistido da nossa amizade no momento mais difícil e, pelo contrário, lutares para que dele saísse. Ao Ramiro, por seres o exemplo de integridade, de bom-senso, de calma e de ponderação. Obrigado por seres uma bússola moral e por teres estado lá em tantos momentos com uma palavra sempre certa, e por seres um GRANDE amigo. Ao Paulão, companheiro já de tantas aventuras que vão desde peddy-papers, mergulho, arborismo tantas coisas mais. Mas sobretudo obrigado por toda a sabedoria que consegues passar, sejam os teus sábios conselhos informáticos, químicos, físicos ou de experiência pessoal. A estes três amigos e também aos enormes Xicão e Marília (e ao quase enorme Kiko), muito obrigado pela vossa companhia e amizade que fez destes anos uma animação e uma aprendizagem constantes.

Um muito obrigado a um grupo que, mesmo longe está sempre lá e com quem é sempre uma diversão estar. Obrigado, Bárbara, Mariana, Mello, Sara e Miguéis por ser sempre um épico cada vez que estamos juntos (mesmo que seja muito raramente)

Não poderia falar de amigos sem dois grandes compinchas Menezes e Miguel. Há amigos que passem os anos que passarem, esteamos onde estiverem, vai sempre parecer que foi ontem que nos juntamos e vocês são desses raros. Muito obrigado pelas nossas jantaradas e pelo vosso companheirismo em tantos anos.

Falando de longos e bons amigos, obrigado Catarina, por seres a pessoa que está lá desde o início dos inícios. Disseste que este era o meu ano e assim foi !

Ao Henrique, o meu irmão mais velho aqui no Algarve, pelo teu companheirismo, conselhos sábios, calma e boa disposição (e conversas até às tantas da manhã !) que fizeram dos primeiros tempos no Algarve uma bela experiência.

A um grupo de três pessoas que também foram a minha família nestes últimos anos. Alexandre, Mara e Marina. Muito obrigado pela vossa amizade e pela vossa companhia. Pelos passeios a pé, noitadas a trabalhar/jogar, (pelo gatinho !) e por me fazerem sentir em família sempre que chegava a casa.

E por falar em família, há pessoas que não sendo família de sangue, são bem mais do que se fossem. À Zaré, Zezé, Tó, Né, Pedro, Tita, Kika, Rita, Marta, Zé Santa Clara, Mafalda, Leonor, Ana Lhó, Tomás Grande, Mariazinha, João Maria. Alguns de vocês andaram comigo ao colo e a outros andei eu convosco ao colo. Obrigado por todos os momentos que temos partilhado e vou poder agora passar mais tempo convosco e retribuir-vos todo o carinho que tive de vós.

À minha família de sangue, em especial à Ana Sofia por toda a alegria e exemplo de trabalho e a minha avó Meca, pela pessoa extraordinária que foi, pelo exemplo de vida, pela sabedoria alegre de quem tanto viveu e tanto me ensinou.

Aos meus pais que estiveram sempre ao meu lado nos melhores e nos piores momentos. Obrigado pelo vosso amor, pelo vosso apoio, por tudo aquilo que me ensinaram e que fez de mim a pessoa que hoje sou, por serem o meu porto de abrigo e por estarem sempre lá.

E finalmente à Cristina. Obrigado a ti por me teres dado a força e a visão que me faltavam tantas vezes, por me ensinares a procurar outras soluções, quando tudo parecia estar perdido e por seres um exemplo de força, coragem e resiliência.

Abstract

The segmented signal for vertebral body development is conveyed, in zebrafish, through mineralization of the notochordal sheath and, in chicken, through resegmentation of the most medially located ventral sclerotome cells, with the contribution of the notochord still unclear. Along with the different size of the notochord in these two embryos, this leads to the hypothesis that evolutionary changes in the expression territories of transcription factors could underlie these differences. In the zebrafish axial(notochord)/paraxial(PSM/somite/sclerotome) mesoderm progenitor region, *flh* normally represses *spt* that normally defines paraxial mesoderm fate, leading to an axial mesoderm one instead.

The aims of this thesis were to clarify the role of the notochord in chicken segmented vertebral body formation and investigate the role of transcription factor evolutionary changes in this process's differences between zebrafish and chicken. In **chapter II** we thoroughly describe the first morphological landmark of segmented vertebrae, Von Ebner's fissure, using it as a proxy to observe that the notochord and dermomyotome are not responsible for vertebral body segmented signal initiation. In **chapter III**, through CNOT2 electroporation experiments, we observe an increase in the axial mesoderm size (notochord and floor plate), accompanied by a shortening of axial length and downregulation of TBX6L. We conclude that CNOT2 represses TBX6L, leading axial/paraxial progenitor cells to assume an axial mesoderm cell fate. In **chapter IV**, we fill in a lingering chicken embryo knowledge gap, by producing a detailed quantification of early axis elongation. At the same time, we provide a reproducible and precise staging system and a morphometric tool to analyze experimental data.

This thesis demonstrates the evolutionary shift in preponderance from the notochord to the PSM/somites/sclerotome in the role on segmented signal location and axial elongation. It also proposes that changes in the *flh*/CNOT2 and *spt*/TBX6L expression territories in the axial/paraxial mesoderm region are underlying these shifts.

Keywords: Vertebral body development, notochord, sclerotome, axial/paraxial mesoderm progenitors, Axial elongation, CNOT2

This page is intentionally left blank

Resumo

A segmentação é uma característica comum a uma grande percentagem de animais que permite uma organização funcional e estrutural do corpo. Esta característica é particularmente evidente nos animais vertebrados que possuem um esqueleto axial formado por estruturas ósseas repetidas ao longo do eixo antero-posterior do corpo, as vértebras. Estas são compostas por um núcleo ósseo central denominado "corpo vertebral" e por arcos localizados dorsalmente e/ou ventralmente ao corpo vertebral, denominados "arcos vertebrais".

A formação do corpo vertebral é um processo muito interessante do ponto de vista da Biologia Evolutiva e do Desenvolvimento, já que ocorre de diferentes maneiras em diferentes grupos de animais. Geralmente, o corpo vertebral forma-se graças à contribuição de duas estruturas embrionárias, a notocorda e o sómito. A notochorda é uma estrutura embrionária axial alongada composta por células vacuolizadas no lúmen e coberta por uma bainha envolvente com células denominadas cordoblastos. Esta estrutura representa o primeiro esqueleto embrinário, tendo várias funções, estruturais e de sinalização genética. Os sómitos são esferas de células mesenquimatosas localizadas em pares, flanqueando a notocorda. Estes formam-se sequencialmente a partir da mesoderme pré-somitica, através de transições epitélio-mesênquima num processo é altamente regulado por um conjunto de genes expressos ciclicamente denominado "relógio embrionário". Cada sómito dá origem a vários compartimentos (dependendo das espécies) que irão dar origem a diferentes tecidos: o esclerótomo que dá origem a tecidos ósseos e o miótomo que origina tecidos musculares e o dermamiótomo que origina vários tecidos como derme e músculo, entre outros. Apesar do corpo da vértebra ter uma contribuição destas duas estruturas, a importância de cada para o processo é diferente entre vários grupos de animais, sobretudo na estrutura que confere o sinal necessário para a formação de corpos vertebrais segmentados. Em peixes como o peixe-zebra, este sinal provém da mineralização da baínha da notocorda pelos cordoblastos. Em amniotas, como a galinha, este sinal começa por aparecer sob a forma de uma divisão rostro-caudal do esclerótomo em dois compartimentos. Esta padronização é mantida na formação do corpo vertebral através do processo de resegmentação. Neste, cada vértebra é formada pela junção da metade caudal de um esclerótomo com a metade rostral do esclerótomo seguinte. A fissura que separa as duas metades do esclerótomo, denominada "fissura de Von Ebner", é então o primeiro sinal morfológico da segmentação das vértebras. Nestes animais o papel da notocorda é ainda

uma incógnita, já que experiências de remoção desta estrutura resultam na formação de corpos de vértebra fundidos.

Por outro lado, o tamanho da notocorda relativamente ao embrião é consideravelmente maior no embrião de peixe-zebra do que no de galinha. O contrário acontece com o esclerótomo, em que este corresponde à maior percentagem de tamanho do sómito maduro no embrião de galinha, sendo apenas uma fina linha de células no embrião de peixe-zebra. Isto leva-nos questionar que transformações poderão ter ocorrido que explicariam estas diferenças. A chave para a resposta a esta pergunta está no processo de desenvolvimento, já que, muitas vezes, as diferenças neste processo são a razão para as diferenças morfológicas observadas entre espécies.

Tanto a notocorda como os sómitos provém de células da mesoderme, mais especificamente da mesoderme axial e paraxial, respectivamente. Durante o processo de desenvolvimento, existem zonas progenitoras que contém factores de transcrição, cuja expressão controla o seu destino. Mutações nestes genes podem causar transformações homeóticas, isto é, conversão das células de uma estrutura noutra diferente. Dois genes descobertos em peixe-zebra, quando mutados, causam alterações deste género: O gene *flating head* (*flh*), quando mutado, leva à transformação total da notocorda em sómito, enquanto o gene *spadetail* (*spt*) leva a uma conversão parcial de células dos sómitos em notocorda. Foi então descoberto que o *flh* reprime o *spt* em células progenitoras de notocorda, levando-as a assumir um destino de notocorda em vez de sómito.

Assim sendo, os objectivos desta tese foram 1) clarificar o papel da notocorda na formação do corpo da vértebra; 2) investigar se a razão das diferenças observadas no papel da notocorda neste processo se deve à alteração nos territórios de expressão de genes como o *flh* ou o *spt*.

No **capítulo II** procedemos ao estudo do efeito da notocorda e do dermamiótomo na segmentação do corpo da vértebra, usando para tal a fissura de Von Ebner como indicador desta segmentação. Para o fazer, começamos por descrever este marco morfológico, tendo descoberto que ele aparece em embriões a partir do sómito IX, Com este conhecimento adquirido, procedemos a experiências de remoção da notocorda e do dermomiótomo e avaliação da presença da fissura de Von Ebner. Em ambas as experiências, a fissura manteve-se inalterada, sugerindo que as duas estruturas não possuem um papel na segmentação do corpo da vértebra.

No entanto um trabalho publicado por outros autores realizou a mesma experiência de remoção da notocorda, deixando o embrião desenvolver-se até formar corpos vertebrais. Os autores descobriram que as vértebras se formavam separadas. Os nossos resultados, em conjunto com estes sugerem então que a notocorda não é responsável por iniciar o sinal de segmentação do corpo vertebral, mas sim por mantê-lo.

No **capítulo III** investigámos a possibilidade dos genes CNOT2, ortólogo de embrião de galinha do *flh* e TBX6L, ortólogo de embrião de galinha do *spt*, controlarem o destino das células progenitoras da mesoderme, levando-as a formar notocorda no embrião de galinha. Para tal, começamos por fazer uma análise conjunta dos seus padrões de expressão, tendo descoberto que ambos estão expressos na zona de origem de células progenitoras de mesoderme axial e paraxial, com uma pequena área de sobreposição. Assim sendo, produzimos experiências de electroporação de um plasmídeo de sobre-expressão do CNOT2 na zona de progenitores de mesoderme axial/paraxial. Os nossos resultados mostraram que a electroporação, com consequente aumento de expressão de CNOT2, levou a várias alterações morfológicas: 1) Um encurtamento da zona segmentada e de mesoderme pré-somitica do embrião; 2) Defeitos na mesoderme paraxial, incluindo segmentação anómala de sómitos e ausência de células na mesoderme pré-somitica e 3) O alargamento das estruturas originárias da mesoderme axial, notocorda e pavimento do tubo neural, de forma altamente relacionada. Através do estudo da expressão do TBX6L, descobrimos que este tinha a sua expressão diminuída em embriões electroporados com CNOT2. De modo a investigar a possibilidade de que o CNOT2 pudesse estar a reprimir o TBX6L no embrião de galinha. Para tal fizemos uma análise da região promotora do TBX6L e mostrámos que existem motivos de ligação de genes da família do CNOT2, apoiando esta possibilidade. Todos estes resultados levaram-nos a sugerir que, no embrião de galinha, o CNOT2 está a controlar o destino das células progenitoras da mesoderme axial/paraxial, ao reprimir o TBX6L, levando-as a seguir o destino de mesoderme axial.

A comparação do alongamento de embriões tratados com embriões controlo mostrou-se difícil, dada a ausência de um estudo quantitativo que descrevesse este processo no seu modo normal. Dado que esta era também a necessidade de um grupo de investigação vizinho, iniciámos uma colaboração que resultou no trabalho apresentado no **Capítulo IV**. Neste estudo fizemos uma cuidadosa análise do alongamento de embriões das fases iniciais do desenvolvimento, descrevendo a alteração de comprimento do embrião inteiro e das suas diferentes secções ao longo do tempo. Através desta análise observámos que as porções

segmentada e pré-somitica são das que mais contribuem para o alongamento total do embrião. Com estes dados verificamos que duas destas podem ser usadas como indicador do tempo de desenvolvimento. Com estes resultados desenvolvemos um método de estadiamento altamente preciso e reprodutível e desenvolvemos uma ferramenta que permite analisar o alongamento do embrião na sua totalidade ou nas suas diferentes secções, detectando e comparando alterações devidas a tratamentos experimentais em relação a embriões controlo.

Com os resultados obtidos nesta tese apercebemo-nos que, durante a evolução, a notocorda está a sofrer uma perda de preponderância considerando a escala evolutiva dos vertebrados, desde os peixes aos humanos em vários aspectos: 1) O seu tamanho relativo ao embrião está a diminuir, acompanhado de um aumento no esclerótomo. 2) A sua importância na formação do corpo vertebral segmentado mudou de ser a fonte do sinal de segmentação para ser importante para a manutenção deste sinal. 3) O seu papel no alongamento do eixo embrionário nas fases iniciais do desenvolvimento está também a sofrer alterações. Enquanto no peixe-zebra a notocorda é a principal força motriz do alongamento, esse papel é assumido pela mesoderme pré-somitica.

Tendo em conta esta informação e que alterações nos territórios de expressão de genes como o *flh*/CNOT2 e o *spt*/TBX6L nas células progenitoras podem causar alterações no tamanho das estruturas, propomos o seguinte: Durante o decurso da evolução, houve uma diminuição do território de expressão dos genes de mesoderme axial concomitantemente com um aumento do território de genes de mesoderme paraxial. Isto levou a que células que pertenceriam à notocorda em vertebrados mais basais, passassem a pertencer a mesoderme pré-somitica/sómito/esclerótomo. Dado que estas células seriam as que teriam importância para a formação do corpo da vértebra segmentado e para o alongamento, a transferência de localização destas células traduziu-se numa transferência de função de uma estrutura para outra.

Table of Contents

List of Figures

List of Tables

This page is intentionally left blank

List of Abbreviations and Acronyms

AF	Annulus Fibrosus
AP	Antero-Posterior
ALP	Alcaline Phosphatase
APH	Axial-Paraxial Hinge
bHLH	Basic Helix-Loop-Helix
BMP	Bone Morphogenic Protein
CEP	Cartilage end-plates
CNH	Chordoneural Hinge
DL	Deep Layer
DV	Dosro-Ventral
ECM	Extracellular Matrix
EMT	Epithelial to mesenchymal transition
EVL	Enveloping layer
FGF	Fibroblast Growth Factor
GFP	Green Fluorescent Protein
HH	Hamburger and Hamilton
HN	Hensen's Node
Hox	Homeobox
Mesp	Mesoderm Posterior
MET	Mesenchymal to epithelial transition
ML	Medio-Lateral
mRNA	Messenger Ribonucleic Acid
MRF	Myogenic Regulatory Factor
MZ	Marginal Zone
NMPs	Neuromesodermal Progenitors
NP	Nucleus pulposus
NSB	Node-streak border
PAPC	Paraxial protocadherin
PAX	Paired-box
PS	Primitive Streak

PSM	Presomitic Mesoderm
RA	Retinoic Acid
SEM	Scanning Electron Microscopy
SHH	Sonic Hedgehog
TBX	T-Box transcription factor
TEM	Transmission Electron Microscopy
WNT	Wingless/Integrated
WT	Wild-Type
YSL	Yolk Syncytial Layer

Chapter I – General introduction

The way I see it, if you're gonna build a time machine into a car, why not do it with some style? (Dr. Emmet Brown)

In *Back to the Future (1985)*

When 900 years old you reach, look as good you will not ! (Master Yoda)

In *Star Wars: The Empire strikes back (1980)*

Introduction

"Evolution of form is very much a matter of teaching very old genes new tricks!"
Sean B. Carroll, in Endless Forms Most Beautiful: The New Science of Evo Devo

Nature has provided us with a multitude of living creatures, of which the Animal kingdom contains some of the most interesting and fascinating ones. Animals come in all shapes and sizes, from the strangely looking Portuguese man o' war, to the elegant Lusitano horse, from the 0.5 mm tardigrades to the 170 ton blue whale. Yet in the midst of all these "endless forms most beautiful and most wonderful" as Charles Darwin referred in "The origin of Species", many common features remain between different species. All animals need to move, feed, produce offspring and have found both different and similar ways of doing so. Insects and birds and mammals found different ways to take to skies and fly, while the limbs of mammals are used for such different functions as to swim, run or collect chicken embryos and write PhD theses.

A striking feature many animals have in common is segmentation, which is generally defined as a "repetition of units along the Antero-Posterior (AP) axis", although this definition is still under debate (Hannibal and Patel, 2013). This characteristic, present in animals so different from one another, as the common earthworm, the scary tarantula or you, the magnificent reader of this document, allows for a larger array of body movements and the appearance of more complex structures and functions (Hickman et al., 2004). Segmentation assumes a very specific shape in the form of the vertebrae. These AP repetitive structures are present in so many different animals and is so defining, that lends its name to a whole group, the subphylum Vertebrata, or how they are more commonly known, the vertebrates. But do all vertebrates possess identical vertebrae ? Definitely not !! There are numerous types of vertebrae as there are numerous types of animals (Figure 1.1) (Fleming et al., 2015). And what could explain all this variety ? As the brilliant Sean Carrol explains in his book "Endless Forms Most Beautiful: The New Science of Evo Devo", we can look for the causes of the phenotypic differences by studying the development of each species.

Of course, as with all matters of Biology, not even the collective human knowledge so far has had the capacity to study all existing variety, and thus, some species are studied as a model for biological processes (Fields and Johnston, 2005). This is the

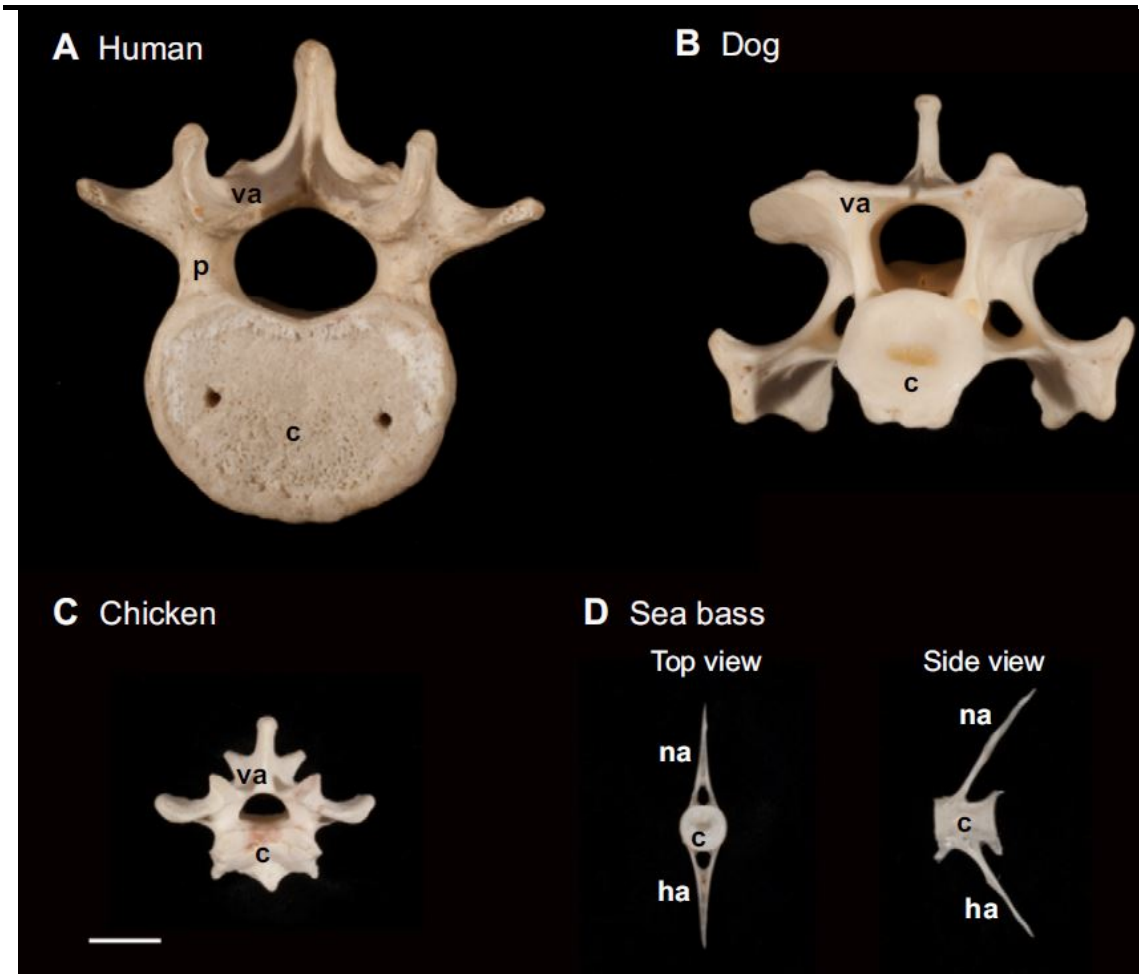

Figure 1. 1 Diverse structure vertebrae of different vertebrate animals.
(A) Human thoracic vertebra. **(B)** Dog cervical vertebra **(C)** Chicken thoracic vertebra **(D)** Sea bass thoracic vertebra. Amniote vertebrae (A-C) show the vertebral body or centrum (c) connected to the dorsally located vertebral arch (va) through the pedicle (p) represented in the human vertebra. The anamniote vertebra (D) shows the vertebral body or centrum (c) connected to the dorsally located neural arch (na) and to the ventrally located haemal arch (ha). Adapted from (Fleming et al., 2015). Scale bar: 1cm

essence of the concept of "model organism". Two of these have been extensively used in Developmental Biology (Müller, 1997), the zebrafish and the chicken. They represent two substantially different groups of vertebrates, the avians and the teleosts and, thus, were used in this work to study the evolution of the process of vertebrae formation. For the purpose of this thesis, whenever it was necessary to stage or refer to any of zebrafish or chicken stages of development, the appropriate reference papers were used, specifically (Kimmel et al., 1995) for zebrafish and (Hamburger and Hamilton, 1951) for chicken.

In this chapter, I will review the current knowledge of vertebral body development and origin on the zebrafish and chicken. I will start by briefly analyzing vertebrae

composition and variations, specifically in these two models. I will next describe the two structures that participate in its formation, the notochord, and the somite. Next, I will explore the actual process of vertebral body formation, highlighting the differences and similarities between the processes in the two species and the role of the notochord and somites. Afterwards, I will explore the possible explanations of these differences, by looking at the developmental origins of the notochord and the somites. Finally, I will hypothesize on the developmental changes that could have occurred during evolution between the two species/groups and the possible role of two genes: CNOT2 and TBX6L.

1 The vertebra

As the saying goes, you must "crawl before you walk". This way, before we can study vertebral body development and the possible origins of the differences in these processes, we must first ask "What is a vertebra ?" The Oxford dictionary defines the vertebra as "each of the series of small bones forming the backbone, having several projections for articulation and muscle attachment, and a hole through which the spinal cord passes". Of course this definition, while enough for the general public, is very reductive for us scientists, as not only there are many types of vertebrae as the vertebra itself is composed of several subcomponents which have themselves different developmental origins (Arratia et al., 2001) and (Fleming et al., 2015). As a testament to this and as a result of this complexity, even the definition of vertebra has changed along history. Early research on vertebrae and vertebral development was conducted by (Gadow and Abbott, 1894; Gadow, 1896). In these works, they formulated the hypothesis that, in all vertebrates, the different parts of a vertebra were formed by four bilateral and symmetrically arranged cartilaginous elements collectively called *arcualia*. The differences in the vertebrae of each group were explained by the presence or absence of each of these elements. As the developmental origins of the different vertebral components were further studied in each group of animals, this notion was progressively dismissed (Arratia et al., 2001; Williams, 1959) and the terminology changed. While there is no definitive definition of vertebra, I personally find the one in (Schultze and Arratia, 1988) to be one of the more complete: The term "vertebra" includes all serially repeated ossified, cartilaginous, and ligamentous elements around the notochord, consisting of centrum, neural arch and spine, and haemal arch and spine." Although the "around the notochord" part is more appliable to fish, as we will see below, it states the basics of

vertebrae composition, in that is composed of two key elements: the *centrum* and the arches (with or without spines). The vertebral *centrum* or vertebral body form the thick core of the vertebra, while lending it its axial structural support and are classified according to their developmental origin. The arches encompass both the dorsally located neural arches and the ventrally positioned haemal arches. The former envelops and protects the spinal cord whereas the latter does the same to the axial blood vessels. While this is true for some animals, like the zebrafish, in other animals like the chicken or the human only have one set of vertebral arches, located dorsally to the vertebral body (reviewed in (Fleming et al., 2015)). Between two adjacent vertebrae there is a structure called the intervertebral disc. It is formed by a central *nucleus pulposus* (NP) composed primarily of proteoglycans, and the surrounding *annulus fibrosus* (AF) made up of collagen fibers and the cartilage end-plates (CEP) that connect the disc to the neighbor vertebrae (reviewed in (McCann and Seguin, 2016) and (Williams et al., 2019).

This thesis will be focused on the development of the vertebral centrum, also referred as vertebral body, as its differences and similarities between vertebrates present a remarkable opportunity to study different ways animals produce the same structure and the possible evolution paths that connect these different ways. In choosing how to refer to this structure, as vertebral centrum, or body, we found that articles on fish studies refer to it as centrum and works that use other animals as models use the term body. We have chosen to use the term "vertebral body", except in sections 1.1 and 1.2. The reason for these exceptions was that the majority of the literature cited in these two sections uses the term centrum.

1.1 Vertebrae homology

In order to compare the developmental process of vertebral centrum in teleosts and avians, we must first ask ourselves if they are homologous. Answering such a question, however, means opening a true Pandora's box, as the concept of homology itself is still widely debated. There are several classifications, each one worthy of writing entire essays analyzing them, but I would like to call to this discussion two of the most important and discussed: cladistic and broad-sense (West-Eberhard, 2003). Let us start by briefly describing the former: cladistic homology states that in order for a characteristic to be considered homologous in two or more *taxa*, its expression has to be unbroken inside monophyletic group that includes these *taxa*. This means that one characteristic must be

present in all taxa of a group, including its most recent common ancestor. For example, in the gnathostome (jawed fish) group, there are groups that have vertebral centra and groups that do not (Fleming et al., 2015). As such, according to the cladistic definition of homology, the centra are not to be considered homologous between gnathostomes. This was explained in Gloria Arratia's seminal 2001 paper (Arratia et al., 2001), in which it was proposed that centra arose independently in the various gnathostome groups. Additionally, as we will see in more detail bellow, the process of vertebral centra formation differs from teleosts to amniotes, which would lead us not to consider vertebrae as homologous in vertebrates. However, there is another interpretation, some consider more parsimonious (Fleming et al., 2015), which is that vertebral centra might have just been lost in the gnathostome groups that do not possess them. Enter the concept of broad-sense homology (West-Eberhard, 2003) ! By this definition, a trait may have been lost in members of a certain group but reappear in its descendants. This definition also allows for homology between two structures that have two different developmental paths leading to its formation. Regarding this, as Wes-Eberhard states in his 2003 paper, evolution acts upon the phenotype and not upon the developmental pathway leading to it. As such the structure itself (its functions, position, etc) should be the main focus of homology considerations. Thus, this definition encourages studies that try to understand how different development strategies lead to "homologous" structures. Not only that, but it also encourages studies that use model organisms to study structures in different species that would not be considered homologous.With all this in mind, the concept of broad-sense homology will be used for this thesis, as we uncover the exciting world of evolution of development.

1.2 Vertebral centra types

As stated earlier vertebral centra can have various classifications, depending on their origin. For this thesis, we will follow the classifications used by several authors in the field (reviewed in (Arratia et al., 2001), (Bensimon-Brito et al., 2012), (Fleming et al., 2015)): The centra can either be chordacentra or perichordal centra. Chordacentra are formed inside the fibrous sheath that envelops the notochord, while perichordal centra are formed outside this sheath. Inside these two groups, there are several subtypes. The

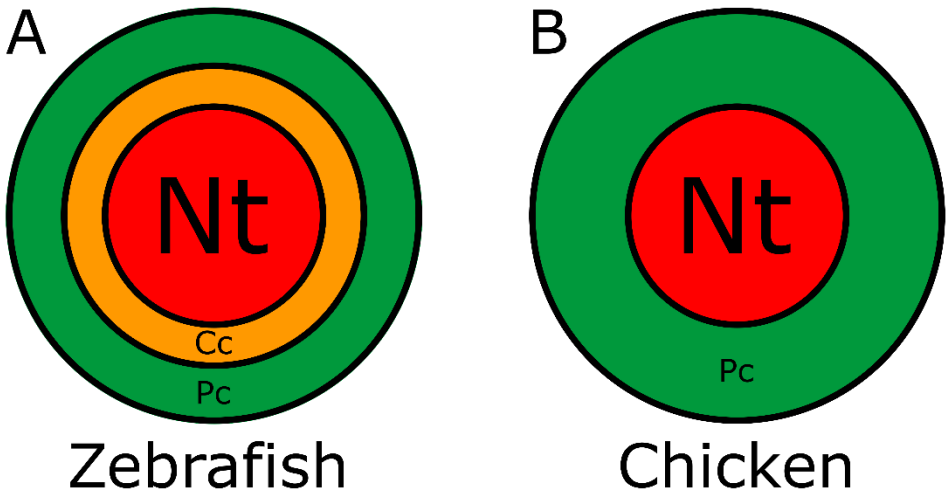

Figure 1. 2 Types of vertebral body/centrum in zebrafish and chicken embryos.
(A) Zebrafish embryos form an initial chordacentrum (Cc) through mineralization of the notochordal sheath followed by a perichordal centrum (Pc) through direct mineralization of sclerotome derived cells, with no cartilage anlage. (B) Chicken embryos form only a perichordal centrum from migration of sclerotome cells, with formation of a cartilage anlage.

chondrictian (cartilaginous fish) chordacentra is formed when cartilaginous cells coming from the arches migrate to the inside notochordal sheath, while the actinopterygian (ray-finned fish) chordacentra forms from mineralization in the middle of the notochordal sheath. Perichordal centra include arcocentra that forms from mineralization of cartilage that comes from the arches, holocentra that develop from proliferating cartilage cells located around the notochord sheath and autocentra that arise by direct ossification, with no intermediate cartilage formation. Although these are different types of centra, they can co-exist in the same organism. That is the case with teleosts such as the zebrafish (Figure 1.2 A), where there is a first phase where a chordacentrum is formed from mineralization of the notochordal sheath and a second phase where sclerotome cells migrate to the vicinity of the notochordal sheath and mineralize directly with no cartilage anlage, forming an autocentrum. In the case of tetrapods like chicken (Figure 1.2 B), there is only the formation of a perichordal centrum, in this case beginning with a template of cartilage formed by sclerotome cells that subsequentially mineralize.

What then is the reason for having such differences in such a key structure of these animals ? One can think of the hundreds of different types of steaks or codfish dishes. All of them have the same protein (the steak and the cod), but their preparation is what makes them unique. The same can be said for the different types of vertebrae as the key to their difference lies in their process of development. How, then, is a vertebra and more

specifically the vertebral body “cooked” (reviewed in (Pais de Azevedo et al., 2012). First you start with two main “ingredients”: the notochord and the somites.

2 Notochord

Located at the center of the elongating AP axis of all chordate embryos, from ascidians to humans and giving its name to this group of animals is the notochord (Stemple, 2005), (Corallo et al., 2015). This structure has been studied since as early as 1834 (Müller, 1834) and since then, its structure and function and origins were or are being uncovered. Structurally, the notochord varies between different chordate groups, but its key features and organization are similar. As with the rest of this thesis, I will focus on the teleost and avian notochords, first describing its structure and morphological development and general functions. When describing the morphological development, I won’t specifically state all the stages where the respective processes occur, as there is an anteroposterior gradient of development, with the rostral portion of the embryo being more differentiated than the caudal part.

In anamniotes such as the zebrafish and salmon, as well as in amphibians such as the axolotl and xenopus, the notochord has its origin on a specific group of dorsal organizer cells that form the chordamesoderm (Scott and Stemple, 2005), (Grotmol et al., 2006), (Ellis et al., 2013a), the origin of which will be discussed later. These cells undergo convergent extension movements, converging towards the midline, which results in a longitudinal elongation (Adams et al., 1990; Glickman et al., 2003). Cells are thus arranged in the so-called “stack-of-coins”, which, in turn” starts to give rise to the no less characteristic rod shape of the notochord. When the zebrafish embryo reaches the 15-somite stage or 16.5 hours post-fertilization (hpf), the chordamesoderm cells start to differentiate in two layers, each with a specific cell type, depending on notch signaling (Yamamoto et al., 2010). The outermost layer, also called notochord epithelium is formed by the chordoblasts (reviewed in (Grotmol et al., 2006)). These are non-vacuolated cells that start to secrete a basal lamina and extracellular matrix (ECM) components, originating the notochordal sheath. This perinotochordal sheath is composed by three layers: An internal *basal lamina* composed of laminins, a medial layer composed of collagen and an external layer formed by loosely organized matrix (Figure 1.3) (reviewed in Scott and Stemple, 2005 and Corallo et al., 2015). The core of the notochord

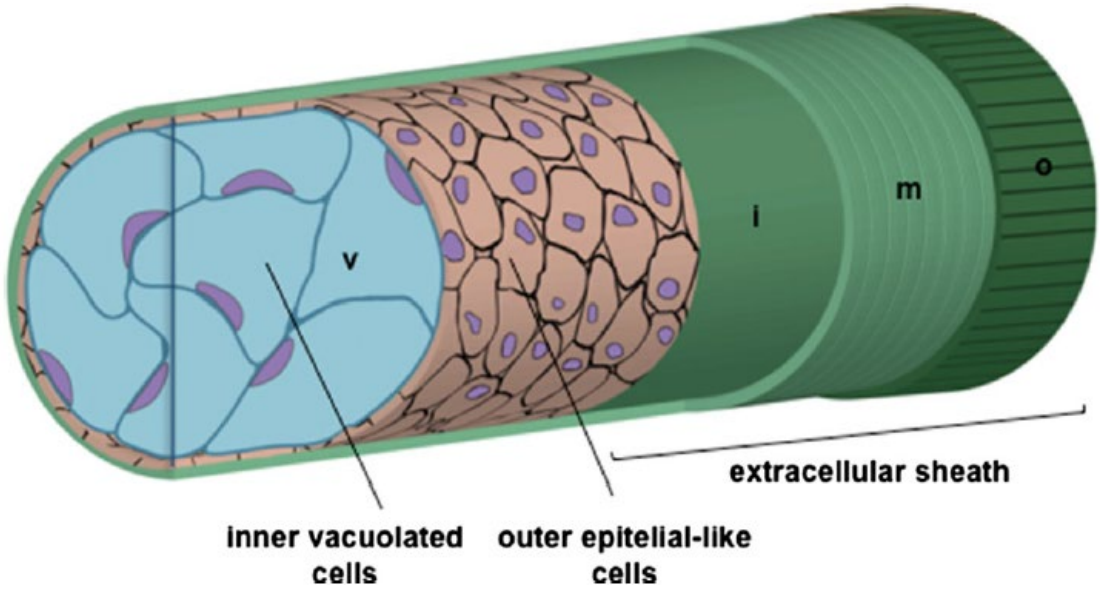

Figure 1. 3 Schematic representation of the zebrafish notochord and its surrounding sheath layers. The core of the notochord is composed of vacuolated cells (v), which are surrounded by the outer layer of chordoblasts (c). The sheath of extracellular matrix is formed by the inner basal lamina (i), the medial layer of collagen fibrils (m) and the outer layer of loosely organized matrix (o). Adapted from (Corallo et al., 2015)

in composed of chordocytes, cells that inflate large vacuoles, forming the bulk of the notochord volume.

In chicken embryo (as well as in other amniotes), the notochord follows a similar structure and development as in zebrafish. In 1976, (Bancroft and Bellairs, 1976), using scanning electron microscopy (SEM) and transmitted electron microscopy (TEM) and corroborating the observations of (Jurand, 1962) established three phases for notochord development from HH5 to HH23: 1) Bilaminar phase; 2) Rod-like unvacuolated phase and 3) Rod-like vacuolated. As with the zebrafish, notochord cells are laid down from the organizer (Hensen's node) as it is migrating posteriorly. In the first phase, the notochord is composed of two layers of loosely packed cells, the dorsal ones dorso-ventrally oriented and the ventral ones mediolaterally oriented and the notochord borders are still difficult to distinguish from the surrounding tissue. In the second phase, this situation changes as the notochord sheath starts to form around the notochord, gaining its rod-like appearance. In the third phase, cells start to become vacuolated and become more densely packed, as the notochord increases its diameter. The notochordal sheath also follows a similar structure (Corallo et al., 2015) with an inner *basal lamina* surrounded by ECM components such as collagen and proteoglycans (Camon et al., 1990), (Hayes et al., 2001). One fundamental difference in the chicken notochordal sheath structural

organization is that it is acellular i.e. there is no outer layer of cells corresponding to the zebrafish chordoblasts. If these cells are not present, which cells then produce the sheath components in the chicken embryo ? To our surprise, this is not an answered question, as the only works that shed some light on this subject are morphological/histological/histochemical studies done in the 1960s and 1970s. Some authors describe the notochord cells as acquiring a secretory morphology and producing the components found in the sheath, proposing that the sheath is produced from within by the notochord cells (Bancroft and Bellairs, 1976), reviewed in (Ruggeri, 1972)). On the other hand, (Jurand, 1962) describe the sheath as originally being formed from microfibrillar components and suggest that these are produced from outside the notochord. All authors unanimously agree that more studies are needed to definitely uncover this question and I subscribe this entirely !

As an embryonic structure, what then is its final destination in the adult animal ? Well, that deeply depends on the animal about which you ask this question. It is usually said that the notochord is a transient structure but that is not true for a wide variety of animals. This is the case in cephalochordates like the amphioxus (Holland et al., 2004) agnathans like lampreys, in Actinopterygii like the sturgeon (Stemple, 2005). On the other hand, in ascidians, the larval phase, which most resembles the chordate basal plan has a notochord and it is essential for locomotion (Satoh, 2003). In so-called higher vertebrates, the situation is a bit different, as the notochord goes on to originate or contribute to other structures. Besides the notochord's function on vertebral body development (which I will not explain here, as it will constitute a heavy spoiler for an important section bellow !), the notochord is generally described as originating the NP of the intervertebral discs and several experiments in mouse prove so (Choi et al., 2008; Choi and Harfe, 2011). However, while that is widely studied in the case of mouse embryos, a study (Bruggeman et al., 2012) using several different organisms representative of fish, amphibians, reptiles and avians, including chicken discovered that it is not the case in non-mammalian vertebrates. They found that, in these animals, there is no formation of NP and the authors suggest several ideas: in amphibians the intervertebral disc is formed by a primitive form of NP possibly originating from notochord cells; in other non-mammalians there is no NP and the disc is entirely formed of an *annulus fibrosus*. Specifically in the chicken embryo the authors observe that the notochord persists throughout all stages of embryogenesis. As for the adult fate, they refer that it is still unclear.

What then leads scientists to devote their time to a seemingly transient structure ? The reason is its wide range of functions, both structurally and functionally. Structurally, its mechanical properties make it the first axial skeleton of all embryos. The vacuolated cells exert pressure against the notochordal sheath, which confers resistance and flexibility at the same time (Stemple, 2005), much like a hose filled with water balloons, the hose being the outer sheath and the balloons the vacuolated cells. This is crucial in at least two capacities: 1) It allows for elongation and straightening in zebrafish and xenopus embryos (Adams et al., 1990); (Koehl et al., 2000); (Ellis et al., 2013a; Ellis et al., 2013b)) and 2) it is an essential part of the mechanical system required for swimming in amphibian tadpoles and zebrafish larvae ((Nishikawa and Wassersug, 1989); reviewed in (Stemple, 2005). Functionally, the notochord is an important signaling center that helps pattern surrounding tissues (reviewed in (Corallo et al., 2015), such as the neural tube (reviewed in (Briscoe and Ericson, 1999)), somites (Resende et al., 2010); (Sheeba et al., 2016)), the zebrafish slow-twitching muscles (Devoto et al., 1996) heart (Danos1996) and even endoderm and pancreas (Cleaver et al., 2000); Kim et al., 1997), just to name a few. This mainly through the production of key signaling molecules such as sonic hedgehog (SHH), chordin and noggin.

One final consideration on the notochord that we consider it is relevant for the purpose of this thesis is one pointed out in the legend of figure 1 of the excellent notochord review by (Stemple, 2005): When we analyze the tree of life of animals that possess a notochord, it is quite remarkable that its size proportionally to the embryo is clearly decreasing from fish, to amphibians, to reptiles to avians and mammals. In zebrafish, for example the notochord is almost the same size of the neural tube, while in the chicken embryo it does not even reach ¼ of its axial roommate.

3 Somites

3.1 Somite formation

The next main “ingredient” for the formation of our vertebra are the somites. These structures are spheres of epithelial cells that flank the notochord and neural tube on both sides and bud off sequentially and in pairs from presomitic mesoderm (PSM). And if this description sounds as plagiarism and seems familiar, as if it is the same as something you have read before, it is only normal, as so many works have been published

describing these structures. The earliest descriptions of somites are the drawings of Marcello Malpighi in his "*Dissertatio epistolica de formatione pulli in ovo*" (Malpighi, 1693). The first terms used to describe the somite were: "rudimenta vertebrarum" (translated from latin, meaning rudimentary vertebra) used by Wolff and "Urwirbeln" (translated from german, meaning protovertebra) used by Remak (reviewed in (Verbout, 1976). These terms however meant that the somites only originated vertebrae, which we now know is not the case. Years later, in 1880, Francis Balfour started using the term "mesoblastic somites", which resulted in the designation of somites.

Much of the morphological and molecular events that lead to somite formation have been and continue to be thoroughly studied, although many questions remain, especially concerning the molecular signals and how they operate (Pais de Azevedo et al., 2018).

In both the zebrafish and chicken embryo the process of somite formation is rather similar in its molecular and morphological events, with a few differences that will be described posteriorly. Just like the notochord, there is quite a cellular journey before somites are formed and this part of the journey begins with the PSM. This structure is in fact two rows of mesenchymal cells flanking the notochord and neural tube, from which the somites will periodically bud off at its anterior end. In order to help visualize this process, one can imagine two traditional Portuguese "chouriços" flanking the axial notochord and neural tube being made on one end and cut on the opposite one, from a cylindrical row of tasty meat and spices. Of course, this simple description, while very appealing for a hungry reader is not enough and a more scientific one is on order. When doing so, the conventionally agreed nomenclature (Ordahl and Le Douarin, 1992); (Christ and Ordahl, 1995); (Pourquie and Tam, 2001) states that forming somite is designated S0, just like the last somites to be formed are called SI, SII, SIII, ect. (highest number being the oldest to have been formed), and the next to start to be formed are S-I, S-II, S-III, etc (the lowest number being the one to be formed immediately next). Over the period of formation of one somite, the most anterior PSM cells undergo several movements and transformations that result in two key changes that occur concomitantly: 1) mesenchymal to epithelial transition (MET) of most of the cells of the future somite and 2) formation of the somitic border. Several studies have brilliantly studied such movements (Kulesa and Fraser, 2002), (Sato et al., 2002); (Nakaya et al., 2004); (Martins et al., 2009) and a brief summary is as follows: The first cells to undergo MET are the most medial ones,

located next to the neural tube and notochord, doing so as early as S-II. This epithelialization spreads to the dorsal and ventral sides of S0 with cells at the posterior end of S0 doing so before the ones at the anterior end. The last cells to epithelialize are the lateral PSM ones. It is very interesting that the first cells to undergo MET are the most medially located ones, as it has been described that these cells are the ones possessing the information for somite segmentation (Freitas et al., 2001).

In this process, a small set of cells remain in the core of the somite, called the somitocoel. Its cell population, however, is not fixed, as several of these cells have been observed as moving to the outer epithelial layer at the same time as outer epithelial cells are seen moving to the somitocoel (Martins et al., 2009).

But what drives the formation of the border between the two somites and cell MET (reviewed in Watanabe and Takahashi, 2010) ? In the chicken embryo all starts in the anterior compartment of S-I, where basic-helix-loop-helix (bHLH) transcription factors Mesoderm Posterior (Mesp) family of transcription factors (like the chicken ortholog c-Meso1, (Buchberger et al., 1998), become restrictively expressed. In this region, (Watanabe et al., 2009) they upregulate the expression of EphA4, a ligand for the ephrin receptor tyrosine kinase family (reviewed in Poliakov et al., 2004). This family of membrane bound proteins are known to regulate cell-cell adhesion and cytoskeletal conformation in the formation of several tissues in various animals. In this case, EphA4 from the anterior compartment of S-I binds to ephrinB2 receptors on the posterior compartment of S-0, which leads to cell-cell repulsion and the beginning of the formation of a gap between these two regions. Additionally, ephrinB2 represses the activity of Cdc42, a member of the Rho family of GTPases, by phosphorylation of its cytoplasmatic tyrosine residues (Pasquale, 2008). This reduction, in turn, leads to epithelialization of the cells of the posterior compartment of S-0 (Nakaya et al., 2004). With MET underway and the formation of a space between two future somites, another key player in somite boundary formation, the ECM enters the fray (literally as in this case the ECM will fill the referred space). Another way by which Eph-ephrin signaling leads to somite border formation, ephrinB2 signaling leads to clustering (Julich et al., 2009) of integrin α1 (Itgα1), the main integrin responsible for fibronectin matrix assembly. This leads to the formation of an ECM composed of fibronectin and other components such as laminins and N-cadherin (Martins et al., 2009; Rifes et al., 2007; Rifes and Thorsteinsdottir, 2012),

which helps further separate the caudal border of one somite and the rostral border of the next.

So now that we know the "how somites are formed", two of the most interesting aspects of somite formation remains unexplained: What determines the "where" and "when" of somite formation ? The first model to try to answer these two questions was the two-component "clock and wavefront" model proposed in 1976 by Cooke and Zeeman (Cooke and Zeeman, 1976). Regarding the first component, the clock, this model assumes that cells possess an intrinsic oscillator that allows them to know when to form the somitic boundary. The second component, the wavefront informs the cells on the location where they will form the boundary. This model, with a few modifications has stood the test of time and is still considered the predominant one (Oates et al., 2012; Pais de Azevedo et al., 2018; Richmond and Oates, 2012) in explaining "What underlies timely somite formation ?" (Andrade et al., 2007). However, it does not explain all the experimental evidence of recent works. As such, a very elegant view that I have decided to adopt in this chapter is the three-tier conceptual framework proposed by Andrew Oates (Gomez et al., 2008; Oates et al., 2012; Richmond and Oates, 2012). In it, the molecular mechanisms and interactions that lead to somite formation are interpreted as a combination of three main components, acting at different levels. The first one and its importance can be realized when we observe that vertebrate embryo somites are formed with a fixed periodicity that depends on the species (Gomez et al., 2008; Oates et al., 2012; Richmond and Oates, 2012), 30 minutes for zebrafish, 60 minutes for the house snake (*Lamprophis fuliginosus*), 90 minutes for *Xenopus Laevis* and chicken, 120 minutes for mouse and six hours in humans. With the risk of anthropomorphizing cells, it almost seems that cells have a pocket or wristwatch to keep time and know exactly when to form a somite. Well, it turns out that cells actually do have a Molecular Clock and it was discovered precisely by my supervisor, Isabel Palmeirim (Palmeirim et al., 1997) (Figure 1.4), when she realized that hairy1, the chicken homolog of the *drosophila* hairy gene had an oscillatory expression pattern, which was later observed by live-imaging experiments (Aulehla et al., 2008; Masamizu et al., 2006). In both cases as discovered later for other species, the time it takes for this expression pattern to repeat itself, i.e. to complete a cycle, is the same it takes for a somite to form. Since then, many genes have been found

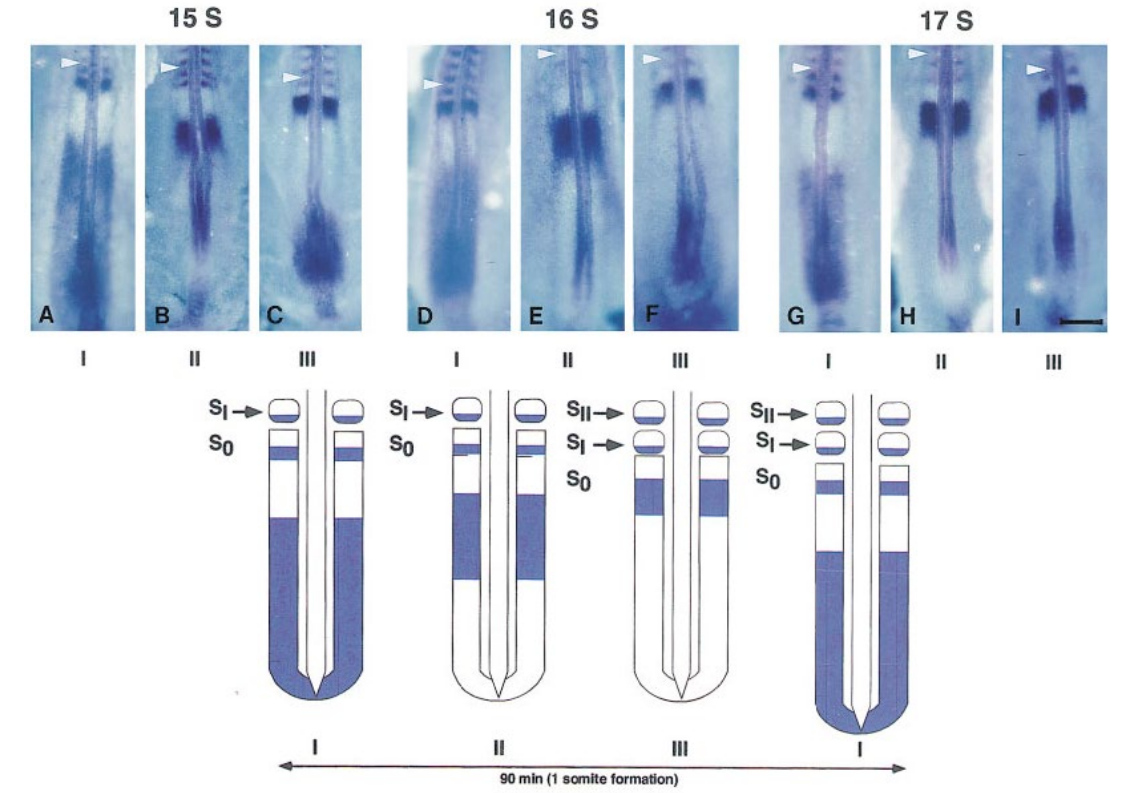

Figure 1. 4 cHAIRY1 mRNA cyclic expression in the PSM.
The top figure shows the three expression pattern phases of the oscillation on embryos with 15 to 17 somites. The bottom drawing represents each of these phases during the cyclic formation of one somite. Scale bar: 200µm. Adapted from (Palmeirim et al., 1997)

to have an oscillatory expression pattern (Andrade et al., 2007) all of which with a period equal to the time of somite formation. This is the nature of the first component: an oscillator operating inside each cell in the PSM. The mechanism by which the oscillator operates depends on mechanisms of negative feedback loop (Burstyn-Cohen et al., 2004) generated by repression of transcription factor genes by their own protein products (Lewis, 2003). Such was discovered to be the case for several of these segmentation clock genes (Bessho2003, Dale2003), with a very curious high variability of which genes oscillate, depending on which species (Krol et al., 2011).

Each somite is formed by many cells and its formation requires coordination of gene expression between them. The way that is achieved is the second component of the three-tier model: synchronization of these oscillations. The delta-notch juxtracrine ligand and receptor signaling system has long been known as a very important cell-cell communication system (reviewed in (Hori et al., 2013; Lai, 2004). More so, that many of the clock cycling genes are part of the notch signaling pathway. As so, it was suggested it as the mechanism of synchronization (Jiang et al., 2000), an hypothesis that was

strongly backed by various experiments on delta-notch mutant zebrafish (Oates and Ho, 2002; Riedel-Kruse et al., 2007).

If the first and second components of the three-tier model correspond to the clock in the clock and wavefront model, the third and final component, the global arrest of oscillation corresponds to the determination front. This was discovered when portions of anterior PSM were inverted in different locations along its whole length and only the ones inverted rostral to a certain antero-posterior (AP) position were found to have changed their AP orientation (Dubrulle et al., 2001). This meant that there is a frontier called the determination front, from which AP somite compartments are already determined, which is essential for somite boundary formation. This frontier is the result of opposing gradients (DiezdelCorral2003, Olivera-Martinez2007) of FGF (Dubrulle and Pourquie, 2004) and Wingless/Integrated (Wnt) (Aulehla et al., 2008) signaling originating from the tailbud and Retinoic Acid (RA) from the formed somites (Vermot et al., 2005). This front is located at different levels in different species, between S-1 and S0 in the mouse embryo (Morimoto2005), between S-II and S-I in zebrafish (Sawada et al., 2000) and more posteriorly in S-IV in chicken (Dubrulle et al., 2001). As cells are approaching the determination front, the oscillations are gradually slowing down (reviewed by Oates et al., 2012) arresting as they cross the front to the anterior PSM. By leaving the area of influence of the FGF/Wnt gradients, cells become competent to start the specific stripe expression of Mesp (reviewed by (Hubaud and Pourquié, 2014) leading to the start of the epithelization process.

While the previous description of the process of somite formation is derived from knowledge of amniotes such as the chicken, most of the morphological and molecular mechanisms are very similar in anamniotes such as the zebrafish. There are, however, several differences (reviewed in (Piatkowska et al., 2021), the main ones, residing in the core genes of the segmentation clock (reviewed by (Krol et al., 2011), the signaling cascade that leads to Mesp expression (reviewed in (Hubaud and Pourquié, 2014) and in the somite shape and furrow formation (reviewed in (Stickney et al., 2000)). Since these differences do not seem to be related to the difference between zebrafish and chicken vertebral body formation, these will not be described in this thesis.

After all that adventure, what do somite cells end up becoming ? As we will see in the next section, somite cells originate several tissues and structures such as elements of the axial skeleton, different types of muscles, tendons, and ligaments, as well as

peripheral nerves and blood vessels (reviewed in (Christ et al., 2007; Piatkowska et al., 2021). The fact that the progenitors of all these different cell types are organized in a metameric pattern such as in the somites is essential for the organization of the vertebrate body.

How then can a small epithelial sphere of cells contribute to such a large variety of structures in the adult ? It all becomes clear when we realize the fascinating metamorphosis the somite undergoes as it matures. Like a colorful butterfly comes out of a monochromatic moth, so too does the somite divide into different compartments that will originate its different derivates.

3.2 Somite differentiation and sclerotome formation

As the somite matures, it will start to differentiate into different compartments, depending on the species considered. Generally, the dermomyotome gives rise to muscle and dermis of the back, the myotome forms all body muscles (except those on the head) and the sclerotome forms several axial skeletal elements (reviewed in Christ et al., 2007). This differentiation is dependent on different signaling molecules and cascades. Depending on the structure each cell is closer to, it will receive specific signals from these structures, defining its fate. As our object of study is the vertebral body and it derives from the sclerotome, we will focus our description on development of this compartment.

And it is in this structure that we can already notice one of the big differences between anamniotes and amniotes (reviewed in (Piatkowska et al., 2021) that is relevant to the process of vertebral body formation. In anamniotes like the zebrafish, the somite mostly differentiates into myotome, with the sclerotome being a much smaller compartment formed from a small cluster of ventromedial somite cells (Morin-Kensicki and Eisen, 1997). In contrast, in amniote embryos like the chicken, the somite gives rise to two major compartments, the dorsolateral dermomyotome and the huge ventromedial sclerotome (reviewed in Christ et al., 2007)).

3.2.1 Sclerotome development in the amniote embryo

As there is much more knowledge on the development of the sclerotome in the amniote embryos (chicken and mouse), we will start our description of sclerotome development in this group of animals.

3.2.1.1 Sclerotome formation and migration

The formation of the sclerotome is a complex process that involves both molecular events, such as induction and expression of different signaling molecules and morphological events such as EMT and cell migration (reviewed by (Christ et al., 2004; Christ et al., 2000; Scaal, 2016).

In chicken embryos, this process begins at somite stage III (Ordahl and Le Douarin, 1992), where, although all the somite cells maintain their epithelial form, a molecular regionalization starts to occur: Cells of the ventromedial side of the somite start to express Paired box 1 (Pax1) (Deutsch et al., 1988), a member of the paired-box transcription factor family (Noll, 1993; Walther et al., 1991). This expression is known to be induced by signals coming from the notochord and floor plate (Ebensperger et al., 1995), identified to be SHH (Fan and Tessier-Lavigne, 1994; Johnson et al., 1994) and Noggin (Dockter, 1999; McMahon et al., 1998). At somite stages IV/V, another member of this family, Pax9 (Muller et al., 1996), also starts to be expressed in the same region. Besides the expression of Pax1, the notochord is also known to be important for induction, proliferation, and survival of the sclerotome (Fan et al., 1995; Fan and Tessier-Lavigne, 1994; Teillet and Le Douarin, 1983).

Immediately after, these sclerotome precursor cells start to lose the expression of the cell adhesion molecule N-cadherin (Hatta et al., 1985; Hatta et al., 1987) which allows them to undergo Epithelial-to-Mesenchymal transition (EMT), (Duband et al., 1987). This permits them to become mobile, acquiring filopodia (Trelstad, 1977) and starting migration to the vicinity of the notochord and neural tube (Jacob et al., 1975). This migration is also known to be dependent on extracellular matrix produced by the notochord and sclerotome cells themselves, at least in the case of the ventral sclerotome (see below) (reviewed by Christ et al., 2000; Christ et al., 2004).

Although some studies have been done on the signaling necessary for sclerotome differentiation, some issues are still not clear (Christ et al., 2007; Scaal, 2016). In the absence of notochord and neural tube, a sclerotomal compartment still formed, although with a decrease in cell number (Hirano et al., 1995). On the other hand, Pax1/9 mutants

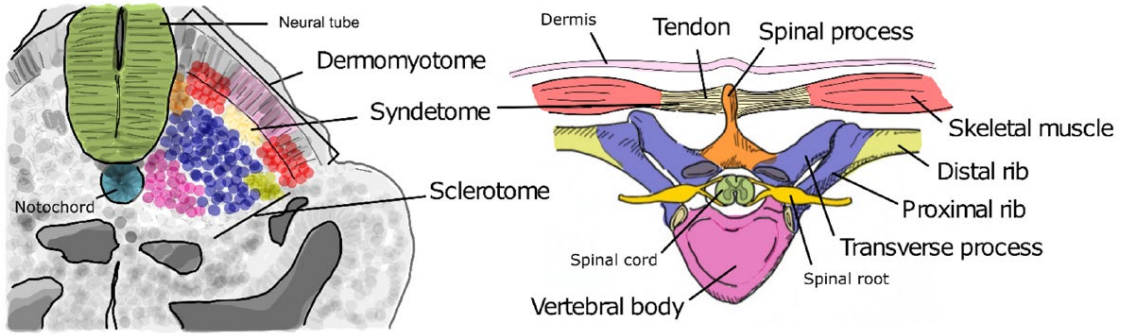

Figure 1.5 The derivatives of the amniote somite.
The several compartments and cells of the somite represented with a different color on the left give rise to different tissues and structures shown on the right with the same color. Adapted from (Nobrega et al., 2021)

(Peters et al., 1999) still produce mesenchymal sclerotome cells, although condensation and growth are affected. Curiously, this leads to absence of vertebral bodies and intervertebral discs, but not of arches. The authors of these and other similar studies refer that these signals may be important to maintain, rather than start sclerotomal differentiation (Christ et al., 2007; Scaal, 2016).

Accompanying the differentiation of the somite compartments and as a consequence of the ventral folding of the embryo, the somite suffers a medio-lateral (ML) rotation, such that the presumptive sclerotome cells become shifted medially and the future dermomyotome cells move to a more lateral position (Brand-Saberi et al., 1996).

3.2.1.2 Sclerotome differentiation and compartmentalization

And just like Spain is actually a collective of different regions that were once separated and independent kingdoms, so is the set of cells that form the sclerotome actually belong to different smaller compartments, that will later give rise to different structures. These sclerotome subunits differentiate not only along mediolateral and dorsoventral axis as it is usually shown in transverse sections, but there is also an AP rostro-caudal division, which will be discussed later. (Figure 1.5) (Christ et al., 2004; Christ et al., 2007; Scaal, 2016). These are the dorsal, the lateral, the central and the ventral sclerotomes and the syndetome and arthrotome. The way by which the sclerotome compartmentalizes is different for each sclerotome subdivision, but to quote Barresi and Gilbert (Barresi, 2020) in the latest version of their Developmental Biology bible, “it all depends on three things: location location location.” Meaning that it depends, like in many other situations during development, on the signals from the surrounding tissues.

Analizing, the different components, we start with 1) the dorsal sclerotome, which is composed of cells that migrate to a space lateral to the dorsal neural tube and under the dorsomedial (epaxial) lip of the dermomyotome and ectoderm. This compartment differentiates under BMP signalling from the ectoderm and roof plate of the neural tube (Monsoro-Burq et al., 1996; Watanabe and Le Douarin, 1996) and gives rise to the dorsal part of the spinous process and dorsal part of the neural arch. Another compartment is 2) the lateral sclerotome, located ventraly to the ventrolateral (hypaxial) lip of the dermomyotome. These cells originate the distal part of the ribs (Olivera-Martinez et al., 2000) and contribute to the tendons, and do so, under the influence of BMP4 signalling from the lateral plate mesoderm (Pourquie et al., 1995; Pourquie et al., 1996) and FGF4 from the myotome (Brent et al., 2003). Both the dorsal and lateral sclerotome downregulate their expression of Pax1 upon their differenciation (Ebensperger et al., 1995). Next on our list is 3) the central sclerotome, that takes up the bulk of initial sclerotome cells located in the centre, located just bellow the demomyotome and later myotome. This compartment will develop due to FGF-8 signalling from a specific set of myotome cells (Huang et al., 2003). Ultimately central sclerotome cells will give rise to the pedicle, the proximal part of the ribs and the ventral portion of the arches (Christ and Wilting, 1992). As for compartment 4), in the central sclerotome it was discovered that the cells located in the cranial and caudal borders of contact with the myotome give rise to the tendon progenitors. This happens due to FGF signalling from the myotome that triggers the expression of the transcription factor scleraxis (Brent et al., 2003), which led the authors to suggest that this compartment should henceforth be called syndetome. To know more about the next compartment, 5) the arthrotome (Mittapalli et al., 2005), we have to go back to our earlier description of somite cells. Remember the somitocoel, which was composed of mesenchymal cells that never ended up epithelializing ? When the somite matures, they are integrated in the sclerotome forming a triangular-shaped region on the rostral half of the caudal half-sclerotome. Although the molecular mechanisms at work in arthrotome differenciation are still unkown (Scaal, 2016), it has been shown that its cells contribute to the intervertebral discs and proximal ribs (Bagnall et al., 1988; Bagnall et al., 1989; Huang et al., 1996; Huang et al., 1994). Later on, it was discovered that they also give rise to the intervertebral joints (Mittapalli et al., 2005) and, because this was the first evidence of sclerotome cells giving rise to joints, this compartment was named arthrotome.

And last but certainly not least is 6) the ventral sclerotome, which originates the vertebral body, the main focus of this thesis and the intervertebral discs (Christ et al., 2004; Christ et al., 2007; Christ et al., 2000; Scaal, 2016). What is interesting about this domain is that initially it does not contain any cells ! Instead, it contains an extracellular matrix sheath that envelops the notochord (Jacob et al., 1975; Newgreen et al., 1986). The ventral sclerotome develops when, after EMT, cells start to migrate and invade this perinotochordal space. To do this, they use this matrix as a substrate (Jacob et al., 1975; Newgreen et al., 1986). On the other hand, the sclerotome cells themselves seem to produce an extracellular matrix that also contributes to their migration (Chernoff and Lash, 1981; Solursh et al., 1979). The formation of this extracellular matrix sheath around the notochord requires the expression of the transcription factors *Sox5* and *Sox6*, in both the notochord and in the sclerotome (Smits and Lefebvre, 2003). In their absence, expression of genes corresponding to key components of the sheath matrix is lacking also both in the notochord and sclerotome. This leads to cartillage deficiencies in the vertebral bodies and no formation of intervertebral discs. This reinforces that, in amniones, sheath formation may be dependant on both notochord and sclerotome cells (Scaal, 2016). Migrating sclerotome cells then form the perinotochordal tube (Tondury, 1958). In it, mesenchymal cell condensations start to appear at the future location of the intervertebral discs (Christ and Wilting, 1992). Between these condensations, where the vertebral bodies will appear, Pax1, known to be a repressor of chondrocyte maturation is downregulated (Takimoto et al., 2013). Formation of the cartilage anlage thus begins, with expression of chondrogenesis genes such as chondroitin-6-sulphate proteoglycan (Wilting et al., 1994). Later ocurring endochondral ossification completes the formation of the vertebral body. As for the signalling required for formation of segmented vertebral bodies, much is still unknown as we will describe in 5.2.

3.2.2 Sclerotome development in the anamniote embryo

As referred earlier, the zebrafish sclerotome is much smaller proportionally to the rest of the embryo than in the chicken. Perhaps because of this fact, there are not many works that explore the formation and differentiation of the sclerotome. One of the first to attempt to do so, used fluorescent dextran to mark somite 5 to 17 individual cells in order to follow sclerotome cell movement (Morin-Kensicki and Eisen, 1997). They describe an initial cluster of ventromedial cells that become mesenchymal and migrate dorsally, towards the notochord and neural tube, contributing, among others, to vertebral cartilages

as the sclerotome cells in amniotes also do. However, they observed that not all these cells give rise to sclerotome and classified three groups according to the fate of their cells: 1) the anterior compartment composed of anterior cells that all become sclerotome; 2) the posterior compartment that contained 1/3 of the posterior cells that gave rise to sclerotome, with the remaining 2/3 of posterior cells forming muscle, and 3) some posterior ventromedial cells that originated both sclerotome and muscle. These different groups also migrated through different locations and at different times, with anterior cells migrating before posterior ones. The anterior cells migrated dorsally between the myotome and the notochord, reaching the neural tube at a point between the borders of two adjacent somites and spreading both anteriorly and posteriorly from that point. Posterior cells followed a similar but broader path. Sclerotome development can also be visualized through expression of *twist* (Stickney et al., 2000). Curiously there are four *twist* genes in the zebrafish embryo (Germanguz et al., 2007; Gitelman, 2007) and the one usually referred as the "zebrafish *twist*" is actually *twist2*. Along with *twist1a*, both genes have been shown to be expressed in zebrafish migrating sclerotome cells (Germanguz et al., 2007). As for the regulation of zebrafish sclerotome, there is little information on the possible relevant signals. Nevertheless, Hh signaling changes have been shown to affect sclerotome formation, albeit with possibly contradictory results (Stickney et al., 2000)

In the same manner we described for the notochord, when analyzing the sclerotomes of different groups, there are clear size differences from anamniotes like the teleosts or the amphibians to the amniotes like the avians and mammals (Morin-Kensicki and Eisen, 1997; Piekarski and Olsson, 2014). The sclerotome of animals like the zebrafish is composed of a thin layer of cells, while in animals like the chicken, it takes up more than half of the size of the differentiated somite

We have just described two key structures that take part in the formation of the vertebral body. Now it is time to explore how the actual process takes place, including the cellular organization, movements and signals involved.

4 Resegmentation

In terms of cellular organization, there is a very curious fact about the position of the vertebrae in relationship to the muscle. As stated before, the somite subdivides into segmented bones and muscles. However if one unit of muscle connected directly to one

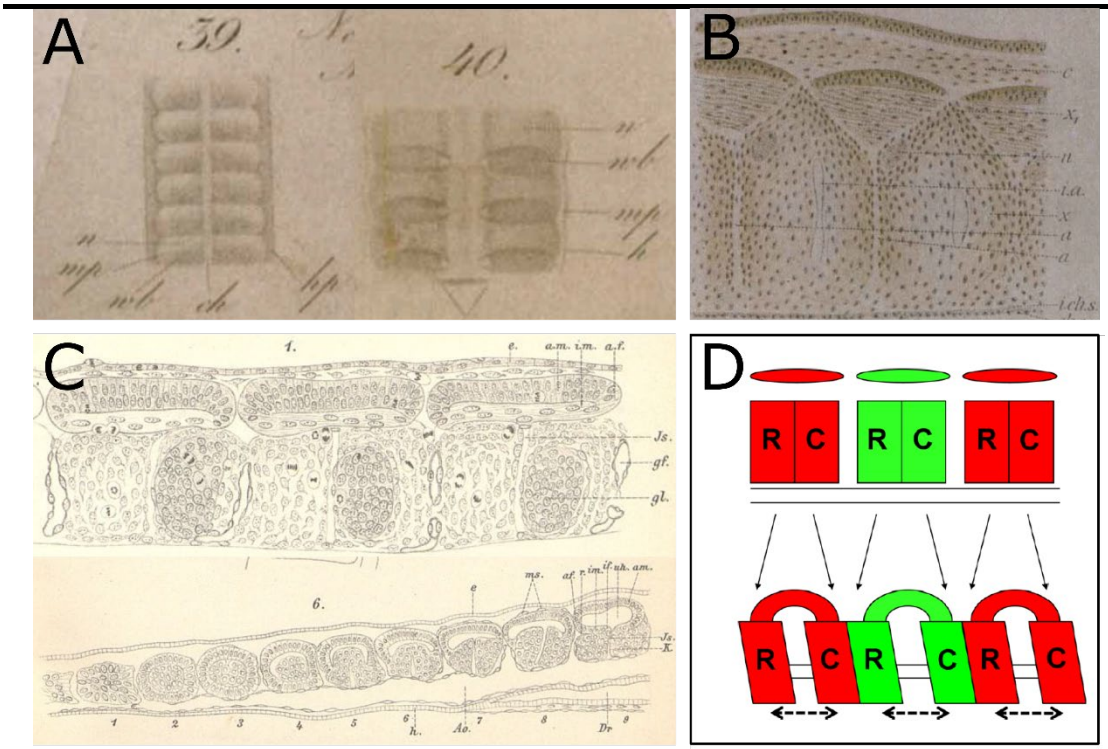

Figure 1.6 Different representations of the resegmentation hypothesis in the last 150 years. Different representations of the resegmentation hypothesis in the last 150 years. (A-B) Representation of resegmentation in chicken embryos according to Remak (1850) (A) and Corning (1881) (C) Schematic of resegmentation in reptile embryos according to Von Ebner (1888). (D) Resegmentation-shift model in chicken embryos according to Ward (2017). Adapted from (Corning, 1881; Remak, 1855; Von Ebner, 1888; Ward et al., 2017)

unit of vertebra, the vertebral column would not be able to do bending movements. What allows these movements to occur is the fact that each axial muscle is, in fact, inserted between two consecutive vertebrae. The question of how this is achieved during development has been a subject of research and debate for more than 100 years (Brand-Saberi and Christ, 1999; Ward et al., 2017). It all started with the concept of resegmentation (Neugliederung), a term created by Robert Remak in 1855. In his work in chicken embryos, he describes that each vertebra is composed of the caudal half sclerotome of one somite and the rostral half sclerotome of the next adjacent somite (Remak, 1855), (Figure. 1.6 A). Curious is the use of the term resegmentation, as the original term actually means New (Neue) Segmentation (Gliederung) (Division). This view was supported by the discovery of an intrasegmental fissure separating both AP halves of the

sclerotome by (Corning, 1881) (Figure 1.6 B). This landmark was later also described by Von Ebner in reptile embryos as an intervertebral fissure (Von Ebner, 1888) (Figure 1.6 C), now commonly referred as Von Ebner's fissure. This idea of resegmentation was not

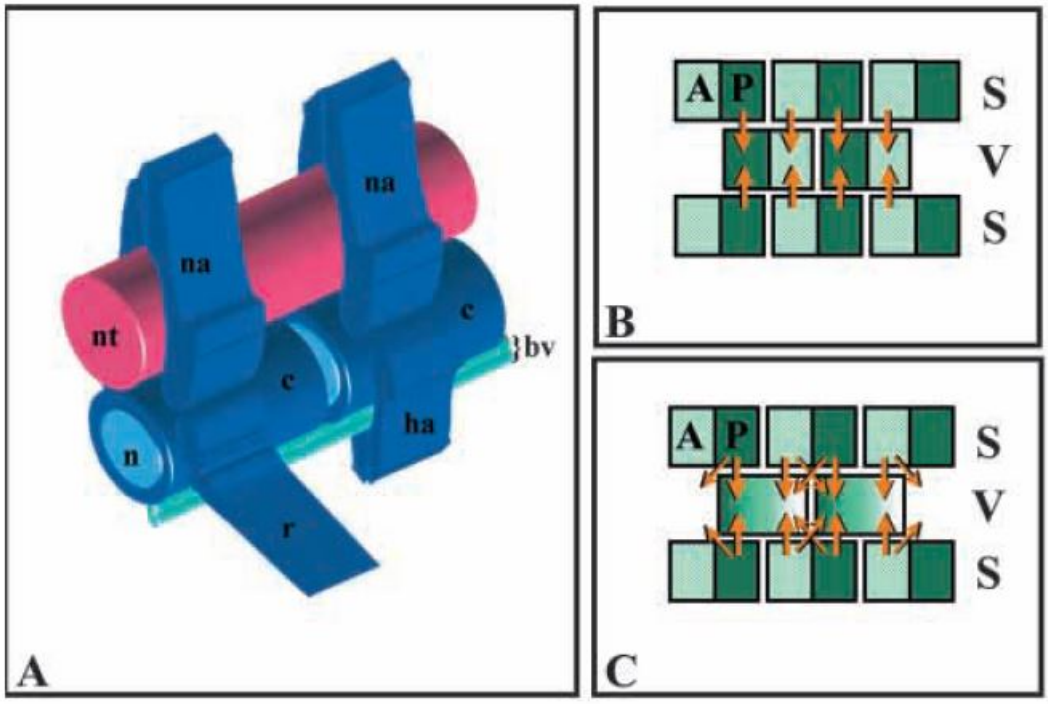

Figure 1.7 Models of resegmentation.
(A) Zebrafish neural and haemal arches and location in relarion to the notochord. (B) Classical compartmental resegmentation model where each anterior (A) or posterior (P) half sclerotome (S) contributes cells to just one vertebra. (C) "Leaky resegmentation" model proposed to explain zebrafish vertebrae formation. In this case, one half sclerotome contributes with cells to more than on vertebra. Adapted from (Morin-Kensicki et al., 2002)

consensual and even Von Ebner's fissure was interpreted as an artifact of fixation (Verbout, 1976). However, not only was the fissure proven to exist (Stern and Keynes, 1987), as several later works supported the idea of resegmentation, through experiments done with several techniques (reviewed in (Brand-Saberi and Christ, 1999; Christ et al., 2004; Ward et al., 2017). Using the quail-chick chimaera system (Le Douarin, 1973), resegmentation was confirmed for the vertebra as a whole and for its different components (Beresford, 1983; Huang et al., 2000; Huang et al., 1996), including the vertebral body (Aoyama and Asamoto, 2000; Bagnall et al., 1988). Besides this, it was also discovered that both halves of the sclerotome are non-miscible (Stern and Keynes, 1987). More recently, results of lineage tracing using an *Uncx4.1-LacZ* transgenic reporter to determine the fate of the caudal sclerotome of thoracic and lumbar vertebrae of mouse embryos were also found to be consistent with resegmentation for the vertebral body (Takahashi et al., 2013). As some of the previous methods may be considered fallible

(Ward et al., 2017), another recent study using again chicken embryo used improved carbocyanine dyes to reanalyze somite contribution to the vertebral bodies and neural

arches. The results of this study were once again consistent and supported the resegmentation hypothesis (Ward et al., 2017). Not only that, but they revealed that, in the lumbosacral region, there is a shift in the rostro-caudal position of the dorsal and ventral sclerotome cells. This led the authors to propose a "resegmentation-shift" model, in which there is resegmentation of the various elements of the vertebra, with local rostro-caudal shifts that depend on the axial position (Ward et al., 2017) (Figure 1.6 D).

The information so far has dealt mostly with resegmentation in the avian embryo, as well as mammal and reptile. What about amphibians and teleosts ? Starting with the latter group, as far as we know, there is only one study that intently addressed this question (Morin-Kensicki et al., 2002). In this work, the authors labelled the somitic ventromedial cell cluster of zebrafish embryos with vital fluorescent dyes and analyzed the relationship of the somite to the vertebra. Their results showed that cells from one somite contributed just to two consecutive vertebrae, which supports the resegmentation model. However, they showed that one half somite could contribute cells to more than one vertebra, independently of its AP position. That is, the cells of the posterior half sclerotome of one somite could end up in either the posterior half of one vertebra or the anterior half of another (Figure 1.7). As this is contrary to the strict regulation observed for resegmentation experiments, the authors classified it as "Leaky resegmentation" (Morin-Kensicki et al., 2002). Since the amphibians are a group that is usually placed between the birds/reptiles and teleosts, it would be interesting to know if there is resegmentation in its embryos and if it is more similar to one group or another. As is the case for the teleosts, we found only one study experimentally addressing this issue (Piekarski and Olsson, 2014). In it, the authors used embryos of Mexican axolotl (*Ambystoma mexicanum*) and performed two labelling techniques, DiI fluorescein dextran marker injection and cell transplantation using GFP transgenic embryos. Using these, they labelled individual somites and observe their fate in the vertebrae. They found that, like other vertebrates, one somite contributed cells to just one vertebra, but contrary to the zebrafish, in a strict manner such as in the chicken. They observed that the posterior half of one vertebra and the anterior half of another adjacent one are both derived from the same somite (Piekarski and Olsson, 2014). Whether being leaky or strict, the truth is that the phenomenon we refer to as "Resegmentation" seems to be a conserved feature among various groups of vertebrates.

5 Vertebral body formation

How then are vertebrae formed through the collaboration of two such different structures ? Well, like being a child of two parents, its biology and upbringing will depend, amongst other things, on the role and preponderance of each parent. The father's brown eyes might be dominant and pass on to the child or he or she could have inherited the mother's fondness for talking. In the same way, this difference in the importance of the "parent" structure, in this case the notochord and the somites, will define the processing of vertebrae formation. And in this lie the big differences on this process between different species.

5.1 Vertebral body formation in the zebrafish

Zebrafish vertebral bodies are composed of an inner chordacentrum formed by mineralization of the notochordal sheath by the chordoblasts, and a peripheral perichordal centrum, dependent on sclerotome cells. It is in the formation of the chordacentrum that we see that, in the case of the zebrafish vertebral body, contrary to the chicken (or maybe not so much as we will later see) we observe a bigger preponderance of the "notochord parent".

At the end of the 1990s and start of the 2000s, the works previously performed in avian and mammalian embryos had established the resegmentation model and the importance of the sclerotome for the segmentation signal of vertebral bodies (Fleming et al., 2001; Grotmol et al., 2003). However, the discovery of the "leaky resegmentation" (see above) on the zebrafish and the much smaller sclerotome size of teleost embryos lead researchers to propose that other structures might be more important for this process. Additionally, there was the discovery of the *fused somites* (*fss*) mutant, in which somite boundaries did not form due to incorrect AP patterning of the somites (van Eeden et al., 1996). When the vertebral column of these mutants was analyzed, there were fusions of haemal arches, but the vertebral bodies were surprisingly normal (Fleming et al., 2004; van Eeden et al., 1996). Due to its role in chondrogenesis and sclerotome induction, the notochord was then suggested to have a major contribution to the process of vertebral body segmentation (Fleming et al., 2001). Several works discovered that this was in fact true. Firstly, in Atlantic salmon (*Salmo salar*) it was discovered that the process of vertebral body formation started with the formation of rings of chordoblasts (Grotmol et

al., 2003), the cells of the outer layer of the notochord that form the notochordal sheath (see above). These rings mark the position of the future vertebral body. Subsequent mineralization within the notochordal sheath in these rings originates the *chordacentra*. It is only then that sclerotome cells migrate to the surface of the chordacentra, differentiating into osteoblasts and forming the perichondral *autocentra* using the previously mineralized chordacentra locations as foundations. These findings were found to be true also for the zebrafish embryos (Fleming et al., 2004). Additionally, these authors discovered that laser ablation of notochord cells at specific positions blocked formation of vertebral bodies. Several works that followed supported the importance of the notochord for vertebral body formation in teleosts: In salmon (Grotmol et al., 2005) it was observed that segmented expression of alkaline phosphatase (ALP) in the notochord occurs at the same time as mineralization of the notochordal sheath and matches with future location of the vertebral bodies. This expression is never seen at this time in the sclerotomal cells. Additionally in salmon the notochord was found to not only produce and maintain the notochordal sheath, but also transcription factors responsible for mineralization and skeletogenesis (Wang et al., 2013). In zebrafish (Bensimon-Brito et al., 2012), mineralization of all vertebrae except the caudal fin ones, was observed to start also as a ring within the notochordal sheath. Like for the salmon, expression of ALP was observed in the mineralizing sheath, along with other factors such as Collagen type II and Osteocalcin, usually expressed in skeletogenic cells. The zebrafish gene for Entpd5 (ectonucleoside triphosphate/diphosphohydrolase 5) (Huitema et al., 2012) was shown to be expressed in a segmented pattern in the notochordal sheath cells, before the beginning of its mineralization (Lleras Forero et al., 2018). Additionally, this expression coincided with the locations where mineralization occurs and was appeared, even when there were disruptions on the segmentation clock. This suggested that vertebral body segmentation is independent on somite segmentation. Another study using zebrafish published in the same year (Wopat et al., 2018), showed that other genes, besides *entpd5* had segmented expression patterns. This work also demonstrated that these patterns corresponded to the future mineralized vertebral body and cartilage-like intervertebral disc domains. They demonstrated the sequential process of vertebral body formation, from the formation of mineralizing and non-mineralizing domains of the notochordal sheath, to the recruitment of osteoblasts to the surface of the mineralized sheath. As for the signaling cascade required for the molecular segmentation of the notochord, it was shown that, at least Notch and RA signaling are important (Pogoda et al., 2018; Wopat et al., 2018).

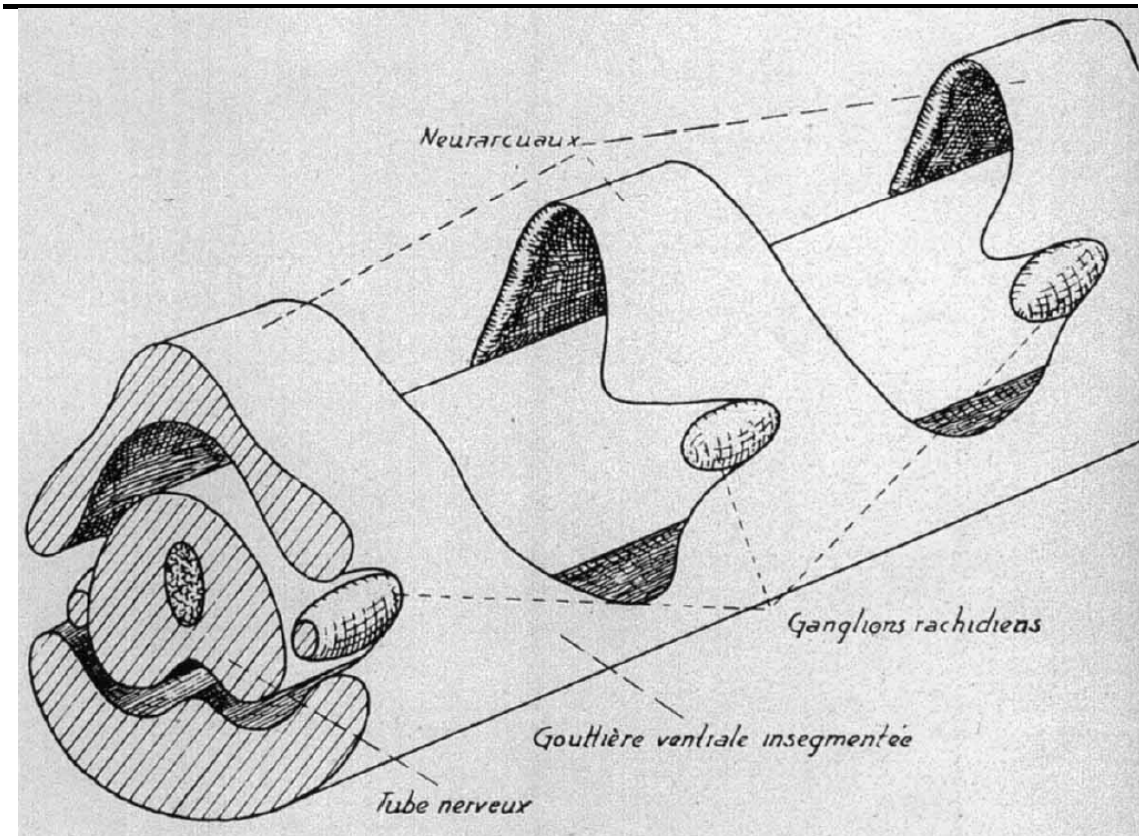

Figure 1.8 Result of notochord removal experiments.
Schematic representation of the results obtained by Strudel (1955) after removal of the notochord. Instead of segmented vertebral bodies, an unsegmented row of cartilage forms in operated embryos. Adapted from (Strudel, 1955)

5.2 Vertebral body formation in the chicken

As referred earlier, the vertebral bodies in the chicken embryo derive from the ventral sclerotome. If in the zebrafish it is clear that the signal to form segmented vertebral bodies comes from the nothocordal sheath chordoblasts, in the chicken embryo, and despite all the works performed, this is still not clear. Classically it is thought that the AP polarity of the somite and the consequent subdivision into both halves of the sclerotome into non-miscible units (Stern and Keynes, 1987), along with phenomenon of resegmentation is sufficient to confer the segmented signal for separate vertebrae formation (Senthinathan et al., 2012). However, in Mesp1/2 and Ripply1/ mutant mice, in which AP polarity is disrupted, the pattern of the vertebral bodies is disrupted, although it did not completely disappear (Takahashi et al., 2013). This suggests that other factors might be necessary for vertebral body segmentation. Could the notochord have a function in this process like it has in teleosts ? Consistent with this hypothesis, surgical removal

of the notochord (Strudel, 1955; Watterson et al., 1954) yielded embryos with an unsegmented rod of cartilage instead of the segmented vertebral bodies, with no formation of intervertebral discs (Figure1.8). Curiously, in these embryos the neural arches were normally segmented. On the other hand, in another study in which the notochord was removed, the authors observed no disruption of the segmented pattern of PAX1 expression in most of the sclerotome, although with exception of the most ventral portion (Senthinathan et al., 2012).

Since the vertebral and muscle segments are shifted by half a segment, could it be that segmentation of the vertebral bodies might have some influence by the muscle components of the somite ? Mouse mutant embryos for Myf-5 (Braun et al., 1992) showed absence of the major distal part of the ribs and mutants for both Myf5 and MyoD (Rot-Nikcevic et al., 2006) revealed several skeletal defects, including fusion of vertebrae. Both genes are part of the myogenic regulatory factor (MRF) family, known to be essential for muscle development (Rudnicki and Jaenisch, 1995).

5.3 What underlies the evolutionary difference between segmented vertebral body formation in teleosts and avians ?

We have thus seen that the cells and the corresponding signals that begin the formation of separate vertebral bodies have different locations in anamniotes like the zebrafish and amniotes like the chicken. In zebrafish, as well as some other teleosts, they are located within the notochordal sheath, while in the chicken, these cells are now found in the most medial ventral sclerotome, although the notochord might have conserved some of that signaling. Could these cells have been somehow co-opted from the notochord to the ventral somite/sclerotome during evolution ? And, if so, how could have this happened ? While this may at first sound like a far-fetched hypothesis, if we think about it, there are already some clues that this could be true: 1) As referred earlier, the notochord and somite/sclerotome have changed their sizes in an inverse proportion, almost as if the former is losing cells as the latter is gaining them; 2) There are remarkable similarities between the notochord and cartilage tissues (Huysseune et al., 2010; Pais de Azevedo et al., 2012; Stemple, 2005): These include the expression of common genes such as type II Collagen, Aggrecan, Sox9 or Chondromodulin (Dietz et al., 1999; Sachdev et al., 2001; Zhao et al., 1997). The study of the gene regulatory network of both tissues has led some authors to propose that they have a common evolutionary origin (Cole,

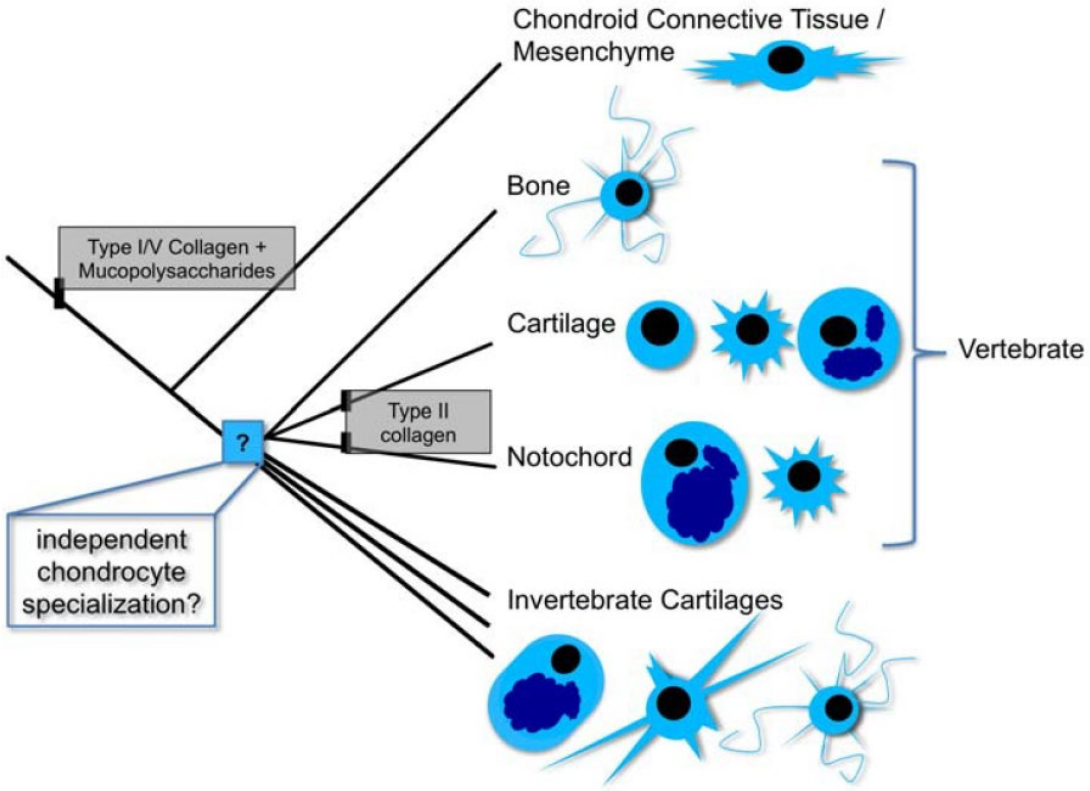

Figure 1.9 Schematic representation of the proposed evolutionary relationship between various connective tissues.
The suggested relationships between different tissues are based on features such as common expression of genes such as type II Collagen. In this model, the notochord is seen as evolutionarily related to cartilage and bone. Adapted from (Cole, 2011)

2011) (Figure 1.9). There are also the interesting on knife fish (*Eigenmannia virescens*), a species in which the notochord persists on its tail. When amputated, the tail regenerates, but the notochord is replaced with cartilage (Kirschbaum and Meunier, 1981). 3) In chicken embryos, as we will see later, the notochord and the medial part of the PSM (which will give rise to the ventromedial sclerotome) derive from the same region in Hensen's node (HN) (Selleck and Stern, 1991; Solovieva et al., 2022).

If indeed the cells responsible for the vertebral body segmented signal in zebrafish are evolutionarily related to the ones in the chicken, but are just located in different structures, how could have this have occurred during evolution ? How can we then shed some light into these questions ? Well, one thing we learned from any good superhero comic book or movie is to always show the main character's origin story order to better understand his behavior and personality. So too we must search for the origin of the notochord and somites to helps us better understand the role they had in these possible

evolutionary changes. This is done by going to the early stages of development and looking for the progenitor cells that will give rise to each of these structures.

6 Somite and notochord origin

Where do then the notochord and somite cells come from and how do they end up forming their respective structures ? The path of a cell from an initial stem state to a fully differentiated part of a tissue or structure can be compared with the path of a human, from birth to adulthood. Imagine one of these cells as a baby that has just been born, with a bright future up ahead that could one day become such different things a painter, an accountant or even a scientist. That baby is one of the first few cells of every animal and, very early in its life, it will have one of the most important times of his life (as the great Lewis Wolpert once said) - gastrulation

6.1 Gastrulation and progenitor cell location

The famous Lewis Wolpert sentence is indeed very true, as it is during this period that some of the most important transformations of the embryo take place. These include, for example, the establishment of the three embryonic axes: the antero-posterior (AP), the dorso-ventral (DV) and the left-right (LR). Another important event that occurs during gastrulation is the formation of the organizer (Martinez Arias and Steventon, 2018; Spemann and Mangold, 1924), a structure that contains a group of cells that has the ability to induce neighboring cells into a certain developmental fate. When transplanted, the organizer has the capability of inducing a whole embryonic axis, as demonstrated by the brilliant experiments by Spemann and Mangold with newt embryos (Spemann and Mangold, 1924), one of the most fascinating and important discoveries of developmental biology. What then is gastrulation and when does it happen ? After the first cleavages occur, the embryo is now a mass of undifferentiated cells called blastoderm with two layers of cells, the epiblast, and the hypoblast. Gastrulation is the process by which these two layers of cells give rise to the three embryonic layers, ectoderm, mesoderm, and endoderm, from which all embryonic tissues will derive. Once again, anamniotes like the zebrafish and *Xenopus* do so in a different manner than amniotes like the chicken and mouse.

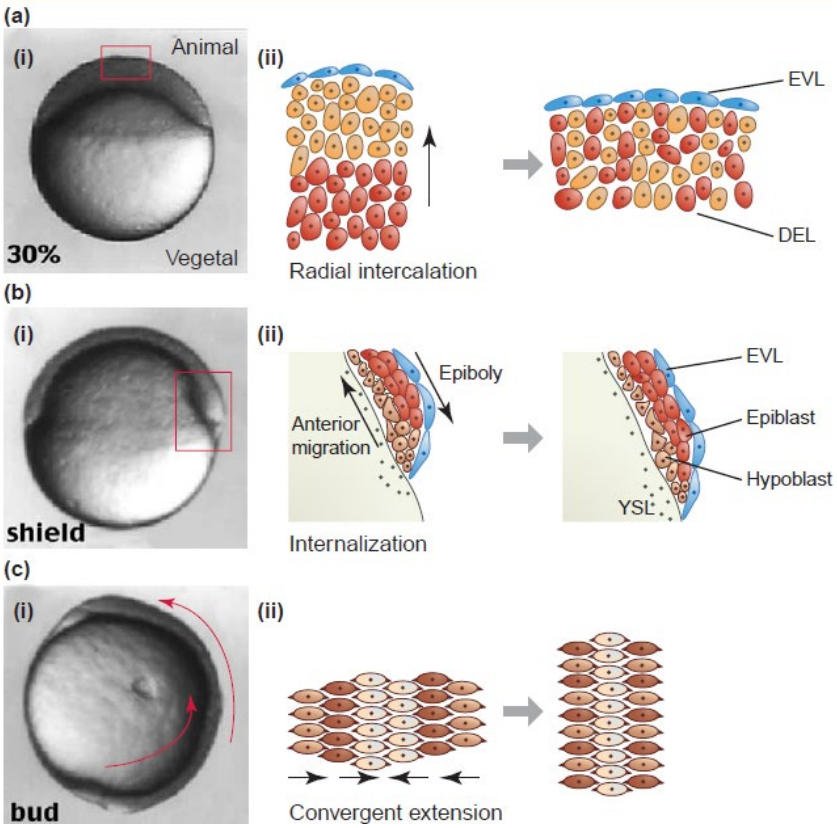

Figure 1.10 The three types of movements that occur during zebrafish gastrulation
The embryonic location where each movement is taking place is shown in (i) and the schematic representation of the corresponding movement is shown in (ii) (A) At 30% epiboly, radial cell intercalation drives epiboly of the DL. (B) At shield stage, mesendodermal forming the hypoblast cells start to internalize. (C) Convergent extension of mesendoderm progenitors leads to early elongation of the forming body axis. EVL – Enveloping layer, DEL – Deep layer Adapted from (Montero and Heisenberg, 2004)

6.1.1 Gastrulation and notochord/somite progenitor location in the zebrafish

In the zebrafish embryo, the blastoderm is a large cellular mass sitting atop the yolk and is composed of three layers (Barresi, 2020; Rohde and Heisenberg, 2007): An outer epithelial monolayer called the enveloping layer (EVL), the yolk syncytial layer (YSL), a ring of nuclei that is formed from the fusion of marginal blastomeres at the vegetal pole to the yolk cell and the deep layer (DL) formed by the majority of blastomeres and which will give rise to the embryo proper. Gastrulation in the zebrafish is a process composed of several events with its different cell movements (Montero and Heisenberg, 2004; Warga and Kimmel, 1990): All three layers initiate movements of epiboly around the yolk, with the DL cells doing so, thanks to Radial intercalation. When that epiboly reaches around 50%, the DL cells begin to form the three germ layers (Figure 1.10). These cells start to accumulate in the marginal zone of the blastoderm all around the yolk forming the germ ring. Here, two layers of cells are formed: The first is composed

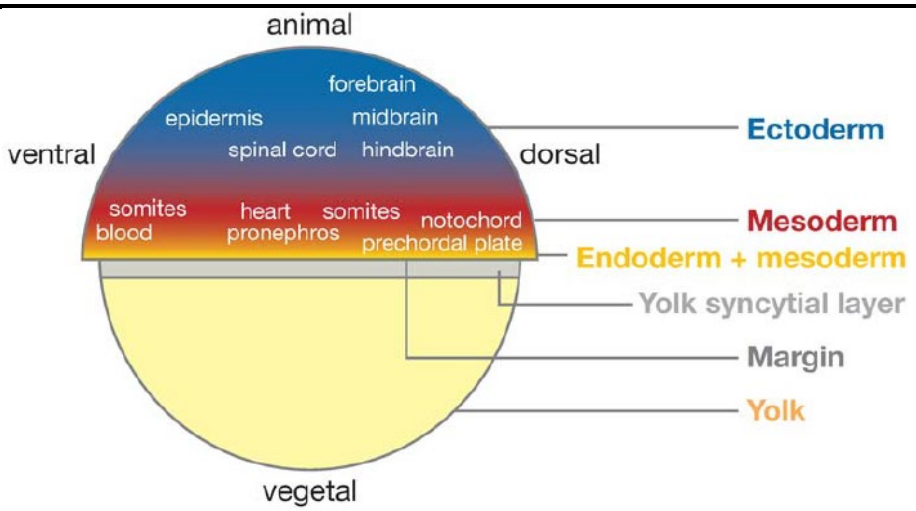

Figure 1.11 Zebrafish fate map at 50% epiboly.
Although the germ layers are arranged along the DV axis, there is a considerable overlap between different presumptive tissue territories due to frequent intermingling of progenitor cells. Adapted from (Schier and Talbot, 2005)

of the mesendodermal progenitors that form the hypoblast, which will later give rise to the mesoderm and endoderm. The second layer is formed by the epiblast, that will form the ectoderm. These cells do not internalize and, thus, the hypoblast ends up located bellow the epiblast (Figure 1.10). The next and final movement cells from both layers undergo mediolateral cell intercalations that lead to convergence toward the dorsal side of the embryo and extension of the AP axis (Schmitz and Campos-Ortega, 1994). This also leads to the formation of the zebrafish's organizer, the shield (Koshida et al., 1998; Schmitz and Campos-Ortega, 1994; Shih and Fraser, 1995; Shih and Fraser, 1996). During gastrulation, where do the cells that will form the notochord and somites come from ? This question is not easy to answer: First, it is only at mid/late gastrula stages that cells begin to commit to a particular fate (Ho and Kane, 1990; Schier and Talbot, 2005). Second, a fate map at the onset of gastrulation does not have defined borders (Figure 1.11) do Schier2005), as there is intermingling between different progenitor cells and, consequently, overlap (Figure 1.11) (Kimmel et al., 1990; Schier and Talbot, 2005). Despite this, two studies produced a detailed fate map of the shield and found some interesting information that sheds some light into this subject (Shih and Fraser, 1995; Shih and Fraser, 1996): The majority of the notochord progenitors were located in the dorsal midline, being flanked on either side by the somitic progenitors. Despite this, they also found that, besides the notochord, other progenitor cells originating from the shield, including somite, neural and endoderm. A later study (Melby et al., 1996) did not confirm

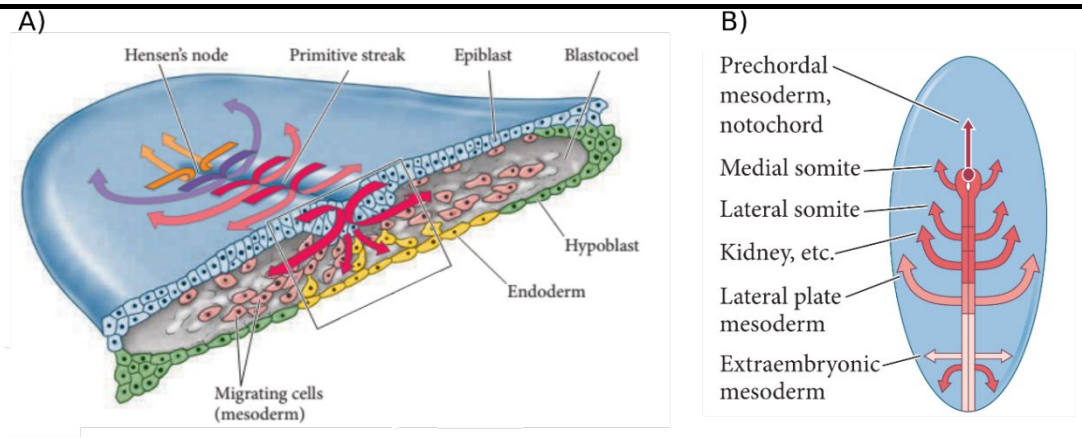

Figure 1.12 Gastrulation and mesoderm fate in the chicken embryo.
(A) Scheme depicting the formation of the three embryonic germ layers (ectoderm, mesoderm, and endoderm). This occurs due to migration of epiblast cells through Hensen's node and the primitive streak. (B) Fate of the migrating mesoderm cells depends on the AP axial level at which the cells migrate. Adapted from (Barresi, 2020; Rohde and Heisenberg, 2007)

that neural cells also originate from the shield, but nevertheless, they observed that cells in the notochord-forming domain in the shield also originate trunk somite/muscle. They also observed a very close proximity between shield cells that originate notochord and trunk somite/muscle.

6.1.2 Gastrulation and notochord/somite progenitor location in the chicken

In the chicken blastoderm, there are two areas, the centrally located *area pellucida*, from where the embryo proper will be formed and the peripheral *area opaca*. It is in the former that gastrulation begins with the formation of the primitive streak (PS) (Barresi, 2020). This structure is formed from a local thickening of epiblast cells called Koller's sickle and the epiblast cells located above it. These cells start to digest the extracellular matrix located bellow them and extend in the AP axis. This is carried out through a combination of movements like cell intercalation (Lawson and Schoenwolf, 2001; Voiculescu et al., 2007) and oriented cell division (Wei and Mikawa, 2000). At its anterior tip, a very important structure is formed, Hensen's node (HN) (called just node in the mouse embryo), which will serve as the chicken embryo's organizer (Waddington, 1932). After the streak reaches its full extension, epiblast cells start to undergo EMT and ingress ventrally migrating in several directions (Figure 1.12 A). This migration is done both through HN as well as through the streak. What is especially interesting in this migration is that there is a correspondence between the AP position where the mesoderm cells ingress and the ML structure they will be part of (Schoenwolf et al., 1992) (Figure

12 B.) Cells from the notochord and medial half of the somite originate from the anterior portion of HN (Selleck and Stern, 1991; Selleck and Stern, 1992). The next cells to migrate are the lateral somite, heart, and kidneys, that do so through the middle of the primitive streak region located caudally to HN. Finally, the lateral plate and extraembryonic mesoderm cells migrate through the posterior portion of the PS (Schoenwolf et al., 1992).

Regarding the medial somite cells and the notochord, although both come from the anterior portion of HN, they do so from different regions. The notochord derives from a V shaped area at the anterior tip of the node and medial somite cells from the two locations immediately adjacent to that V-shaped region (Figure 1.13). It is also described that there is an overlap in these two regions, where cells located therein can originate the two structures (Selleck and Stern, 1991; Selleck and Stern, 1992). The origin of the medial somite cells was later confirmed to be true for all levels of the paraxial mesoderm (Iimura et al., 2007). A very recent work (Solovieva et al., 2022) not only confirms that the anterior portion of HN gives rise to somite and notochord cells but describes the existence therein of a stem cell niche.

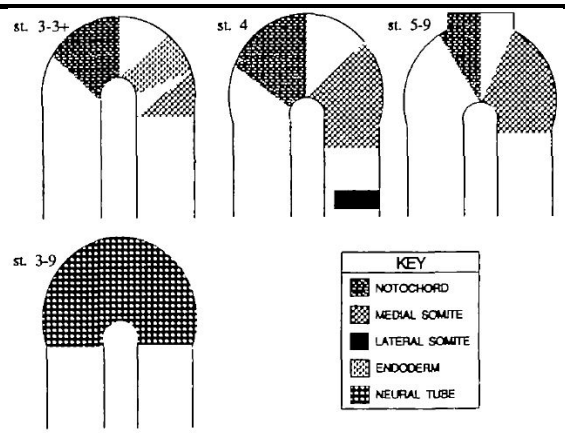

Figure 1.13 Fate map of Hensen's node at stages HH3-9, produced from cell labelling.
The three top drawings represent the fate of the mesoderm and endoderm cells of the different areas of Hensen's node. The regions corresponding to the notochord and medial somite are represented on one side only, although they are bilaterally symmetrical. Especially interesting are the proximity and overlap of the notochord and medial somite territories. The single bottom drawing pertains to the fate of the neural tube specifically. Adapted from (Selleck and Stern, 1991).

At later stages, when located in the tailbud (Le Douarin and Halpern, 2000; Teillet et al., 1998), HN is referred to as chordoneural hinge (CNH) (Catala et al. 1995, Pasteels, 1937). This region was thoroughly studied at 5-6 somite stages in a seminal work (Charrier et al., 1999) and found to be functionally and molecularly subdivided in three zones (Figure

1.14): Zone a corresponds to the rostral portion the CNH, where cells have already committed to a notochord or floor plate fate; zone b to the middle, with cells that are becoming committed to their respective fates; and zone c, corresponding to the most caudal portion where cell commitment has not yet occurred. This zone, together with the anterior tip of the PS, forms the axial-paraxial hinge (APH), which was found to be capable of originating both axial and paraxial derivate cells.

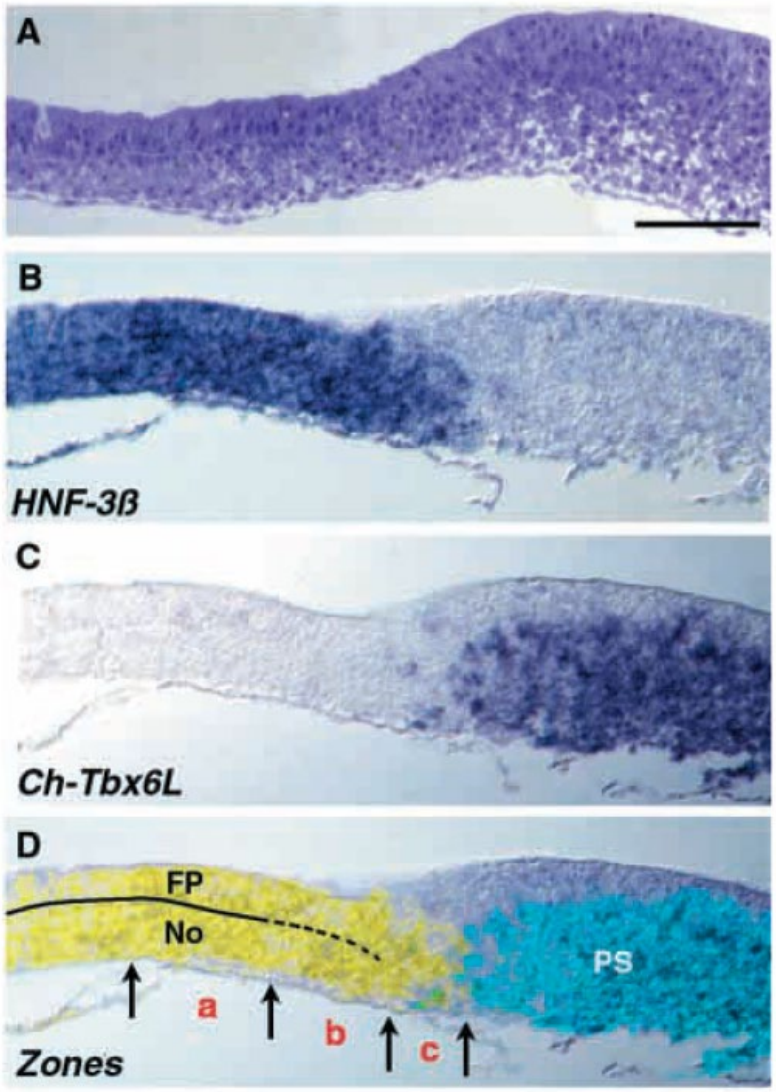

Figure 1.14 The three areas of Hensen's node region.
(A) Sagittal 1 mm section of an HH8+ to HH9- chicken embryo showing cellular arrangement. (B-C) sagittal 7mm consecutive serial sections of the embryo in A or similar, showing expression of FOXA2 (at this time designated HNF3-β) (B) and TBX6L (C). (D) Superimposition of the expression patterns in (B) and (C). The combined analysis of the cellular disposition and the expression patterns allows the establishment of the three Hensen's node zones: Zone a corresponds to the territory of expression of FOXA2 with separation of the floor plate (FP) and notochord (No) by a basement membrane; Zone b containing the core of the node, without separation of the dorsal and ventral portions; and Zone c where the expression pattern of FOXA2 ends, being in close proximity to the TBX6L primitive streak (PS) expressing domain. Scale bar: 100µm. Adapted from (Charrier et al., 1999)

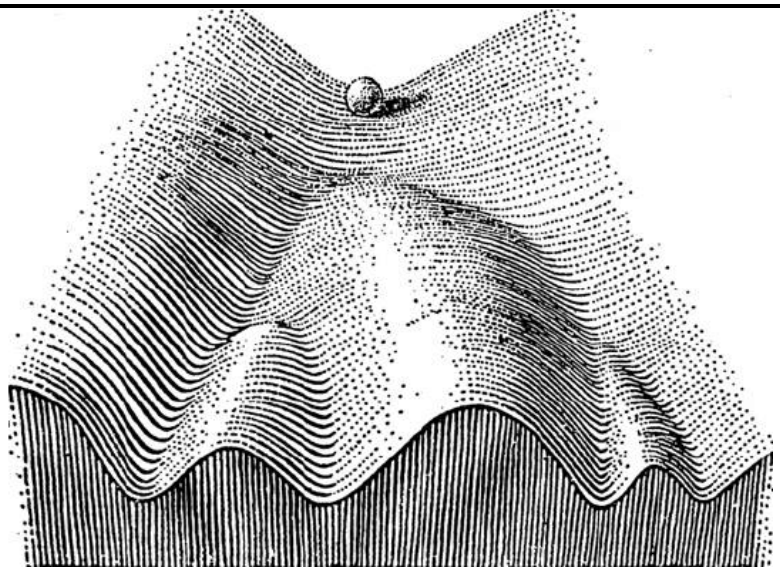

Figure 1.15 Representation of the original drawing of Waddington's epigenetic landscape
The marble is meant to be compared to a progenitor cell. The descent of the marble through the different bifurcating valleys represents the different developmental fates a progenitor cell can progressively commit to. Adapted from (Waddington, 1957)

6.1.3 Notochord/somite progenitor proximity

As described, both in zebrafish and chicken, the regions containing axial and paraxial mesoderm progenitors are located in very close proximity or even overlapping one another. This is also observed in other species: In mouse E8.5 embryos, the interface between the node and the PS is called the node-streak border (NSB) (Wymeersch et al., 2021) and is the equivalent of the APH. This region contains both notochord (ventrally located) and somite (dorsally located) progenitor cells (Cambray and Wilson, 2007). In *Xenopus*, the dorsal portion of the late blastopore lip (stage 13) (Nieuwkoop et al., 2020) originates notochord cells, while the lateral region gives rise to somite precursor cells (Gont et al., 1993), while in blastula stage (stage 6), both notochord and somites arise from common blastomeres (Lane and Smith, 1999).

As we have seen, the cells that will form the notochord and the somites come from different but very close places in the early embryo and this has a major influence on their fate. Continuing with our metaphor of the babies that were born before gastrulation, these babies are now a child growing up and the environment where they do so is very important, as it will define who they will be in the future as adults. We can recall the concept of Waddington's landscape (Figure 1.15) (Waddington, 1957; Wang et al., 2011). In this framework, the path of a cell during development is compared to a marble descending a landscape through a series of valleys. Frequently these valleys branch into two paths, with the cell following one and not the other, which represents the cell fate

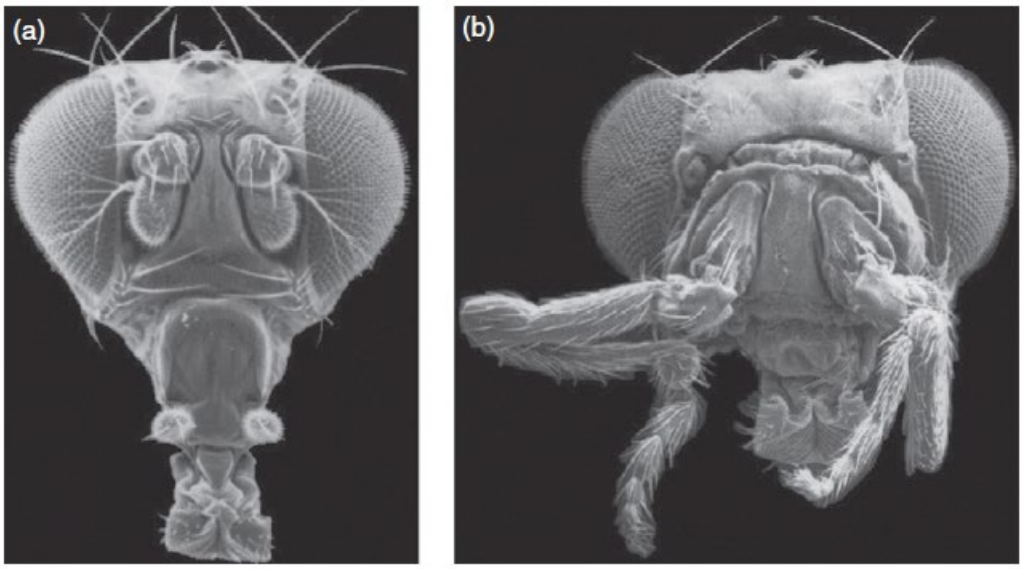

Figure 1.16 Scanning electron micrographs of heads of Drosophila melanogaster adults.
(A) Wild-type head showing the presence of normal antennae in its expected location. (B) Antennapedia mutant head showing a homeotic transformation of antennae into legs. Adapted from (Bürglin, 2013)

decision and increase commitment of a certain fate. What makes the marble, or the child choose each path and not the other ?

6.2 Progenitor specification

It has long been known that certain genes have a very important role in establishing the fate of progenitor cells in early embryos. This knowledge came in part from the discovery of homeotic transformations (McGinnis, 1994). Homeosis is defined in the Brenner's Encyclopedia of Genetics as "something has been changed into the likeness of something else." (Bürglin, 2013). Indeed, mutations in which certain structures transform into other structures helped establish the role of the corresponding genes in the structure's development. Notable examples include the *Antennapedia* (*Antp*) mutant flies, where antennae are replaced with legs (Schneuwly et al., 1987) (Figure 1.16), that led to the description of the role of this homeobox gene in the formation of leg segments during *Drosophila* development. Another well-known example is the Homeobox (hox) gene code (Weldon and Munsterberg, 2021) and its importance for the identity of segments, specifically of somites and vertebrae in vertebrate animals.

These genes are usually expressed in specific progenitor cells, defining their future identity. This can be assessed by several techniques, including: fate map studies where cells and their descendants are followed throughout development, revealing the structure

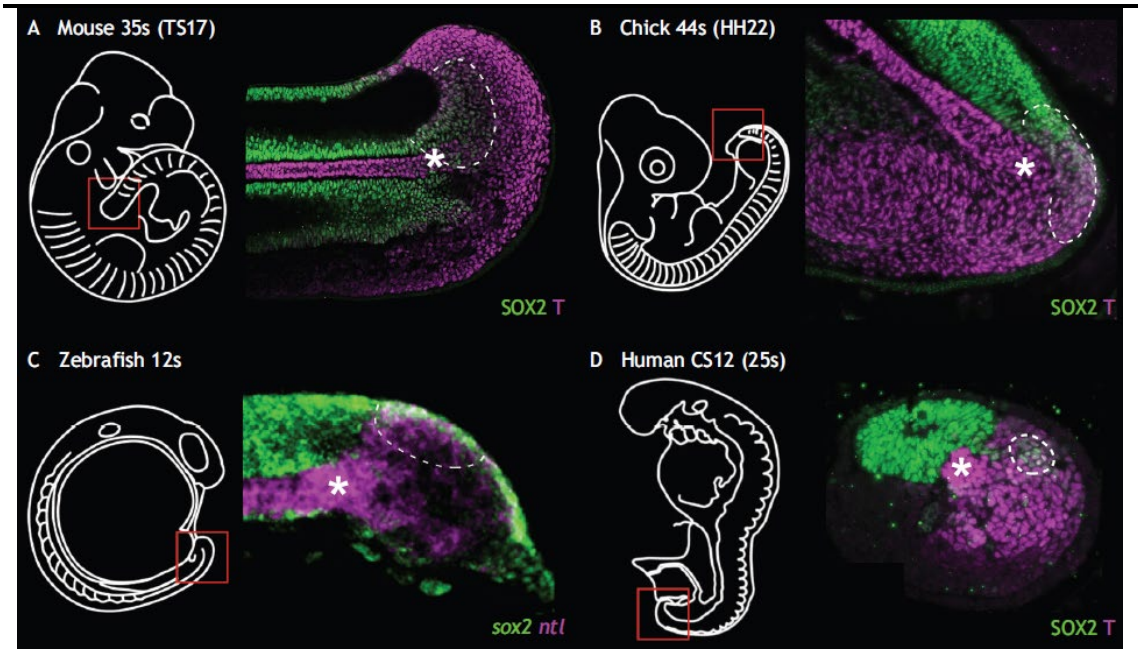

Figure 1.17 Micrographs of the tailbuds of different vertebrate embryos showing the location of the Neuromesodermal progenitor cells
(A) Mouse 35 somite stage embryo (B) Chicken 44 somite stage embryo (C) Zebrafish 12 somite stage embryo (D) Human 25 somite stage embryo. All four images are taken from the posterior tip of the tailbud, represented inside a red square. In all embryos, there is an area (shown inside dashed circle lines) where both the markers for neural and mesodermal progenitors (SOX2 and T, respectively) are expressed. The white asterisks mark the posterior end of the notochord in all images. Adapted from (Wymeersch et al., 2021).

they will belong to; heterotopic studies, where cells are transplanted to a new environment where they keep their fate or adopt a new one, revealing their potency; and retrospective clonal analysis (Bonnerot and Nicolas, 1993; Meilhac et al., 2003), a technique that allows analysis of progeny of single cells. Since this technique finds the clones of each labelled cells, it allows for the identification of progenitors that belong to one region or structure but are commonly descendant of a progenitor that belongs to another region or structure. This allowed for the discovery (Tzouanacou et al., 2009) of an area in the tailbud of the mouse embryo that contains progenitor cells that can originate both mesoderm and neural ectoderm. Since then, these neuromesodermal progenitors (NMPS) have been found in different species like zebrafish (Martin, 2016; Martin and Kimelman, 2012; Row et al., 2016), chicken (Guillot et al., 2021), and human (Olivera-Martinez et al., 2012), and the genes that are needed to be expressed for each cell fate are being explored. As a brief reference of this subject we will give just a few examples, since this is an ongoing topic in research with already a lot of information to summarize here. Mesoderm progenitors express T and neural ectoderm ones express Sox2, with the NMPs being cells that are both T and Sox2 positive (Figure 1.17) (Wymeersch et al., 2021). When focusing

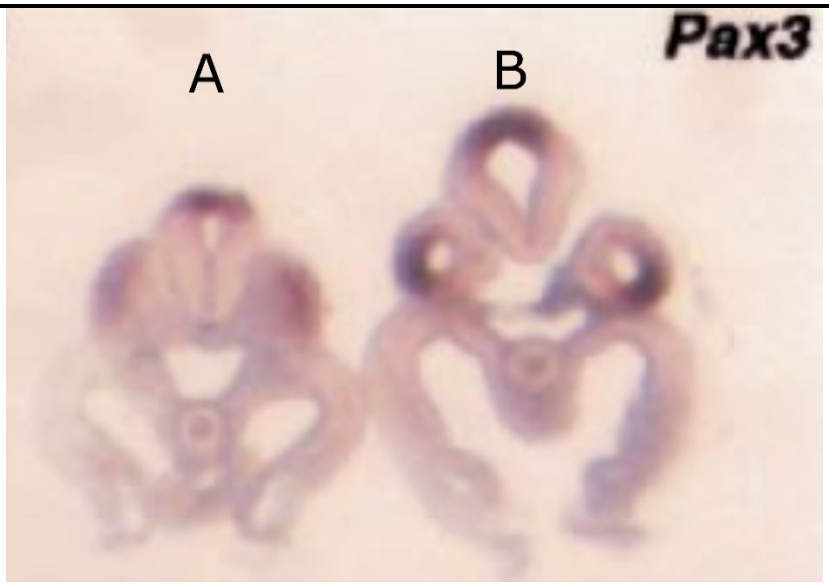

Figure 1.18 Transverse sections of WT and Tbx6 mutant e10.5 mouse embryos.
(A) Transverse section of a WT mouse embryo showing one medially located neural tube flanked by a pair of somites on each side. (B) Transverse section of a Tbx6 mutant mouse embryo showing transformation of the two rows of somites in two neural tubes. Expression of Pax3 is shown in each embryo. Adapted from (Chapman and Papaioannou, 1998).

specifically on the notochord, somites and neural tube, there were several mutations that produce homeotic transformations: One of the most cited ones is the mutant mouse for T-Box transcription factor 6 (*Tbx6)*, where posterior paraxial tissue does not form and instead flanking the normal axially located neural tube are two other neural tubes, with dorsoventral patterning (Chapman and Papaioannou, 1998) Figure 1.18. Two other examples include the mouse mutant for *Wnt3a*, that lack posterior paraxial mesoderm and showed a duplicate neural tube bellow the normal one (Takada et al., 1994). On the other hand, an increase in *Msgn1* expression leads to a decrease in neural tube size and to the restitution of paraxial mesoderm in *Wnt3a* mutants (Chalamalasetty et al., 2014). Together, these and other works helped establish the role of these three genes in the paraxial mesodermal cascade: *Wnt3a* maintains mesoderm progenitors and later activates *Msgn1*, that initiates the PSM genetic program, leading to, among others, expression of *Tbx6* and repression of neural fate (Chalamalasetty et al., 2014) (Figure 1.19).

When looking more specifically to genes that could produce homeotic transformations between notochord and somites, the orthologs of two interacting genes show very interesting expression patterns and mutation phenotypes: CNOT2 and TBX6L.

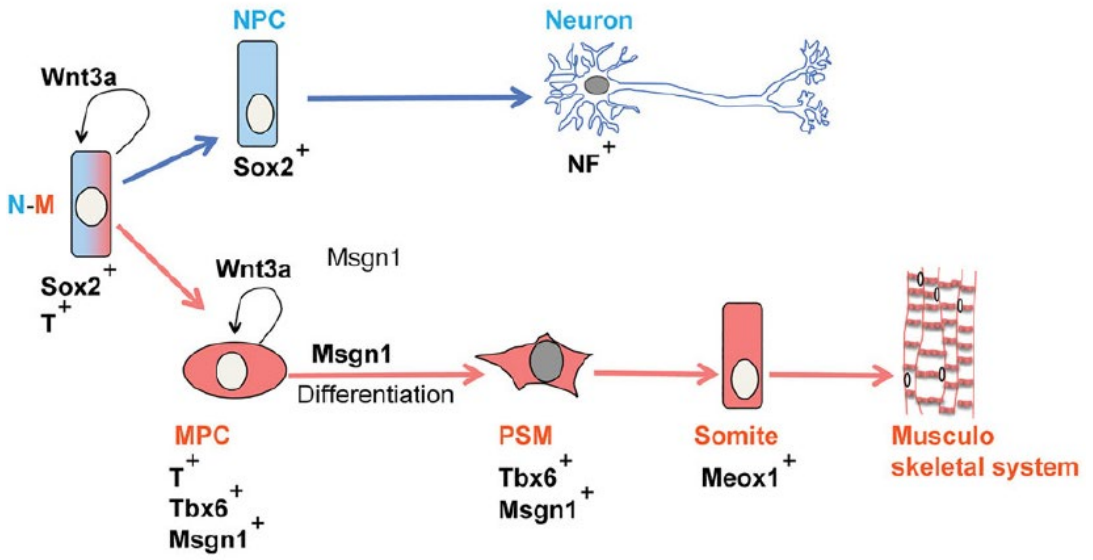

Figure 1.19 Neuromesodermal cascade leading NMPs to neural or muscle fate.
Bipotential progenitor cells express both Sox2 and T. Depending on the expression of genes like Msgn1, different genetic programs are activated, leading to neural or mesodermal cell fates. Adapted from (Chalamalasetty et al., 2014).

6.3 CNOT2 and its gene family are regulators of notochord specification

CNOT2 (Stein et al., 1996b) is a homeobox transcription factor (Lemaire and Kessel, 1997; Stein et al., 1996a) that belongs to the Antennapedia class of genes. It is part of a family that has representatives in many vertebrate animals (Plouhinec et al., 2004) such as the zebrafish *floating head* (*flh*) (Talbot et al., 1995), *Xenopus XNot1* (von Dassow et al., 1993) and *Xnot2* (Gont et al., 1993), and mouse with *Noto* (Plouhinec et al., 2004). In chicken, there is also another related gene, CNOT1 (Stein and Kessel, 1995), suggested to have appeared due to a duplication of CNOT2. From various phylogenetic analysis of this gene family, (Abdelkhalek et al., 2004; Plouhinec et al., 2004; Stein et al., 1996b) based on their sequence similarity, two groups can be formed: one containing the chicken CNOT2, the mouse *Noto* and the zebrafish *flh* and another containing both Xenopus, *Xnot1* and *Xnot2*, as well as chicken CNOT1 (Figure 1.20). It is important to refer that more recently, CNOT2, CNOT1 and *floating head* (*flh*) have changed their designation to GNOT2, GNOT1 and *notochord homeobox* (*noto*), respectively. For the purpose of this manuscript, we will use the previous designations CNOT2, CNOT1 and *flh* as these are the used ones for most of the literature cited here.

As for the expression patterns, briefly and with a few small differences, all of them are strongly expressed in the organizer in the beginning of gastrulation. Progressing in

development, in segmentation stages, it is expressed in the notochord in a decreasing anterior to posterior gradient, later on remaining expressed in the tailbud (Ranson et al., 1995; Stein and Kessel, 1995; Stein et al., 1996b; Talbot et al., 1995; von Dassow et al., 1993).

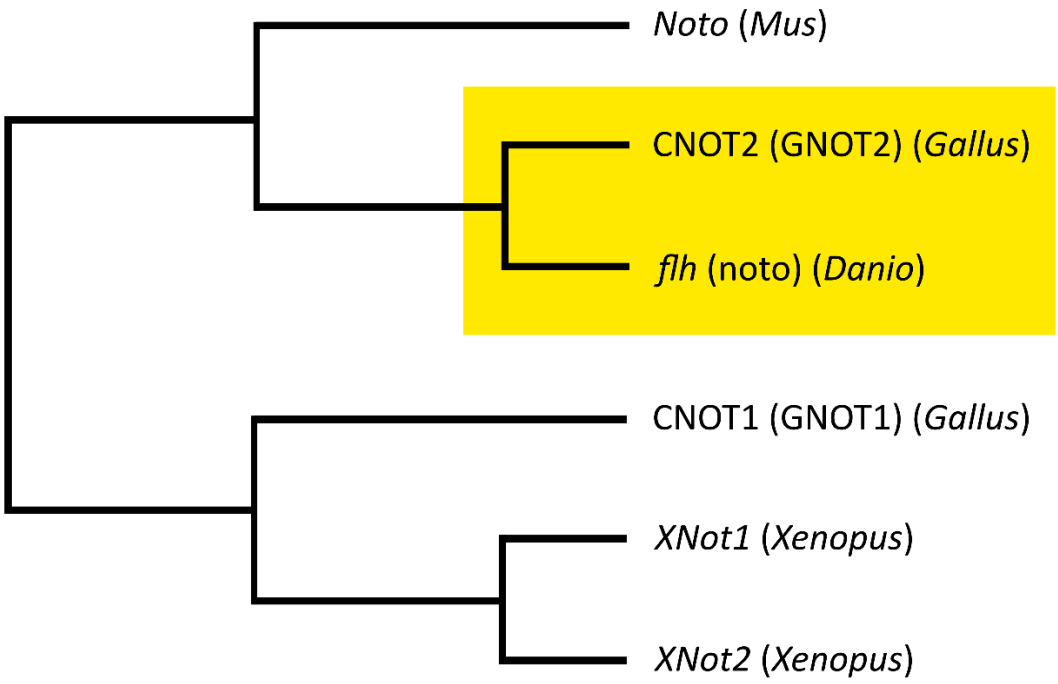

Figure 1.20 Phylogenetic relationships of Not gene family members.
Dendogram representing the relationships between Not gene family members of four vertebrate models: zebrafish (Danio rerio), african clawed frog (Xenopus laevis), chicken (Gallus gallus) and mouse (Mus musculus). This dendogram summarizes the information of the various phylogenetic trees contained in (Abdelkhalek et al., 2004; Plouhinec et al., 2004; Stein et al., 1996b). Because of the various changes to each gene's nomenclature, previous gene names are presented between brackets next to the currently accepted gene name, except for flh/noto, CNOT2/GNOT2 and CNOT1/GNOT2. For these genes, the original name is presented first, as it is the name by which it is referred to in the majority of the bibliography cited in this thesis. Highlighted in yellow are the branches containing zebrafish flh and chicken CNOT2.

One of the first hints of a role in the formation of the axial mesoderm structures, more specifically in the notochord, was in the analysis of the *floating head* zebrafish. In this mutant, the notochord was totally absent from the embryo (Talbot et al., 1995) with somites being fused in the middle. This was the reason for the mutant's curious name, as the head was "floating" by not having a notochord to be attached to. Additionally, the (ventral neural tube) floor plate of the posterior trunk and tail is shown to be only a few scattered clusters of cells. In the place where the notochord is normally located, *flh* mutants showed muscle tissue instead (Halpern et al., 1995; Talbot et al., 1995). Since

the prechordal plate was normal, as well as the derivates of the non-axial mesoderm, this mutation was considered particularly interesting as it was specific of axial mesoderm derivatives. Also, this was a very important discovery as it was the first example of a mutation that had the effect of turning the fate of cells in a determined position from one tissue to another one altogether (Halpern et al., 1995). Another additional detail is the nature of this mutation: the *notail* (*ntl*) zebrafish mutant (ortholog of Brachyury or T) shows the presence of a few axial mesoderm precursor cells that were not able to form notochord (Halpern et al., 1993). In the case of *flh*, there were no such cells present and, in their normal location, muscle tissue was found. This led the authors to suggest that the notochord precursors differentiated in muscle instead of notochord in *flh* mutants. Other experiments supported these findings (Halpern et al., 1995): When WT cells were transplanted to *flh* mutants, embryos were able to produce notochords and when *flh* mutant cells transplanted in a large number to WT embryos, they were not able to do so, producing muscle instead. Continued work on *flh* discovered that, in the dorsal marginal region of the early gastrula of zebrafish embryos, there is a domain where the majority of its cells originate notochord. This domain coincides with the expression domain of *flh* and in the *flh* mutant, these cells originate muscle fibers (Melby et al., 1996). All these lines of evidence pointed to a role of *flh* in the specification of axial progenitor cells to a notochord fate and that, in its absence, these cells respecified into a paraxial mesoderm fate and later muscle. As referred earlier, *ntl* is another gene required for formation of the notochord, as it was shown that, when mutated, embryos lack a notochord (Halpern et al., 1993; Schulte-Merker et al., 1994). As such, it was interesting to know what the interactions between these two transcription factors (*flh* and *ntl*) could be. In order to do so, the expression of one was assessed in the other's mutant (Melby et al., 1997; Talbot et al., 1995): At the beginning of gastrulation, there were no changes in their expression patterns. However, by midgastrulation, expression of both *flh* and *ntl* was reduced, but not totally absent in the axial mesoderm. This meant each gene was required for maintenance, but not initiation of the other's expression. The authors suggest that another gene then could be responsible for the initiation of expression of *flh* and *ntl*. They refer *foxa2* (at that time called *HNF-3β*), as it is required for the formation of the notochord, and expression of T (*ntl*) is totally absent *foxa2* mutants (Ang and Rossant, 1994; Weinstein et al., 1994). But the most interesting interaction discovered (Amacher and Kimmel, 1998) was with *spadetail* (*spt*) (Kimmel et al., 1989), a t-box transcription factor associated with paraxial mesoderm cell fate (ortholog of TBX6L in the chicken embryo,

see more detailed description below). In order to study the interaction between *flh* and *spt*, double mutants for both genes were produced. The phenotypes and expression patterns of several genes were studied for these double mutants, as well as for the single *flh* and *spt* ones (*flh*$^{-}$ and *spt*$^{-}$). Since the midline of *flh*$^{-}$ cells converted to a muscle fate and expressed muscle markers (see above), the first question to be asked was whether this would happen in *flh*$^{-}$;*spt*$^{-}$. Very interestingly, that was not the case. Not only no muscle cells were found in the midline of *flh*$^{-}$;*spt*$^{-}$, but *myoD* expression was irregular flanking the midline resembling *spt*$^{-}$ instead of *flh*$^{-}$. Authors concluded that for *flh*$^{-}$ to have muscle in the midline, *spt* function had to be present. Additionally, *flh*$^{-}$;*spt*$^{-}$ showed formation of differentiated notochord tissue from the hindbrain region extending to the anterior trunk. These mutants also demonstrated expression of the notochord marker *shh*, showing that loss of *spt* function leads to notochord formation, even if *flh* function is also lost. Finally, it was demonstrated that *flh*$^{-}$;*spt*$^{-}$ showed expression of *ntl* where the anterior notochord formed, with this expression being stronger than in *flh*$^{-}$. This meant that there could be some sort of repression on *ntl* by *spt* that was lifted in double mutants, allowing for expression of *ntl* even if *flh* function was not present. From all these results, a model was suggested that explains the genetic interactions in the midline of zebrafish embryos leading to the decision of progenitor cells in producing notochord or paraxial mesoderm and later somite and muscle (Amacher and Kimmel, 1998). So far, this model has been supported by following studies (He et al., 2014; Kodjabachian et al., 1999; Yamamoto et

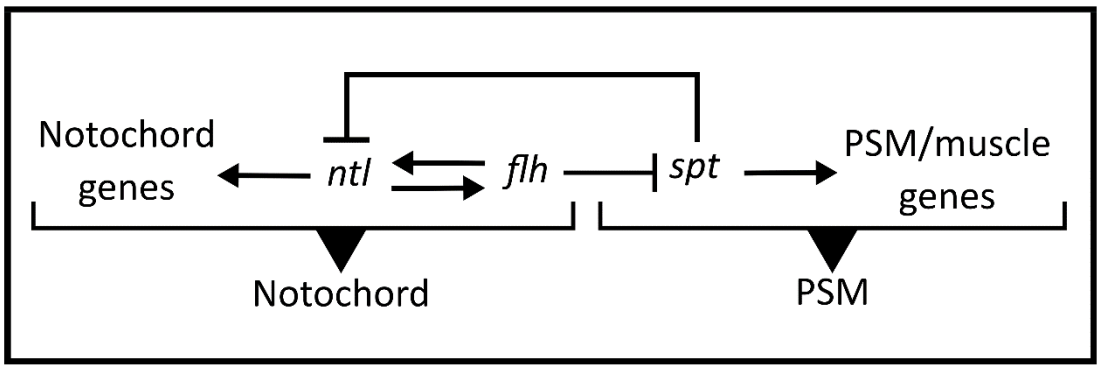

Figure 1.21 In the zebrafish, flh represses spt repression of notochord genes like ntl, leading axial/paraxial mesoderm progenitors to originate notochord.
Simplified version of proposed model for the relationship between flh and spt in the cell fate decision between notochord and PSM, based on the literature. spt is suggested to repress notochord genes like ntl and upregulate the expression of PSM/muscle genes leading to the formation of PSM progenitor cells. In notochord progenitors, flh represses spt action allowing the action of notochord genes like ntl in driving cells to a notochord fate. Additionally in these progenitors, ntl and flh are required for maintenance of each other's expression.

al., 1998) both in zebrafish and in other animal models, but not in the chicken embryo (see below) and a simplified version of it is presented here (Figure 1.21). Briefly, in the axial/paraxial mesoderm progenitors, cells can go in two separate paths: 1) *flh* expression leads to the differentiation of progenitor cells into notochord by repressing *spt*. To that end, *flh* and *ntl* cooperate in maintaining their mutual expression. 2) Conversely, in the remaining mesoderm progenitors, *spt* represses *ntl* and is not repressed by *flh*, resulting in cells forming paraxial mesoderm.

While zebrafish embryos provided a lot of information on the role of CNOT2 in notochord formation, another water-dwelling vertebrate, the *Xenopus* also provided useful data on this subject. As described earlier, there are two genes belonging to the Not family, *Xnot1* (von Dassow et al., 1993) and *Xnot2* (Gont et al., 1993). Gain-of-function studies were made where synthetic *Xnot2* m-RNA was microinjected at 4-cell stage (Gont et al., 1996). This resulted in enlarged notochords in a larger quantity of embryos if the injection was performed in the dorsal blastomeres, although a few ectopic patches of notochord were shown when the ventral blastomeres were injected. In 69% of injected embryos, there was an observable reduction of somitic tissue, leading the authors to suggest the notochord enlargement was produced at the cost of paraxial mesoderm. When lineage tracing was performed to uncover the fate of injected cells, it was confirmed that they contributed mainly to the enlarged or ectopic notochords and in a small manner to the floor plate. Another line of evidence in the *Xenopus* supports the role of *flh* in notochord formation (Yasuo and Lemaire, 2001): In embryos where BMP signaling is inhibited on its ventral side, a new secondary trunk is formed, lacking only notochord. Later on, during development, in order for this ectopic trunk to be maintained, repression of Wnt signaling is also necessary. When synthetic m-RNA of *Xnot2* was injected in these embryos, notochord formation was observed. The authors also discovered that *Xnot2* acted as a transcription repressor. Since it was previously described that *Xwnt-8* represses *Xnot2* (Hoppler and Moon, 1998), the authors (Yasuo and Lemaire, 2001) suggest that in the normal conditions, Xwnt-8 repression of Xnot2 does not occur in the notochord progenitor region through the effects of either the Wnt antagonist, *frzb* or by action of the transcription repressor *Gsc*.

Of course, no bibliographical review on CNOT2 would be complete without information collected from the mammalian ortholog, *Noto*. This member of the Not family was first discovered as being the mutated gene in the Truncate mouse mutant

(Abdelkhalek et al., 2004). This was immediately confirmed by phylogenetic analysis (Plouhinec et al., 2004). Unlike zebrafish *flh* mutants, *Noto* mutant mice showed notochord defects only in the posterior trunk and tail (posterior to the lumbar region) (Abdelkhalek et al., 2004). Also, in *T* mutants, *Noto* is not expressed and in *Noto* mutants, *T* is normally expressed. This suggests that, in mouse, *T* is necessary for the initial expression of *Noto* in the notochord. Also of interest is the absence of *Noto* expression in *Foxa2* mouse mutants (Abdelkhalek et al., 2004; Plouhinec et al., 2004). This would imply an AP regionalization of the regulation of notochord formation in mice (Figure 1.22). Confirming the existence of this regionalization, it was observed that different AP portions of the notochord of mouse embryos have different origins (Yamanaka et al., 2007): The most anterior head process originating from the most anterior cells of the node, the trunk, derived from the node and the tail coming also from the node migrating posteriorly. The same authors produced a version of the *Noto* mutant in which *eGFP* was knocked into the *Noto* locus (Abdelkhalek et al., 2004). In this mutant, this allowed them to find Noto-GFP^{+} originating from the node in the paraxial mesoderm, confirming that, just like in zebrafish mutant, progenitor cells assume a different mesodermal fate (Yamanaka et al., 2007). Since *Noto* could have the same function as *flh*, the authors

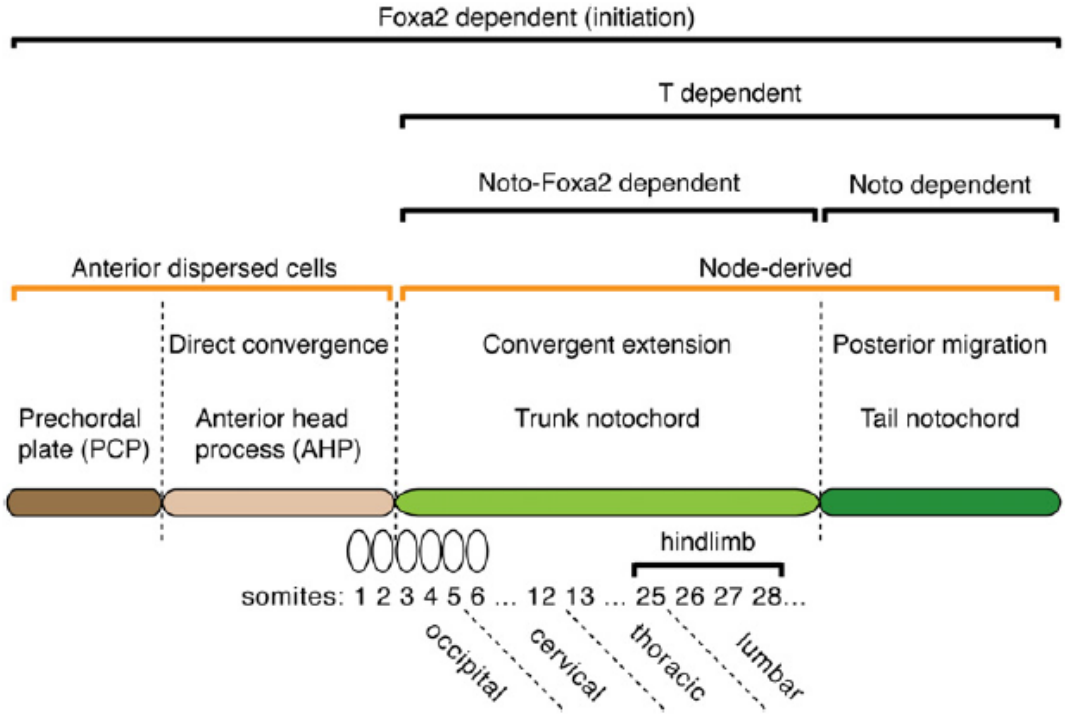

Figure 1.22 Model of the regionalization of the notochord in the mouse embryo.
In the mouse embryo, different sections of the notochord are dependent on different transcription factors. Also, different types of morphogenetic movements are necessary to form each of the different notochord portions. Adapted from (Yamanaka et al., 2007)

suggested that the lack of problems in the trunk notochord could be due to some compensation from other genes in this region. This was indeed confirmed, as it was shown that the failure to form notochord only happening in the tail was also shown in the trunk posteriorly to somites 3-4 in double *Noto Foxa2* mutants. The authors then suggested that, in the formation of the three notochord regions established by them, the middle one is dependent on both *Noto* and *Foxa2*, while the most posterior one is solely reliant on *Noto* (Yamanaka et al., 2007). Based on results from a previous study (Herrmann, 1991), they added that *T* is also needed for formation of the notochord of both of these regions.

All these examples from different vertebrate embryos clearly show that CNOT2's orthologs are very important players in the formation of axial mesoderm, especially notochord, from mesoderm progenitor cells. As stated earlier, in this decision CNOT2 seems to interact with another transcription factor which we will explore now.

6.4 TBX6L and its gene family are regulators of PSM specification

The second gene that shows an interesting potential is TBX6L, the chicken ortholog of zebrafish *spt*. As referred earlier, CNOT2's zebrafish ortholog *flh* represses *spt*, which would otherwise normally lead to formation of paraxial mesoderm.

Spadetail is a mutation on a T-box transcription factor, and it was discovered that this gene was in fact *tbx16* (Griffin et al., 1998; Ruvinsky et al., 1998). Even though this nomenclature has changed, for the purpose of this manuscript, it will still be designated *spt*, as most of the works cited here that describe its function follow this nomenclature. This gene is a member of a huge family of T-box transcription factors, characterized by the presence of the T binding domain (Wymeersch et al., 2019), first discovered in the mouse *T* (Herrmann, 1991).

In terms of orthology, there are only two other genes than are orthologs of tbx16 (Ahn et al., 2012; Griffin et al., 1998; Lardelli, 2003; Papaioannou and Silver, 1998; Ruvinsky et al., 1998): the chicken TBX6L (Knezevic et al., 1997) and Xenopus VegT (Zhang and King, 1996), also called Xombi (Lustig et al., 1996), Antipodean (Stennard et al., 1996) and Brat (Horb and Thomsen, 1997). The three genes of the three species belong to the Tbx6/16 subfamily (Ahn et al., 2012), which phylogenetically "(…) has been plagued by uncertain phylogenetic relationships among its members." to quote the author of a huge study on the phylogeny of this family (Ahn et al., 2012). Two other

members of this subfamily include the zebrafish tbx6 (Nikaido et al., 2002) and its mouse ortholog Tbx6 (Chapman and Papaioannou, 1998), as well as the zebrafish tbx6l (Hug et al., 1997). The reason these genes are mentioned here, are to provide the reader a guide to the nomenclature while searching the literature. This is necessary as these genes have changed their names and both the new and old ones might cause some confusion: Zebrafish tbx6 was formerly called tbx24 and fss (Ahn et al., 2012); the zebrafish tbx6l was formerly called tbx6 (Windner et al., 2012). Their respective relationships and designations are shown in a simplified dendrogram Figure 1.23. The reason for these confusions is the fact that the once called tbx6 had that designation because it was initially thought to be the ortholog of the mammalian Tbx6. In fact, not only is it very distant phylogenetically to mammalian Tbx6, but it is also closer to the cluster containing tbx16, TBX6L and VegT. On the other hand, tbx24/fss was found to be closer, both in sequence and function to Tbx6, which led to the change in name.

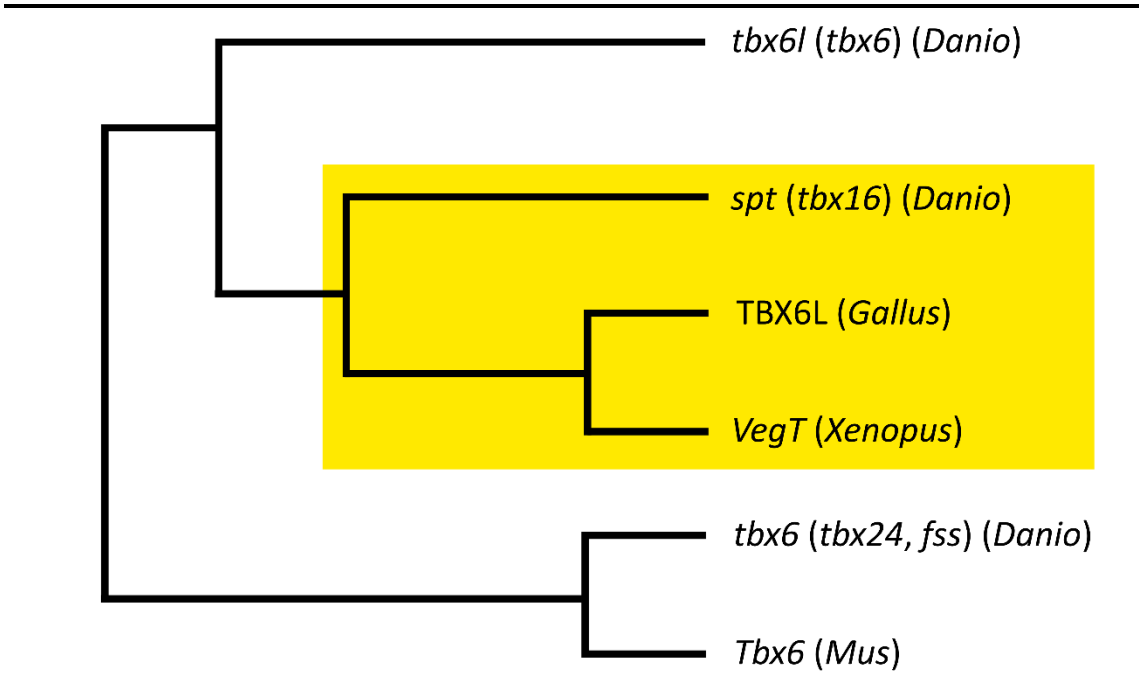

Figure 1.23 Phylogenetic relationships of Tbx6/16 gene family members.
Dendogram representing the relationships between Tbx6/16 gene family members of four vertebrate models: zebrafish (Danio rerio), african clawed frog (Xenopus laevis), chicken (Gallus gallus) and mouse (Mus musculus). This dendogram summarizes the information of the various phylogenetic trees contained in (Ahn et al., 2012; Griffin et al., 1998; Lardelli, 2003; Windner et al., 2012). Because of the various changes and similarity of each gene's nomenclature, previous gene names are presented between brackets next to the currently accepted gene name, except for spt/tbx16. For this gene, the original name is presented first, as it is the name by which it is referred to in the majority of the bibliography cited in this thesis. Highlighted in yellow are the branches containing zebrafish spt and chicken TBX6L.

Starting with zebrafish *spt*, it is expressed (Griffin et al., 1998; Ruvinsky et al., 1998) initially in all the marginal cells of the late blastula and early gastrula. As gastrulation is occurring, it loses its expression in the axial mesoderm progenitor region. Later on, during somitogenesis, it becomes restricted to paraxial and lateral mesoderm in the posterior tail area at 10-somite stage. In zebrafish *spt* mutants, trunk somites do not form, with just a few mesenchymal cells being present next to the notochord (Kimmel et al., 1989). Besides this, there is an accumulation of cells in the tailbud, from which came the original name of the mutation "spadetail". When traced, many of the cells that should originate the trunk somites migrated posteriorly and were instead translocated to the notochord. Later works (Ho and Kane, 1990) confirmed that translocation to the notochord and discovered, through transplantation experiments, that the mutation affected only the trunk mesoderm. They also found that mutant cells transplanted to WT embryos did not have their phenotype rescued. Additionally, *spt* embryos were shown to have a broader axial mesoderm, confirmed by a broadening of the expression pattern of *ntl* both at 80% epiboly (Thisse et al., 1995) and at 4-somite stage (Hammerschmidt et al., 1996). As for the nature of the cells in the enlarged tailbud, unfortunately, we were not able to find a good study describing which marker genes are expressed in this area. Most of the analysis performed in the papers described earlier were of pre-segmentation stages and in only one (Amacher and Kimmel, 1998), did we find that *shh* was expressed in this area, although the picture shown is not clear on the quantity of cells in which it is expressed.

In *Xenopus*, *VegT* expression is very similar to zebrafish *tbx16* (Fukuda et al., 2010). It is expressed (Zhang and King, 1996) in mesoderm precursors of the dorsal marginal zone at early gastrula. In late gastrula this expression is maintained, except in the dorsal region that will give rise to the notochord. (Showell et al., 2004). Functionally, in *VegT* knockdown experiments using morpholinos (Fukuda et al., 2010) revealed very similar phenotypes to *spt* mutants. Specifically, embryos showed both disruption of somite formation and an accumulation of cells in the posterior tip of the tail (Fukuda et al., 2010).

As such, from the expression patterns and functional experiments, it is clearly shown that the orthologs of TBX6L are very important for the formation of the PSM.

6.5 Chicken CNOT2 and TBX6L are expressed in the axial and paraxial progenitor cell regions juxtaposed to each other

As described earlier, the orthologs of CNOT2 and TBX6L have both an expression pattern and functional roles consistent with major functions in determining the fate of notochord and PSM cells. What about the two genes in the chicken embryo ? While the expression patterns of both genes have already been described, no functional studies have revealed their role in the chicken embryo so far.

Expression of CNOT2 in chicken embryos was first described in 1996 after its initial cloning (Stein et al., 1996b). It starts very early in development in a large area of the epiblast of XI blastoderms, becoming reduced to its caudal part by EK stage XIII (Eyal-Giladi and Kochav, 1976). When the PS is being formed, CNOT2 expression is restricted to its anterior part, becoming only expressed in the node of HH4 embryos. From this point forward, expression remains in the node and is observed mainly in the recently formed notochord, showing a fading posterior to anterior gradient. At HH10, CNOT2 is expressed in the *sinus rhomboidalis* (the area that contains the node at this stage (Catala et al., 1996) and later on in the tailbud. At HH23 expression ceases as notochord formation is also ending.

TBX6L was first cloned in chicken in 1997 and its expression pattern was also then described (Knezevic et al., 1997). Its expression starts in blastoderms of stages X-XI in the posterior marginal zone epiblast and the anteriorly juxtaposed *area pellucida*. At the start of PS formation, the expression in the marginal zone is reduced and is concentrated in the more central region. Afterwards, expression is detected in the whole primitive streak (PS as it is extending until HH4). After HH5, as mesoderm is being formed, expression appears only in the paraxial mesoderm forming the segmental plate, not being present in any axial mesoderm cells or their progenitors in HN. In segmentation stages, expression is strong in the PSM, being downregulated as the first somites are formed, persisting weakly in the last formed somite. This pattern is maintained through tailbud stages until it disappears around stages HH26-28.

As described, both genes are expressed in the progenitor cells of the somites and notochord, disappearing as each corresponding structure is formed. When the territories of expression of both genes are analyzed more specifically in the regions where the

progenitor cells are located (Charrier et al., 1999), interesting patterns are found. In the *sinus rhomboidalis* of HH6 embryos, more specifically in the median pit, lies the chordoneural hinge (CNH), the equivalent of HN in neurulation stages and forward. This region is functionally and molecularly subdivided in three zones: *Zone a* corresponds to the rostral portion the CNH, where cells have already committed to a notochord or floor plate fate, *zone b* to the middle, with cells that are becoming committed to their respective fates and *zone c*, corresponding to the most caudal portion where cell commitment has not yet occurred. This zone, together with the anterior tip of the PS, forms the axial-paraxial hinge, a region described as being capable of originating both axial and paraxial progenitor cells. In this seminal work (Charrier et al., 1999), the authors also analyzed the expression of CNOT2 and TBX6L. They describe CNOT2 as expressed in all three zones, while TBX6L being expressed in the anterior tip of the PS, the two domains being juxtaposed, but not overlaping.

7 Aims and objectives

To sum up the story so far, formation of the vertebral body of zebrafish and chicken embryos differs in the structure that possesses the segmented signal. In the zebrafish, it is the notochord and in the chicken, the medial somite cells, with the contribution of the notochord still unclear. Additionally, we can observe proportionally different sizes of both structures in both species. The sclerotome seems to be following the inverse path of the notochord in the sense that it is increasing its size. From teleosts, where it is no more than a row of cells between the dermomyotome and the notochord to avians, where it takes up more than 2/3rds of the mature somite. This knowledge begs the question of what could be underlying such differences between two species. By looking for the origin of the notochord and somites, we found that: 1) Progenitor cell regions of both structures are located extraordinarily close to each other, if not overlapping; 2) Two genes, *flh* (along with its orthologs) and *spt* (along with its orthologs) play major roles in regulating their respective cell fate; 3) These two genes are also expressed in the progenitor regions of their respective structures, and, consequentially, 4) *flh*/CNOT2 and *spt*/TBX6L also have juxtaposed expression patterns.

As such, one can hypothesize that the cells that contain the information for vertebral body segmentation can be the same in both species but located in different territories/structures. In the zebrafish, these cells are in the axial mesoderm territory, in this case, the peripheric notochord, and in the chicken, they belong to the paraxial mesoderm territory, specifically in the medial somite and later sclerotome, the two locations being quite close to each other.

With all this knowledge, there are three main questions we aim to answer in this thesis, addressed by three of the five chapters of this thesis.

1) What is the role of the notochord in the formation of segmented vertebral bodies ? This question will be addressed in **Chapter 2**

2) Could CNOT2 and TBX6L be controlling axial-paraxial mesoderm cell fate in the chicken embryo as it is happening in the zebrafish ? This question will be tackled in **Chapter 3**

3) Could changes in the expression territories of flh/CNOT2 and spt/TBX6L have resulted in the transfer of these cells from one structure to another, while at the same time

account for some of the size changes between both species ? This will be discussed in **Chapter 5**

During the realization of the experimental work, we found the need to better understand the elongation dynamics of the chicken embryo. As such, **Chapter 4** concerns this analysis

References

Abdelkhalek, H. B., Beckers, A., Schuster-Gossler, K., Pavlova, M. N., Burkhardt, H., Lickert, H., Rossant, J., Reinhardt, R., Schalkwyk, L. C., Muller, I., et al. (2004). The mouse homeobox gene Not is required for caudal notochord development and affected by the truncate mutation. *Genes Dev* 18, 1725-1736.

Adams, D. S., Keller, R. and Koehl, M. A. (1990). The mechanics of notochord elongation, straightening and stiffening in the embryo of Xenopus laevis. *Development* **110**, 115-130.

Ahn, D., You, K. H. and Kim, C. H. (2012). Evolution of the tbx6/16 subfamily genes in vertebrates: insights from zebrafish. *Mol Biol Evol* **29**, 3959-3983.

Amacher, S. L. and Kimmel, C. B. (1998). Promoting notochord fate and repressing muscle development in zebrafish axial mesoderm. *Development* **125**, 1397-1406.

Andrade, R. P., Palmeirim, I. and Bajanca, F. (2007). Molecular clocks underlying vertebrate embryo segmentation: A 10-year-old hairy-go-round. *Birth Defects Res C Embryo Today* **81**, 65-83.

Ang, S. L. and Rossant, J. (1994). HNF-3 beta is essential for node and notochord formation in mouse development. *Cell* **78**, 561-574.

Aoyama, H. and Asamoto, K. (2000). The developmental fate of the rostral/caudal half of a somite for vertebra and rib formation: experimental confirmation of the resegmentation theory using chick-quail chimeras. *Mech Dev* **99**, 71-82.

Arratia, G., Schultze, H. P. and Casciotta, J. (2001). Vertebral column and associated elements in dipnoans and comparison with other fishes: development and homology. *J Morphol* **250**, 101-172.

Aulehla, A., Wiegraebe, W., Baubet, V., Wahl, M. B., Deng, C., Taketo, M., Lewandoski, M. and Pourquie, O. (2008). A beta-catenin gradient links the clock and wavefront systems in mouse embryo segmentation. *Nat Cell Biol* **10**, 186-193.

Bagnall, K., Higgins, S. and Sanders, E. (1988). The contribution made by a single somite to the vertebral column: experimental evidence in support of resegmentation using the chick-quail chimaera model. *Development* **103**, 69-85.

Bagnall, K., Higgins, S. and Sanders, E. (1989). The contribution made by cells from a single somite to tissues within a body segment and assessment of their integration with similar cells from adjacent segments. *Development* **107**, 931-943.

Bancroft, M. and Bellairs, R. (1976). The development of the notochord in the chick embryo, studied by scanning and transmission electron microscopy. *J Embryol Exp Morphol* **35**, 383-401.

Barresi, M. J., Gilbert, S. F. (2020). *Developmental Biology* (12th edition edn).

Bensimon-Brito, A., Cancela, M. L., Huysseune, A. and Witten, P. E. (2012). Vestiges, rudiments and fusion events: the zebrafish caudal fin endoskeleton in an evo-devo perspective. *Evol Dev* **14**, 116-127.

Beresford, B. (1983). Brachial muscles in the chick embryo: the fate of individual somites. *J Embryol Exp Morphol* **77**, 99-116.

Bonnerot, C. and Nicolas, J.-F. (1993). Clonal analysis in the intact mouse embryo by intragenic homologous recombination. *Comptes Rendus de L'academie des sciences. Serie III, Sciences de la vie* **316**, 1207-1217.

Brand-Saberi, B. and Christ, B. (1999). 1 Evolution and Development of Distinct Cell Lineages Derived from Somites. In *Somitogenesis - Part 2*, pp. 1-42.

Brand-Saberi, B., Wilting, J., Ebensperger, C. and Christ, B. (1996). The formation of somite compartments in the avian embryo. *Int J Dev Biol* **40**, 411-420.

Braun, T., Rudnicki, M. A., Arnold, H.-H. and Jaenisch, R. (1992). Targeted inactivation of the muscle regulatory gene Myf-5 results in abnormal rib development and perinatal death. *Cell* **71**, 369-382.

Brent, A. E., Schweitzer, R. and Tabin, C. J. (2003). A somitic compartment of tendon progenitors. *Cell* **113**, 235-248.

Briscoe, J. and Ericson, J. (1999). The specification of neuronal identity by graded Sonic Hedgehog signalling. In *Seminars in cell & developmental biology*, pp. 353-362: Elsevier.

Bruggeman, B. J., Maier, J. A., Mohiuddin, Y. S., Powers, R., Lo, Y., Guimaraes-Camboa, N., Evans, S. M. and Harfe, B. D. (2012). Avian intervertebral disc arises from rostral sclerotome and lacks a nucleus pulposus: implications for evolution of the vertebrate disc. *Dev Dyn* **241**, 675-683.

Buchberger, A., Seidl, K., Klein, C., Eberhardt, H. and Arnold, H. H. (1998). cMeso-1, a novel bHLH transcription factor, is involved in somite formation in chicken embryos. *Dev Biol* **199**, 201-215.

Bürglin, T. R. (2013). Homeotic Mutation. In *Brenner's Encyclopedia of Genetics*, pp. 510-511.

Burstyn-Cohen, T., Stanleigh, J., Sela-Donenfeld, D. and Kalcheim, C. (2004). Canonical Wnt activity regulates trunk neural crest delamination linking BMP/noggin signaling with G1/S transition. *Development* **131**, 5327-5339.

Cambray, N. and Wilson, V. (2007). Two distinct sources for a population of maturing axial progenitors. *Development* **134**, 2829-2840.

Camon, J., Degollada, E. and Verdu, J. (1990). Ultrastructural aspects of the production of extracellular matrix components by the chick embryonic notochord in vitro. *Acta Anat (Basel)* **137**, 114-123.

Catala, M., Teillet, M. A., De Robertis, E. M. and Le Douarin, M. L. (1996). A spinal cord fate map in the avian embryo: while regressing, Hensen's node lays down the notochord and floor plate thus joining the spinal cord lateral walls. *Development* **122**, 2599-2610.

Catala, M., Teillet, M. A. and Le Douarin, N. M. (1995). Organization and development of the tail bud analyzed with the quail-chick chimaera system. *Mech Dev* **51**, 51-65.

Chalamalasetty, R. B., Garriock, R. J., Dunty, W. C., Jr., Kennedy, M. W., Jailwala, P., Si, H. and Yamaguchi, T. P. (2014). Mesogenin 1 is a master regulator of paraxial presomitic mesoderm differentiation. *Development* 141, 4285-4297.

Chapman, D. L. and Papaioannou, V. E. (1998). Three neural tubes in mouse embryos with mutations in the T-box gene Tbx6. *Nature* **391**, 695-697.

Charrier, J. B., Teillet, M. A., Lapointe, F. and Le Douarin, N. M. (1999). Defining subregions of Hensen's node essential for caudalward movement, midline development and cell survival. *Development* **126**, 4771-4783.

Chernoff, E. A. and Lash, J. W. (1981). Cell movement in somite formation and development in the chick: inhibition of segmentation. *Dev Biol* **87**, 212-219.

Choi, K. S., Cohn, M. J. and Harfe, B. D. (2008). Identification of nucleus pulposus precursor cells and notochordal remnants in the mouse: implications for disk degeneration and chordoma formation. *Dev Dyn* **237**, 3953-3958.

Choi, K. S. and Harfe, B. D. (2011). Hedgehog signaling is required for formation of the notochord sheath and patterning of nuclei pulposi within the intervertebral discs. *Proc Natl Acad Sci U S A* **108**, 9484-9489.

Christ, B., Huang, R. and Scaal, M. (2004). Formation and differentiation of the avian sclerotome. *Anat Embryol (Berl)* **208**, 333-350.

Christ, B., Huang, R. and Scaal, M. (2007). Amniote somite derivatives. *Dev Dyn* **236**, 2382-2396.

Christ, B., Huang, R. and Wilting, J. (2000). The development of the avian vertebral column. *Anatomy and embryology* **202**, 179-194.

Christ, B. and Ordahl, C. P. (1995). Early stages of chick somite development. *Anat Embryol (Berl)* **191**, 381-396.

Christ, B. and Wilting, J. (1992). From somites to vertebral column. *Annals of Anatomy - Anatomischer Anzeiger* **174**, 23-32.

Cleaver, O., Seufert, D. W. and Krieg, P. A. (2000). Endoderm patterning by the notochord: development of the hypochord in Xenopus. *Development* **127**, 869-879.

Cole, A. G. (2011). A review of diversity in the evolution and development of cartilage: the search for the origin of the chondrocyte. *Eur Cell Mater* **21**, 122-129.

Cooke, J. and Zeeman, E. C. (1976). A clock and wavefront model for control of the number of repeated structures during animal morphogenesis. *Journal of theoretical biology* **58**, 455-476.

Corallo, D., Trapani, V. and Bonaldo, P. (2015). The notochord: structure and functions. *Cell Mol Life Sci* **72**, 2989-3008.

Corning, H. (1881). Über die sogenannte Neugliederung der Wirbelsäule und über das Schicksal der Urwirbelhöhle bei Reptilien. *Morph Jb* **17**, 611-622.

Deutsch, U., Dressler, G. R. and Gruss, P. (1988). Pax 1, a member of a paired box homologous murine gene family, is expressed in segmented structures during development. *Cell* **53**, 617-625.

Devoto, S. H., Melançon, E., Eisen, J. S. and Westerfield, M. (1996). Identification of separate slow and fast muscle precursor cells in vivo, prior to somite formation. *Development* **122**, 3371-3380.

Dietz, U. H., Ziegelmeier, G., Bittner, K., Bruckner, P. and Balling, R. (1999). Spatio-temporal distribution of chondromodulin-I mRNA in the chicken embryo: expression during cartilage development and formation of the heart and eye. *Dev Dyn* **216**, 233-243.

Dockter, J. L. (1999). 3 Sclerotome Induction and Differentiation. In *Somitogenesis - Part 2*, pp. 77-127.

Duband, J. L., Dufour, S., Hatta, K., Takeichi, M., Edelman, G. M. and Thiery, J. P. (1987). Adhesion molecules during somitogenesis in the avian embryo. *J Cell Biol* **104**, 1361-1374.

Dubrulle, J., McGrew, M. J. and Pourquie, O. (2001). FGF signaling controls somite boundary position and regulates segmentation clock control of spatiotemporal Hox gene activation. *Cell* **106**, 219-232.

Dubrulle, J. and Pourquie, O. (2004). Coupling segmentation to axis formation. *Development* **131**, 5783-5793.

Ebensperger, C., Wilting, J., Brand-Saberi, B., Mizutani, Y., Christ, B., Balling, R. and Koseki, H. (1995). Pax-1, a regulator of sclerotome development is induced by notochord and floor plate signals in avian embryos. *Anatomy and embryology* **191**, 297-310.

Ellis, K., Bagwell, J. and Bagnat, M. (2013a). Notochord vacuoles are lysosome-related organelles that function in axis and spine morphogenesis. *J Cell Biol* **200**, 667-679.

Ellis, K., Hoffman, B. D. and Bagnat, M. (2013b). The vacuole within: how cellular organization dictates notochord function. *Bioarchitecture* **3**, 64-68.

Eyal-Giladi, H. and Kochav, S. (1976). From cleavage to primitive streak formation: a complementary normal table and a new look at the first stages of the development of the chick. I. General morphology. *Dev Biol* **49**, 321-337.

Fan, C.-M., Porter, J. A., Chiang, C., Chang, D. T., Beachy, P. A. and Tessier-Lavigne, M. (1995). Long-range sclerotome induction by sonic hedgehog: direct role of the amino-terminal cleavage product and modulation by the cyclic AMP signaling pathway. *Cell* **81**, 457-465.

Fan, C.-M. and Tessier-Lavigne, M. (1994). Patterning of mammalian somites by surface ectoderm and notochord: evidence for sclerotome induction by a hedgehog homolog. *Cell* **79**, 1175-1186.

Fields, S. and Johnston, M. (2005). Cell biology. Whither model organism research? *Science* **307**, 1885-1886.

Fleming, A., Keynes, R. and Tannahill, D. (2004). A central role for the notochord in vertebral patterning. *Development* **131**, 873-880.

Fleming, A., Keynes, R. J. and Tannahill, D. (2001). The role of the notochord in vertebral column formation. *J Anat* **199**, 177-180.

Fleming, A., Kishida, M. G., Kimmel, C. B. and Keynes, R. J. (2015). Building the backbone: the development and evolution of vertebral patterning. *Development* **142**, 1733-1744.

Freitas, C., Rodrigues, S., Charrier, J. B., Teillet, M. A. and Palmeirim, I. (2001). Evidence for medial/lateral specification and positional information within the presomitic mesoderm. *Development* **128**, 5139-5147.

Fukuda, M., Takahashi, S., Haramoto, Y., Onuma, Y., Kim, Y. J., Yeo, C. Y., Ishiura, S. and Asashima, M. (2010). Zygotic VegT is required for Xenopus paraxial mesoderm formation and is regulated by Nodal signaling and Eomesodermin. *Int J Dev Biol* **54**, 81-92.

Gadow, H. and Abbott, E. (1894). On the Evolution of the Vertebral Column of Fishes. *Proceedings of the Royal Society of London* **56**, 296-299.

Gadow, H. F. (1896). I. On the evolution of the vertebral column of amphibia and amuivta. Philosophical Transactions of the Royal Society of London. Series B, Containing Papers of a Biological Character, 1-57.

Germanguz, I., Lev, D., Waisman, T., Kim, C. H. and Gitelman, I. (2007). Four twist genes in zebrafish, four expression patterns. *Dev Dyn* **236**, 2615-2626.

Gitelman, I. (2007). Evolution of the vertebrate twist family and synfunctionalization: a mechanism for differential gene loss through merging of expression domains. *Mol Biol Evol* **24**, 1912-1925.

Glickman, N. S., Kimmel, C. B., Jones, M. A. and Adams, R. J. (2003). Shaping the zebrafish notochord. *Development* 130, 873-887.

Gomez, C., Ozbudak, E. M., Wunderlich, J., Baumann, D., Lewis, J. and Pourquie, O. (2008). Control of segment number in vertebrate embryos. *Nature* 454, 335-339.

Gont, L. K., Fainsod, A., Kim, S. H. and De Robertis, E. M. (1996). Overexpression of the homeobox gene Xnot-2 leads to notochord formation in Xenopus. *Dev Biol* **174**, 174-178.

Gont, L. K., Steinbeisser, H., Blumberg, B. and de Robertis, E. M. (1993). Tail formation as a continuation of gastrulation: the multiple cell populations of the Xenopus tailbud derive from the late blastopore lip. *Development* **119**, 991-1004.

Griffin, K. J., Amacher, S. L., Kimmel, C. B. and Kimelman, D. (1998). Molecular identification of spadetail: regulation of zebrafish trunk and tail mesoderm formation by T-box genes. *Development* **125**, 3379-3388.

Grotmol, S., Kryvi, H., Keynes, R., Krossoy, C., Nordvik, K. and Totland, G. K. (2006). Stepwise enforcement of the notochord and its intersection with the myoseptum: an evolutionary path leading to development of the vertebra? *J Anat* **209**, 339-357.

Grotmol, S., Kryvi, H., Nordvik, K. and Totland, G. K. (2003). Notochord segmentation may lay down the pathway for the development of the vertebral bodies in the Atlantic salmon. *Anat Embryol (Berl)* **207**, 263-272.

Grotmol, S., Nordvik, K., Kryvi, H. and Totland, G. K. (2005). A segmental pattern of alkaline phosphatase activity within the notochord coincides with the initial formation of the vertebral bodies. *J Anat* **206**, 427-436.

Guillot, C., Djeffal, Y., Michaut, A., Rabe, B. and Pourquie, O. (2021). Dynamics of primitive streak regression controls the fate of neuromesodermal progenitors in the chicken embryo. *Elife* **10**.

Halpern, M. E., Ho, R. K., Walker, C. and Kimmel, C. B. (1993). Induction of muscle pioneers and floor plate is distinguished by the zebrafish no tail mutation. *Cell* **75**, 99-111.

Halpern, M. E., Thisse, C., Ho, R. K., Thisse, B., Riggleman, B., Trevarrow, B., Weinberg, E. S., Postlethwait, J. H. and Kimmel, C. B. (1995). Cell-autonomous shift from axial to paraxial mesodermal development in zebrafish floating head mutants. *Development* 121, 4257-4264.

Hamburger, V. and Hamilton, H. L. (1951). A series of normal stages in the development of the chick embryo. *J Morphol* **88**, 49-92.

Hammerschmidt, M., Pelegri, F., Mullins, M. C., Kane, D. A., Brand, M., van Eeden, F. J., Furutani-Seiki, M., Granato, M., Haffter, P., Heisenberg, C. P., et al. (1996). Mutations affecting morphogenesis during gastrulation and tail formation in the zebrafish, Danio rerio. *Development* 123, 143-151.

Hannibal, R. L. and Patel, N. H. (2013). What is a segment? *EvoDevo* **4**, 1-10.

Hatta, K., Okada, T. S. and Takeichi, M. (1985). A monoclonal antibody disrupting calcium-dependent cell-cell adhesion of brain tissues: possible role of its target antigen in animal pattern formation. *Proc Natl Acad Sci U S A* **82**, 2789-2793.

Hatta, K., Takagi, S., Fujisawa, H. and Takeichi, M. (1987). Spatial and temporal expression pattern of N-cadherin cell adhesion molecules correlated with morphogenetic processes of chicken embryos. *Dev Biol* **120**, 215-227.

Hayes, A. J., Benjamin, M. and Ralphs, J. R. (2001). Extracellular matrix in development of the intervertebral disc. *Matrix Biology* **20**, 107-121.

He, Y., Xu, X., Zhao, S., Ma, S., Sun, L., Liu, Z. and Luo, C. (2014). Maternal control of axial-paraxial mesoderm patterning via direct transcriptional repression in zebrafish. *Dev Biol* **386**, 96-110.

Herrmann, B. G. (1991). Expression pattern of the Brachyury gene in whole-mount TWis/TWis mutant embryos. *Development* **113**, 913-917.

Hickman, C. P., Roberts, L., Larson, A. and I'Anson, H. (2004). *Integrated Principles of Zoology* (12th edn). New York, USA: Mcgraw-Hill.

Hirano, S., Hirako, R., Kajita, N. and Norita, M. (1995). Morphological analysis of the role of the neural tube and notochord in the development of somites. *Anat Embryol (Berl)* **192**, 445-457.

Ho, R. K. and Kane, D. A. (1990). Cell-autonomous action of zebrafish spt-1 mutation in specific mesodermal precursors. *Nature* **348**, 728-730.

Holland, L. Z., Laudet, V. and Schubert, M. (2004). The chordate amphioxus: an emerging model organism for developmental biology. *Cell Mol Life Sci* **61**, 2290-2308.

Hoppler, S. and Moon, R. T. (1998). BMP-2/-4 and Wnt-8 cooperatively pattern the Xenopus mesoderm. *Mech Dev* **71**, 119-129.

Horb, M. E. and Thomsen, G. H. (1997). A vegetally localized T-box transcription factor in Xenopus eggs specifies mesoderm and endoderm and is essential for embryonic mesoderm formation. *Development* **124**, 1689-1698.

Hori, K., Sen, A. and Artavanis-Tsakonas, S. (2013). Notch signaling at a glance. *J Cell Sci* **126**, 2135-2140.

Huang, R., Stolte, D., Kurz, H., Ehehalt, F., Cann, G. M., Stockdale, F. E., Patel, K. and Christ, B. (2003). Ventral axial organs regulate expression of myotomal Fgf-8 that influences rib development. *Developmental Biology* **255**, 30-47.

Huang, R., Zhi, Q., Brand-Saberi, B. and Christ, B. (2000). New experimental evidence for somite resegmentation. *Anat Embryol (Berl)* **202**, 195-200.

Huang, R., Zhi, Q., Neubuser, A., Muller, T. S., Brand-Saberi, B., Christ, B. and Wilting, J. (1996). Function of somite and somitocoele cells in the formation of the vertebral motion segment in avian embryos. *Acta Anat (Basel)* **155**, 231-241.

Huang, R., Zhi, Q., Wilting, J. and Christ, B. (1994). The fate of somitocoele cells in avian embryos. *Anat Embryol (Berl)* **190**, 243-250.

Hubaud, A. and Pourquié, O. (2014). Signalling dynamics in vertebrate segmentation. *Nature reviews Molecular cell biology* **15**, 709-721.

Hug, B., Walter, V. and Grunwald, D. J. (1997). tbx6, a Brachyury-related gene expressed by ventral mesendodermal precursors in the zebrafish embryo. *Dev Biol* **183**, 61-73.

Huitema, L. F., Apschner, A., Logister, I., Spoorendonk, K. M., Bussmann, J., Hammond, C. L. and Schulte-Merker, S. (2012). Entpd5 is essential for skeletal mineralization and regulates phosphate homeostasis in zebrafish. *Proc Natl Acad Sci U S A* **109**, 21372-21377.

Huysseune, A., Sire, J. Y. and Witten, P. (2010). A revised hypothesis on the evolutionary origin of the vertebrate dentition. *Journal of Applied Ichthyology* **26**, 152-155.

Iimura, T., Yang, X., Weijer, C. J. and Pourquie, O. (2007). Dual mode of paraxial mesoderm formation during chick gastrulation. *Proc Natl Acad Sci U S A* **104**, 2744-2749.

Jacob, M., Jacob, J. H. and Christ, B. (1975). [The early differentiation of the perinotochordal connective tissue. A scanning and transmission electron microscopic study on chick embryos (author's transl)]. *Experientia* **31**, 1083-1086.

Jiang, Y.-J., Aerne, B. L., Smithers, L., Haddon, C., Ish-Horowicz, D. and Lewis, J. (2000). Notch signalling and the synchronization of the somite segmentation clock. *Nature* **408**, 475-479.

Johnson, R. L., Laufer, E., Riddle, R. D. and Tabin, C. (1994). Ectopic expression of Sonic hedgehog alters dorsal-ventral patterning of somites. *Cell* **79**, 1165-1173.

Julich, D., Mould, A. P., Koper, E. and Holley, S. A. (2009). Control of extracellular matrix assembly along tissue boundaries via Integrin and Eph/Ephrin signaling. *Development* **136**, 2913-2921.

Jurand, A. (1962). The development of the notochord in chick embryos. *J Embryol Exp Morphol* **10**, 602-621.

Kimmel, C. B., Ballard, W. W., Kimmel, S. R., Ullmann, B. and Schilling, T. F. (1995). Stages of embryonic development of the zebrafish. *Dev Dyn* 203, 253-310.

Kimmel, C. B., Kane, D. A., Walker, C., Warga, R. M. and Rothman, M. B. (1989). A mutation that changes cell movement and cell fate in the zebrafish embryo. *Nature* **337**, 358-362.

Kimmel, C. B., Warga, R. M. and Schilling, T. F. (1990). Origin and organization of the zebrafish fate map. *Development* **108**, 581-594.

Kirschbaum, F. and Meunier, F. J. (1981). Experimental regeneration of the caudal skeleton of the glass knifefish, Eigenmannia virescens (Rhamphichthydae, Gymnotoidei). *J Morphol* **168**, 121-135.

Knezevic, V., De Santo, R. and Mackem, S. (1997). Two novel chick T-box genes related to mouse Brachyury are expressed in different, non-overlapping mesodermal domains during gastrulation. *Development* **124**, 411-419.

Kodjabachian, L., Dawid, I. B. and Toyama, R. (1999). Gastrulation in zebrafish: what mutants teach us. *Developmental biology* **213**, 231-245.

Koehl, M., Quillin, K. J. and Pell, C. A. (2000). Mechanical design of fiber-wound hydraulic skeletons: the stiffening and straightening of embryonic notochords. *American Zoologist* **40**, 28-041.

Koshida, S., Shinya, M., Mizuno, T., Kuroiwa, A. and Takeda, H. (1998). Initial anteroposterior pattern of the zebrafish central nervous system is determined by differential competence of the epiblast. *Development* **125**, 1957-1966.

Krol, A. J., Roellig, D., Dequeant, M. L., Tassy, O., Glynn, E., Hattem, G., Mushegian, A., Oates, A. C. and Pourquie, O. (2011). Evolutionary plasticity of segmentation clock networks. *Development* 138, 2783-2792.

Kulesa, P. M. and Fraser, S. E. (2002). Cell dynamics during somite boundary formation revealed by time-lapse analysis. *Science* **298**, 991-995.

Lai, E. C. (2004). Notch signaling: control of cell communication and cell fate. *Development* **131**, 965-973.

Lane, M. C. and Smith, W. C. (1999). The origins of primitive blood in Xenopus: implications for axial patterning. *Development* **126**, 423-434.

Lardelli, M. (2003). The evolutionary relationships of zebrafish genes tbx6, tbx16/spadetail and mga. *Dev Genes Evol* **213**, 519-522.

Lawson, A. and Schoenwolf, G. C. (2001). Cell populations and morphogenetic movements underlying formation of the avian primitive streak and organizer. *Genesis* **29**, 188-195.

Le Douarin, N. (1973). A biological cell labeling technique and its use in experimental embryology. *Developmental biology* **30**, 217-222.

Le Douarin, N. M. and Halpern, M. E. (2000). Discussion point. Origin and specification of the neural tube floor plate: insights from the chick and zebrafish. *Curr Opin Neurobiol* **10**, 23-30.

Lemaire, L. and Kessel, M. (1997). Gastrulation and homeobox genes in chick embryos. *Mech Dev* **67**, 3-16.

Lewis, J. (2003). Autoinhibition with Transcriptional Delay. *Current Biology* **13**, 1398-1408.

Lleras Forero, L., Narayanan, R., Huitema, L. F., VanBergen, M., Apschner, A., Peterson-Maduro, J., Logister, I., Valentin, G., Morelli, L. G., Oates, A. C., et al. (2018). Segmentation of the zebrafish axial skeleton relies on notochord sheath cells and not on the segmentation clock. *Elife* 7.

Lustig, K. D., Kroll, K. L., Sun, E. E. and Kirschner, M. W. (1996). Expression cloning of a Xenopus T-related gene (Xombi) involved in mesodermal patterning and blastopore lip formation. *Development* **122**, 4001-4012.

Malpighi, M (1693). *Dissertatio epistolica de formatione pulli in ovo*. *Apud Joannem Martyn*.

Martin, B. L. (2016). Factors that coordinate mesoderm specification from neuromesodermal progenitors with segmentation during vertebrate axial extension. *Semin Cell Dev Biol* **49**, 59-67.

Martin, B. L. and Kimelman, D. (2012). Canonical Wnt signaling dynamically controls multiple stem cell fate decisions during vertebrate body formation. *Dev Cell* **22**, 223-232.

Martinez Arias, A. and Steventon, B. (2018). On the nature and function of organizers. *Development* **145**.

Martins, G. G., Rifes, P., Amandio, R., Rodrigues, G., Palmeirim, I. and Thorsteinsdottir, S. (2009). Dynamic 3D cell rearrangements guided by a fibronectin matrix underlie somitogenesis. *PLoS One* **4**, e7429.

Masamizu, Y., Ohtsuka, T., Takashima, Y., Nagahara, H., Takenaka, Y., Yoshikawa, K., Okamura, H. and Kageyama, R. (2006). Real-time imaging of the somite segmentation clock: revelation of unstable oscillators in the individual presomitic mesoderm cells. *Proc Natl Acad Sci U S A* **103**, 1313-1318.

McCann, M. R. and Seguin, C. A. (2016). Notochord Cells in Intervertebral Disc Development and Degeneration. *J Dev Biol* **4**.

McGinnis, W. (1994). A century of homeosis, a decade of homeoboxes. *Genetics* **137**, 607-611.

McMahon, J. A., Takada, S., Zimmerman, L. B., Fan, C. M., Harland, R. M. and McMahon, A. P. (1998). Noggin-mediated antagonism of BMP signaling is required for growth and patterning of the neural tube and somite. *Genes Dev* **12**, 1438-1452.

Meilhac, S. M., Kelly, R. G., Rocancourt, D., Eloy-Trinquet, S., Nicolas, J. F. and Buckingham, M. E. (2003). A retrospective clonal analysis of the myocardium reveals two phases of clonal growth in the developing mouse heart. *Development* **130**, 3877-3889.

Melby, A. E., Kimelman, D. and Kimmel, C. B. (1997). Spatial regulation of floating head expression in the developing notochord. *Dev Dyn* **209**, 156-165.

Melby, A. E., Warga, R. M. and Kimmel, C. B. (1996). Specification of cell fates at the dorsal margin of the zebrafish gastrula. *Development* **122**, 2225-2237.

Mittapalli, V. R., Huang, R., Patel, K., Christ, B. and Scaal, M. (2005). Arthrotome: a specific joint forming compartment in the avian somite. *Dev Dyn* **234**, 48-53.

Monsoro-Burq, A. H., Duprez, D., Watanabe, Y., Bontoux, M., Vincent, C., Brickell, P. and Le Douarin, N. (1996). The role of bone morphogenetic proteins in vertebral development. *Development* 122, 3607-3616.

Montero, J. A. and Heisenberg, C. P. (2004). Gastrulation dynamics: cells move into focus. *Trends Cell Biol* **14**, 620-627.

Morin-Kensicki, E. M. and Eisen, J. S. (1997). Sclerotome development and peripheral nervous system segmentation in embryonic zebrafish. *Development* **124**, 159-167.

Morin-Kensicki, E. M., Melancon, E. and Eisen, J. S. (2002). Segmental relationship between somites and vertebral column in zebrafish. *Development* **129**, 3851-3860.

Müller, J. P. (1834). Vergleichende Anatomie der Myxinoiden.

Muller, T. S., Ebensperger, C., Neubuser, A., Koseki, H., Balling, R., Christ, B. and Wilting, J. (1996). Expression of avian Pax1 and Pax9 is intrinsically regulated in the pharyngeal endoderm, but depends on environmental influences in the paraxial mesoderm. *Dev Biol* **178**, 403-417.

Müller, W. A. (1997). Model organisms in developmental biology. In *Developmental biology*, pp. 21-121: Springer.

Nakaya, Y., Kuroda, S., Katagiri, Y. T., Kaibuchi, K. and Takahashi, Y. (2004). Mesenchymal-epithelial transition during somitic segmentation is regulated by differential roles of Cdc42 and Rac1. *Dev Cell* **7**, 425-438.

Newgreen, D. F., Scheel, M. and Kastner, V. (1986). Morphogenesis of sclerotome and neural crest in avian embryos. In vivo and in vitro studies on the role of notochordal extracellular material. *Cell Tissue Res* **244**, 299-313.

Nieuwkoop, P. D., Faber, J., Gerhart, J. and Kirschner, M. (2020). Normal table of Xenopus laevis (Daudin): a systematical and chronological survey of the development from the fertilized egg till the end of metamorphosis: Garland Science.

Nikaido, M., Kawakami, A., Sawada, A., Furutani-Seiki, M., Takeda, H. and Araki, K. (2002). Tbx24, encoding a T-box protein, is mutated in the zebrafish somite-segmentation mutant fused somites. *Nat Genet* **31**, 195-199.

Nishikawa, K. and Wassersug, R. (1989). Evolution of spinal nerve number in anuran larvae. *Brain, behavior and evolution* **33**, 15-24.

Nobrega, A., Maia-Fernandes, A. C. and Andrade, R. P. (2021). Altered Cogs of the Clock: Insights into the Embryonic Etiology of Spondylocostal Dysostosis. *J Dev Biol* **9**.

Noll, M. (1993). Evolution and role of Pax genes. *Current opinion in genetics & development* **3**, 595-605.

Oates, A. C. and Ho, R. K. (2002). Hairy/E (spl)-related (Her) genes are central components of the segmentation oscillator and display redundancy with the Delta/Notch signaling pathway in the formation of anterior segmental boundaries in the zebrafish.

Oates, A. C., Morelli, L. G. and Ares, S. (2012). Patterning embryos with oscillations: structure, function and dynamics of the vertebrate segmentation clock. *Development* **139**, 625-639.

Olivera-Martinez, I., Coltey, M., Dhouailly, D. and Pourquie, O. (2000). Mediolateral somitic origin of ribs and dermis determined by quail-chick chimeras. *Development* **127**, 4611-4617.

Olivera-Martinez, I., Harada, H., Halley, P. A. and Storey, K. G. (2012). Loss of FGF-dependent mesoderm identity and rise of endogenous retinoid signalling determine cessation of body axis elongation. *PLoS Biol* **10**, e1001415.

Ordahl, C. and Le Douarin, N. (1992). Two myogenic lineages within the developing somite. *Development* **114**, 339-353.

Pais de Azevedo, T., Magno, R., Duarte, I. and Palmeirim, I. (2018). Recent advances in understanding vertebrate segmentation. *F1000Res* **7**, 97.

Pais de Azevedo, T. P., Witten, P. E., Huysseune, A., Bensimon-Brito, A., Winkler, C., To, T. T. and Palmeirim, I. (2012). Interrelationship and modularity of notochord and somites: a comparative view on zebrafish and chicken vertebral body development. *Journal of Applied Ichthyology* **28**, 316-319.

Palmeirim, I., Henrique, D., Ish-Horowicz, D. and Pourquie, O. (1997). Avian hairy gene expression identifies a molecular clock linked to vertebrate segmentation and somitogenesis. *Cell* **91**, 639-648.

Papaioannou, V. E. and Silver, L. M. (1998). The T-box gene family. *Bioessays* **20**, 9-19.

Pasquale, E. B. (2008). Eph-ephrin bidirectional signaling in physiology and disease. *Cell* **133**, 38-52.

Pasteels, J. (1937). Etudes sur la gastrulation des vertébrés méroblastiques. III. Oiseaux. IV Conclusions générales. *Arch. Biol.* **48**, 381-488.

Peters, H., Wilm, B., Sakai, N., Imai, K., Maas, R. and Balling, R. (1999). Pax1 and Pax9 synergistically regulate vertebral column development. *Development* **126**, 5399-5408.

Piatkowska, A. M., Evans, S. E. and Stern, C. D. (2021). Cellular aspects of somite formation in vertebrates. *Cells Dev* **168**, 203732.

Piekarski, N. and Olsson, L. (2014). Resegmentation in the Mexican axolotl, Ambystoma mexicanum. *J Morphol* **275**, 141-152.

Plouhinec, J. L., Granier, C., Le Mentec, C., Lawson, K. A., Saberan-Djoneidi, D., Aghion, J., Shi, D. L., Collignon, J. and Mazan, S. (2004). Identification of the mammalian Not gene via a phylogenomic approach. *Gene Expr Patterns* 5, 11-22.

Pogoda, H. M., Riedl-Quinkertz, I., Lohr, H., Waxman, J. S., Dale, R. M., Topczewski, J., Schulte-Merker, S. and Hammerschmidt, M. (2018). Direct activation of chordoblasts by retinoic acid is required for segmented centra mineralization during zebrafish spine development. *Development* 145.

Poliakov, A., Cotrina, M. and Wilkinson, D. G. (2004). Diverse roles of eph receptors and ephrins in the regulation of cell migration and tissue assembly. *Dev Cell* **7**, 465-480.

Pourquie, O., Coltey, M., Breant, C. and Le Douarin, N. M. (1995). Control of somite patterning by signals from the lateral plate. *Proc Natl Acad Sci U S A* **92**, 3219-3223.

Pourquie, O., Fan, C. M., Coltey, M., Hirsinger, E., Watanabe, Y., Breant, C., Francis-West, P., Brickell, P., Tessier-Lavigne, M. and Le Douarin, N. M. (1996). Lateral and axial signals involved in avian somite patterning: a role for BMP4. *Cell* 84, 461-471.

Pourquie, O. and Tam, P. P. (2001). A nomenclature for prospective somites and phases of cyclic gene expression in the presomitic mesoderm. *Dev Cell* **1**, 619-620.

Ranson, M., Tickle, C., Mahon, K. A. and Mackem, S. (1995). Gnot1, a member of a new homeobox gene subfamily, is expressed in a dynamic, region-specific domain along the proximodistal axis of the developing limb. *Mechanisms of development* **51**, 17-30.

Remak, R. (1855). Untersuchungen über die Entwicklung der Wirbelthiere: Reimer.

Resende, T. P., Ferreira, M., Teillet, M. A., Tavares, A. T., Andrade, R. P. and Palmeirim, I. (2010). Sonic hedgehog in temporal control of somite formation. *Proc Natl Acad Sci U S A* **107**, 12907-12912.

Richmond, D. L. and Oates, A. C. (2012). The segmentation clock: inherited trait or universal design principle? *Curr Opin Genet Dev* **22**, 600-606.

Riedel-Kruse, I. H., Muller, C. and Oates, A. C. (2007). Synchrony dynamics during initiation, failure, and rescue of the segmentation clock. *Science* **317**, 1911-1915.

Rifes, P., Carvalho, L., Lopes, C., Andrade, R. P., Rodrigues, G., Palmeirim, I. and Thorsteinsdottir, S. (2007). Redefining the role of ectoderm in somitogenesis: a player in the formation of the fibronectin matrix of presomitic mesoderm. *Development* **134**, 3155-3165.

Rifes, P. and Thorsteinsdottir, S. (2012). Extracellular matrix assembly and 3D organization during paraxial mesoderm development in the chick embryo. *Dev Biol* **368**, 370-381.

Rohde, L. A. and Heisenberg, C. P. (2007). Zebrafish Gastrulation: Cell Movements, Signals, and Mechanisms. pp. 159-192.

Rot-Nikcevic, I., Reddy, T., Downing, K. J., Belliveau, A. C., Hallgrímsson, B., Hall, B. K. and Kablar, B. (2006). Myf5−/−: MyoD−/− amyogenic fetuses reveal the importance of early contraction and static loading by striated muscle in mouse skeletogenesis. *Development genes and evolution* **216**, 1-9.

Row, R. H., Tsotras, S. R., Goto, H. and Martin, B. L. (2016). The zebrafish tailbud contains two independent populations of midline progenitor cells that maintain long-term germ layer plasticity and differentiate in response to local signaling cues. *Development* **143**, 244-254.

Rudnicki, M. A. and Jaenisch, R. (1995). The MyoD family of transcription factors and skeletal myogenesis. *Bioessays* **17**, 203-209.

Ruggeri, A. (1972). Ultrastructural histochemical and autoradiographic studies on the developing chick notochord. *Zeitschrift für Anatomie und Entwicklungsgeschichte* **138**, 20-33.

Ruvinsky, I., Silver, L. M. and Ho, R. K. (1998). Characterization of the zebrafish tbx16 gene and evolution of the vertebrate T-box family. *Dev Genes Evol* **208**, 94-99.

Sachdev, S. W., Dietz, U. H., Oshima, Y., Lang, M. R., Knapik, E. W., Hiraki, Y. and Shukunami, C. (2001). Sequence analysis of zebrafish chondromodulin-1 and expression profile in the notochord and chondrogenic regions during cartilage morphogenesis. *Mech Dev* **105**, 157-162.

Sato, Y., Yasuda, K. and Takahashi, Y. (2002). Morphological boundary forms by a novel inductive event mediated by Lunatic fringe and Notch during somitic segmentation.

Satoh, N. (2003). The ascidian tadpole larva: comparative molecular development and genomics. *Nat Rev Genet* **4**, 285-295.

Sawada, A., Saga, Y. and Takeda, H. (2000). [Zebrafish somitogenesis-roles of mesp- and hairy-related genes]. *Tanpakushitsu Kakusan Koso* **45**, 2738-2744.

Scaal, M. (2016). Early development of the vertebral column. *Semin Cell Dev Biol* **49**, 83-91.

Schier, A. F. and Talbot, W. S. (2005). Molecular genetics of axis formation in zebrafish. *Annu Rev Genet* **39**, 561-613.

Schmitz, B. and Campos-Ortega, J. A. (1994). Dorso-ventral polarity of the zebrafish embryo is distinguishable prior to the onset of gastrulation. *Rouxs Arch Dev Biol* **203**, 374-380.

Schneuwly, S., Klemenz, R. and Gehring, W. J. (1987). Redesigning the body plan of Drosophila by ectopic expression of the homoeotic gene Antennapedia. *Nature* **325**, 816-818.

Schoenwolf, G. C., Garcia-Martinez, V. and Dias, M. S. (1992). Mesoderm movement and fate during avian gastrulation and neurulation. *Dev Dyn* **193**, 235-248.

Schulte-Merker, S., Van Eeden, F., Halpern, M. E., Kimmel, C. and Nusslein-Volhard, C. (1994). no tail (ntl) is the zebrafish homologue of the mouse T (Brachyury) gene. *Development* **120**, 1009-1015.

Schultze, H. P. and Arratia, G. (1988). Reevaluation of the caudal skeleton of some actinopterygian fishes: II. Hiodon, Elops, and Albula. *Journal of Morphology* **195**, 257-303.

Scott, A. and Stemple, D. L. (2005). Zebrafish notochordal basement membrane: signaling and structure. *Curr Top Dev Biol* **65**, 229-253.

Selleck, M. A. and Stern, C. D. (1991). Fate mapping and cell lineage analysis of Hensen's node in the chick embryo. *Development* **112**, 615-626.

Selleck, M. A. and Stern, C. D. (1992). Commitment of mesoderm cells in Hensen's node of the to notochord and somite. *Development* **114**, 403-415.

Senthinathan, B., Sousa, C., Tannahill, D. and Keynes, R. (2012). The generation of vertebral segmental patterning in the chick embryo. *J Anat* **220**, 591-602.

Sheeba, C. J., Andrade, R. P. and Palmeirim, I. (2016). Mechanisms of vertebrate embryo segmentation: Common themes in trunk and limb development. *Semin Cell Dev Biol* **49**, 125-134.

Shih, J. and Fraser, S. E. (1995). Distribution of tissue progenitors within the shield region of the zebrafish gastrula. *Development* **121**, 2755-2765.

Shih, J. and Fraser, S. E. (1996). Characterizing the zebrafish organizer: microsurgical analysis at the early-shield stage. *Development* **122**, 1313-1322.

Showell, C., Binder, O. and Conlon, F. L. (2004). T-box genes in early embryogenesis. *Dev Dyn* **229**, 201-218.

Smits, P. and Lefebvre, V. (2003). Sox5 and Sox6 are required for notochord extracellular matrix sheath formation, notochord cell survival and development of the nucleus pulposus of intervertebral discs. *Development* **130**, 1135-1148.

Solovieva, T., Lu, H. C., Moverley, A., Plachta, N. and Stern, C. D. (2022). The embryonic node behaves as an instructive stem cell niche for axial elongation. *Proc Natl Acad Sci U S A* **119**.

Solursh, M., Fisher, M., Meier, S. and Singley, C. T. (1979). The role of extracellular matrix in the formation of the sclerotome. *J Embryol Exp Morphol* **54**, 75-98.

Spemann, H. and Mangold, H. (1924). über Induktion von Embryonalanlagen durch Implantation artfremder Organisatoren. *Archiv für mikroskopische Anatomie und Entwicklungsmechanik* **100**, 599-638.

Stein, S., Fritsch, R., Lemaire, L. and Kessel, M. (1996a). Checklist: vertebrate homeobox genes. *Mech Dev* **55**, 91-108.

Stein, S. and Kessel, M. (1995). A homeobox gene involved in node, notochord and neural plate formation of chick embryos. *Mech Dev* **49**, 37-48.

Stein, S., Niss, K. and Kessel, M. (1996b). Differential activation of the clustered homeobox genes CNOT2 and CNOT1 during notogenesis in the chick. *Dev Biol* **180**, 519-533.

Stemple, D. L. (2005). Structure and function of the notochord: an essential organ for chordate development. *Development* **132**, 2503-2512.

Stennard, F., Carnac, G. and Gurdon, J. B. (1996). The Xenopus T-box gene, Antipodean, encodes a vegetally localised maternal mRNA and can trigger mesoderm formation. *Development* **122**, 4179-4188.

Stern, C. D. and Keynes, R. J. (1987). Interactions between somite cells: the formation and maintenance of segment boundaries in the chick embryo. *Development* **99**, 261-272.

Stickney, H. L., Barresi, M. J. and Devoto, S. H. (2000). Somite development in zebrafish. *Dev Dyn* **219**, 287-303.

Strudel, G. (1955). L'influence morphogene du tube nerveux et de la corde sur la differenciation de la colonne vertebrale et de sa musculature chez l'embryon de poulet. *Comptes rendus des seances de la societé de biologie et de ses filiales* **149**, 188-190.

Takada, S., Stark, K. L., Shea, M. J., Vassileva, G., McMahon, J. A. and McMahon, A. P. (1994). Wnt-3a regulates somite and tailbud formation in the mouse embryo. *Genes Dev* **8**, 174-189.

Takahashi, Y., Yasuhiko, Y., Takahashi, J., Takada, S., Johnson, R. L., Saga, Y. and Kanno, J. (2013). Metameric pattern of intervertebral disc/vertebral body is generated independently of Mesp2/Ripply-mediated rostro-caudal patterning of somites in the mouse embryo. *Dev Biol* **380**, 172-184.

Takimoto, A., Mohri, H., Kokubu, C., Hiraki, Y. and Shukunami, C. (2013). Pax1 acts as a negative regulator of chondrocyte maturation. *Experimental cell research* **319**, 3128-3139.

Talbot, W. S., Trevarrow, B., Halpern, M. E., Melby, A. E., Farr, G., Postlethwait, J. H., Jowett, T., Kimmel, C. B. and Kimelman, D. (1995). A homeobox gene essential for zebrafish notochord development. *Nature* 378, 150-157.

Teillet, M. A., Lapointe, F. and Le Douarin, N. M. (1998). The relationships between notochord and floor plate in vertebrate development revisited. *Proc Natl Acad Sci U S A* **95**, 11733-11738.

Teillet, M. A. and Le Douarin, N. M. (1983). Consequences of neural tube and notochord excision on the development of the peripheral nervous system in the chick embryo. *Dev Biol* **98**, 192-211.

Thisse, C., Thisse, B. and Postlethwait, J. H. (1995). Expression of snail2, a second member of the zebrafish snail family, in cephalic mesendoderm and presumptive neural crest of wild-type and spadetail mutant embryos. *Dev Biol* **172**, 86-99.

Tondury, G. (1958). Entwicklungsgeschichte und fehlbildungen der wirbelsaule. *Die Wirbelsaule in Forschung und Praxis*.

Trelstad, R. L. (1977). Mesenchymal cell polarity and morphogenesis of chick cartilage. *Dev Biol* **59**, 153-163.

Tzouanacou, E., Wegener, A., Wymeersch, F. J., Wilson, V. and Nicolas, J. F. (2009). Redefining the progression of lineage segregations during mammalian embryogenesis by clonal analysis. *Dev Cell* **17**, 365-376.

van Eeden, F. J., Granato, M., Schach, U., Brand, M., Furutani-Seiki, M., Haffter, P., Hammerschmidt, M., Heisenberg, C. P., Jiang, Y. J., Kane, D. A., et al. (1996). Mutations affecting somite formation and patterning in the zebrafish, Danio rerio. *Development* 123, 153-164.

Verbout, A. (1976). A critical review of the 'neugliederung'concept in relation to the development of the vertebral column. *Acta biotheoretica* **25**, 219-258.

Vermot, J., Gallego Llamas, J., Fraulob, V., Niederreither, K., Chambon, P. and Dolle, P. (2005). Retinoic acid controls the bilateral symmetry of somite formation in the mouse embryo. *Science* **308**, 563-566.

Voiculescu, O., Bertocchini, F., Wolpert, L., Keller, R. E. and Stern, C. D. (2007). The amniote primitive streak is defined by epithelial cell intercalation before gastrulation. *Nature* **449**, 1049-1052.

von Dassow, G., Schmidt, J. E. and Kimelman, D. (1993). Induction of the Xenopus organizer: expression and regulation of Xnot, a novel FGF and activin-regulated homeo box gene. *Genes Dev* **7**, 355-366.

Von Ebner, V. (1888). Urwirbel und neugliederung der wirbelsäule. *Sitzungsber Akad Wiss Wien* **3**, 194-206.

Waddington, C. H. (1932). III. Experiments on the development of chick and duck embryos, cultivated in vitro. *Philosophical Transactions of the Royal Society of London. Series B, Containing Papers of a Biological Character* **221**, 179-230.

Waddington, C. H. (1957). *The strategy of the genes*: Allen &Unwin, London.

Walther, C., Guenet, J.-L., Simon, D., Deutsch, U., Jostes, B., Goulding, M. D., Plachov, D., Balling, R. and Gruss, P. (1991). Pax: a murine multigene family of paired box-containing genes. *Genomics* 11, 424-434.

Wang, J., Zhang, K., Xu, L. and Wang, E. (2011). Quantifying the Waddington landscape and biological paths for development and differentiation. *Proc Natl Acad Sci U S A* **108**, 8257-8262.

Wang, S., Kryvi, H., Grotmol, S., Wargelius, A., Krossoy, C., Epple, M., Neues, F., Furmanek, T. and Totland, G. K. (2013). Mineralization of the vertebral bodies in Atlantic salmon (Salmo salar L.) is initiated segmentally in the form of hydroxyapatite crystal accretions in the notochord sheath. *J Anat* **223**, 159-170.

Ward, L., Evans, S. E. and Stern, C. D. (2017). A resegmentation-shift model for vertebral patterning. *Journal of Anatomy* **230**, 290-296.

Warga, R. M. and Kimmel, C. B. (1990). Cell movements during epiboly and gastrulation in zebrafish. *Development* **108**, 569-580.

Watanabe, T., Sato, Y., Saito, D., Tadokoro, R. and Takahashi, Y. (2009). EphrinB2 coordinates the formation of a morphological boundary and cell epithelialization during somite segmentation. *Proceedings of the National Academy of Sciences* **106**, 7467-7472.

Watanabe, T. and Takahashi, Y. (2010). Tissue morphogenesis coupled with cell shape changes. *Curr Opin Genet Dev* **20**, 443-447.

Watanabe, Y. and Le Douarin, N. M. (1996). A role for BMP-4 in the development of subcutaneous cartilage. *Mech Dev* **57**, 69-78.

Watterson, R. L., Fowler, I. and Fowler, B. J. (1954). The role of the neural tube and notochord in development of the axial skeleton of the chick. *Am J Anat* **95**, 337-399.

Wei, Y. and Mikawa, T. (2000). Formation of the avian primitive streak from spatially restricted blastoderm: evidence for polarized cell division in the elongating streak. *Development* **127**, 87-96.

Weinstein, D. C., Ruiz i Altaba, A., Chen, W. S., Hoodless, P., Prezioso, V. R., Jessell, T. M. and Darnell, J. E., Jr. (1994). The winged-helix transcription factor HNF-3 beta is required for notochord development in the mouse embryo. *Cell* **78**, 575-588.

Weldon, S. A. and Munsterberg, A. E. (2021). Somite development and regionalisation of the vertebral axial skeleton. *Semin Cell Dev Biol*.

West-Eberhard, M. J. (2003). *Developmental plasticity and evolution*: Oxford University Press.

Williams, E. E. (1959). Gadow's arcualia and the development of tetrapod vertebrae. *The Quarterly Review of Biology* **34**, 1-32.

Williams, S., Alkhatib, B. and Serra, R. (2019). Development of the axial skeleton and intervertebral disc. *Curr Top Dev Biol* **133**, 49-90.

Wilting, J., Kurz, H., Brand-Saberi, B., Steding, G., Yang, Y. X., Hasselhorn, H. M., Epperlein, H. H. and Christ, B. (1994). Kinetics and differentiation of somite cells forming the vertebral column: studies on human and chick embryos. *Anat Embryol (Berl)* **190**, 573-581.

Windner, S. E., Bird, N. C., Patterson, S. E., Doris, R. A. and Devoto, S. H. (2012). Fss/Tbx6 is required for central dermomyotome cell fate in zebrafish. *Biol Open* **1**, 806-814.

Wopat, S., Bagwell, J., Sumigray, K. D., Dickson, A. L., Huitema, L. F. A., Poss, K. D., Schulte-Merker, S. and Bagnat, M. (2018). Spine Patterning Is Guided by Segmentation of the Notochord Sheath. *Cell Rep* 22, 2026-2038.

Wymeersch, F. J., Skylaki, S., Huang, Y., Watson, J. A., Economou, C., Marek-Johnston, C., Tomlinson, S. R. and Wilson, V. (2019). Transcriptionally dynamic progenitor populations organised around a stable niche drive axial patterning. *Development* **146**.

Wymeersch, F. J., Wilson, V. and Tsakiridis, A. (2021). Understanding axial progenitor biology in vivo and in vitro. *Development* **148**.

Yamamoto, A., Amacher, S. L., Kim, S.-H., Geissert, D., Kimmel, C. B. and De Robertis, E. (1998). Zebrafish paraxial protocadherin is a downstream target of spadetail involved in morphogenesis of gastrula mesoderm. *Development* **125**, 3389-3397.

Yamamoto, M., Morita, R., Mizoguchi, T., Matsuo, H., Isoda, M., Ishitani, T., Chitnis, A. B., Matsumoto, K., Crump, J. G., Hozumi, K., et al. (2010). Mib-Jag1-Notch signalling regulates patterning and structural roles of the notochord by controlling cell-fate decisions. *Development* 137, 2527-2537.

Yamanaka, Y., Tamplin, O. J., Beckers, A., Gossler, A. and Rossant, J. (2007). Live imaging and genetic analysis of mouse notochord formation reveals regional morphogenetic mechanisms. *Dev Cell* **13**, 884-896.

Yasuo, H. and Lemaire, P. (2001). Role of Goosecoid, Xnot and Wnt antagonists in the maintenance of the notochord genetic programme in Xenopus gastrulae. *Development* **128**, 3783-3793.

Zhang, J. and King, M. L. (1996). Xenopus VegT RNA is localized to the vegetal cortex during oogenesis and encodes a novel T-box transcription factor involved in mesodermal patterning. *Development* **122**, 4119-4129.

Zhao, Q., Eberspaecher, H., Lefebvre, V. and De Crombrugghe, B. (1997). Parallel expression of Sox9 and Col2a1 in cells undergoing chondrogenesis. *Dev Dyn* **209**, 377-386.

This page is intentionally left blank

Chapter II – The role of the notochord and dermomyotome in formation of segmented vertebral bodies

When you have eliminated the impossible, whatever remains, however improbable, must be the truth? (Sherlock Holmes)

In *The sign of the Four (1890)*

The greatest teacher, failure is. (Master Yoda)

In *Star Wars: The last Jedi (2017)*

Introduction

The formation of segmented vertebral bodies is a process that involves the participation of two different structures, the notochord and the somites (Pais de Azevedo et al., 2012). However, the structures and processes responsible for the signal to originate segmented vertebral bodies is different between various animal species.

In the teleosts like the zebrafish, this begins with the expression of specific genes and extracellular matrix molecules on the cells of the notochordal sheath, the chordoblasts (Lleras Forero et al., 2018; Wopat et al., 2018). This expression is segmented and corresponds to the future location of the vertebral bodies and intervertebral discs and leads to mineralization of the notochordal sheath (Bensimon-Brito et al., 2012; Fleming et al., 2004), establishing the pattern for segmented vertebral body formation.

In the chicken embryo the cells that form the vertebral body derive from the sclerotome compartment of the mature somite, more specifically from the ventral sclerotome (Christ et al., 2004). These cells migrate to the vicinity of the notochord (Jacob et al., 1975), due to signals coming from it, as well as the floor plate (Ebensperger et al., 1995) and using an extracellular matrix for migration (Smits and Lefebvre, 2003). It is classicaly described that formation of segmented vertebrae implies the process of resegmentation (Remak, 1855; Ward et al., 2017). Through this process, the sclerotome is rostrocaudally subdivided in two compartments, one vertebrae being formed by the caudal half sclerotome and the rostral half sclerotome of the next somite (Aoyama and Asamoto, 2000; Bagnall et al., 1988). The two half sclerotomes are separated by Von Ebner's fissure (Christ and Ordahl, 1995; Stern and Keynes, 1987; Von Ebner, 1888), this being the first morphological landmark of sclerotome segmentation.

However, it is unkown if other structures can be important in the signalling for the formation of segmented vertebral bodies. For example, mutations in muscle genes such as Myf5 and MyoD (Rot-Nikcevic et al., 2006) revealed several skeletal defects, including fusion of vertebrae. The notochord role, specifically is still under debate, as classical experiments of notochord ablation (Strudel, 1955; Watterson et al., 1954) resulted in fusion of vertebral bodies. In contrast, in another study in which the notochord was removed, there was no observed effect on the segmented pattern of PAX1 expression in most of the sclerotome, although with exception of the most ventral portion

(Senthinathan et al., 2012). In this chapter, we address the issue of the role of the sclerotome surrounding structures, notochord and dermomyotome, in the formation of the Von Ebner's fissure, as a proxy of segmented vertebrae initial formation.

Materials and methods

Chicken embryos

Fertilized eggs were obtained from commercial sources (Sociedade Agrícola da Quinta da Freiria, Portugal) and incubated until the desired stages in a SMA Coudelou SMA 60 or a Termaks KB8400 incubators in humidified atmosphere and controlled temperature (37.5oC). After incubation, embryos were collected in PBS without Ca2+/Mg2+ and staged according to Hamburger and Hamilton classification system (Hamburger and Hamilton, 1951). Following staging, embryos were fixed overnight at 4ºC in a 4% formaldehyde solution and then progressively dehydrated in methanol series and stored in 100% methanol at -20oC. When necessary, somites were classified according to the conventionally agreed nomenclature (Christ and Ordahl, 1995; Ordahl and Le Douarin, 1992; Pourquie and Tam, 2001).

DAPI staining

Embryos were fixed overnight at 4ºC in a 4% formaldehyde solution, washed in PBS, permeabilized in triton x-100 0.5% and washed in PBS again. Staining was performed through incubation with DAPI (1:500 of the stock solution 2mg/ml) overnight at 4ºC (Sandell et al., 2012) on Nunc 179820 4-well culture dishes (Thermo). Next, embryos were washed again in PBS, post-fixed with paraformaldehyde (0.2%) for 2 hours, rewashed in PBS and slowly dehydrated in methanol through a series of higher concentration solutions for 2 hours. Finally, embryos were transferred to 1.5ml tubes and cleared through incubation with methyl salicylate at room temperature. Mounting was performed in methyl salicylate in MatTek 35mm Glass Bottom Microwell Dishes (P35G-1.5-14-C).

Embryo Imaging

Whole mount in situ hybridization embryos were placed in 1% agar (in distilled water) 60mm petri dishes and imaged in a Zeiss SteREO Lumar.V12 stereomicroscope coupled with a Zeiss MRc5 camera and using Axiovision Rel. 4.8 software. Imaging of sections of in situ hybridization embryos was performed in a Zeiss Axioimager Z2 coupled with a Zeiss ICc3 camera and using Axiovision Rel. 4.8 software. Mounted and

DAPI stained embryos were imaged in an LSM710 confocal microscope (Zeiss) with the ZEN Black software and using the 405nm laser. Z-stack scans of various thicknesses were performed. Image adjustments for brightness/contrast and Von Ebner's fissure assessment through observations of the corresponding stacks were performed using ZEN 3.2 (Lite) or FIJI.

Notochord removal

Chicken embryos were incubated until stages HH12+ to HH14, collected and mounted in the EC culture technique (Chapman et al., 2001). Microsurgery was performed as follows: The embryo was positioned ventrally, and the ectoderm was opened in an area comprising the last 5 to 8 somites and about 10% of the PSM. A few drops of pancreatin (Sigma P1750) were added for 5 to 8 seconds in order to destroy the extracellular matrix around the operated area, facilitating the surgery. After pancreatin action, goat serum (Gibco 16210-072) was added to stop pancreatin's action. The section of notochord removed corresponded to the 4-8 most recently formed somites. Notochord ablation was performed by first doing an incision in the anterior end of the section to be removed with a sharpened tungsten needle. Then, the notochord was pulled by aspiration using a custom-made mouth pipette until the desired length. The embryos were then cultured for 24 hours at 37oC in a New Brunswick Galaxy 48s incubator, after which they were fixed overnight at 4oC in a 4% formaldehyde solution. Finally they were progressively dehydrated in methanol series and stored in 100% methanol at -20oC.

Dermomyotome removal

Eggs were incubated until stages HH13 to HH14, at which embryos were collected and placed dorsal side up on a Petri dish containing a black bottom. A small window was opened in the ectoderm and the dermomyotomes of somites VI to XI were removed using a sharpened tungsten needle. Dermomyotome removal was performed at the right side somites, with the contralateral ones being untouched and used as control. An additional step was performed to counteract the possibility of dermomyotome signal still being present under the form of secreted proteins in the extracellular matrix: After dermomyotome removal, pancreatin (Sigma P1750) was added for 5 to 8 seconds in order to destroy the extracellular matrix around the operated somites. After pancreatin action, goat serum was added to stop pancreatin's action. Embryos were then cultured for 12

hour in 35 mm Petri dishes on over 25mm Polycarbonate filters (0.8 μm; Millipore ATTP02500) floating on top of culture medium composed of Medium199 (Sigma) supplemented with 5% heat inactivated fetal calf serum, 10% chicken serum, 1%L-glutamine and 1% penicillin 5000 IU/ml, 5000 IU/ml. The cultures were done in a New Brunswick Galaxy 48s incubator. After culture, the embryos were fixed in 4% paraformaldehyde (PFA).

RNA probes and Whole mount in situ hybridization

The PAX3 probe (Williams and Ordahl, 1994) plasmid already existed in the lab. Digoxigenin or fluorescein-labelled RNA probes were synthesized using standard techniques of plasmid linearization and transcription as described (Williams and Ordahl, 1994). Whole mount In situ hybridization was performed as described previously (Henrique et al., 1995), with a few modifications: Pre-hybridization and post-hybridization was performed at 70oC instead of 65 oC. Anti-DIG antibodies were used at 1/5000 instead of 1/2000. NBT, BCIP and INT/BCIP were used at 5μl/ml, 3.75μl/ml and 7.5 μl/ml.

Results

Vertebral body's formation implies the process of sclerotome re-segmentation into both an anterior and posterior compartment, separated by the previously described Von Ebner's fissure. In this section we seek to establish the role of sclerotome neighboring structures, such as the medially located notochord and the supra-located dermomyotome, in the formation of Von Ebner's fissure and ultimately of the segmented vertebral bodies, by using modern microscopy techniques.

Von Ebner's fissure starts to form at somite IX

In order to carefully described the dynamics of Von Ebner's fissure formation, whole-mount DAPI stained 30 somites chicken embryos were analyzed by using Confocal Microscopy. The analysis was performed along all the three axes of the embryo and representative sections of the embryo are shown in Figure 2.1. This embryonic stage was chosen as it contains somites at several phases of differentiation.

We analyzed somites 0 to XV (Figure 2.1 A) and found that the fissure can be identified as a cleft that separates the two halves of the sclerotome with a higher cell density shown by a higher fluorescence. As for the onset of fissure formation, we can confirm that it starts to form around somite IX (Figure 2.1 G), around the time the sclerotome is differentiating and performing EMT (Figure 2.1 D). In somite VII we did not observe the presence of any signs of a fissure. Somites IX and X show a fissure, specifically on the medial portion of the sclerotome (Figure 2.1 G). At somite stages XIV to XVI (Figure 2.1 F), as the sclerotome starts to migrate to the vicinity of the notochord (Figure 2.1 C, the fissure is more easily observed. At somite stages XXII to XXIV (Figure 2.1 E, E1-E3) sclerotome cells are migrating to the perinotochordal space surrounding the notochord (Figure 2.1 B). At these stages, the fissure can be seen dividing the sclerotome in two similar sized AP halves and spanning its whole ML extension (Figure 2.1 E, E1-E3). This is of particular importance as this means that, as sclerotome cells surround the notochord, they maintain the segmental pattern acquired with the AP division of the sclerotomes (Figure 2.1 E2). With this description Von Ebner's fissure, the role of the notochord and dermomyotome could now be assessed, using this landmark as a proxy for segmentation of the vertebral bodies.

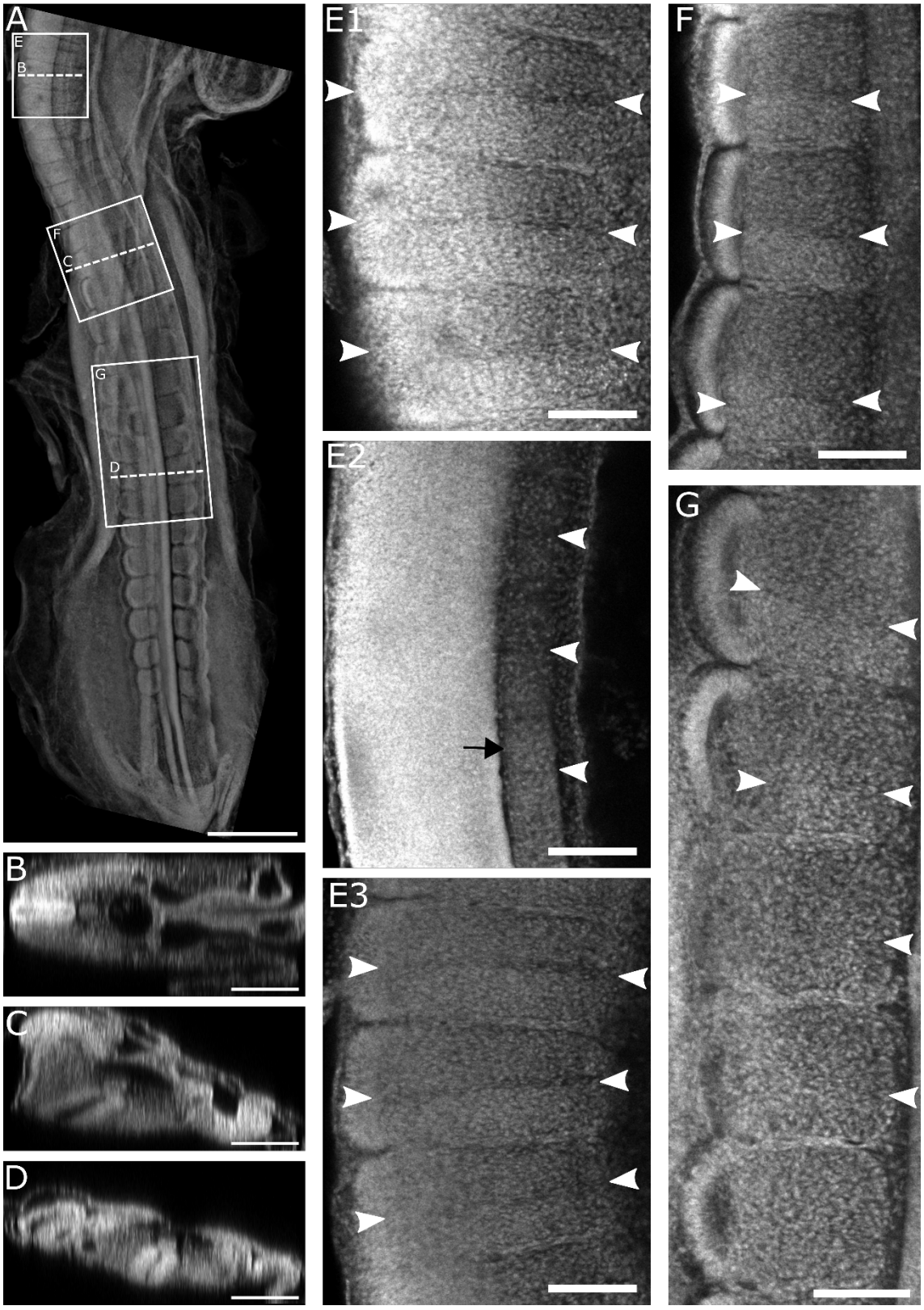
A
E
B
F
C
G
D
B
C
D
E1
E2
E3
F
G

Figure 2.1 Confocal images of a DAPI stained HH17^{-} chick embryo clearly show Von Ebner's fissure.
(A) Average intensity projection of 48 z-stacks showing the entire embryo from the posterior tip of the tail until somite XXV. **(B-D)** XZ projections showing transverse sections corresponding to the axial level of somites XXVII (B), XXII (C) and XII (D). **(B)** Transverse section of embryo in A at the axial level of somite XXVII showing migrating sclerotome cells already invading the perinotochordal space. **(C)** Transverse section of embryo in A at the axial level of somite XXII showing sclerotome cells starting to migrate to the perinotochordal space. **(D)** Transverse section of embryo in A at the axial level of somite XII showing migrating differentiating sclerotome cells. **(E1-E3)** Three different coronal plane sections of embryo in A showing the whole length of Von Ebner's fissure along somites XXII to XXIV. Due to the turning of the embryo, the sections shown here are distributed along the ML plane, showing the fissure on the left somites, axial position where the notochord is located and right somites (white arrowheads or between white arrowheads). Notice that at the level of the notochord (black arrow), the fissures are still observable on the somites that are surrounding the notochord in the perinotochordal space. The fissure is identifiable in the whole ML extension of these three sclerotomes. **(F)** Coronal plane sections of embryo in A showing somites XIV to XVI. Von Ebner's fissure is clearly observable (between white arrowheads) in the whole ML extension of these three sclerotomes. **(G)** Coronal plane sections of embryo in A showing somites VIII to XII. Von Ebner's fissure is observable the whole ML extension of the sclerotomes of somites XI and XII (between white arrowheads), on the medial part of the sclerotomes of somites IX and X (white arrowheads) and not observable on the sclerotome of somite VIII. The embryo in A is shown dorsal side up.
Scale bars: 500μm for A, 200μm for B-D and 100μm for E-G.

Notochord removal does not impair Von Ebner's fissure formation

Previous works in which surgical removal of the notochord in chicken embryos were performed resulted in fusion of the vertebral bodies (Strudel, 1955; Watterson et al., 1954). On the other hand, similar experiments did not alter the segmented expression pattern of PAX1 on sclerotome (Senthinathan et al., 2012). As such, in order to clarify the role of the notochord on the formation of Von Ebner's fissure, used as a proxy for segmented vertebral body initial formation, we designed and produced notochord removal experiments.

Chicken eggs were incubated until embryo stages HH12^{+} to HH14 and the notochord was microsurgically ablated in a section corresponding to the 4 to 8 most recently formed somites (somites without Von Ebner's fissure) (Figure 2.2 A). The absence of notochord could be easily observable immediately after the procedure (Figure 2.2 B). After 24 hours of incubation the effect of notochord removal on Von Ebner's fissure formation was assessed by using confocal microscopy on DAPI stained operated embryos. As previously described by (Charrier et al., 1999), we observed the formation of an enlarged structure comprised of an accumulation of notochord cells at the caudal end of the remainder

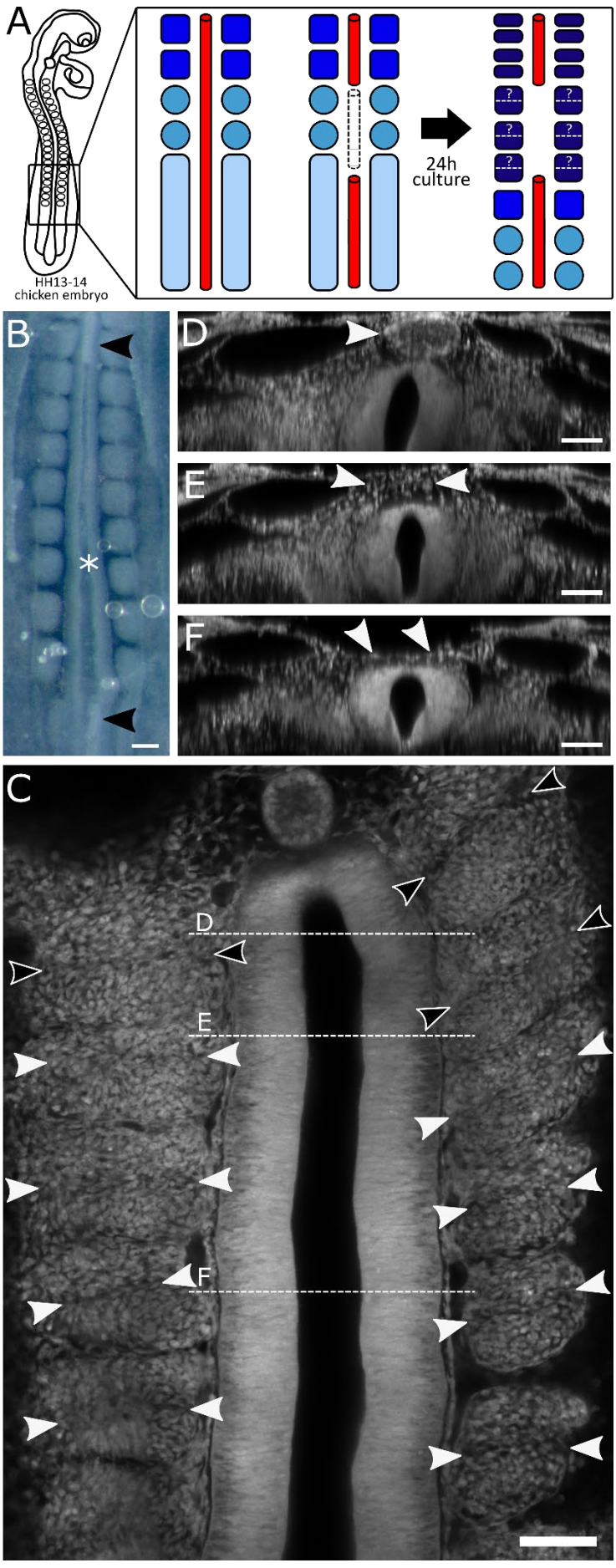
A
HH13-14
chicken embryo
24h
culture
B
D
E
F
C
D
E
F

Figure 2.2 Notochord surgical removal does not impair Von Ebner's fissure formation
(A) Schematic representation of the notochord removal experiments performed on chicken embryos of stages HH12+-14. A portion of notochord was surgically removed next to the most recently formed 4 to 8 somites. After 24h of culture, notochord removal effect is assessed. (B) HH12+ embryo immediately after notochord removal (white asterisk) next to the 8 most recently formed somites. The margins of the remaining notochord are shown (black arrowheads). (C) DAPI staining of the embryo in B after culture showing Von Ebner's fissure present in the somites located next to the operated area (white arrowheads). Fissures on the somites next to the unoperated section of the notochord are also shown (black arrowheads). (D-F) XZ projections showing transverse sections corresponding to the axial level of different somite: (D) Next to a rostral unoperated level still showing the presence of the notochord (white arrowhead); (E) Next to an operated area with a more rostral position; (F) Next to an operated area with a more caudal position. Note that a few sclerotome cells can be observed in the area where the notochord would be, white arrowheads in E and F.
Embryo in A is shown dorsal side up. Embryos in B-F are shown ventral side up. Scale bars: 100μm for A, 50μm for C-F.

cranial portion of the notochord (Figure 2.2 D). This mass of notochord cells extends beyond the cut point, which could mean that somites close to the limit of surgery area, could have received notochord signals due to this extension. To control for this, we always assessed the presence of notochord by looking at the XZ projections showing the transverse section of each axial level (Figure 2.2 D-E). Surprisingly, in the five embryos analyzed, Von Ebner's fissure was present in all somites, even in those whose sclerotomes developed in the absence of notochord (Figure 2.2 C). Additionally, we could observe some sclerotome cells in the axial position where the notochord would be, ventrally to the neural tube (Figure 2.2E, F).

Dermomyotome removal does not impair Von Ebner's fissure formation and/or maintenance

Several mutations in mouse muscle genes expressed in the dermomyotome such as Myf5 (Braun et al., 1992) and MyoD (Rot-Nikcevic et al., 2006) result in vertebral defects including vertebral fusions. This led us to consider the role of the dermomyotome in the formation of segmented vertebral bodies in amniotes, like the chicken. As so, we designed and produced experiments for testing this hypothesis, similar to the ones designed to assess the role of the notochord (Figure 2.3 A).

Chicken eggs were incubated until embryo stages HH13 to HH14. In these embryos, since we observed the onset of formation of Von Ebner's fissure from somite stage IX, we performed dermomyotome removal experiments on somites VI (first presenting a dermomyotome) to XI (Figure 2.3 B). This way, we could assess if dermomyotome ablation

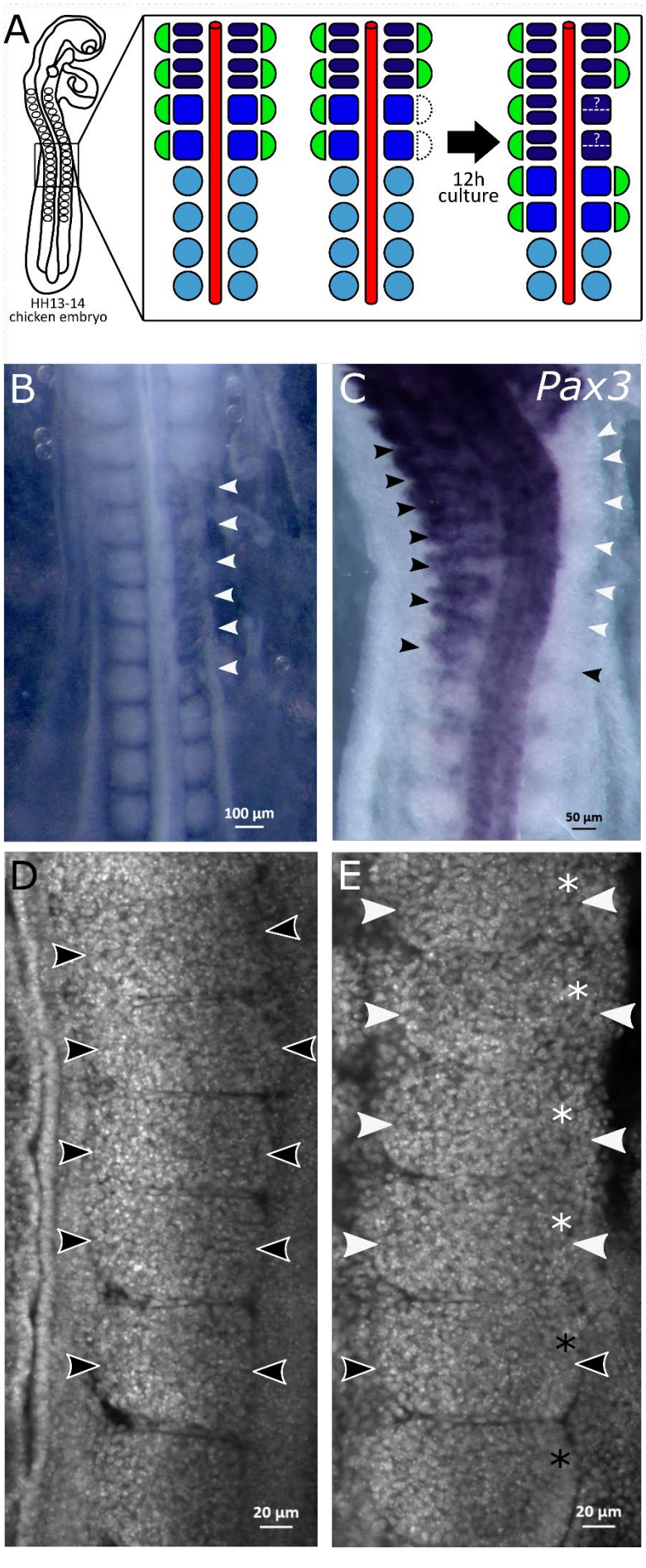
A
HH13-14
chicken embryo
12h
culture
?
?
B
100 µm
C
Pax3
50 µm
D
20 µm
E
20 µm

Figure 2.3 Dermomyotome removal does not impair Von Ebner's fissure formation
(A) Schematic representation of the dermomyotome removal experiments performed on chicken embryos of stages HH13-14. The dermomyotomes were microsurgically removed from somites VI (the first presenting a dermomyotome) to somite XI, in the absence (n=4) and in the presence (n=5) of pancreatin. After 12h of culture, dermomyotome removal effect was assess. (B) HH13 embryo immediately after dermomyotomes removal from right-side somites VI to XI (white arrowheads). (C) In situ hybridization for PAX3 (dermomyotome marker) of embryo in B after 12h of culture, showing complete removal of the dermomyotomes (white arrowheads). The contralateral left side somites and the somite pair located posteriorly to the operated ones shows normal PAX3 staining (black arrowheads). (D) DAPI staining of the control somites of embryo in C showing presence of Von Ebner's fissure in all sclerotomes (black arrowheads). (E) DAPI staining of the operated embryo in C showing presence of Von Ebner's fissure in the sclerotomes of four of the operated somites (white arrowheads). Dermomyotome absence can be observed on the operated somites (white asterisks) as opposed to the two posteriorly non-operated ones (black asterisks).
All embryos are shown dorsal side up.

has an effect on Von Ebner's fissure formation (operation on somites VI to VIII, before fissure formation) and/or maintenance (operation on somites IX to XI, after the onset of fissure formation). To ensure the total removal of dermomyotome, we performed PAX3 *in situ* hybridizations on all operated embryos (Figure 3.2 C).

Initial results showed that Von Ebner's fissure was still present in all somites of four operated embryos (data not shown). However, since these ablations were performed mechanically, i.e., with no proteolytic enzymes, there was the possibility that the dermomyotome signal could still be present under the form of secreted proteins in the extracellular matrix. To assess for this possibility, we added an additional step to the protocol, by treating the operated embryos with pancreatin. However, even in this more stringent condition, Von Ebner's fissure formation occurs in the absence of the dermomyotome, in all embryos analyzed (n=5) (Figure. 2.3 compare D with E).

Discussion

Von Ebner's fissure imaging analysis reveals new and interesting details

Von Ebner's fissure, much like the concept of resegmentation itself was still under heavy debate up until the end of the 20th century (Verbout, 1976). At this time, the fissure was regarded by some authors as a mere artifact of fixation and, as such, an invalid argument supporting resegmentation. In the following years, mainly due to the implementation of lineage tracing techniques such as the quail-chick chimaera system (Le Douarin, 1973) or the use of carbocyanine dyes (Ward et al., 2017), the resegmentation hypothesis was proven to be true (for a more detailed review on the subject, see section 4 of the introduction). Von Ebner's fissure was also proven to exist in chicken embryos thanks to several works performed by key authors such as Bodo Christ (Christ and Wilting, 1992) and Claudio Stern (Stern and Keynes, 1987). To do so, these authors used both light and electron microscopy, producing excellent images that prove the existence of the fissure unequivocally, while at the same time confirming the accuracy of the stunning drawings of previous authors like Von Ebner (Von Ebner, 1888). However, since we intended to use Von Ebner's fissure as a proxy for the initial steps of vertebral body segmentation, we decided to do a thorough study of Von Ebner's fissure on several somite stages using more modern microscopy techniques such as confocal microscopy of DAPI stained embryos (Sandell et al., 2012). This technique offered great advantages, as the fissure is more easily identifiable, since all section planes are contained within one single image, making it easier to navigate between all different coronal planes. Additionally, this allows for the observation of the transverse sections of the embryos through XZ projections, as well as sagittal sections through YZ projections. Our results yielded interesting findings and previously unpublished information:

1) In the four most anterior somites, we never identify Von Ebner's fissure (data not shown). This new finding is not surprising as it is already described that, in the chicken embryo, the first four somites do not contribute to vertebrae formation. In fact, the most anterior four somites, together with the anterior half of the fifth somite, give rise to the basioccipital skeletal elements of the skull (Huang et al., 2000; Maschner et al., 2016). The posterior half of the fifth somite, together with the anterior compartment of the sixth somite, form the first vertebra, the atlas. Importantly, this finding reinforces the

relationship between Von Ebner's fissure and the process of segmented vertebrae formation.

2) Our confocal analysis on DAPI stained embryos reveal the presence of the Von Ebner's fissure from the most lateral part of the sclerotome to the vicinity of the notochord. This is of particular importance as it suggested that, as sclerotome cells surround the notochord, they maintain the segmental pattern acquired with the AP division of the sclerotomes. However, it was previously described that Von Ebner's fissure did not extend all the way to the axial region of the embryo (Christ and Wilting, 1992). We suggest that the discrepancy of these observations could be explained by differences of analyzed embryo stages, since the 30 somite embryos we used in our work are slightly younger than the 3-day older embryos used in Christ's work. To clarify this matter, we suggest the use of DAPI staining in progressively older embryos and a thorough analysis of all the section planes and axial levels.

3) On somites IX and X, the fissure is only identifiable in the medial portion of the sclerotome, leading us to suggest that fissure formation starts in the medial side of the sclerotome. This is in accordance with the original drawings of Von Ebner (Von Ebner, 1888) that shows the fissure appearing first only in the medial part of the sclerotome. Since this work was performed in reptile embryos if our hypothesis is correct, that would mean that this feature could be conserved among different animal species.

Notochord role on segmented vertebral body formation: what we know so far

Shortly after our notochordal and dermomyotome removal experiments were performed, a study also conducting notochord ablation experiments was published (Ward et al., 2018). In this study, the authors use an ingenious procedure for notochord ablation *in ovo* on HH12-13, allowing embryos to develop until the vertebral bodies are formed. With this, they observed vertebral body fusion in the regions where the notochord was ablated. Taking into account our results, we suggest that, in their experiments, the effect of notochord ablation in vertebrae segmentation occurs following the development of Von Ebner's fissure, i.e., after the process of resegmentation. If this is the case, vertebral body segmentation is initiated by an intrinsic sclerotome segmented signal and the notochord is only necessary for the later maintenance of this pattern. Curiously, it has

been already showed that the notochord plays an important role on somite segmentation, through the expression of Shh and upregulation of its receptor Patched1 in neighboring PSM cells, at the level of the determination front (Resende et al., 2010).

In conclusion, this and other works, lead us to propose that 1) the notochord plays an important role on the establishment of the segmented pattern of PSM cells, 2) Von Ebner's fissure formation, as a proxy of vertebral body resegmentation, is only dependent on a segmented signal present within the sclerotome structure, and totally independent from neighboring tissues (notochord and dermomyotome), 3) the notochord is important to drive cells migration to its vicinity and 4) later on in development the notochord tissue seems to be essential to prevent vertebral body fusion.

Importantly, this points out to a huge difference between notochord properties in the teleosts, like the zebrafish, in which vertebrae body segmentation relies on a segmented signal present in the notochordal sheath, and vertebrates, like the chicken, in which segmental information seems to be totally confined to the sclerotome cells.

References

Aoyama, H. and Asamoto, K. (2000). The developmental fate of the rostral/caudal half of a somite for vertebra and rib formation: experimentl confirmation of the resegmentation theory using chick-quail chimeras. *Mech Dev* **99**, 71-82.

Bagnall, K., Higgins, S. and Sanders, E. (1988). The contribution made by a single somite to the vertebral column: experimental evidence in support of resegmentation using the chick-quail chimaera model. *Development* **103**, 69-85.

Bensimon-Brito, A., Cancela, M. L., Huysseune, A. and Witten, P. E. (2012). Vestiges, rudiments and fusion events: the zebrafish caudal fin endoskeleton in an evo-devo perspective. *Evol Dev* **14**, 116-127.

Braun, T., Rudnicki, M. A., Arnold, H.-H. and Jaenisch, R. (1992). Targeted inactivation of the muscle regulatory gene Myf-5 results in abnormal rib development and perinatal death. *Cell* **71**, 369-382.

Chapman, S. C., Collignon, J., Schoenwolf, G. C. and Lumsden, A. (2001). Improved method for chick whole-embryo culture using a filter paper carrier. *Developmental dynamics: an official publication of the American Association of Anatomists* **220**, 284-289.

Charrier, J. B., Teillet, M. A., Lapointe, F. and Le Douarin, N. M. (1999). Defining subregions of Hensen's node essential for caudalward movement, midline development and cell survival. *Development* **126**, 4771-4783.

Christ, B., Huang, R. and Scaal, M. (2004). Formation and differentiation of the avian sclerotome. *Anat Embryol (Berl)* **208**, 333-350.

Christ, B. and Ordahl, C. P. (1995). Early stages of chick somite development. *Anat Embryol (Berl)* **191**, 381-396.

Christ, B. and Wilting, J. (1992). From somites to vertebral column. *Annals of Anatomy - Anatomischer Anzeiger* **174**, 23-32.

Ebensperger, C., Wilting, J., Brand-Saberi, B., Mizutani, Y., Christ, B., Balling, R. and Koseki, H. (1995). Pax-1, a regulator of sclerotome development is induced by notochord and floor plate signals in avian embryos. *Anatomy and embryology* **191**, 297-310.

Fleming, A., Keynes, R. and Tannahill, D. (2004). A central role for the notochord in vertebral patterning. *Development* **131**, 873-880.

Hamburger, V. and Hamilton, H. L. (1951). A series of normal stages in the development of the chick embryo. *J Morphol* **88**, 49-92.

Henrique, D., Adam, J., Myat, A., Chitnis, A., Lewis, J. and Ish-Horowicz, D. (1995). Expression of a Delta homologue in prospective neurons in the chick. *Nature* **375**, 787-790.

Huang, R., Zhi, Q., Patel, K., Wilting, J. and Christ, B. (2000). Contribution of single somites to the skeleton and muscles of the occipital and cervical regions in avian embryos. *Anat Embryol (Berl)* **202**, 375-383.

Jacob, M., Jacob, J. H. and Christ, B. (1975). [The early differentiation of the perinotochordal connective tissue. A scanning and transmission electron microscopic study on chick embryos (author's transl)]. *Experientia* **31**, 1083-1086.

Le Douarin, N. (1973). A biological cell labeling technique and its use in experimental embryology. *Developmental biology* **30**, 217-222.

Lleras Forero, L., Narayanan, R., Huitema, L. F., VanBergen, M., Apschner, A., Peterson-Maduro, J., Logister, I., Valentin, G., Morelli, L. G., Oates, A. C.,

et al. (2018). Segmentation of the zebrafish axial skeleton relies on notochord sheath cells and not on the segmentation clock. *Elife* **7**.

Maschner, A., Kruck, S., Draga, M., Prols, F. and Scaal, M. (2016). Developmental dynamics of occipital and cervical somites. *J Anat* **229**, 601-609.

Ordahl, C. and Le Douarin, N. (1992). Two myogenic lineages within the developing somite. *Development* **114**, 339-353.

Pais de Azevedo, T. P., Witten, P. E., Huysseune, A., Bensimon-Brito, A., Winkler, C., To, T. T. and Palmeirim, I. (2012). Interrelationship and modularity of notochord and somites: a comparative view on zebrafish and chicken vertebral body development. *Journal of Applied Ichthyology* **28**, 316-319.

Pourquie, O. and Tam, P. P. (2001). A nomenclature for prospective somites and phases of cyclic gene expression in the presomitic mesoderm. *Dev Cell* **1**, 619-620.

Remak, R. (1855). *Untersuchungen über die Entwicklung der Wirbelthiere*: Reimer.

Resende, T. P., Ferreira, M., Teillet, M. A., Tavares, A. T., Andrade, R. P. and Palmeirim, I. (2010). Sonic hedgehog in temporal control of somite formation. *Proc Natl Acad Sci U S A* **107**, 12907-12912.

Rot-Nikcevic, I., Reddy, T., Downing, K. J., Belliveau, A. C., Hallgrímsson, B., Hall, B. K. and Kablar, B. (2006). Myf5−/−: MyoD−/− amyogenic fetuses reveal the importance of early contraction and static loading by striated muscle in mouse skeletogenesis. *Development genes and evolution* **216**, 1-9.

Sandell, L. L., Kurosaka, H. and Trainor, P. A. (2012). Whole mount nuclear fluorescent imaging: convenient documentation of embryo morphology. *Genesis* **50**, 844-850.

Senthinathan, B., Sousa, C., Tannahill, D. and Keynes, R. (2012). The generation of vertebral segmental patterning in the chick embryo. *J Anat* **220**, 591-602.

Smits, P. and Lefebvre, V. (2003). Sox5 and Sox6 are required for notochord extracellular matrix sheath formation, notochord cell survival and development of the nucleus pulposus of intervertebral discs. *Development* **130**, 1135-1148.

Stern, C. D. and Keynes, R. J. (1987). Interactions between somite cells: the formation and maintenance of segment boundaries in the chick embryo. *Development* **99**, 261-272.

Strudel, G. (1955). L'influence morphogene du tube nerveux et de la corde sur la differenciation de la colonne vertebrale et de sa musculature chez l'embryon de poulet. **149**, 188-190.

Verbout, A. (1976). A critical review of the 'neugliederung'concept in relation to the development of the vertebral column. *Acta biotheoretica* **25**, 219-258.

Von Ebner, V. (1888). Urwirbel und neugliederung der wirbelsäule. *Sitzungsber Akad Wiss Wien* **3**, 194-206.

Ward, L., Evans, S. E. and Stern, C. D. (2017). A resegmentation-shift model for vertebral patterning. *Journal of Anatomy* **230**, 290-296.

Ward, L., Pang, A. S. W., Evans, S. E. and Stern, C. D. (2018). The role of the notochord in amniote vertebral column segmentation. *Dev Biol* **439**, 3-18.

Watterson, R. L., Fowler, I. and Fowler, B. J. (1954). The role of the neural tube and notochord in development of the axial skeleton of the chick. *Am J Anat* **95**, 337-399.

Williams, B. A. and Ordahl, C. P. (1994). Pax-3 expression in segmental mesoderm marks early stages in myogenic cell specification. *Development* **120**, 785-796.

Wopat, S., Bagwell, J., Sumigray, K. D., Dickson, A. L., Huitema, L. F. A., Poss, K. D., Schulte-Merker, S. and Bagnat, M. (2018). Spine Patterning Is Guided by Segmentation of the Notochord Sheath. *Cell Rep* **22**, 2026-2038.

Chapter III – Cell fate decision between Axial and Paraxial mesoderm: The role of CNOT2

Mr. Kim: We're Starfleet officers. 'Weird' is part of the job (Captain Janeway)
In *Star Trek: Voyager (1995-2001)*

Do. Or do not. There is no try. (Master Yoda)
In *Star Wars: The Empire strikes back (1980)*

Introduction

Vertebrate embryo development is a very coordinated process with different cells originating very different tissues. One of the first events in which cells commit to a specific developmental fate is gastrulation. In this process, two layers of cells originate the three germ layers, ectoderm, mesoderm and endoderm (Barresi2020). Cell fate decision between these different outcomes depends upon the expression of different transcription factors. Crucial for normal development is the fate decision between mesoderm (that originates bone and muscle tissue, among others) and neural ectoderm (originating neural tissues). Knowledge on this issue was greatly increased with the discovery of an embryonic area within the tailbud of mouse embryos containing cells that can originate both mesoderm and neuroectoderm, the NMPs (Tzouanacou et al., 2009). Since then, these cells have been described to be present in the tailbud of embryos of several species like zebrafish (Martin and Kimelman, 2012), chicken (Guillot et al., 2021), and human (Olivera-Martinez et al., 2012). While many recent studies have dedicated themselves to explore the biology of the NMPs, there is much less information on cell fate decision within the mesodermal layer.

The mesoderm gives rise to many different tissues, two of them being playing key roles in vertebral body development, the notochord and the somites (Pais de Azevedo et al., 2012). The notochord is the first axial skeleton of the embryo, having important structural and functional roles in development (Corallo et al., 2015). Somites are spheres of epithelial cells that form in pairs flanking the notochord on each side. They are formed through sequential MET of mesenchymal cells that form the unsegmented PSM (Martins et al., 2009). This process is tightly regulated through the existence of the embryonic clock (Pais de Azevedo et al., 2018). The notochord and the somites/PSM represent two types of mesodermal tissues, the axial and paraxial mesoderm, respectively. What is known about cell fate decision between the axial and paraxial mesoderm ?

In the zebrafish embryo mutant floating head the notochord is totally absent from the embryo, being completely replaced by somitic tissue (Halpern et al., 1995; Talbot et al., 1995). In another mutant, spadetail, cells that would normally originate PSM and muscle, were observed to translocate to the notochord (Kimmel et al., 1989). It was later discovered (Amacher and Kimmel, 1998) that, in the notochord progenitor region of zebrafish embryos, flh represses spt that would normally activate PSM and muscle genes,

leading cells to originate notochord. The importance of flh and spt also corroborated in studies performed for other vertebrate models such as Xenopus (Fukuda et al., 2010; Gont et al., 1993) and mouse (Yamanaka et al., 2007).

In the chicken there are two very close orthologs of flh and spt, CNOT2 (Stein et al., 1996b), and TBX6L (Griffin et al., 1998; Ruvinsky et al., 1998), respectively. These two genes are expressed in the notochord and PSM progenitor regions of chicken embryos, but their functional role is not yet known. In this chapter we address if CNOT2 and TBX6L have a role in axial/paraxial mesoderm cell fate decision in the chicken embryo.

Materials and methods

Chicken embryos

Fertilized eggs were obtained from commercial sources (Sociedade Agrícula Quinta da Freiria or Pintobar Exploração Avícula Lda, Portugal) and incubated until the desired HH stages (Hamburger and Hamilton, 1951)in a SMA Coudelou SMA 60 or a Termaks KB8400 incubators in humidified atmosphere and controlled temperature (37.5ºC).

After incubation, embryos were collected in PBS without $Ca2^{+}$/$Mg2^{+}$ and staged according to Hamburger and Hamilton classification system (Hamburger and Hamilton, 1951). When necessary, somite staging was performed using the conventionally agreed nomenclature (Christ and Ordahl, 1995; Ordahl and Le Douarin, 1992; Pourquie and Tam, 2001), as follows: The forming somite is designated S0, just like the last somites to be formed are called SI, SII, SIII, ect. (highest number being the oldest to have been formed), and the next to start to be formed are S-I, S-II, S-III, etc (the lowest number being the one to be formed immediately next).

Following staging, embryos were fixed overnight at 4ºC in a 4% formaldehyde solution and then progressively dehydrated in methanol series and stored in 100% methanol at -20ºC.

RNA probes

Plasmids containing CNOT2, TBX6L, and FOXA2 probes were kindly provided by Michael Kessel, Susan Mackem and Claudio Stern (Knezevic et al., 1997; Ruiz i Altaba et al., 1995; Stein et al., 1996b). SHH probe plasmid already existed in the lab having been produced according to (Riddle et al., 1993). Digoxigenin or fluorescein-labelled RNA probes were synthesized using standard techniques of plasmid linearization and transcription as described (Knezevic et al., 1997; Riddle et al., 1993; Ruiz i Altaba et al., 1995; Stein et al., 1996b).

Whole mount in situ hybridization

Whole mount *In situ* hybridization was performed as described previously (Henrique et al., 1995), with a few modifications: Pre-hybridization and post-hybridization was performed at 70ºC instead of 65 ºC. Anti-DIG antibodies were used at 1/5000 instead of 1/2000. NBT, BCIP and INT/BCIP were used at 5µl/ml, 3.75µl/ml and 7.5 µl/ml.

Double whole mount *In situ* hybridization was performed as described previously (Freitas et al., 2001).

Cryoembedding and histology

Selected embryos were embedded in 15% sucrose, 7.5% gelatin, frozen in liquid nitrogen or dry ice and sectioned (14 mm) in a Thermo CryoStar NX50 cryostat. After drying, sections were washed in PBS and distilled water for gelatin removal and mounted in Aquatex® (Merck)

Construct production

The pCAT expression plasmid already existed in the lab. It was previously generated by cloning the IRES-MCS region from a pIRES2-GFP (Clontech) into pCAGGS-AFP (kindly provided by Tsuyoshi Momose) pCAT-CNOT2 and were generated from insertion of the CNOT2 in the MCS of pCAT.

Embryo electroporation

HH4-5 embryos were collected and set up for the Early Chick (EC) culture, by being placed in filter paper carriers as described in (Chapman et al., 2001). The electroporation (Figure 3.1) was performed as described in (Voiculescu et al., 2008), with a few adjustments. After culture setup, the embryo was placed ventral side up in an electrode chamber (CUY700-P2E, NEPA GENE) filled with Tyrode's saline. A solution containing 0.2-0.5µl of fast green (0.4% wt/v) and either 0.2-2 mg/µl of pCAT (henceforth designated pCAT-empty) or pCAT-CNOT2 (Figure 3.1 B) was loaded onto glass needles prepared from glass capillaries (World Precision Instruments TW100F-4) using a puller (SUTTER INSTRUMENT CO., Model P-87, Flaming/Brown

Micropippete) with the following settings: Time: 150; Heat: 720; Pull: 75; Velocity: 60). Embryos in the filter paper were injected with this solution in an area of the node corresponding to the location of axial and paraxial mesoderm progenitors (Figure 3.1 B), using an IM 300 (Narishige Japan) microinjector. Immediately after, five 50 ms pulses of 10 V, with an interval of 350 ms were applied using the eletroporator BTX ECM 830, Eletro Square Porator (Harvard Apparatus). The embryo was then processed following the rest of EC culture procedure and cultured for 12-24h at 37ºC in a New Brunswick Galaxy 48s incubator. After culture, embryos were assessed for their morphology and fluorescence and imaged as described below, finally being fixed and stored as described earlier.

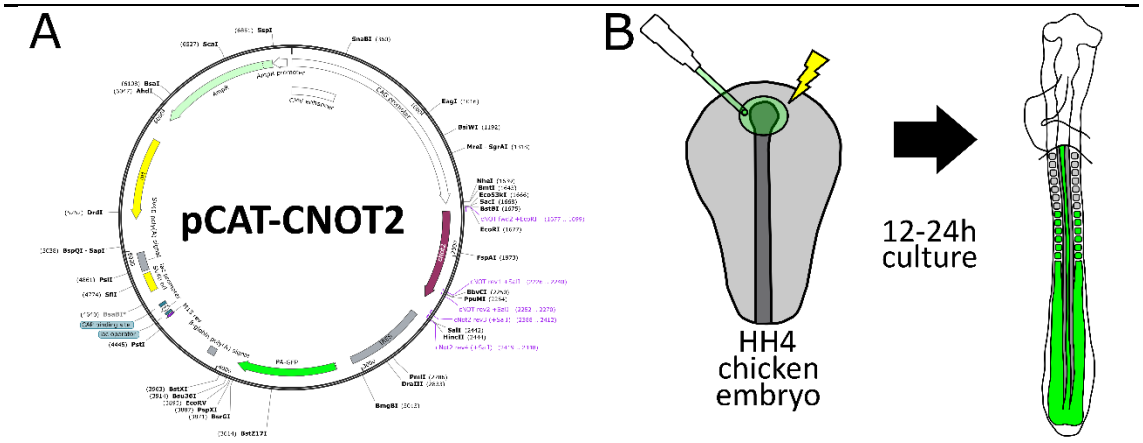

Figure 3.1. Electroporation of pCAT-CNOT2 in HH4 chick embryos results in CNOT2 gene upregulation in electroporated cells.
(A) Schematic representation of pCAT-CNOT2 construct used in the electroporation experiments. **(B)** Schematic representation of the electroporation experiments performed. HH4 chicken embryos were electroporated with pCAT empty vector or pCAT-CNOT2 construct in the node region corresponding to the location of axial and paraxial mesoderm progenitors. Embryos were then cultured for 12 to 24 hours.

Sample imaging

Whole mount *in situ* hybridization embryos were placed in 1% agar (in distilled water) 60mm petri dishes and imaged in a Zeiss SteREO Lumar.V12 stereomicroscope coupled with a Zeiss MRc5 camera and using Axiovision Rel. 4.8 software. Imaging of sections of *in situ* hybridization embryos was performed in a Zeiss Axioimager Z2 coupled with a Zeiss ICc3 camera and using Axiovision Rel. 4.8 software.

Embryo measuring, image and statistical analysis

Images were adjusted for brightness/contrast and embryo measurements were performed in the Zeiss Zen 3.2 (blue edition) software. Four measurements were performed: 1) Head Fold (HF), corresponding to the length between the anterior tip of the embryo and the head fold, 2) Segmented (Seg), corresponding to the length from the anterior border of the most anterior somite to the posterior border of the most posterior somite, 3) Presomitic mesoderm (PSM), corresponding to the length between the posterior border of the most posterior somite and the node and 4) Total Trunk (TT), corresponding to the sum of Seg and PSM (see methods section in chapter IV for more details on HF, Seg and PSM).

A Mann–Whitney U test was performed for the four measurements described, comparing two conditions: Electroporated with pCAT-empty vector and electroporated with pCAT-CNOT2, using IBM SPSS Statistics 28.0.

Results

CNOT2 and TBX6L have slightly overlapping patterns in the chicken axial/paraxial mesoderm

In order to search for a possible function of CNOT2 and TBX6L on the decision between axial and paraxial mesoderm fates, we decided to perform our own analysis of their expression pattern in the chicken embryo. As previously described, we observed that at stage HH13$^-$ CNOT2's expression territory begins in the anterior part of the CNH (where notochord progenitor cells are located) and spans to the posterior notochord, fading well before the level of the first somites (Figure 3.2 A). As for TBX6L, it is expressed in the posterior part of HN and very strongly in the PSM territory (Figure 3.2 B). It was previously described that PSM expression starts to disappear while the first somites are being formed, remaining in the medial portion of the two to three newly formed somites. However we found out that, when the NBT-BCIP color reaction was further developed, the expression extended to the 7 to 8 most recently formed somites (Supplementary figure 3.1).

Because we detected a complementary expression of both genes, we decided to perform double in situ hybridizations on several stages of the first three days of development (Figure 3.3). Interestingly, we found that, from as early as HH1, and throughout the stages analyzed, the two genes are expressed in the presumptive axial and paraxial mesoderm territories, with a small overlap region. In HH1 (Figure 3.3 A), both genes are expressed in the posterior portion of the blastoderm, CNOT2 anteriorly to TBX6L with an overlap region between both territories. HH4 shows CNOT2 expressed in HN and the most anterior part of the PS, while TBX6L is expressed in the most posterior area of HN (slightly overlapping with the CNOT2 expression domain) and the whole PS (Figure 3.3 B). HH13 embryos show the expression pattern previously described for HH13$^-$ with the CNOT2/TBX6L overlap region in the tailbud (Figure 3.3 C), where axial/paraxial mesoderm progenitors are located.

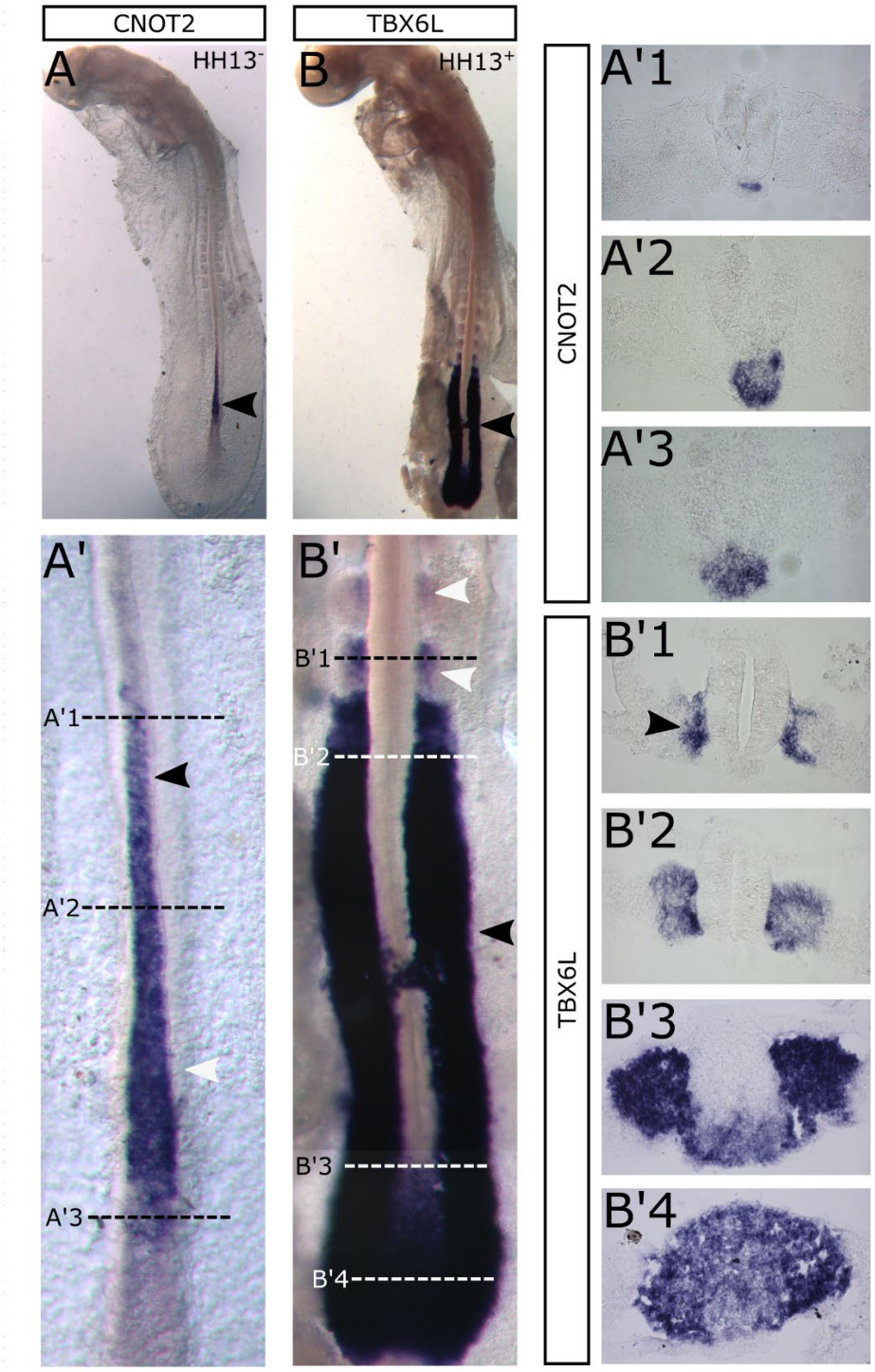

Figure 3.2. CNOT2 and TBX6L are expressed in the chick axial and paraxial mesoderm and their progenitor regions, respectively.
(A, A') HH13$^-$ chick embryo showing CNOT2 expression in the anterior part of the node, and posterior notochord facing the PSM (white arrowhead in A'). Expression in the notochord fades anteriorly (black arrowhead in A'). **(A'1-A'3)** 25µm transverse sections of embryo in A'. **(B, B')** HH13$^+$ chick embryo showing TBX6L expression in the posterior half of the node, PSM progenitors and PSM (black arrowhead). Expression starts to disappear with somites being formed, remaining in the two to three most recently formed somites (somites I to III) (white arrowheads). **(B'1-B'4)** 14µm transverse sections of embryo in B'. In the most recently formed somites, expression is restricted to their medial portions (black arrowhead in B'1).

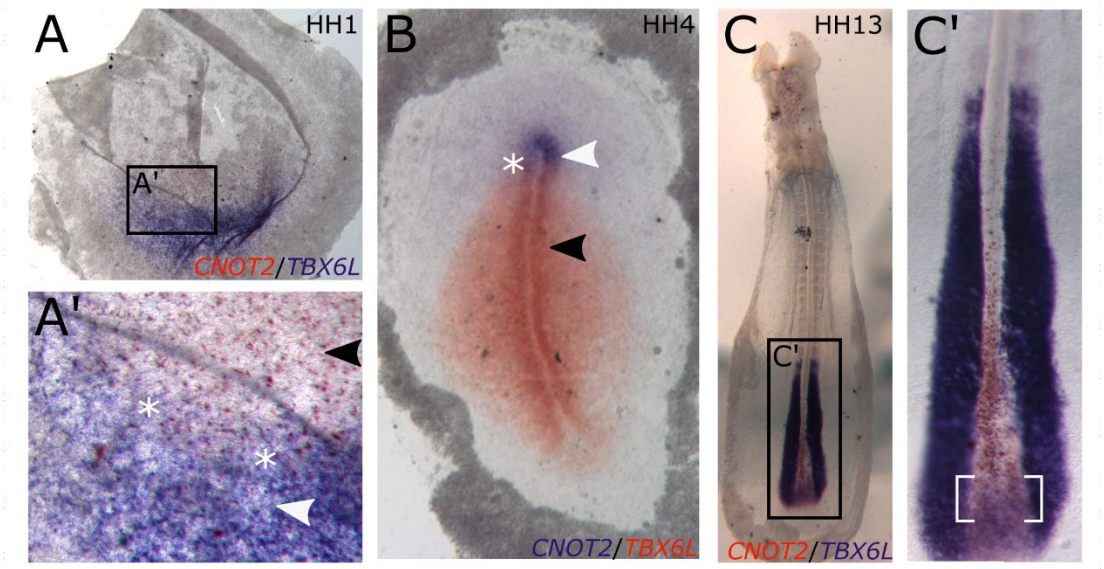

Fig. 3.3. CNOT2 and TBX6L have complementary expression patterns with an overlap region in the axial/paraxial mesoderm progenitor zone.
Double in situ hybridization of CNOT2 and TBX6L in chick embryos of stages HH1 to HH13. **(A, A')** HH1 chick embryo showing CNOT2 expression (red orange) and TBX6L (purple blue) in the posterior end of the epiblast. CNOT2 (black arrowhead in A') is expressed anteriorly to TBX6L (white arrowhead in A') with a small overlap region (white asterisks in A'). **(B)** HH4 chick embryos showing CNOT2 (purple blue) in Hensen's Node and most anterior primitive streak (white arrowhead) and TBX6L (red orange) expression in the most posterior portion of Hensen's Node and the whole primitive streak (black arrowhead). As in A, there is a small overlap area in the most posterior zone of the node and most anterior part of the primitive streak (white asterisk). **(C, C')** HH13 chick embryo showing the complementary expression patterns of CNOT2 (red orange) and TBX6L (purple blue) in the posterior half of the embryo. Note the overlap region of expression in the tailbud (between white brackets).

Upregulation of CNOT2 expression in axial/paraxial progenitors produces several effects on chick embryo development

The overlap of the previously described CNOT2/TBX6L's expression patterns and the phenotypes of their mutations in zebrafish are consistent with a role of these genes in the determination of the chick axial/paraxial mesodermal fate. In order to investigate this possible function, we produced expression constructs of CNOT2 (Figure 3.4 A), henceforth designated pCAT-CNOT2. Chick embryos at stages HH4 and 5 were electroporated in a region corresponding to Hensen's node/anterior tip of the primitive streak (the APH), which contain the progenitor cells of the axial and paraxial mesoderm (Charrier et al., 1999; Selleck and Stern, 1991; Solovieva et al., 2022) (Figure 3.4 B). To test the success of the electroporation we performed in situ hybridizations for CNOT2. We found that 1) pCAT-CNOT2 electroporation led to ectopic expression of CNOT2 in

both the PSM and the somites, corresponding to areas of high fluorescence (Figure 3.4 C D) and 2) There was an overexpression of CNOT2 in the axial mesoderm region, as this expression extends anteriorly to the regions flanking the PSM, progressing through the somitic area, and eventually reaching the head.

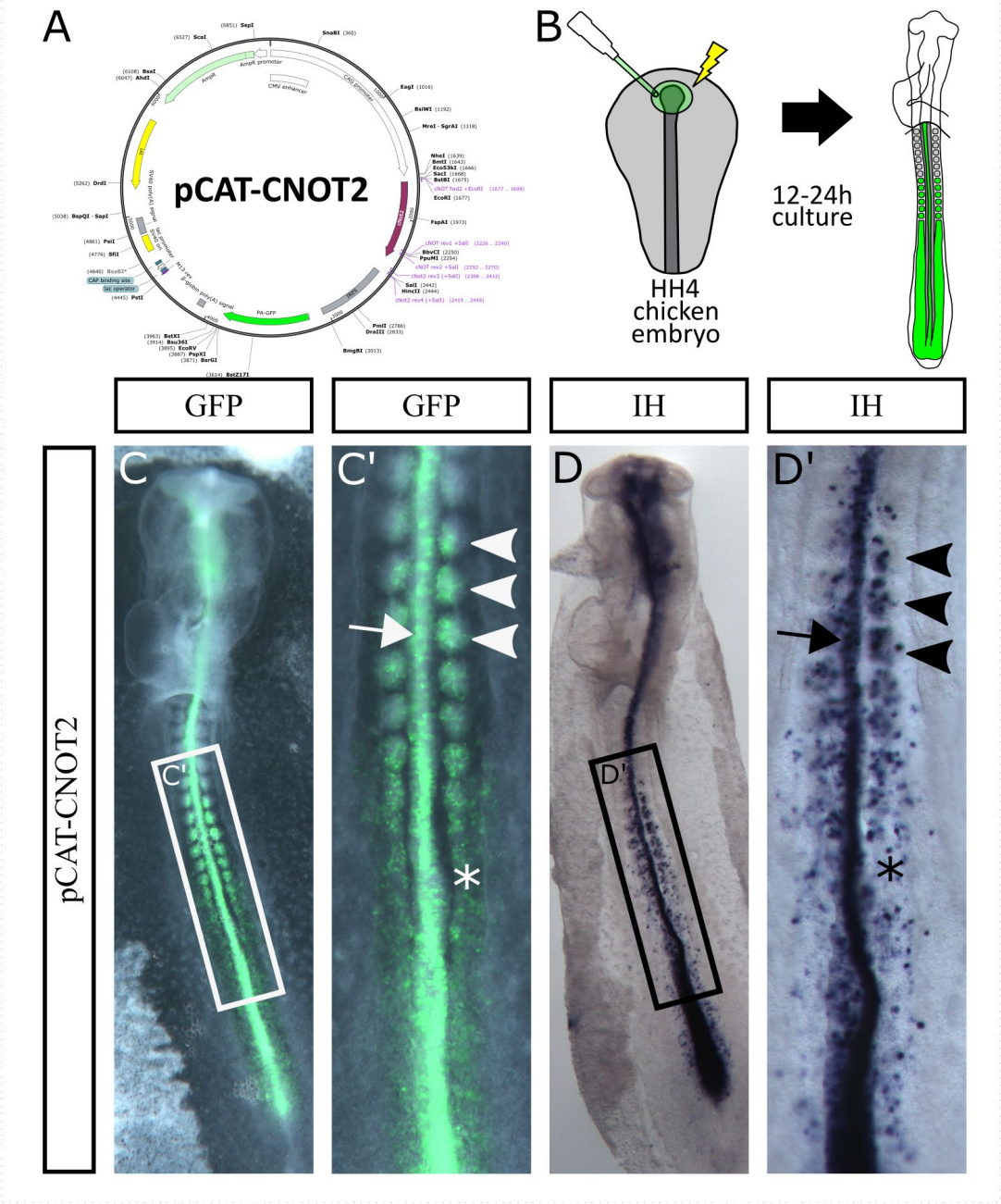

Figure 3.4 Electroporation of pCAT-CNOT2 in HH4 chick embryos results in CNOT2 upregulation in electroporated cells.
(A) Schematic representation of pCAT-CNOT2 construct used in the electroporation experiments. **(B)** Schematic representation of the electroporation experiments performed. HH4 chicken embryos were electroporated with pCAT empty vector or pCAT-CNOT2 construct in the node region corresponding to the location of axial and paraxial mesoderm progenitors. Embryos were then cultured for 12 to 24 hours. **(C, C')** HH11- embryo showing GFP fluorescence (green) in electroporated cells of the axial mesoderm (white arrow), PSM (white asterisk) and somites (white arrowheads). **(D, D')** In situ hybridization for CNOT2 of the embryo in C showing expression in electroporated cells of the axial mesoderm (black arrow), PSM (black asterisk) and somites (black arrowheads)..

After confirming the success of the plasmid construction and the electroporation technique (Figure 3.4), we proceeded to electroporate HH4-5 chick embryos in the axial and paraxial mesoderm progenitor region described above. As a control experiment, the empty vector designated pCAT-empty was electroporated in the same conditions described earlier. A total of 131 embryos were electroporated, 81 with pCAT-CNOT2 and 50 with pCAT-empty. After electroporation, the embryos were cultured for 12-24h, collected, imaged, fixed and stored for further processing. Of the 131 embryos, 112 were collected, 78 electroporated with pCAT-CNOT2 and 34 with pCAT-empty, the remaining ones being discarded when showing contamination and/or severe rupture or scarring of tissues. Immediately after culture, embryos were selected for the presence or absence of fluorescence with 17 of the 112 showing no fluorescence at all, 11 electroporated with pCAT-CNOT2 and 6 with pCAT-empty. A total of 95 embryos showed visible fluorescence, 67 electroporated with pCAT-CNOT2 and 28 with pCAT-empty. When assessing for fluorescence, each embryo was imaged, and the exposure time (milliseconds) needed to observe a good quantity of fluorescent cells in the embryo was registered. Since some of the embryos showed fluorescence but only at very low levels, with a high exposure time being necessary for observation, we decided on a criterion for selection of embryos to be analyzed. As such, we selected the embryos which needed an exposure time of less than 400ms and proceeded with their analysis. Of the 95 embryos that showed fluorescence, a total of 66 filled this criterium, 45 electroporated with pCAT-CNOT2 and 21 with pCAT-empty.

When assessing the morphology of the selected embryos and comparing the control pCAT-empty with pCAT-CNOT2 electroporated ones, there were immediately three main observable differences (Figure 3.5, compare A1-2 with B1-2), which are detailed bellow:

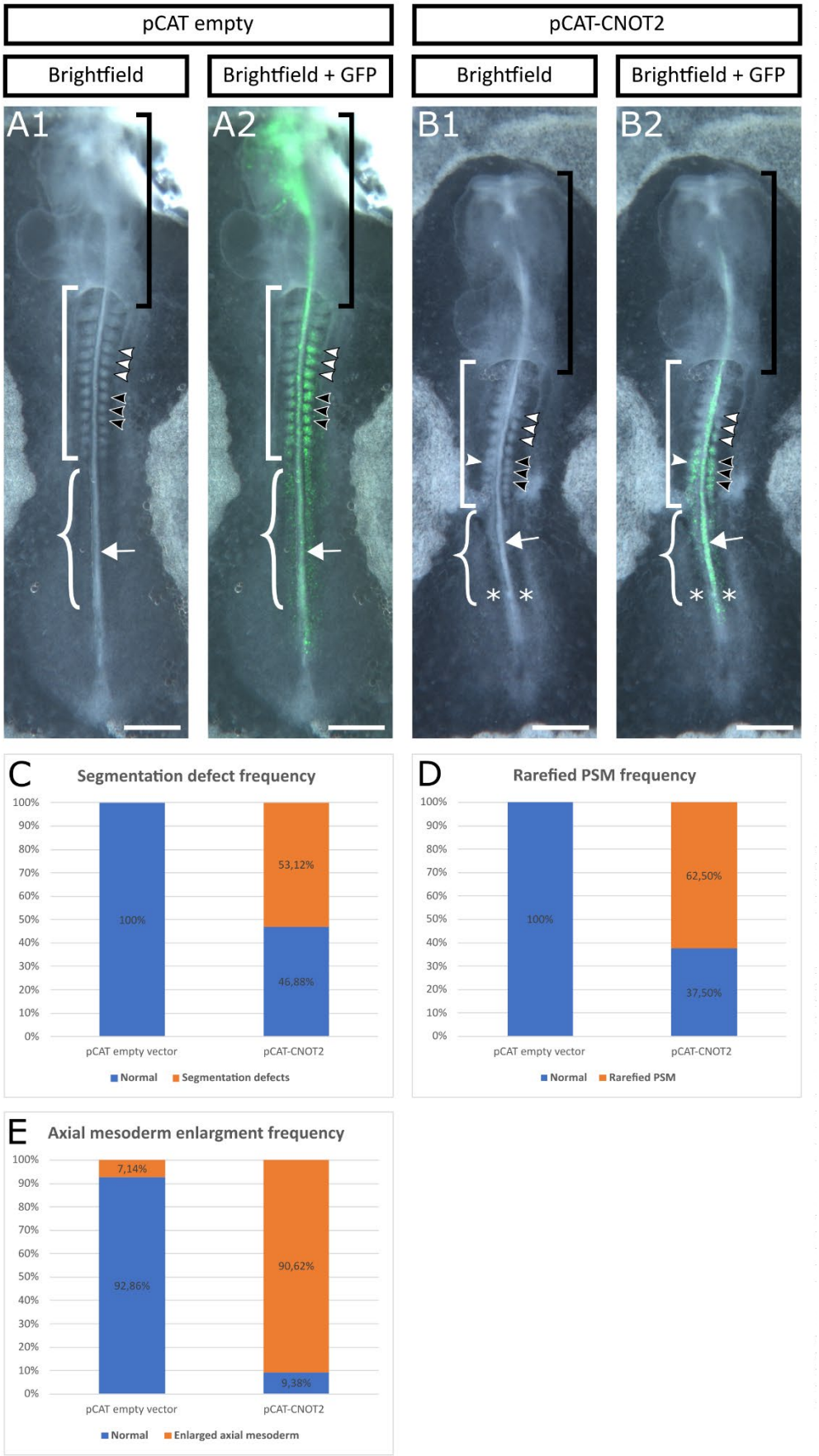
pCAT empty
pCAT-CNOT2
Brightfield
Brightfield + GFP
Brightfield
Brightfield + GFP
A1
A2
B1
B2
C
Segmentation defect frequency
100%
90%
80%
70%
60%
50%
40%
30%
20%
10%
0%
100%
53,12%
46,88%
pCAT empty vector
pCAT-CNOT2
Normal
Segmentation defects
D
Rarefied PSM frequency
100%
62,50%
37,50%
pCAT empty vector
pCAT-CNOT2
Normal
Rarefied PSM
E
Axial mesoderm enlargment frequency
7,14%
92,86%
90,62%
9,38%
pCAT empty vector
pCAT-CNOT2
Normal
Enlarged axial mesoderm

Figure 3.5. pCAT-CNOT2 electroporated embryos, show AP shortened segmented and PSM regions, segmental defects, rarefied PSM and enlarged axial mesoderm.
(A1-A2) HH11+ chick embryo electroporated with pCAT-empty showing normal morphology. (A1) HH11+ electroporated embryo fixed immediately after culture showing normal length of the different portions of the embryo and normal morphology of the somites, PSM and axial mesoderm. (A2) HH11+ electroporated embryo fixed immediately after culture, showing GFP fluorescence (green) in electroporated cells of the axial mesoderm, PSM and somites. **(B1-B2)** HH11 chick embryo electroporated with pCAT-CNOT2 showing reduced segmented and PSM region AP lengths, segmentation defects, rarefied PSM and enlarged axial mesoderm. (B1) HH11 electroporated embryo fixed immediately after culture. While the head length is roughly the same size as in the embryo in A (black brackets), the lengths of the segmented (white bracket) and PSM (white curved bracket) are distinctively reduced. There are also segmentation defects that include AP fusion of somites (white arrowhead), reduced somite size (white arrowheads with black contour), especially in the mediolateral axis and reduced AP distance between somites (black arrowheads with white contour). Additionally, the PSM presents a rarefied appearance (white asterisks). Finally, there is a clear enlargement of the axial mesoderm (white arrow). (B2) HH11 electroporated embryo fixed immediately after culture, showing GFP fluorescence (green) in electroporated cells of the axial mesoderm, PSM and somites. All the phenotypes described in B1 appear in structures/tissues that contain electroporated cells. **(C)** Bar graph showing the percentage of embryos showing the segmentation defects described above. No segmentation defects appeared in embryos electroporated with pCAT-empty (14 out of 14), while 53.12% of embryos electroporated with pCAT-CNOT2 (17 out of 32) showed at least one of the defects described. **(D)** Bar graph showing the percentage of embryos presenting rarefied PSMs. No embryos electroporated with pCAT-empty (14 out of 14) showed this phenotype, while in 62.5% of embryos electroporated with pCAT-CNOT2 (20 out of 32) did so. **(E)** Bar graph showing the percentage of embryos presenting enlarged axial mesoderm. While only 7.14% (1 out of 14) of embryos electroporated with pCAT-empty showed an enlargement of the axial mesoderm, in a huge percentage of 90.62% (29 out of 32) of embryos electroporated with pCAT-CNOT2 there was a clearly visible enlargement of the axial mesoderm.
All in toto embryos are shown ventral side up. Scale bars: 500µm for A1-A2 and B1-B2.

Analysis of the impact on embryo elongation

Since we noticed a shortening of pCAT-CNOT2 electroporated embryos, we decided to quantify the differences in embryo elongation, by measuring and comparing experimental and control embryos. As such, we divided the chicken embryo into four regions (Figure 3.6 A): Head Fold (HF), corresponding to the length between the anterior tip of the embryo and the head fold, Segmented (Seg), corresponding to the distance between the anterior border of the most anterior somite to the posterior border of the most posterior somite, Presomitic mesoderm (PSM), corresponding to the length between the caudal limit of the most posterior somite and the node/CNH and, finally, Total Trunk (TT), corresponding to the sum of Seg and PSM. The length values of the four measurements taken for entirely observable and measurable embryos electroporated with both pCAT-empty (n=14) and pCAT-CNOT2 (n=32) were plotted against each other (Figure 3.6 B-E). The statistical difference of the measurement values between control and experimental embryos was assessed using a nonparametric Independent-Samples Mann-Whitney U Test (Table 3.1). These results showed us that the HF values are indistinguishable between both groups (Table 3.1) (p=0.599). On the contrary, for the

Seg, PSM and TT, the measurements of the embryos electroporated with pCAT-CNOT2 are significantly lower (Table 3.1) (p=0.030, p=0.012, p=0.022 respectively) than the ones from embryos electroporated with pCAT-empty.

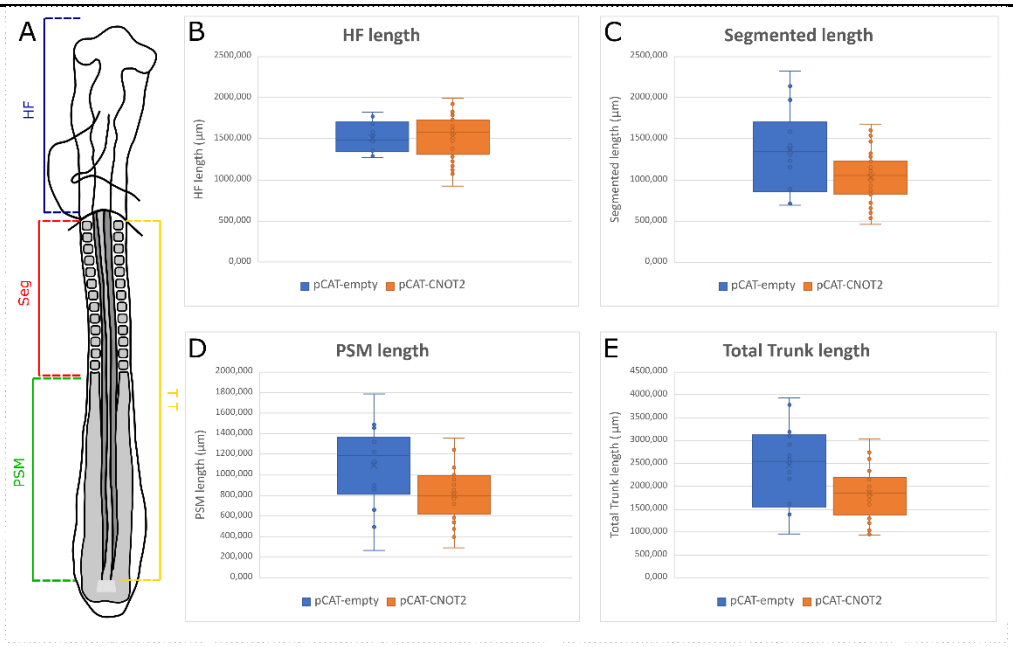

Figure 3.6 pCAT-CNOT2 electroporated embryos, show AP shortening of segmented and PSM regions.
(A) Schematic representation of an HH11 chick embryo showing the four measurements taken: Head Fold (HF) – Length between the anterior tip of the embryo and the head fold, Segmented (Seg), – Length from the anterior border of the most anterior somite to the posterior border of the most posterior somite, Presomitic mesoderm (PSM) – Length between the posterior border of the most posterior somite and the node and Total Trunk (TT) – Sum of Seg and PSM. **(B-E)** Box plot of the HF, Seg, PSM and TT (B, C, D and E, respectively) length measurements in pCAT-empty (blue) and pCAT-CNOT2 (orange).

Table 3.1. Segmented, PSM and Total Trunk lengths have significantly lower values in pCAT-CNOT2 electroporated embryos
Summary of a nonparametric Independent-Samples Mann-Whitney U Test performed, comparing the measurements of HF, Seg, PSM and TT between embryos electroporated with pCAT-empty and pCAT-CNOT2. Results show statistical similarity between HF measurements (p>0.05) and statistically significant difference between measurements of Seg, PSM and TT ((p<0.05).
Test was performed in IBM SPSS Statistics 28.0.

Hypothesis Test Summary

	Null Hypothesis	Test	Sig.[a,b]	Decision
1	The distribution of HF_Length is the same across categories of Electroporation.	Independent-Samples Mann-Whitney U Test	,599	Retain the null hypothesis.
2	The distribution of Segmented_Length is the same across categories of Electroporation.	Independent-Samples Mann-Whitney U Test	,030	Reject the null hypothesis.
3	The distribution of PSM_Length is the same across categories of Electroporation.	Independent-Samples Mann-Whitney U Test	,012	Reject the null hypothesis.
4	The distribution of Total_Trunk_Length is the same across categories of Electroporation.	Independent-Samples Mann-Whitney U Test	,022	Reject the null hypothesis.

a. The significance level is ,050.
b. Asymptotic significance is displayed.

This indicated that CNOT2 upregulation in the chick axial/paraxial mesoderm progenitor region perturbs embryo elongation leading to a shortening of the trunk (Segmented and PSM regions), with no apparent differences in the size of the head (HF).

As this work was being performed, we noticed the lack of a work quantifying the elongation behavior of chick embryos at early stages. This need was shared with a neighboring group from our institute and prompted a collaboration that resulted in two papers (one accepted and one in preparation), which are presented in chapter IV. In one of these works, we found that, for chicken early embryo stages, the HF measurement can be used as a proxy for the embryonic stage.

In order to overcome the difficulty on staging our experimental embryos by counting the number of somites (due to the segmentation defects caused by CNOT2 upregulation), we aimed to evaluate if at the later stages obtained in our results, we could also use HF measurement as a proxy for embryo stage of development. With this in mind we plotted HF measurement values of all pCAT-empty embryos (control embryos), against their corresponding stage. The result (Supplementary figure 3.2) showed a clear trend of increase in HF values associated with increase in embryo stage. As such and taking into account that the HF measure was statistically unchanged in CNOT2 electroporated embryos, we decided to use HF as a proxy for both control and experimental embryo staging.

Fueled by these findings, we plotted the measures of Seg, PSM and TT against the corresponding HF values. We then compared these three measurements between embryos electroporated with pCAT-empty and pCAT-CNOT2 (Figure 3.7). Confirming the results described earlier, there was a clear difference between the dynamics of embryo growth of both groups, with elongation rate of pCAT-CNOT2 embryos being lower than that of control pCAT-empty ones. Additionally, we performed the same plots but comparing also pCAT-CNOT2 embryos in which imaging of fluorescence was performed at values higher than 400ms (Supplementary figure 3.3). Doing so, we observed that the trend was very similar between the two groups of embryos with different levels of fluorescence. This indicated that the elongation dynamics were the same, with embryos with lower fluorescence having higher length measurement levels than the ones with higher fluorescence.

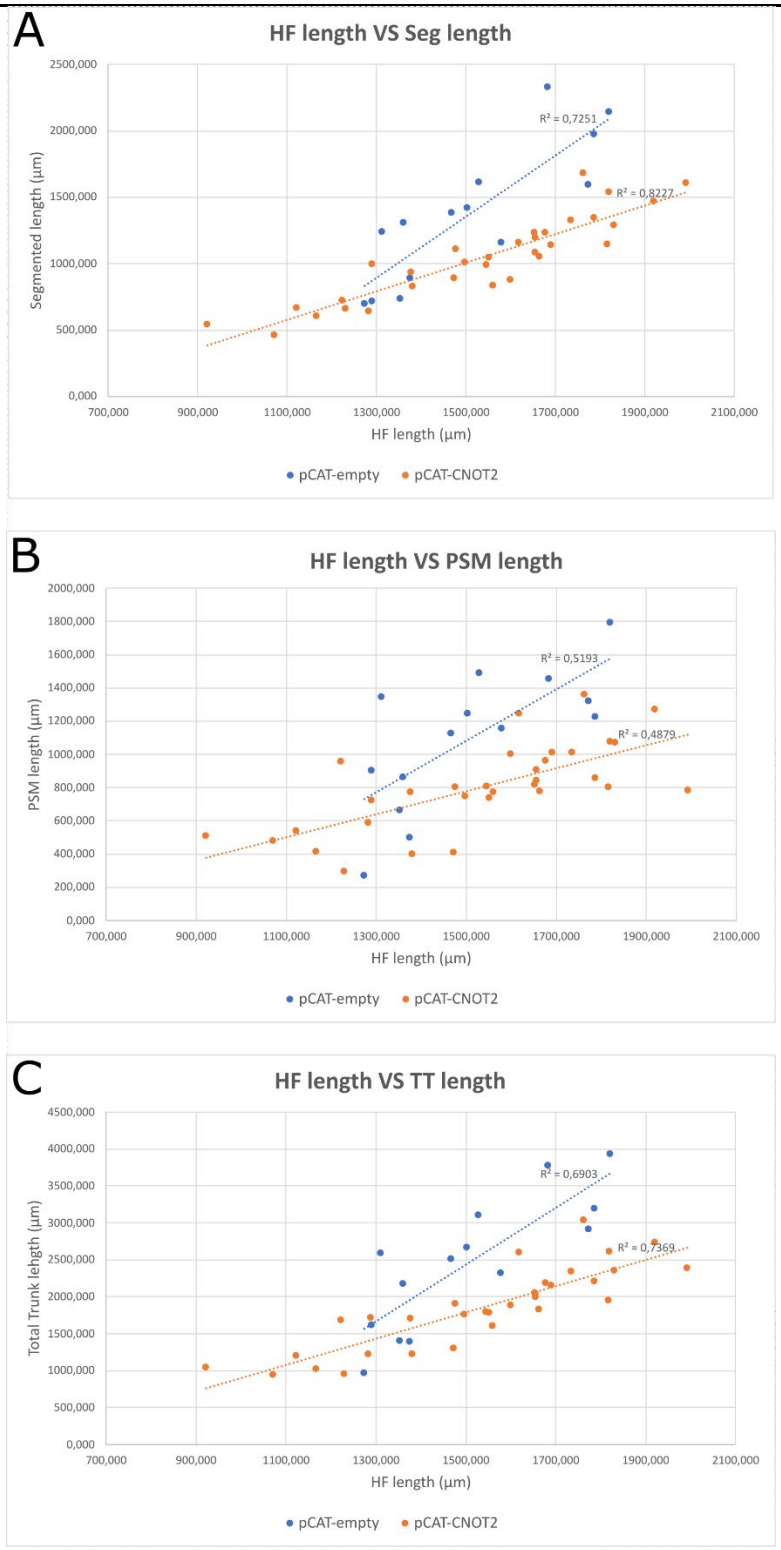

Figure 3.7. pCAT-empty and pCAT-CNOT2 electroporated embryos, show different elongation dynamics for Seg, PSM and TT portions of the embryo.
(A-C) The length measurement values of the Seg, PSM and TT (A, B and C, respectively) portions of the embryo are plotted against the length measurement values of the HF for pCAT-empty and pCAT-CNOT2 electroporated embryos that showed fluorescence imaged at less than 400ms. pCAT-CNOT2 embryos show a lower elongation rate than pCAT-empty ones. The linear trend and its R^2 value are both shown for all groups

Analysis of the impact on somite and PSM morphology

In the trunk region of pCAT-CNOT2 electroporated embryos, there were clear defects both in the segmented and unsegmented paraxial mesodermal regions. Firstly, the somites appeared to be overall smaller, especially in the ML axis and with smaller AP distances between them, when compared with pCAT-empty electroporated ones, some of them even being fused. Due to these defects, somite counting was very difficult to perform. We observed that more than a half of pCAT-CNOT2 embryos (53.12%, 17 out of 32) (Figure 3.5 B1, B2, C) showed one or more of the described defects, while none of the pCAT-empty control embryos did so. Besides this, the PSM region of more than half of the pCAT-CNOT2 embryos presented a rarefied appearance (62.5%, 20 out of 32) (Figure 3.5 B1, B2, D), while again none of the pCAT-empty control embryos did so. The rarefied appearance of PSM in CNOT2 electroporated embryos is an indicative of lack of cells in this paraxial mesoderm region. This prompted us to try to understand the possible causes for these findings.

Analysis of the impact on axial mesoderm structures

While the morphological changes previously reported occurred in slightly more than half of the experimental embryos, it was the effect electroporation had on the axial mesoderm structures that was observed in a higher percentage of embryos. We observed that there was an enlargement of the axial mesoderm in the vast majority of pCAT-CNOT2 embryos (90,62%, 20 out of 32%) (Fig. 3.5, B1, B2, E) compared to pCAT-empty controls with only 1 out of 14 embryos showing this phenotype. However, just by observing the morphology of said embryos, in which axial mesoderm structure it had more effect: the notochord or the floor plate.

CNOT2 upregulation in axial/paraxial mesoderm progenitors leads to both notochord and floor plate enlargement

Since we detected an enlarged axial mesoderm phenotype in a staggering 90,62% of pCAT-CNOT2 electroporated embryos, we decided to evaluate the changes in the axial mesoderm of the electroporated embryos in more detail. For that, we performed in situ

hybridizations of both pCAT-CNOT2 and pCAT empty vector electroporated embryos, using two well-known markers of axial mesoderm, specifically of the notochord and the floor plate. The markers used were; 1) SHH (Riddle et al., 1993) (n=8 pCAT-CNOT2 and n=6 pCAT empty vector), which is expressed in the notochord facing PSM and in the notochord and floor plate at the somitic level and 2) FOXA2 (Ruiz i Altaba et al., 1995) (n=6 pCAT-CNOT2 and n=2 pCAT empty vector), which is expressed in both structures (notochord and floor plate) at the level of the PSM and just in the floor plate at the somite level.

We started by comparing the expression patterns of FOXA2 and SHH in electroporated embryos with their control empty vector counterparts. By looking at the *in toto* embryos, it is easily noticeable that there is an enlargement in the axial mesoderm region, shown by a broader expression region of both FOXA2 (Fig. 3.8 B2 compared to A2) and SHH (Fig. 3.9 B2 compared to A2). This broader expression pattern was coincidental with regions of higher fluorescence intensity (Fig. 3.8 B1 and B2).

In order to explore the nature of this expression pattern enlargement, we produced 14µm transverse sections of electroporated embryos where *in situ* hybridizations were performed for both FOXA2 (n=4) and SHH (n=6). In these cross-sections, we observed a clear increase in size in both the floor plate (n=8) and the notochord (n=7), as shown by the expression of FOXA2 (Fig. 3.8 B'-B''' compared to A'-A''') and SHH (Fig. 3.9 B'-B'' compared to A'-A''). In addition, while the notochord maintained its characteristic round shape, the floor plate appeared as a round or irregular shaped structure, losing its characteristic apical constriction (n=9) (Fig. 3.8 B2'-B2''' compared to A2'-A2'''). In these embryos, the neural tube showed a total absence or incomplete closure of its neural folds (n=7) (Fig. 3.8 B2'-B2''). These size and shape changes yielded varied consequences for the spatial organization of the axial structures: in some embryos there was a such considerable enlargement of the floor plate, that its size reached about the same as the notochord's. In these cases, we observed that floor plate cells were no longer located between the two halves of the neural tube as in control embryos (n=3) (Fig. 3.8 B2''-B2''' compared to A2''-A2'''). In these cases, the notochord was displaced, being located side by side with the floor plate.

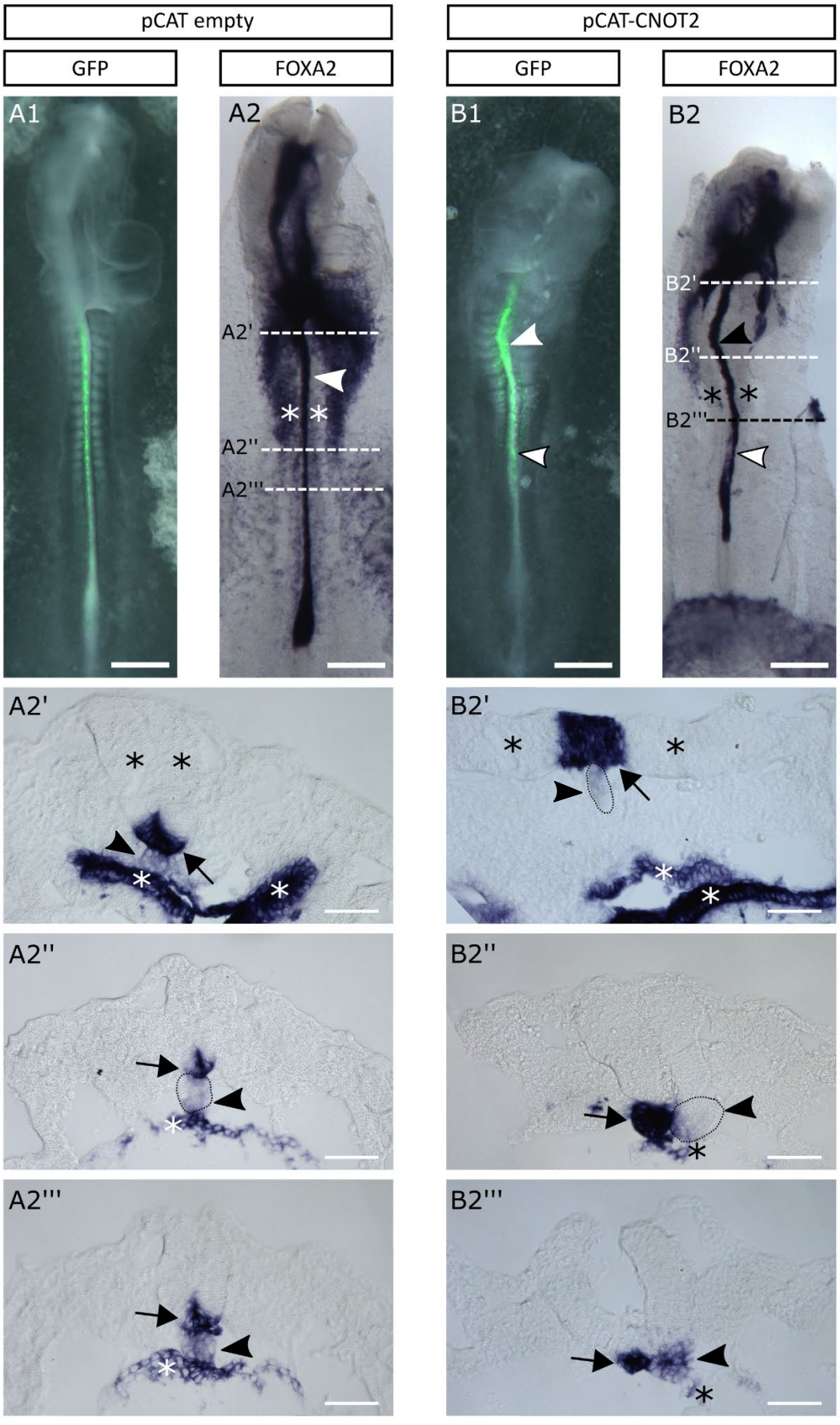
pCAT empty
pCAT-CNOT2
GFP
FOXA2
GFP
FOXA2
A1
A2
B1
B2
A2'
A2''
A2'''
B2'
B2''
B2'''
A2'
B2'
A2''
B2''
A2'''
B2'''

Figure 3.8 . pCAT-CNOT2 electroporated embryos, show an enlargement of axial mesoderm demonstrated by FOXA2 expression.
(A1-A2) HH11+ chick embryo electroporated with pCAT empty vector showing normal expression of FOXA. (A1) HH11- electroporated embryo fixed immediately after culture, showing GFP fluorescence (green) in electroporated cells of the axial mesoderm, PSM and somites. (A2) In situ hybridization of embryo in A1 showing normal FOXA2 expression in the axial mesoderm (notochord and floor plate) (white arrowhead) and endoderm (white asterisks). (A2'-A2''') 14μm transverse sections of embryo in A2 showing normal notochord (black arrowheads) and floor plates (with normal apical constriction) (black arrow) and endoderm (white asterisks in A2'-A2'''), all expressing FOXA2. The neural tube (black asterisks) has closed normally. **(B1-B2)** HH11+ chick embryo electroporated with pCAT-CNOT2 showing a clear enlargement of the axial mesoderm as demonstrated by expression of FOXA2. (B1) HH11- electroporated embryo fixed immediately after culture, showing GFP fluorescence (green) in electroporated cells of the axial mesoderm (white arrowhead), PSM and somites. (B2) FOXA2 In situ hybridization of embryo in B1 showing a clear enlargement of the axial mesoderm (black arrowhead) in a region where electroporated cells are present (compare with B1). The axial mesoderm enlargement is higher in regions of higher fluorescence (white arrowhead in B1 and black arrowhead in B2) compared with regions of lower fluorescence (white arrowheads with black outline in B1 and B2). Notice the absence of FOXA2 expression in the endoderm in a grand majority of the embryo (white asterisks, compare with A2). There is also no ectopic FOXA2 expression in other regions showing electroporated cells, like the somites or PSM. (B2'-B2''') 14μm transverse sections of embryo in B2, revealing details on the enlargement of the axial mesoderm. (B2') Transverse section of embryo in B2 showing a clear enlargement of the notochord (black arrowhead, compare with A2''). Additionally, there is an absence of the apical constriction usually present in the floor plate (compare with A2'). Also notice the complete failure of neural tube closure (black asterisks). Additionally, the endoderm is present and showing expression of FOXA2 (white asterisks). (B2'') Transverse section of embryo in B2 showing a clear enlargement of both the notochord (black arrowhead, compare with A2'') and floor plate (black arrow, compare with A2''). Additionally, the floor plate shows no apical constriction and is located bellow the neural tube instead of its usual location (compare with A2''). The notochord is also displaced to the right, perhaps due to the abnormal location and enlargement of the floor plate. Also notice the almost complete absence of endoderm, save for a few cells showing expression of FOXA2 (black asterisk, compare with A2''). (B2''') Transverse section of embryo in B2 showing abnormalities in the notochord and floor plate. Just as in B2'' there is a displacement of both the notochord (black arrowhead, compare with A3''') and floor plate (black arrow, compare with A3'''). Also, as in B2'', the floor plate shows no apical constriction (compare with A3'''). In this section, only the notochord is slightly enlarged. Notice that this region corresponds to an area where there is less fluorescence (black and white arrowheads in B1 and B2), compared to a more anterior region (white arrowhead in B1 and black arrowhead in B2). Again, just as in B2'' notice the almost complete absence of endoderm, save for a few cells showing expression of FOXA2 (black asterisk, compare with A2''').
All in toto embryos are shown ventral side up. Scale bars: 500μm for A1-A2 and B1-B2 and 50μm for A2'-A2''' and B2'-B2'''. In B2', A2'' and B2'' the unstained notochord is highlighted with a dashed line for better visualization.

Another interesting finding in some p-CAT-CNOT2 electroporated embryos where *in situ* hybridization for FOXA2 was performed, was the partial or complete absence of endoderm (n=3), usually expressing this gene (Fig. 3.8 compare B2 to A2 and compare B2'' and B2''' to A2'' and A2''' respectively). Dorsal endoderm cells are described to share the same cellular origin with the notochord and medial floor plate ones (Catala et al., 1996). Unfortunately, in these embryos we could not be sure if the endoderm was not removed at the time of the fixation of the embryos.

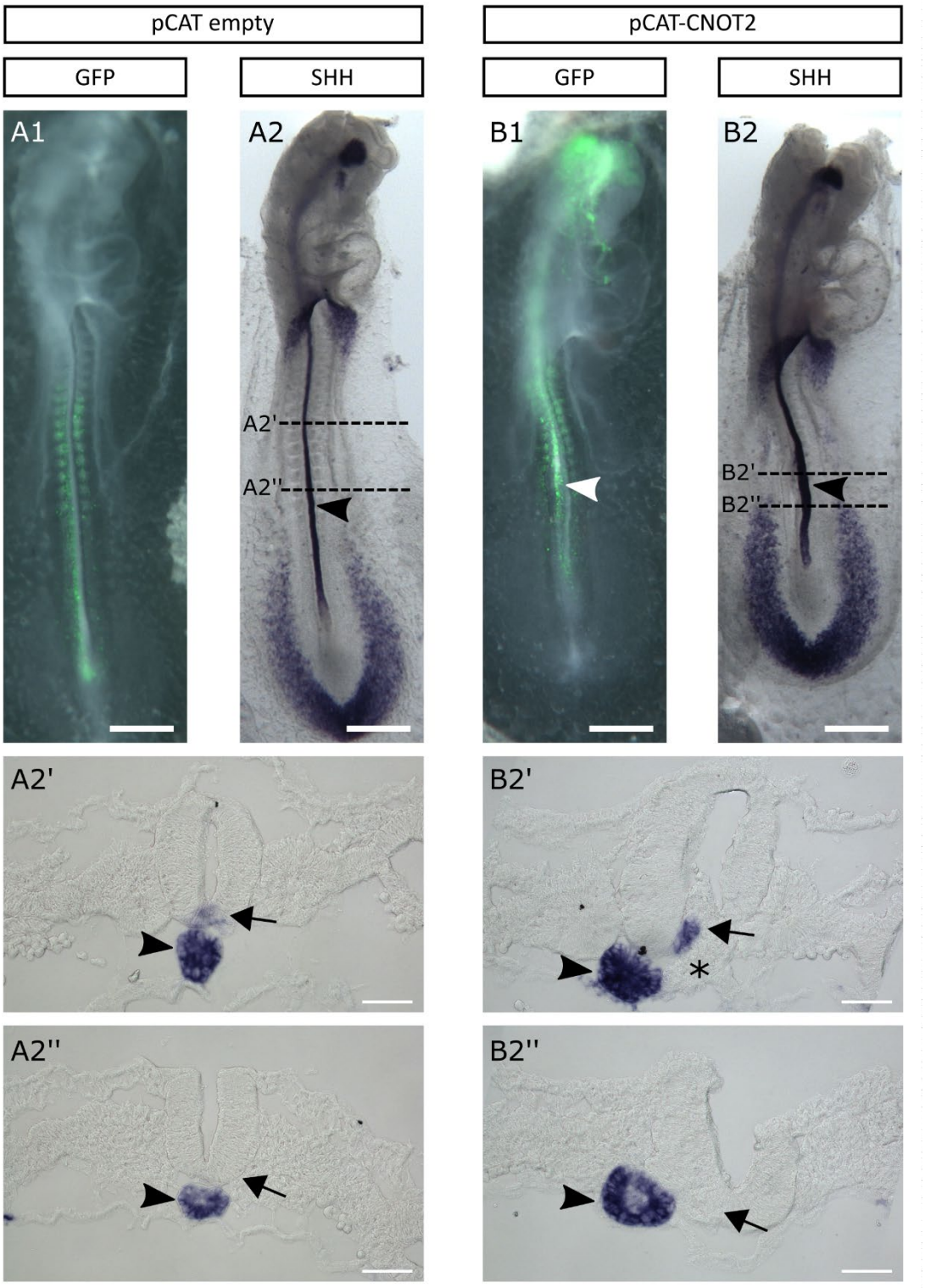

Figure 3.9. pCAT-CNOT2 electroporated embryos, show enlargement of axial mesoderm demonstrated by SHH expression.
(A1-A2) HH12^{+} chick embryo electroporated with pCAT empty vector showing normal expression of SHH. **(A1)** HH11^{-} electroporated embryo fixed immediately after culture, showing GFP fluorescence (green) in electroporated cells of the axial mesoderm, PSM and somites. **(A2)** *In situ* hybridization of embryo in A1 showing normal SHH expression in the axial mesoderm (notochord and floor plate) (black arrowhead). **(A2'-A2'')** 14µm transverse sections of embryo in A2 showing normal notochord (black arrowhead) expressing SHH and floor plate (black arrow). **(B1-B2)** HH12^{+} chick embryo electroporated with pCAT-CNOT2 showing a clear enlargement of the axial mesoderm as demonstrated by expression

of SHH. **(B1)** HH11^{-} electroporated embryo fixed immediately after culture, showing GFP fluorescence (green) in electroporated cells of the axial mesoderm (white arrowhead), PSM, somites and cephalic region. **(B2)** SHH *In situ* hybridization of embryo in B1 showing a clear enlargement of the axial mesoderm (black arrowhead) in a region where electroporated cells are present (compare with B1). There is also no ectopic SHH expression in other regions showing electroporated cells, like the somites, PSM or in the cephalic region where electroporated cells where present.. **(B2'-B2'')** 14μm transverse sections of embryo in A, revealing details on the enlargement of the axial mesoderm. **(B2')** Transverse section of embryo in B2 showing a clear enlargement of the notochord (black arrowhead, compare with A2') and a big accumulation of cells in the region where the floor plate is usually located, in the middle and under the neural tube (black asterisk). Some of these cells show expression of SHH (black arrow). Notice the displacement of the notochord to the left side of the section, perhaps due to the accumulation of cells in the middle and under the neural tube. **(B2'')** Transverse section of embryo in B2 showing a clear enlargement of both the notochord (black arrowhead, compare with A2'') and floor plate region (black arrow, compare with A2''). Notice the displacement of the notochord to the left side of the section, perhaps due to the enlargement of the floor plate.

All *in toto* embryos are shown ventral side up. Scale bars: 500μm for A1-A2 and B1-B2 and 50μm for A2'-A2'' and B2'-B2''.

In all electroporated embryos in which i*n situ* hybridizations were performed, we observed the phenotypes described above with varying degrees of strength. However, the most severe ones (n=4) yielded some very interesting findings. In the embryos where the notochord was highly enlarged, we observed an accumulation of seemingly mesenchymal cells between the two halves of the ventral part of the neural tube. These cells did not form a regularly shaped structure, instead spreading themselves even to the lumen of the neural tube and separating its ventral halves (Fig. 3.9 B2', 3.10 A2',B2'C2'). These accumulations varied from showing expression of FOXA2 (Fig. 3.10 B2') or SHH (Fig. 3.10 C2') in some but not all of its cells or none of these (Fig. 3.10 A2'). In these embryos, the lateral floor plate that normally expresses both FOXA2 and SHH (Charrier et al., 2002) can be identified by the normal expression of these two genes (Fig. 3.10 A2', B2', C2') and is shown split in its two halves by the existence of the cell accumulations. This, in conjunction with the fact that there is no identifiable medial floor plate, leads us to suggest that the cells in this accumulation were destined to form the medial floor plate.

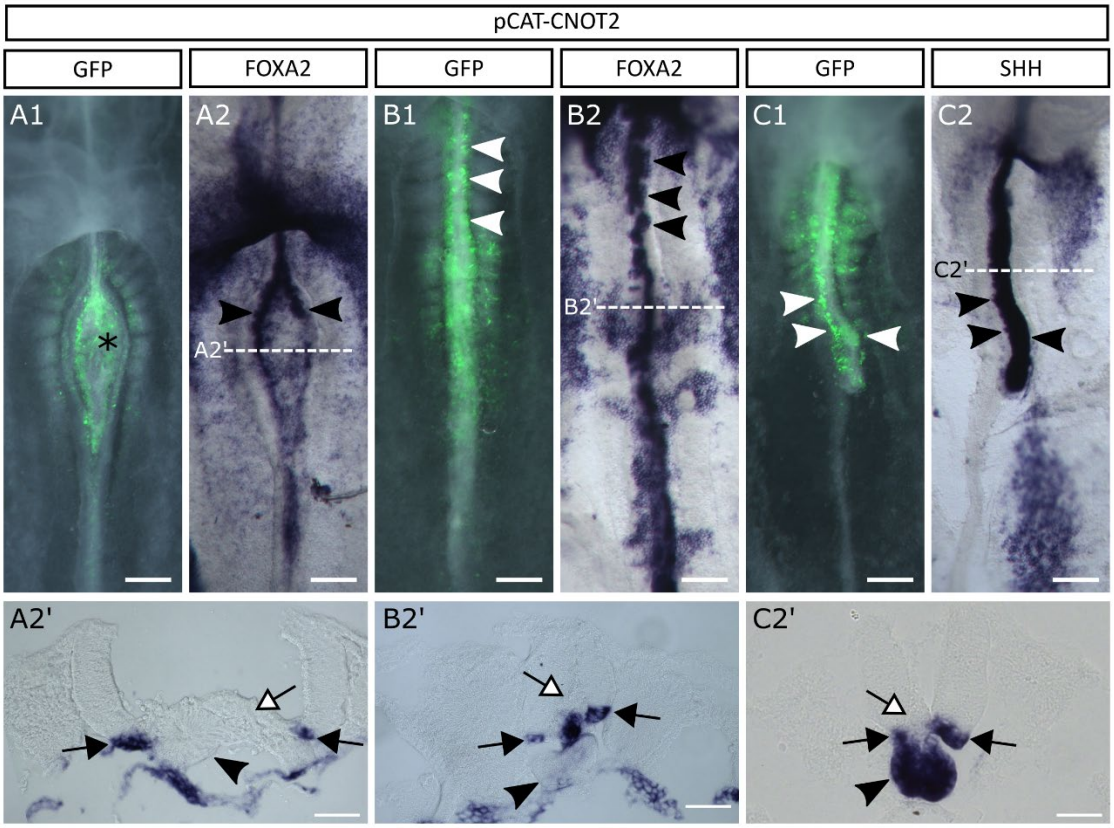

Figure 3.10. The most severe CNOT2 electroporation phenotypes show an accumulation of cells in the floor plate cells and greatly enlarged notochords

(A1-A2) HH11 embryos electroporated with pCAT-CNOT2 showing a greatly enlarged notochord and an accumulation of cells in the axial mesoderm. (A1) HH11 electroporated embryo fixed immediately after culture showing a mass of cells in the axial mesoderm region. Note that the composition of this mass is mainly by CNOT2 electroporated cells (GFP in green). (A2) In situ hybridization of embryo in A1 showing FOXA2 expression in the axial mesoderm. Notice the two halves of the lateral floor plate split by the described cell mass (black arrowheads). (A2') 14µm transverse section of embryo in A showing a greatly enlarged notochord (black arrowhead) and a large accumulation of cells in the axial mesoderm region (black and white arrow) located between the two halves of the neural tube. FOXA2 shows no expression in any of the cells of the mass but is expressed in the two separated lateral floor plate halves. **(B1-B2)** $HH10^{+}$ embryos electroporated with pCAT-CNOT2 showing a greatly enlarged notochord and an accumulation of cells in the axial mesoderm. (B1) HH10+ electroporated embryo fixed immediately after culture showing patches of a large quantity of CNOT2 electroporated (GFP positive in green) in the axial mesoderm. (white arrowheads) (B2) In situ hybridization of embryo in B1 showing enlarged floor plate as shown by FOXA2 expression (black arrowheads). (B2') 14µm transverse section of embryo in B showing a greatly enlarged notochord (black arrowhead) and an accumulation of cells in the axial mesoderm region (black and white arrow) located between the two halves of the neural tube. In this case, FOXA2 is expressed in some, but not all the mass's cells, as well as in the two separated lateral floor plate halves. **(C1-C2)** $HH11^{+}$ embryos electroporated with pCAT-CNOT2 showing a greatly enlarged notochord and an accumulation of cells in the axial mesoderm. (C1) HH11+ electroporated embryo fixed immediately after culture showing patches of a large quantity of CNOT2 electroporated (GFP positive in green) in the axial mesoderm (white arrowheads). (C2) In situ hybridization of embryo in B1 showing a great enlargement of the notochord as demonstrated by SHH expression (black arrowheads). (C2') 14µm transverse section of embryo in C showing a greatly enlarged notochord (black arrowhead) and an accumulation of cells in the axial mesoderm region (black and white arrow) located between the two halves of the neural tube. In this case, SHH is expressed in the accumulation of cells, as well as in the two separated lateral floor plate halves.

All in toto embryos are shown ventral side up. Scale bars: 200µm for A1-A2, B1-B2 and C1-C2 and 50µm for A2' and B2' and C2'.

As described above, we observe that notochord and the floor plate suffer changes of various degrees in CNOT2 electroporated embryos which lead us to propose a sequence of severity phenotypes depending on the level of expression induced by the electroporation technique. (Figure 3.11).

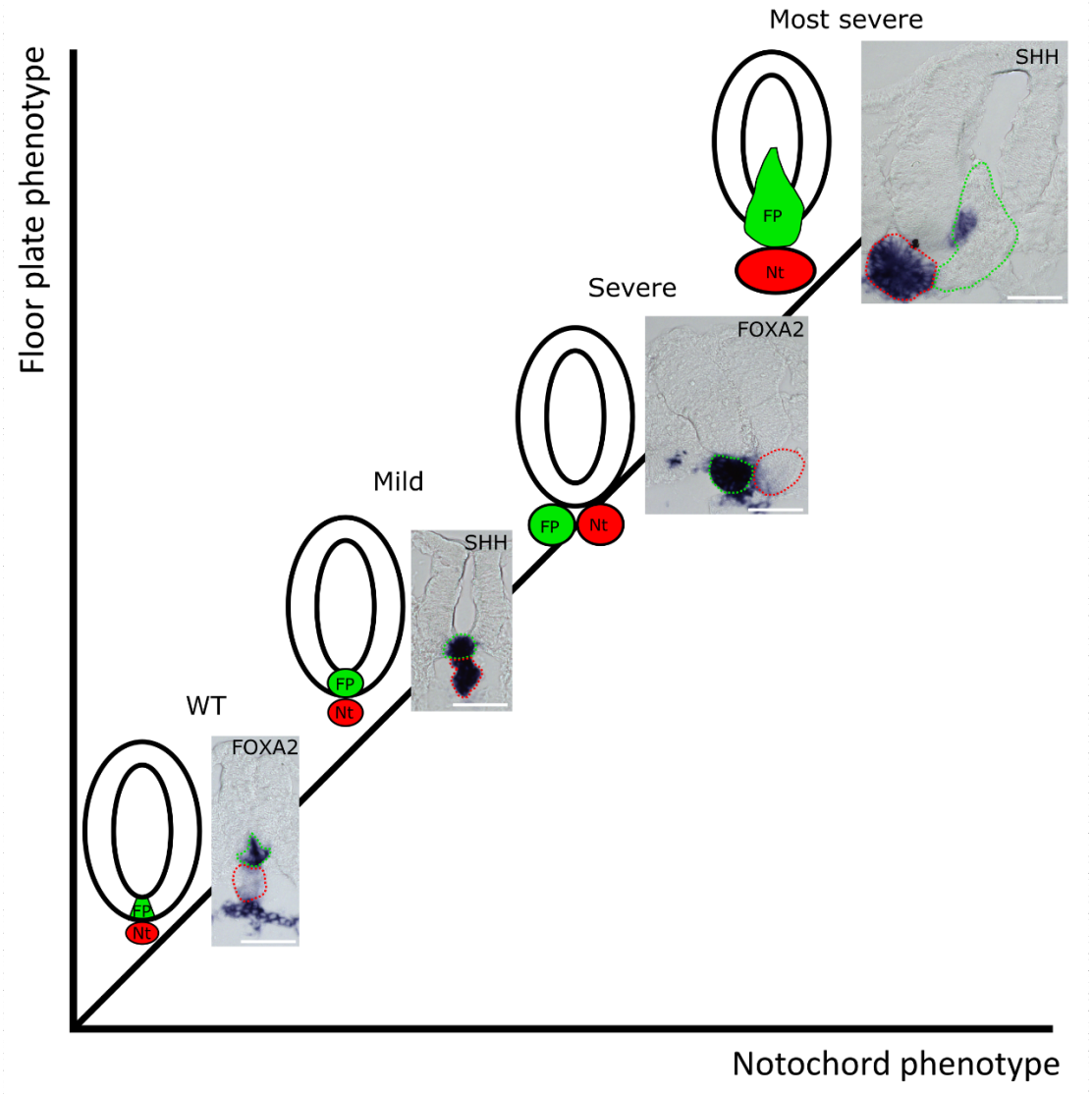

Figure 3.11 The degree of CNOT2 electroporation correlates with the severity of the phenotype in the floor plate and notochord.
Images and schematic representations of transverse sections of wild type and CNOT2 electroporated embryos showing the floor plate (green) and notochord (red) and their respective phenotypes in correlated growing severity. In wild type embryos, the floor plate is located in the middle of the ventral neural tube and the notochord is located just ventrally. In the "mild" phenotype, plate loses its characteristic apical constriction and both structures remain in the same location but are slightly increased in size. In the "severe" phenotype, both structures are larger than in the "mild" phenotype and the floor plate is no longer located in the ventral neural tube but is instead bellow it. Accompanying this, the notochord is displaced laterally to either one of the sides, with the two structures now standing ventrally to the neural tube and side by side. In the "most severe" phenotype, the floor plate is now replaced by an accumulation of cells that fills an area spanning from the lumen of the neural tube to the usual location of the notochord. The notochord is thus displaced and its size is larger than in the previous phenotypes.

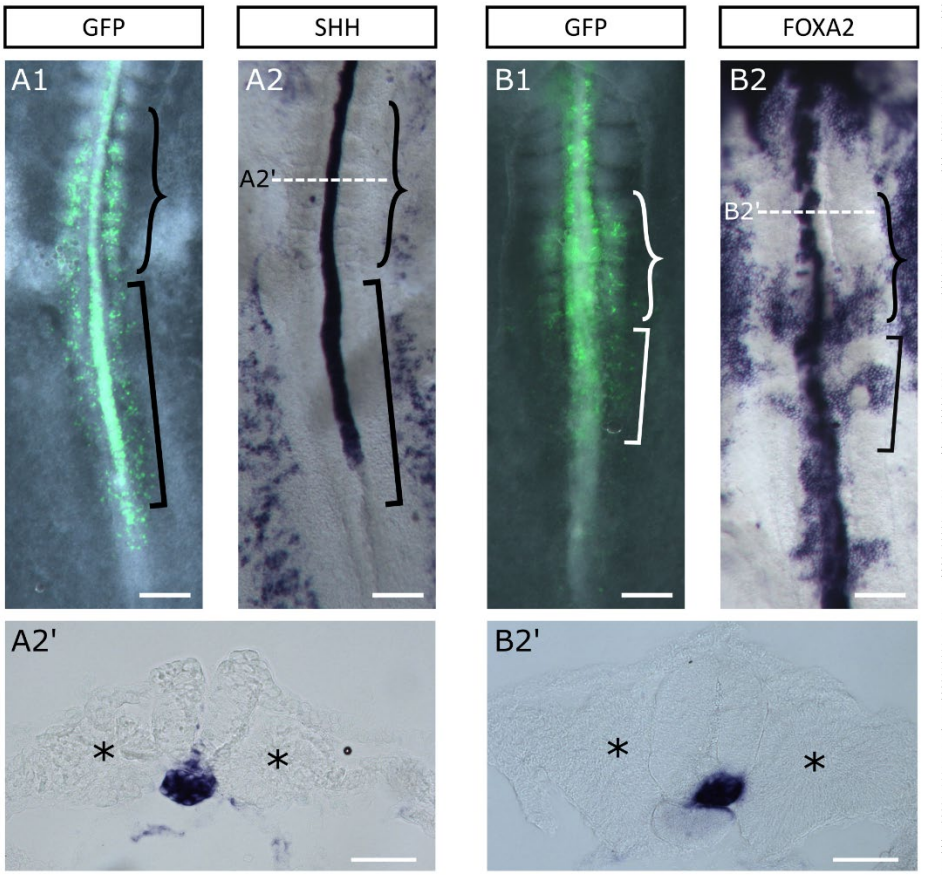

Fig. 3.12. pCAT-CNOT2 upregulation does not result in ectopic expression of SHH or FOXA2 in the paraxial mesoderm
(A1-A2) HH11 chick embryo electroporated with pCAT-CNOT2 showing absence of SHH expression in electroporated cells of the paraxial mesoderm. (A1) HH11 electroporated embryo fixed immediately after culture, showing GFP fluorescence (green) in the electroporated cells of the somites (bracket) and PSM (square bracket). (A2) In situ hybridization of embryo in A1 showing SHH expression in the axial mesoderm and absence of expression in the electroporated cells of the somites (bracket) and PSM (square bracket). (A2') 14µm transverse sections of embryo in A showing absence of SHH expression in the somites (black asterisks). **(B1-B2)** HH10+ chick embryo electroporated with pCAT-CNOT2 showing absence of of FOXA2 expression in electroporated cells of the paraxial mesoderm. (B1) HH10+ electroporated embryo fixed immediately after culture, showing GFP fluorescence (green) in the electroporated cells of the somites (white bracket) and PSM (white square bracket). (B2) In situ hybridization of embryo in B1 showing FOXA2 expression in the axial mesoderm and absence of expression in the electroporated cells of the somites (bracket) and PSM (square bracket). Note that the expression visible in the embryo is in the endoderm and not on the paraxial mesoderm. (B2') 14µm transverse sections of embryo in A showing absence of SHH expression in the somites (black asterisks). All in toto embryos are shown ventral side up. Scale bars: 200µm for A1-A2 and B1-B2 and 50µm for A2' and B2'.

In normal embryos, the floor plate has an apical constriction and is located between the ventral halves of the neural tube. In CNOT2 electroporated embryos, the severity of the floor plate phenotype starts with just a slight increase in size and loss of apical constriction. The next level of severity shows a greater increase in size to such a degree that it is localized bellow the neural tube side-by-side with the notochord. In the most extreme cases, there is no longer a floor plate, but accumulation of presumably floor

plate cells with a considerable size. These degrees of phenotypic severity in the floor plate are accompanied by a gradual increase in the overall size of the notochord, such that a more intense level of floor plate severity corresponds to a bigger sized notochord.

Taken together, these results suggest that CNOT2 electroporation in the axial/paraxial mesoderm progenitor area leads to an increase in the size of these two axial mesoderm structures, notochord and floor plate. As FOXA2 is expressed in the entire floor plate and SHH is expressed the entire notochord, CNOT2 upregulation of these two genes could account for the increase in size of their respective structures. In order to test this, we looked for their expression in ectopic locations where cells had been electroporated with CNOT2, specifically in the paraxial mesoderm. Surprisingly, we found that in the PSM and somites that contained a large number of electroporated cells (Figure 3.12, A1 and B1), there was no ectopic expression of FOXA2 or SHH (Figure 3.12, A2 and B2). Sometimes there was expression of FOXA2 seemingly in this region, but upon analyzing the corresponding sections, this was found to be only expression in the endoderm cells (Figure 3.12 B2, B2'). In conclusion, our results suggest that CNOT2 upregulation in the axial/paraxial mesoderm progenitors leads to both notochord and floor plate enlargement, but this effect is not mediated by the upregulation of SHH or FOXA2.

Low TBX6L expression areas reveal its repression by CNOT2

It was previously described that *flh* (the zebrafish ortholog of CNOT2) represses *spt* (the zebrafish ortholog of TBX6L) leading to an increase in axial mesoderm cells (Amacher and Kimmel, 1998) at the cost of paraxial mesoderm. It was also previously described that *spt*/TBX6L is an important transcription factor in the formation of the PSM and, consequently the somites. We thus decided to study the expression pattern of TBX6L in pCAT-CNOT2 electroporated embryos (Figure 3.13) (n=9). As shown earlier, TBX6L is normally very strongly expressed in the PSM of 48h chicken embryos. However, there are two regions, where its expression is usually weaker: the most recently formed somites and the medial area of the tailbud. In electroporated embryos, we found changes on the TBX6L expression pattern in these two regions. TBX6L expression in the somites is normally restricted to the two to three most recently formed somites. However, by increasing the time of revelation of the NBT-BCIP reaction, the expression is extended anteriorly until somite VII (Figure 3.1S). In some pCAT-CNOT2 electroporated embryos somites from one side show considerably more fluorescence than the contralateral ones (n=5), indicative of higher CNOT2 overexpression. In these somites, we can observe a

clear downregulation of TBX6L (n=4). On the other hand, in the tailbud region, TBX6L expression is reduced, specifically in areas where there is higher fluorescence (7 out of 9). These results strongly suggest a downregulation of TBX6L expression by CNOT2 in the chicken embryo.

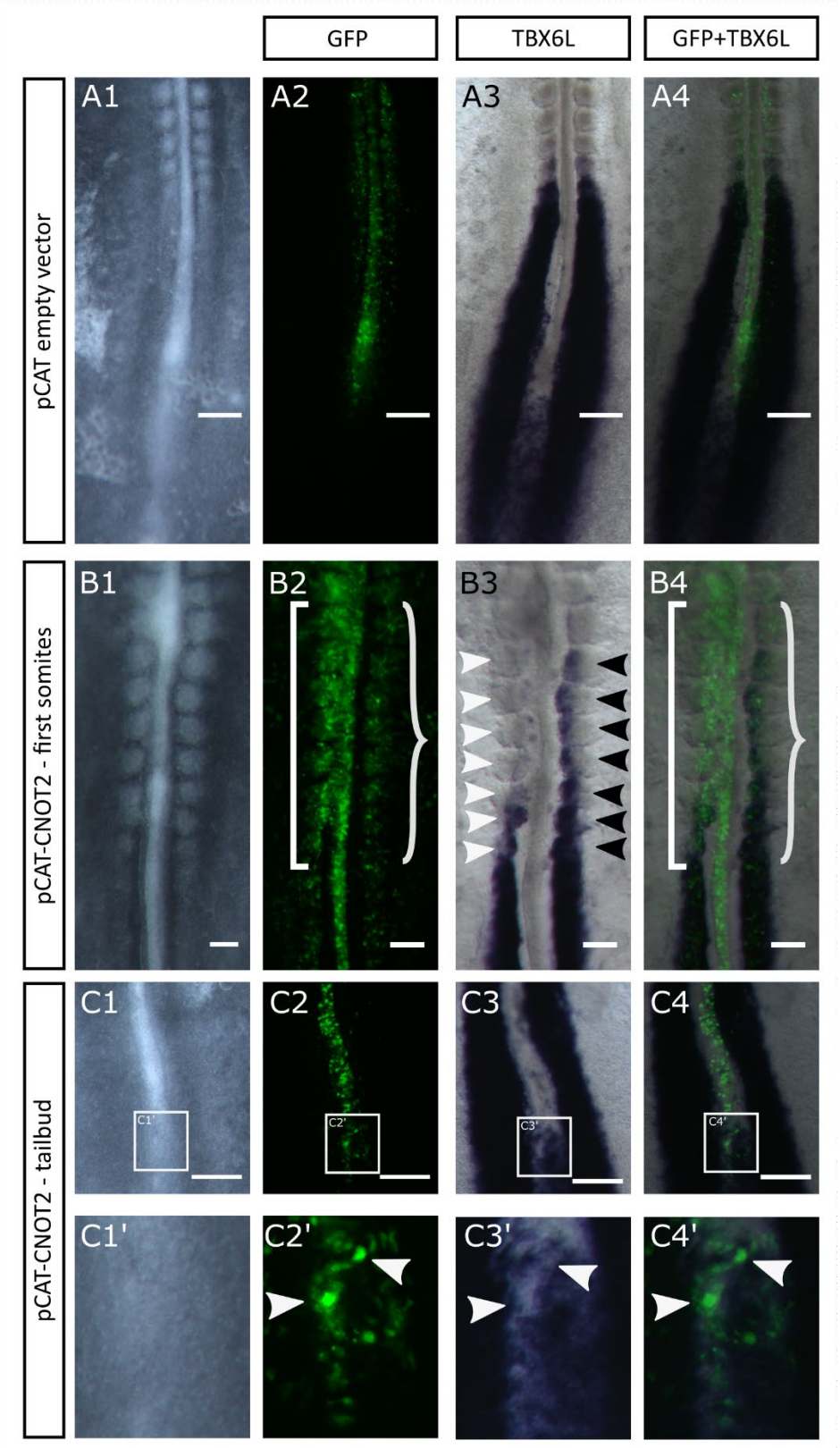

Figure 3.13. In pCAT-CNOT2 electroporated embryos, downregulation of TBX6L is evident in areas of weaker TBX6L expression, revealing its downregulation by CNOT2.
(A1-A4) HH11- chick embryo electroporated with pCAT empty vector showing normal expression of TBX6L. (A1) HH11- electroporated embryo fixed immediately after culture. (A2) Embryo in A1 showing GFP fluorescence (green) in electroporated cells of the notochord, PSM and somites. (A3) In situ hybridization of embryo in A1 showing normal TBX6L expression in the tailbud, PSM and recently formed somites. (A4) Merge of A2 and A4. **(B1-B4)** HH10+ chick embryo electroporated with pCAT-CNOT2 showing a clear reduction of TBX6L expression in somites I-VII (the seven most recently formed somites). (B1) HH10+ electroporated embryo fixed immediately after culture. (B2) Embryo in B1 showing GFP fluorescence (green) in electroporated cells of the notochord, PSM and somites. Notice that GFP expression is higher in the left side somites (bracket) compared to the right side (curved bracket). (B3) In situ hybridization of the embryo in B1 showing a strong reduction of TBX6L expression in somites I-VII located on the left side of the embryo (white arrowheads), when compared with the contralateral ones (black arrowheads). (B4) Merge of B2 and B3. Notice the correspondence of higher GFP expression (corresponding to higher levels of CNOT2) with lower TBX6L expression. See also supplementary. movies 3.1 and 3.2. **(C1-C4)** Close-up of the medial part of the tailbub of an HH10+ chick embryo electroporated with pCAT-CNOT2 showing a match between downregulation of TBX6L expression and high GFP expression. (C1, C1') HH10+ electroporated embryo fixed immediately after culture. (C2, C2') Embryo in C1 showing patches of GFP fluorescence (green) in the axis of the embryo. (C3, C3') In situ hybridization of embryo in C1/C1' showing areas of TBX6L absence of expression in the region of weaker TBX6L expression (white arrowheads). (C4, C4') Merge of C2/C3 and C2'/C3'. Notice the correspondence of patches of GFP expression (corresponding to higher levels of CNOT2) with the areas of TBX6L absence of expression (white arrowheads). See also supplementary. movie 3.3 and 3.4.
All embryos are shown ventral side up. Scale bars: 100µm for A-C and 50µm for D

TBX6L, like spt has Noto family binding motifs in its promoter.

The TBX6L expression patterns of pCAT-CNOT2 electroporated embryos are consistent with a repression of TBX6L by CNOT2. This could happen through other proteins or by direct binding of CNOT2 to the TBX6L promoter region. If the latter hypothesis is to be true, we should be able to detect the consensus binding site for Not in the promotor regions of TBX6L. To investigate that possibility, we used the Regulatory Sequence Analysis Tools (RSAT) (http://rsat.sb-roscoff.fr/index.php, (Nguyen et al., 2018; van Helden, 2003)) to search for the consensus binding site determined for the human (in the lack of chicken genetic information) NOTO protein in the chicken TBX6L promoters. The consensus binding site was retrieved from the Human Transcription Factor Database (HumanTFDB) (http://bioinfo.life.hust.edu.cn/HumanTFDB/, (Hu et al., 2018)). As the relationship between the orthologs of CNOT2 and TBX6L were first described in zebrafish with *flh* and *spt*, we also performed the same analysis for the *spt* promoter. We found that spt/tbx16 has 8 putative binding sites (Table 3.2 A1), one of them located approximately 200bp from the transcription start site (Table 3.2-A2). Chicken TBX6 has 4 binding sites (Table 3.2-B1), one of them at less than 100bp from the start site (Table 3.2 L-B2).

Table 3.2 . spt and TBX6L have Noto family binding motifs in their promoters.
Results obtained from the Regulatory Sequence Analysis Tools (RSAT) showing the number and location of the identified consensus binding sites for Noto gene family binding motifs in the spt/tbx16 and TBX6L promoter sequences. **(A1)** Table showing the 8 Noto consensus binding sites found for zebrafish spt/tbx16 promoter sequence. **(A2)** Schematic representation of the location of the 8 Noto consensus binding sites found for zebrafish spt/tbx16 promoter sequence. **(B1)** Table showing the 8 Noto consensus binding sites found for chicken TBX6L promoter sequence. **(B2)** Schematic representation of the location of the 8 Noto consensus binding sites found for chicken TBX6L promoter sequence.

A1

Matching positions

PatID	Strand	Pattern	SeqID	Start	End	matching_seq	Score
START_END	DR	-	tbx16	-2000	-1	-	0.00
YHMATTA	D	YHMATTA	tbx16	-1501	-1495	caagTTAATTAggtt	1.00
YHMATTA	D	YHMATTA	tbx16	-1132	-1126	tcagTTCATTAaagc	1.00
YHMATTA	D	YHMATTA	tbx16	-631	-625	ttgcCTAATTAccct	1.00
YHMATTA	D	YHMATTA	tbx16	-258	-252	caaaTAAATTAaatg	1.00
YHMATTA	R	YHMATTA	tbx16	-1500	-1494	taacCTAATTAactt	1.00
YHMATTA	R	YHMATTA	tbx16	-1473	-1467	ttgcCTAATTAccct	1.00
YHMATTA	R	YHMATTA	tbx16	-1172	-1166	acacTTCATTAacca	1.00
YHMATTA	R	YHMATTA	tbx16	-1118	-1112	tccaCACATTAgctg	1.00

A2

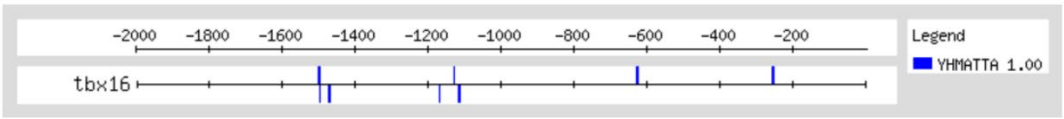

B1

Matching positions

PatID	Strand	Pattern	SeqID	Start	End	matching_seq	Score
START_END	DR	-	TBX6	-2000	-1	-	0.00
YHMATTA	D	YHMATTA	TBX6	-855	-849	taaaCTAATTAaggg	1.00
YHMATTA	D	YHMATTA	TBX6	-80	-74	cctgCTCATTAgcct	1.00
YHMATTA	R	YHMATTA	TBX6	-1408	-1402	gattTTCATTAcggc	1.00
YHMATTA	R	YHMATTA	TBX6	-854	-848	tcccTTAATTAgttt	1.00

B2

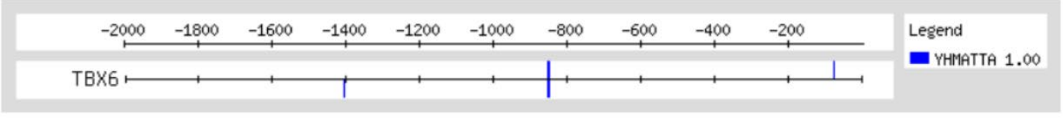

Discussion

The area of overlap of CNOT2/TBX6L expression seems to correspond to the previously described axial/paraxial stem cell niche

Although CNOT2 and TBX6L expression patterns have been previously described (Knezevic et al., 1997; Stein et al., 1996a) we further expanded these studies, observing that both genes are expressed in the posterior half of chick blastoderm stages, becoming restricted to the notochord and PSM progenitor cell regions as gastrulation takes place. An interesting previously undescribed result (Charrier et al., 1999) is the existence of an area of overlap between the expression domains of these two genes. This has been observed by whole-mount double in situ hybridization in several analyzed embryonic stages, HH1, HH4 and HH13. Unfortunately, this technique does not allow us to assess if these genes are co-express in the same cell, but only that there is an ever-present region where both genes are expressed. At stage HH4 the overlap region corresponds to the area containing both notochord and medial somite progenitor regions (Selleck and Stern, 1991; Selleck and Stern, 1992). It also corresponds to a recently described area in stage HH4 and HH8 where there is a stem-cell niche containing cells that will originate both notochord and somite (Solovieva et al., 2022). Despite the location of this axial/paraxial mesoderm stem cell niche not being precisely described at HH13, we propose that it corresponds to the region where we observe the co-expression of CNOT2/TBX6L.

CNOT2 represses TBX6L and paraxial mesoderm fate, leading mesoderm cells to adopt a notochord fate.

Taking into account the co-expression of CNOT2 and TBX6L in the axial/paraxial mesoderm stem cell niche, we hypothesized that, in the chicken embryo, CNOT2 could be involved in the axial/paraxial mesoderm decision of cells in this steam cell niche (Figure 3.14). To test this hypothesis, we overexpressed CNOT2 in the axial/paraxial progenitor region, at HH4, resulting in several morphological effects on the embryo (Figure 3.15). By analyzing our results we present bellow several lines of evidence that clearly support our hypothesis and further suggest that in the axial/paraxial stem cell region, CNOT2 represses TBX6L expression, leading to a notochord cell fate.

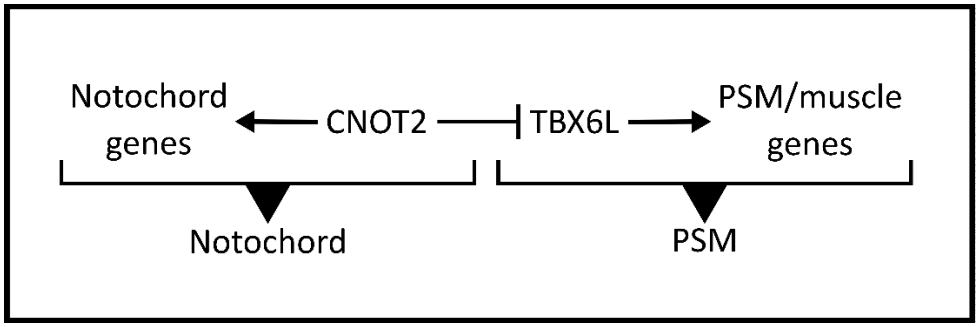

Figure 3.14 CNOT2 represses TBX6L leading axial/paraxial mesoderm progenitors to originate notochord.
Proposed model for the relationship between CNOT2 and TBX6L in the axial/paraxial mesoderm progenitor cell fate, based on our results. Like what is proposed in the zebrafish, in a mesoderm progenitor cell that will originate notochord, CNOT2 represses TBX6L which would upregulate PSM or muscle genes. This, along with possible upregulation of notochord genes (like the case of zebrafish ntl), leads progenitor cells to assume a notochord fate.

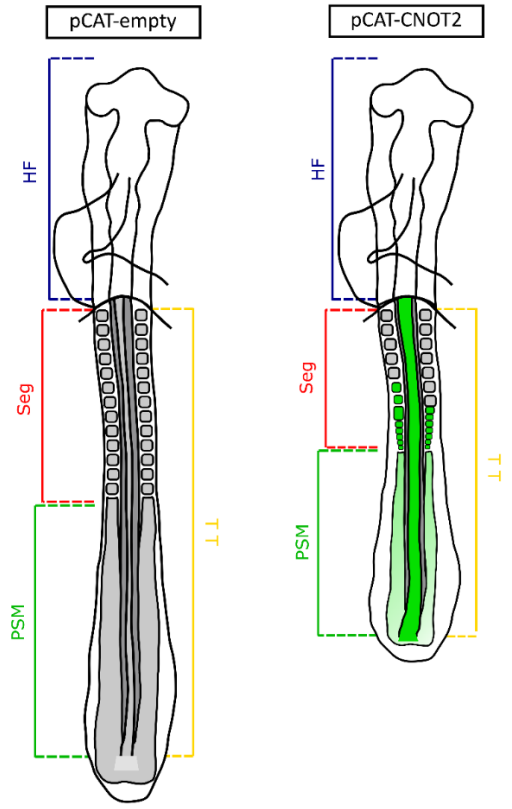

Figure 3.15 CNOT2 causes an increase in axial mesoderm cells at the cost of paraxial mesoderm
Schematic representation of a control embryo electroporated with pCAT-empty (on the left) and an embryo electroporated with pCAT-CNOT2. In the electroporated embryo, there is a shift in the balance between the progenitor axial and paraxial mesoderm cells. Increase in axial mesoderm cells causes an increase in the size of the corresponding structures (notochord and floor plate). Decrease in paraxial mesoderm cells results in a reduction of the lengths of the segmented and PSM regions of the embryo, several somite segmentation defects and rarefied PSMs

Elongation defects caused by CNOT2 electroporation support our hypothesis

The first morphological difference that we can observe in p-CAT-CNOT2 electroporated embryos is the notable shortening of the Seg, PSM and TT portions of the embryo. However, when we consider the head of the embryo, we observed a normal morphology in both control and p-CAT-CNOT2 electroporated embryos. Since we frequently saw green fluorescent cells in this region, this absence of effect could not be due to having no electroporated cells in the head.

What is underlying the reduced length values of Seg, PSM and TT in p-CAT-CNOT2 electroporated embryos ? Are we somehow affecting the structures or mechanisms required for trunk axial elongation ? To answer this question, we must first understand what these structures and mechanisms are.

When we consider the elongation of the primitive streak, it has already been established that convergent and intercalating movements towards the midline (Lawson and Schoenwolf, 2001a; Lawson and Schoenwolf, 2001b; Voiculescu et al., 2007), together with oriented cell division parallel to the anterior-posterior axis (Wei and Mikawa, 2000), produce its extension. As for the following stages, an idea of possible structures that could have a role in elongation can be obtained through the experiments of two historic figures of chick embryo developmental biology, Conrad Hal Waddington and Nelson J. Spratt Jr.. Both produced two very elegant experiments, in which they ablated blastoderms in similar regions: 1) just posterior to the primitive pit, before the appearance of the head process (Waddington, 1932) and 2) the whole blastoderm except a small part of the anterior portion of the embryo, containing the Hensen's Node and 0,4mm of the anterior primitive streak (Spratt Jr, 1947). After culture, both obtained embryos with an elongated "tail", posterior to the cut margin, complete with neural tube, notochord and somites. This experiment demonstrated that the structures that the remaining cells of the ablated embryos originate have the capacity to elongate the embryo axis autonomously. The notochord and the somites/PSM could then be candidate structures to play an important role in axis elongation. In the Masters thesis of this manuscript's author (Pais De Azevedo, 2009), the role of the notochord was tested through ablation experiments. The effect of notochord removal was not statistically significant, although it produced a trend of shorter embryos. This suggests that the notochord might have a role in chicken embryo AP axis elongation but would not be the main driving force. Later works performed by Bertrand Bénazeráf and colleagues,

amongst other authors, started to establish the structures and mechanisms underlying embryo axis elongation (Benazeraf, 2018; Xiong et al., 2020). When ablation experiments on different tissues were performed (Benazeraf et al., 2010), the authors observed that removal of the PSM seemed to produce the stronger effect on elongation speed. In the same work it was discovered that a random posterior-to-anterior gradient of cell motility on the PSM regulated elongation movements. This work was later expanded, and a very interesting model of force and movement relationships was proposed to drive embryo AP axis elongation (Xiong et al., 2020). Briefly, the expansion of the PSM due to the motility gradient compresses the axial tissues and, along with the normal intercalation cell movements cause them to elongate. This pushes the caudal progenitor cell area posteriorly, driving lateral movement of PSM progenitor cells, in turn, feeding the PSM, leading to the maintenance of the motility gradient and PSM expansion. In an insightful analogy, the mechanism is compared to an engine, with the PSM cells serving as the "fuel".

An example of a "loss of fuel" situation is the normal termination of elongation mechanism proposed to occur in chick embryos (Denans et al., 2015). It was discovered that loss of T/Brachyury and of the Retinoic Acid (RA)-degrading enzyme Cyp26A1 due to repression of FGF and Wnt signaling in the tailbud (Olivera-Martinez et al., 2012; Tenin et al., 2010) leads to an increase in RA signaling. This, in turn, results in increase of expression of neural genes in NMPs, leading to a shortage of PSM progenitors. It was discovered that activation of posterior set of Hox genes (9-13) in the tail-bud (Denans et al., 2015) causes a repression of FGF and Wnt signaling in the tailbud (Olivera-Martinez et al., 2012; Tenin et al., 2010) that leads to loss of T/Brachyury and of the Retinoic Acid (RA)-degrading enzyme Cyp26A1. This, in turn, originates an increase in RA signaling. Causing an in increase of expression of neural genes in NMPs, resulting in a shortage of PSM progenitors, which slows down elongation until its termination. These works highlight the PSM as one of the main driving forces of axis elongation.

With the importance of the PSM in mind, we suggest that, in our p-CAT-CNOT2 electroporated embryos, increase in CNOT2 signaling represses TBX6L, causing paraxial mesoderm progenitor cells to commit to axial mesoderm. As in the mechanism of elongation termination, this leads to a shortage of PSM progenitors, causing a lack of PSM cells and a consequent decrease in the PSM length. Supporting this hypothesis, the shortage of PSM cells can be observed in our embryos as the "rarefied aspect" of the

affected PSMs. An interesting way to confirm this lack of PSM cells would be to stain embryos with DAPI and use confocal microscopy to count the real number of PSM cells.

If electroporated embryos are shorter, does this mean that their elongation rates would also be lower ? Because of the aforementioned difficulty in counting somites and, consequently, of staging embryos and comparing lengths of same embryo stages, we used the HF measurement as a proxy for assessing embryonic stage (see results section and chapter 4 for more detailed descriptions). With this, we demonstrated that the elongation rate of p-CAT-CNOT2 electroporated embryos is lower than control ones. However, the difference in trends between both groups of embryos might also have another explanation: All embryos are electroporated between stages HH4 and HH5. As the embryo is progressing its development, the differences between Seg, PSM and TT lengths increase, the higher the stage the embryo develops until. This is consistent with our hypothesis. Since we electroporate p-CAT-CNOT2 in the area where axial and paraxial progenitor cells are located, according to our hypothesis, we are changing the fate of electroporated cells that would originate paraxial mesoderm to an axial mesoderm fate. In the first few hours of culture after electroporation, only a few cells have been affected and, thus, the effect on embryonic length would be low. As more cells that would give rise to paraxial mesoderm shift to axial mesoderm, the effect is increased and elongation is impaired with higher intensity, explaining the differences observed in the trends. When we compared the embryos electroporated with p-CAT-CNOT2 in which fluorescence was stronger against those in which fluorescence was weaker, we discovered that the trends were the same, with absolute length values being higher in embryos with lower fluorescence. This meant that the effect is dependent on the number of electroporated cells, consistent with our hypothesis that more paraxial mesoderm progenitor cells had their fate changed, reducing the size of the PSM.

Segmentation defects caused by CNOT2 electroporation support our hypothesis

Besides the shortened trunks, one of the most conspicuous morphological defects we noticed in the p-CAT-CNOT2 electroporated embryos was the presence of several defects in the segmented portion of the embryo. These ranged from somites with reduced size, especially in the ML axis, fused somites along the AP borders and a decreased AP distance between somites, these last ones we humorously called “concertina” embryos, due to the likeness to the musical instrument.

Somite size can be altered by changing the period of oscillation of the segmentation clock, as was done experimentally in zebrafish embryos (Liao et al., 2016). In this work, the pace of the clock was slowed down leading to the reduction of the segmentation period, which originated shortened somites. However, this also increased the number of somites produced. In our results, and although somite counting was difficult to achieve, we did not notice an increase in the number of somites. Although we do not rule out this hypothesis, pending a more thorough analysis of the number of somites formed, we suggest that p-CAT-CNOT2 electroporation did not cause a change in the pace of the segmentation clock.

What then could explain for the appearance of smaller somites in our electroporated embryos? In a classical experiment performed by Jonathan Cooke (Cooke, 1975), one of the creators of the "Clock and Wavefront Model", removal of up to one-third of early Xenopus blastula cells originated shorter embryos with the expected number of somites, but smaller. More recently, most of the principles of this model were quantified, resulting in an expansion to the model by demonstration of an interdependence between its two components (Lauschke et al., 2013). The authors describe the existence of a phase gradient across whole extension of the PSM that possesses the same amplitude independently of its length. With different PSM lengths, the slope of this gradient changes and was described as a predictor for somite size, showing it works as a scaling mechanism. We suggest that, in our p-CAT-CNOT2 electroporated embryos, the reduction of the PSM size causes a scaling down, effectively reducing somite size.

These hypotheses could explain somite shortening, but what about the cases where we found fused somites ? A possible reason could lie in the role of the paraxial protocadherin (PAPC) in embryo segmentation. In both chicken and mouse embryos this molecule has been shown to couple the segmentation clock to somite segmentation (Chal et al., 2017; Chal and Pourquie, 2017) as expression of PAPC regulated by the segmentation clock leads to endocytosis of N-cadherin (CDH2) at the rostral half of the forming somite. This causes a change in the cell adhesion, leading to the formation of the boundary and the individualization of the somite. What does PAPC have to do with CNOT2 then ? In Xenopus embryos, it was found that microinjection of the Xenopus ortholog of CNOT2 Xnot represses expression of PAPC (Kim et al., 1998). Additionally, in the dorsal midline of flh mutant embryos, where flh should be expressed, besides ectopic expression of spt, there is also expression of papc (Yamamoto et al., 1998). In this

work the authors establish that spt is required for the expression of papc and that both are repressed by flh. This suggests that, either directly or through the action of TBX6L, CNOT2 is upstream of PAPC regulating its expression. As the use of PAPC-RNAi in the rostral half of S-I of chicken embryos resulted in an increase of cell connectivity (Chal and Pourquie, 2017), this suggests that a similar process is occurring in our electroporation experiments. We thus propose that CNOT2 is downregulating the expression of PAPC, directly or through repression of TBX6L, thus leading to an increase in cell connectivity at the future somite border, causing it not to form. As not all the cells of the PSM are electroporated, somite fusion would only occur when enough cells have TBX6L/PAPC repressed and did not change their adhesion. An interesting way to test this hypothesis would be to perform in situ hybridizations of PAPC in electroporated embryos and confirm its downregulation.

Enlargement of notochords due to CNOT2 electroporation support our hypothesis

Another morphological feature of our p-CAT-CNOT2 electroporated embryos was the enlargement of the notochord. In notochords where we detected fluorescent labelling, we observed a clear increase in the width of the notochords, observable by the expression of its known marker, SHH. These results clearly support our hypothesis of a role for CNOT2 in defining chicken notochordal fate in mesodermal progenitor cells as it happens with *flh* in zebrafish. Combining this with our previous observations that showed reduction of PSM, this leads us to suggest that electroporated cells have changed their commitment from paraxial to axial mesoderm fate. This is a perfectly possible hypothesis, as it has been shown that prospective somitic cells on the lateral regions of HN and the rostral PS still have a degree of plasticity. Thus, in the chicken, overexpression of CNOT2 could repress paraxial mesoderm genes such as TBX6L and cells would be converted to an axial fate (Selleck and Stern, 1992). Also supporting this hypothesis, experiments done in Xenopus, where blastomeres of 4-cell stage embryos were injected with synthetic m-RNA of one of this species' ortholog of CNOT2, Xnot2, resulted in greatly enlarged notochords with a reduction of somitic tissue in 69% of injected embryos (Gont et al., 1996). Our results are in accordance with this study, as a strikingly similar percentage of our chicken embryos electroporated with CNOT2 also showed segmentation defects (53%) and rarefied PSM (63%) (indicative of lack of PSM cells).

CNOT2 repression of TBX6L support our hypothesis

In zebrafish, it has been previously described that CNOT2's ortholog flh downregulates TBX6L's ortholog spt, leading to the expression of genes necessary for the formation of the notochord (Amacher and Kimmel, 1998). In order for our hypothesis that the existent model for the relationship between flh and spt to also be valid for the chicken embryo, CNOT2 should also repress TBX6L.

However, at a first glance this was not the case, since in CNOT2 electroporated embryos a quite strong TBX6L expression could be observed along the entire PSM. However, a more careful analysis revealed a reduction of TBX6L expression in regions where the level of its expression is much lower: the medial tailbud region and in the most recently formed somites. This reduction was clearly associated with the presence of GFP fluorescence, meaning CNOT2 overexpression. This could mean that, in the PSM, the level of repression caused by CNOT2 overexpression would not be enough to suppress the strong level of TBX6L expression. Attesting to this is the difference in the NBT-BCIP revelation time necessary to observe TBX6L expression pattern in the PSM and in the recently formed somites.

We can also wonder about the reason why we observe such a strong level of TBX6L expression in PSM. One possibility is that this is related to the half-life of TBX6L mRNA. In mouse embryonic stem cells, it was found (Sharova et al., 2009) that the mouse ortholog Tbx6 has a higher half-life (approximately 11h) than the median of the other 19977 genes analyzed in this study (approximately 7h). It is described that transcription factors usually have a half-life of 1-2h, meaning that Tbx6 has a high half-life for a transcription factor. We found no data about chicken TBX6L, and it would be possible that the half-life of orthologs in different species could be different. However, another study (Yang et al., 2003) analyzed and compared data from human and Saccharomyces cerevisiae mRNA decay and found that the relationship between decay rates and functional classes were true for both species, leading them to suggest that there is a common "organizational scheme" for eukaryotes. Finally, they also describe that mRNA decay is strongly related to specific motifs. Considering all this, it would not be strange that chicken TBX6L would also have a high value half-life like its mouse ortholog.

As such, we suggest that, just like in zebrafish, CNOT2 is repressing TBX6L in axial mesoderm progenitor cells preventing them from assuming a paraxial mesoderm

fate. Although all the previous lines of evidence clearly support our hypothesis, for it to be true, CNOT2 must be able to bind to TBX6L. This could be done in one of two ways, either via direct binding of CNOT2 to TBX6L promoter or through other intermediate transcription factors. To investigate the first possibility, we searched the spt and TBX6L sequences for the consensus binding site determined for the human NOTO protein. We used this consensus binding site, as there is no data available for the specific chicken and zebrafish CNOT2 and flh binding motifs and the consensus sequence is usually a conserved feature. Indeed we found that, both the zebrafish spt and chicken TBX6L have several putative binding sites. This supports our hypothesis of a direct binding of flh/CNOT2 to the promoter regions and strongly suggests that CNOT2 is able to bind to TBX6L, repressing its activity in the chicken embryo.

Morphological similarities between CNOT2 electroporated embryos and zebrafish spt support our hypothesis

If indeed our hypothesis that CNOT2 is repressing TBX6L as in the zebrafish, then the phenotype of CNOT2 electroporated chicken embryos should be similar to the phenotype of spt mutants. Spt mutant embryos (Kimmel et al., 1989) are described as having a depletion of paraxial mesoderm in the trunk somites. Its head structures are normal, as well as other structures like the heart. The axial mesoderm is slightly enlarged as observed by expression of ntl (Hammerschmidt et al., 1996). The main feature of these mutants is the accumulation of cells in the tailbud that gives its characteristic appearance. Cells that would normally give rise to trunk somites originating from the lateral part of the germ ring converge dorsally. Lineage tracing studies in these mutants demonstrated that these cells move posteriorly, entering the tail and end up assuming different fates, such as notochord (Kimmel et al., 1989). All these features correspond to some of the morphological characteristics of the electroporated chicken embryos described above: the rarified and shortened PSM, the normal development of the head and heart structures and the enlargement of the axial mesoderm. As for the characteristic accumulation of cells, electroporated embryos also show an accumulation of cells in the midline, although it does not appear as frequently and is not located specifically in the tailbud. The difference in frequency can be explained by the nature of the electroporation experiments, when compared to mutants. In mutants, all cells have depletion of the specific gene, while in electroporation, there is only a partial quantity of cells that are electroporated. The difference in location might be explained by the fact that, in electroporated embryos it

depends on the AP level which would have a higher concentration of electroporated cells. As for the reduced AP length in the trunk of electroporated embryos, we found no description of a length change in the AP axis of mutant spt embryos. Their notochord is described as having a kinked and twisted appearance, as if compressed (Kimmel et al., 1989). However, this does not seem to be due to impairment of mediolateral cell intercalations in notochord progenitor cells (Ho and Kane, 1990). The authors thus suggest that notochord kinking occurs "secondarily to its extension" (Ho and Kane, 1990). As we already described, one of the main driving forces for chick embryo trunk elongation is the paraxial mesoderm. In the zebrafish embryo the notochord seems to play a more important role (McLaren and Steventon, 2021), as we will explain in more detail later. As notochord elongation would not be affected in mutant spt zebrafish embryos, overall trunk elongation would not be impaired, as it seems to be due to PSM depletion in the chick embryo. This would explain the apparent difference between elongation phenotypes in spt mutant zebrafish and p-CAT-CNOT2 electroporated embryos.

Apart from these two differences (location in the cell accumulations and AP trunk lengths), the chicken p-CAT-CNOT2 electroporated embryos and spt mutant embryos do share a remarkable common set of features.

CNOT2 regulates floor plate formation, possibly by repression of TBX6L

Our CNOT2 electroporation experiments yielded embryos showing changes in the notochord, but also in the floor plate and neural tube.

The first change that we observed was an overall enlargement of the whole floor plate. The increase in size seems to stem from an increase in the quantity of cells. Although we never quantified cell number, looking at the transverse sections, this is easily observable. The floor plate size increase was also very variable, which is consistent with an increase in the number of cells, as it would depend on the number of electroporated ones. In cases where we observed a considerable size increase, the location of the floor plate also changes, with it being located next to the notochord ventrally to the neural tube. We suggest that this is due to the abnormal number of floor plate cells: as cells are laid down by HN, the aberrant number of cells are not able to fully insert themselves between

the ventral halves of the neural tube. This results in the formation of an irregular structure that still has part of it attached to the neural tube. In the most extreme cases, this structure was shown to have cells expressing SHH, FOXA2 or none of these genes. We suggest that, in these situations, the cell accumulation structure could possess notochord progenitor cells, as well as floor plate ones, and even other types of cells. In the future, it would be interesting to characterize the cells present in this apparently heterogenous region.

Another observed change was the loss of the characteristic apical constriction aspect of the floor plate and, frequently in the same embryos, lack of neural tube closure. Normal neural tube closure is achieved through the constriction of the apical side of floor plate cells, forming the Medial Hinge Point (MHP) (Schoenwolf et al., 1992). The increase in the number of floor plate cells could potentially impair the formation of the apical constriction, resulting in incomplete or absence of neural tube closure.

What could lead to this increase in floor plate cell number ? Could it be that, just as we suggested for the notochord, CNOT2 might have a role on floor plate progenitor cell determination ? For this to be true, it would mean that, in our electroporation experiments, we would also be affecting floor plate progenitor cells. To answer these questions, we must look to the nature and origin of the floor plate structure.

The first thing that is essential to mention is that the structure that is referred to as floor plate is actually formed by cells with different developmental origins and with expression of different marker genes (Placzek and Briscoe, 2005; Strahle et al., 2004). Based on these two characteristics, different regions of the floor plate have been identified and classified along the ML and AP axis. This has apparently been a source of great controversies regarding the origin and mode of induction of floor plate cells (Le Douarin and Halpern, 2000; Placzek et al., 2000). Regarding the AP embryo level, two regions have been described in the chicken embryo, each with a different cell origin. The anterior floor plate (Patten et al., 2003) comprises a region positioned anteriorly to the hindbrain. Its cells originate from an area of prenodal epiblast located anteriorly to HN designated “area a” (Garcia-Martinez and Schoenwolf, 1993; Schoenwolf et al., 1989; Schoenwolf and Sheard, 1990). The posterior floor plate comprises the remaining posteriorly located regions along the entire spinal cord. Its cellular origin was first established through various fate-map and lineage-tracing studies as coming from HN (Catala et al., 1996; Charrier et al., 2002; Schoenwolf and Sheard, 1990; Selleck and Stern, 1991; Teillet et

al., 1998). Along its ML axis, there is also a distinction between two different types of floor plate (Charrier et al., 2002): The medial floor plate (MFP) is formed from cells that originate from HN and the lateral floor plate (LFP) is formed by adjacent neural plate cells that are induced by the medial floor plate and possibly by the notochord. MFP cells express markers such as SHH and FOXA2 and, while LFP initially also express them, FOXA2 expression is lost by the 7th day of development. Additionally, LFP always expresses neural markers such as SOX1, which MFP cells do not.

When considering these four different regions of floor plate, the morphological differences we observed in our results were restricted to the medial and posterior floor plate. In p-CAT-CNOT2 electroporated embryos, we did not observe differences in the floor plate located anteriorly to the hindbrain (data not shown). In the most severe cases of floor plate size increase it was clear that the affected region was the medial floor plate (see Figure 3.10 A2', B2', C2'). As such, the two floor plate regions in which p-CAT-CNOT2 electroporation produces changes are precisely the ones that have their origin in HN, which was the targeted region for electroporation. Since these floor plate cells have the same origin as notochord cells, it is plausible that our electroporation experiments are also affecting floor plate progenitor cells. Could CNOT2 then have a role in floor plate development ?

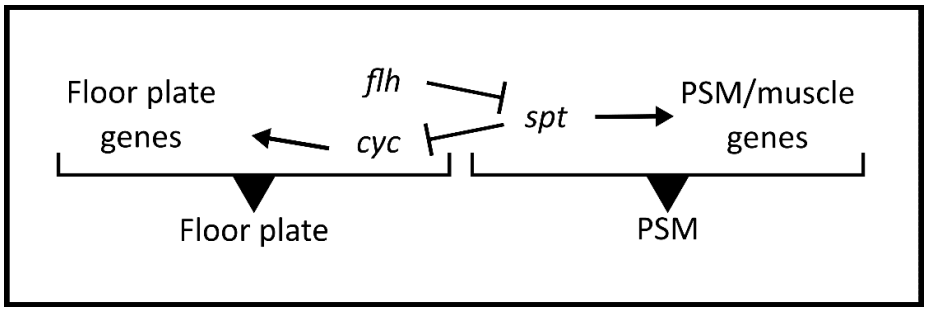

Figure 3.16 flh represses spt repression of floor plate genes like cyc leading axial/paraxial mesoderm progenitors to originate floor plate .
Simplified version of proposed model from for the relationship between flh and spt in the decision between floor plate and PSM cell fate, based on the literature. spt is suggested to repress floor plate genes like cyc and upregulate the expression of PSM/muscle genes leading to the formation of PSM progenitor cells. In floor plate progenitors, flh represses spt action allowing the action of floor plate genes like cyc in driving cells to a floor plate fate.

Indeed mutations in CNOT2's orthologs in other vertebrates have been known to produce changes in the floor plate. In Xenopus embryos injected with synthetic *Xnot2* (Gont et al., 1996) besides an enlargement in the notochord, the authors observed labelled injected cells also contributing to the floor plate (referred to as ventral spinal cord). In

zebrafish *flh* mutants, a continuous floor plate does not form in the trunk and tail (posteriorly to the hindbrain) and only a few islands of cells are present (Halpern et al., 1995; Talbot et al., 1995). However, since *flh*$^{-}$ cells transplanted into WT hosts were able to produce floor plates, this suggested that *flh*$^{-}$ cells are still capable of producing floor plate, when provided with non-autonomous signals from surrounding WT cells. The authors do not rule out a cell-autonomous role for *flh* in floor plate development, stating that "it remains to be demonstrated". There is another gene, *cyclops* (*cyc*) that, when mutated, causes an almost complete loss of floor plate (Hatta et al., 1991). Curiously, double *cyc*:*flh* mutants show total absence of both notochord and floor plate in all axial levels (Halpern et al., 1997), leading the authors to state that their phenotype to midline development is additive. While with *cyc* mutations, *flh* phenotype is accentuated, in double *spt*:*flh* mutants, an almost complete floor plate forms (Amacher and Kimmel, 1998), revealing that *spt* absence is able to correct the defective floor plate phenotype of *flh*. In the same way, *spt* mutation is also able to rescue the absence of floor plate phenotype of *cyc* single mutants, as in *spt*:*cyc* double mutants, the floor plate also forms normally (Amacher et al., 2002). Finally, in *spt* single mutants, the floor plate is slightly expanded and is also formed ectopically (Amacher et al., 2002; Amacher and Kimmel, 1998). With all these combined results, these authors thus suggested that *spt* is functioning as a repressor of midline cell fates such as notochord and floor plate. The authors additionally add that *spt* would then function as a regulator in the number of midline cells (Figure 3.16). Considering the data from other models and our results, we propose that CNOT2 promotes the development of the floor plate by repressing TBX6L, which would otherwise repress floor plate genes. This would lead paraxial mesoderm progenitor cells to adopt a floor plate fate (Figure 3.17).

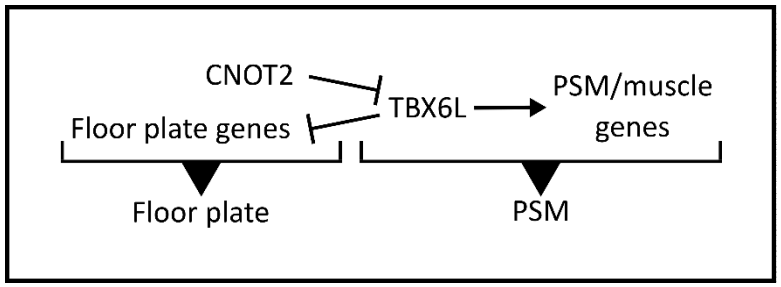

Figure 3.17 CNOT2 represses TBX6L repression of floor plate genes like leading axial/paraxial mesoderm progenitors to originate floor plate.
Proposed model for the relationship between CNOT2 and TBX6L in the decision between floor plate and PSM cell fate, based on our results. We suggest that TBX6L normally represses floor plate genes leading to the formation of PSM progenitor cells. In floor plate progenitors, CNOT2 represses TBX6L action allowing the action of floor plate genes in driving cells to a floor plate fate.

CNOT2 represses TBX6L and paraxial mesoderm fate, leading mesoderm cells to adopt an axial one instead.

As we discussed, our results showed that p-CAT-CNOT2 causes an enlargement of both the notochord and the floor plate. An increase in the notochord size was always accompanied by a corresponding increase in the floor plate. Moreover, the intensities of the phenotypes were clearly correlated, as embryos with the most severe phenotype on one structure always had the most severe phenotype of the other. And while the notochord always maintains its characteristic round shape, the increased floor plate often assumes an irregular one. This can be easily explained by the existence of the notochordal sheath that maintains its regular round shape. Since the floor plate cells does not possess a sheath or membrane around it, the cells would not be constrained to assume any particular shape, resulting in the variability observed in our results. As referred earlier it would be interesting to characterize the seemingly heterogenous population of the cell accumulation in the floor plate location, specifically for genes known to be activated by CNOT2.

On the other hand, we discovered that pCAT-CNOT2 electroporation did not cause an ectopic expression of SHH or FOXA2 on the somites and PSM, even though we observed electroporated cells in these structures. These two genes are two classical markers of notochord and floor plate respectively. This leads us to suggest that the effect of CNOT2 electroporation had one of two different outcomes: 1) Cells had their paraxial mesoderm path changed to axial mesoderm, contributing to the increase of the notochord or floor plate or maintained their paraxial mesoderm fate, even expressing CNOT2. We suggest that electroporation in these cells would still have cause expression of CNOT2, but it would not be enough to produce an effect of cell fate change. This could happen due to various reasons, including the presence of certain genes inhibiting CNOT2's action, the absence of others needed for its function or even epigenetic modifications like chromatin state changes from CNOT2 target genes. Nevertheless, CNOT2 overexpression could still have effects like the repression of PAPC leading to fusion of somites.

Taking in account all our results, we propose that, in the stem cell progenitor niche of chicken embryo's HN, axial mesoderm progenitors are maintained by the action of

CNOT2 in repressing the repressive activity of TBX6L on notochord and floor plate genes, allowing these cells to adopt an axial mesodermal fate (Figure 3.18).

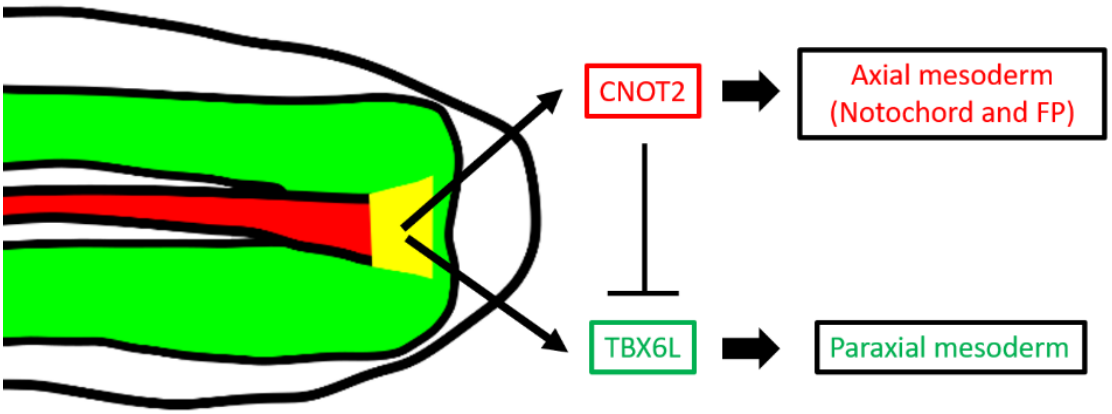

Figure 3.18 Model depicting the interaction between CNOT2 and TBX6L in axial/paraxial mesoderm cell fate decision in the chicken embryo.

References

Amacher, S. L., Draper, B. W., Summers, B. R. and Kimmel, C. B. (2002). The zebrafish T-box genes no tail and spadetail are required for development of trunk and tail mesoderm and medial floor plate. *Development* **129**, 3311-3323.

Amacher, S. L. and Kimmel, C. B. (1998). Promoting notochord fate and repressing muscle development in zebrafish axial mesoderm. *Development* **125**, 1397-1406.

Benazeraf, B. (2018). Dynamics and mechanisms of posterior axis elongation in the vertebrate embryo. *Cell Mol Life Sci* **76**, 89-98.

Benazeraf, B., Francois, P., Baker, R. E., Denans, N., Little, C. D. and Pourquie, O. (2010). A random cell motility gradient downstream of FGF controls elongation of an amniote embryo. *Nature* **466**, 248-252.

Catala, M., Teillet, M. A., De Robertis, E. M. and Le Douarin, M. L. (1996). A spinal cord fate map in the avian embryo: while regressing, Hensen's node lays down the notochord and floor plate thus joining the spinal cord lateral walls. *Development* **122**, 2599-2610.

Chal, J., Guillot, C. and Pourquie, O. (2017). PAPC couples the segmentation clock to somite morphogenesis by regulating N-cadherin-dependent adhesion. *Development* **144**, 664-676.

Chal, J. and Pourquie, O. (2017). Making muscle: skeletal myogenesis in vivo and in vitro. *Development* **144**, 2104-2122.

Chapman, S. C., Collignon, J., Schoenwolf, G. C. and Lumsden, A. (2001). Improved method for chick whole-embryo culture using a filter paper carrier. *Developmental dynamics: an official publication of the American Association of Anatomists* **220**, 284-289.

Charrier, J. B., Lapointe, F., Le Douarin, N. M. and Teillet, M. A. (2002). Dual origin of the floor plate in the avian embryo. *Development* **129**, 4785-4796.

Charrier, J. B., Teillet, M. A., Lapointe, F. and Le Douarin, N. M. (1999). Defining subregions of Hensen's node essential for caudalward movement, midline development and cell survival. *Development* **126**, 4771-4783.

Christ, B. and Ordahl, C. P. (1995). Early stages of chick somite development. *Anat Embryol (Berl)* **191**, 381-396.

Cooke, J. (1975). Control of somite number during morphogenesis of a vertebrate, Xenopus laevis. *Nature* **254**, 196-199.

Corallo, D., Trapani, V. and Bonaldo, P. (2015). The notochord: structure and functions. *Cell Mol Life Sci* **72**, 2989-3008.

Denans, N., Iimura, T. and Pourquie, O. (2015). Hox genes control vertebrate body elongation by collinear Wnt repression. *Elife* **4**.

Freitas, C., Rodrigues, S., Charrier, J. B., Teillet, M. A. and Palmeirim, I. (2001). Evidence for medial/lateral specification and positional information within the presomitic mesoderm. *Development* **128**, 5139-5147.

Fukuda, M., Takahashi, S., Haramoto, Y., Onuma, Y., Kim, Y. J., Yeo, C. Y., Ishiura, S. and Asashima, M. (2010). Zygotic VegT is required for Xenopus paraxial mesoderm formation and is regulated by Nodal signaling and Eomesodermin. *Int J Dev Biol* **54**, 81-92.

Garcia-Martinez, V. and Schoenwolf, G. C. (1993). Primitive-streak origin of the cardiovascular system in avian embryos. *Developmental biology* **159**, 706-719.

Gont, L. K., Fainsod, A., Kim, S. H. and De Robertis, E. M. (1996). Overexpression of the homeobox gene Xnot-2 leads to notochord formation in Xenopus. *Dev Biol* **174**, 174-178.

Gont, L. K., Steinbeisser, H., Blumberg, B. and de Robertis, E. M. (1993). Tail formation as a continuation of gastrulation: the multiple cell populations of the Xenopus tailbud derive from the late blastopore lip. *Development* **119**, 991-1004.

Griffin, K. J., Amacher, S. L., Kimmel, C. B. and Kimelman, D. (1998). Molecular identification of spadetail: regulation of zebrafish trunk and tail mesoderm formation by T-box genes. *Development* **125**, 3379-3388.

Guillot, C., Djeffal, Y., Michaut, A., Rabe, B. and Pourquie, O. (2021). Dynamics of primitive streak regression controls the fate of neuromesodermal progenitors in the chicken embryo. *Elife* **10**.

Halpern, M. E., Hatta, K., Amacher, S. L., Talbot, W. S., Yan, Y. L., Thisse, B., Thisse, C., Postlethwait, J. H. and Kimmel, C. B. (1997). Genetic interactions in zebrafish midline development. *Dev Biol* **187**, 154-170.

Halpern, M. E., Thisse, C., Ho, R. K., Thisse, B., Riggleman, B., Trevarrow, B., Weinberg, E. S., Postlethwait, J. H. and Kimmel, C. B. (1995). Cell-autonomous shift from axial to paraxial mesodermal development in zebrafish floating head mutants. *Development* **121**, 4257-4264.

Hamburger, V. and Hamilton, H. L. (1951). A series of normal stages in the development of the chick embryo. *J Morphol* **88**, 49-92.

Hammerschmidt, M., Pelegri, F., Mullins, M. C., Kane, D. A., Brand, M., van Eeden, F. J., Furutani-Seiki, M., Granato, M., Haffter, P., Heisenberg, C. P., et al. (1996). Mutations affecting morphogenesis during gastrulation and tail formation in the zebrafish, Danio rerio. *Development* **123**, 143-151.

Hatta, K., Kimmel, C. B., Ho, R. K. and Walker, C. (1991). The cyclops mutation blocks specification of the floor plate of the zebrafish central nervous system. *Nature* **350**, 339-341.

Henrique, D., Adam, J., Myat, A., Chitnis, A., Lewis, J. and Ish-Horowicz, D. (1995). Expression of a Delta homologue in prospective neurons in the chick. *Nature* **375**, 787-790.

Ho, R. K. and Kane, D. A. (1990). Cell-autonomous action of zebrafish spt-1 mutation in specific mesodermal precursors. *Nature* **348**, 728-730.

Hu, H., Miao, Y.-R., Jia, L.-H., Yu, Q.-Y., Zhang, Q. and Guo, A.-Y. (2018). AnimalTFDB 3.0: a comprehensive resource for annotation and prediction of animal transcription factors. *Nucleic Acids Research* **47**, D33-D38.

Kim, S. H., Yamamoto, A., Bouwmeester, T., Agius, E. and Robertis, E. M. (1998). The role of paraxial protocadherin in selective adhesion and cell movements of the mesoderm during Xenopus gastrulation. *Development* **125**, 4681-4690.

Kimmel, C. B., Kane, D. A., Walker, C., Warga, R. M. and Rothman, M. B. (1989). A mutation that changes cell movement and cell fate in the zebrafish embryo. *Nature* **337**, 358-362.

Knezevic, V., De Santo, R. and Mackem, S. (1997). Two novel chick T-box genes related to mouse Brachyury are expressed in different, non-overlapping mesodermal domains during gastrulation. *Development* **124**, 411-419.

Lauschke, V. M., Tsiairis, C. D., Francois, P. and Aulehla, A. (2013). Scaling of embryonic patterning based on phase-gradient encoding. *Nature* **493**, 101-105.

Lawson, A. and Schoenwolf, G. C. (2001a). Cell populations and morphogenetic movements underlying formation of the avian primitive streak and organizer. *Genesis* **29**, 188-195.

Lawson, A. and Schoenwolf, G. C. (2001b). New insights into critical events of avian gastrulation. *The Anatomical Record: An Official Publication of the American Association of Anatomists* **262**, 238-252.

Le Douarin, N. M. and Halpern, M. E. (2000). Discussion point. Origin and specification of the neural tube floor plate: insights from the chick and zebrafish. *Curr Opin Neurobiol* **10**, 23-30.

Liao, B. K., Jorg, D. J. and Oates, A. C. (2016). Faster embryonic segmentation through elevated Delta-Notch signalling. *Nat Commun* **7**, 11861.

Martin, B. L. and Kimelman, D. (2012). Canonical Wnt signaling dynamically controls multiple stem cell fate decisions during vertebrate body formation. *Dev Cell* **22**, 223-232.

Martins, G. G., Rifes, P., Amandio, R., Rodrigues, G., Palmeirim, I. and Thorsteinsdottir, S. (2009). Dynamic 3D cell rearrangements guided by a fibronectin matrix underlie somitogenesis. *PLoS One* **4**, e7429.

McLaren, S. B. P. and Steventon, B. J. (2021). Anterior expansion and posterior addition to the notochord mechanically coordinate zebrafish embryo axis elongation. *Development* **148**.

Nguyen, N. T. T., Contreras-Moreira, B., Castro-Mondragon, J. A., Santana-Garcia, W., Ossio, R., Robles-Espinoza, C. D., Bahin, M., Collombet, S., Vincens, P., Thieffry, D., et al. (2018). RSAT 2018: regulatory sequence analysis tools 20th anniversary. *Nucleic Acids Res* **46**, W209-W214.

Olivera-Martinez, I., Harada, H., Halley, P. A. and Storey, K. G. (2012). Loss of FGF-dependent mesoderm identity and rise of endogenous retinoid signalling determine cessation of body axis elongation. *PLoS Biol* **10**, e1001415.

Ordahl, C. and Le Douarin, N. (1992). Two myogenic lineages within the developing somite. *Development* **114**, 339-353.

Pais De Azevedo, T. (2009). Dynamics of embryo axis elongation in amniotes vs. anamniotes: The role of the notochord. In *Faculty of Sciences*. Lisbon, Portugal: University of Lisbon.

Pais de Azevedo, T., Magno, R., Duarte, I. and Palmeirim, I. (2018). Recent advances in understanding vertebrate segmentation. *F1000Res* **7**, 97.

Pais de Azevedo, T. P., Witten, P. E., Huysseune, A., Bensimon-Brito, A., Winkler, C., To, T. T. and Palmeirim, I. (2012). Interrelationship and modularity of notochord and somites: a comparative view on zebrafish and chicken vertebral body development. *Journal of Applied Ichthyology* **28**, 316-319.

Patten, I., Kulesa, P., Shen, M. M., Fraser, S. and Placzek, M. (2003). Distinct modes of floor plate induction in the chick embryo. *Development* **130**, 4809-4821.

Placzek, M. and Briscoe, J. (2005). The floor plate: multiple cells, multiple signals. *Nat Rev Neurosci* **6**, 230-240.

Placzek, M., Dodd, J. and Jessell, T. M. (2000). Discussion point. The case for floor plate induction by the notochord. *Curr Opin Neurobiol* **10**, 15-22.

Pourquie, O. and Tam, P. P. (2001). A nomenclature for prospective somites and phases of cyclic gene expression in the presomitic mesoderm. *Dev Cell* **1**, 619-620.

Riddle, R. D., Johnson, R. L., Laufer, E. and Tabin, C. (1993). Sonic hedgehog mediates the polarizing activity of the ZPA. *Cell* **75**, 1401-1416.

Ruiz i Altaba, A., Placzek, M., Baldassare, M., Dodd, J. and Jessell, T. M. (1995). Early stages of notochord and floor plate development in the chick embryo defined by normal and induced expression of HNF-3 beta. *Dev Biol* **170**, 299-313.

Ruvinsky, I., Silver, L. M. and Ho, R. K. (1998). Characterization of the zebrafish tbx16 gene and evolution of the vertebrate T-box family. *Dev Genes Evol* **208**, 94-99.

Schoenwolf, G. C., Bortier, H. and Vakaet, L. (1989). Fate mapping the avian neural plate with quail/chick chimeras: origin of prospective median wedge cells. *Journal of Experimental Zoology* **249**, 271-278.

Schoenwolf, G. C., Garcia-Martinez, V. and Dias, M. S. (1992). Mesoderm movement and fate during avian gastrulation and neurulation. *Dev Dyn* **193**, 235-248.

Schoenwolf, G. C. and Sheard, P. (1990). Fate mapping the avian epiblast with focal injections of a fluorescent-histochemical marker: ectodermal derivatives. *J Exp Zool* **255**, 323-339.

Selleck, M. A. and Stern, C. D. (1991). Fate mapping and cell lineage analysis of Hensen's node in the chick embryo. *Development* **112**, 615-626.

Selleck, M. A. and Stern, C. D. (1992). Commitment of mesoderm cells in Hensen's node of the to notochord and somite. *Development* **114**, 403-415.

Sharova, L. V., Sharov, A. A., Nedorezov, T., Piao, Y., Shaik, N. and Ko, M. S. (2009). Database for mRNA half-life of 19 977 genes obtained by DNA microarray analysis of pluripotent and differentiating mouse embryonic stem cells. *DNA Res* **16**, 45-58.

Solovieva, T., Lu, H. C., Moverley, A., Plachta, N. and Stern, C. D. (2022). The embryonic node behaves as an instructive stem cell niche for axial elongation. *Proc Natl Acad Sci U S A* **119**.

Spratt Jr, N. T. (1947). Regression and shortening of the primitive streak in the explanted chick blastoderm. *Journal of Experimental Zoology* **104**, 69-100.

Stein, S., Fritsch, R., Lemaire, L. and Kessel, M. (1996a). Checklist: vertebrate homeobox genes. *Mech Dev* **55**, 91-108.

Stein, S., Niss, K. and Kessel, M. (1996b). Differential activation of the clustered homeobox genes CNOT2 and CNOT1 during notogenesis in the chick. *Dev Biol* **180**, 519-533.

Strahle, U., Lam, C. S., Ertzer, R. and Rastegar, S. (2004). Vertebrate floor-plate specification: variations on common themes. *Trends Genet* **20**, 155-162.

Talbot, W. S., Trevarrow, B., Halpern, M. E., Melby, A. E., Farr, G., Postlethwait, J. H., Jowett, T., Kimmel, C. B. and Kimelman, D. (1995). A homeobox gene essential for zebrafish notochord development. *Nature* **378**, 150-157.

Teillet, M. A., Lapointe, F. and Le Douarin, N. M. (1998). The relationships between notochord and floor plate in vertebrate development revisited. *Proc Natl Acad Sci U S A* **95**, 11733-11738.

Tenin, G., Wright, D., Ferjentsik, Z., Bone, R., McGrew, M. J. and Maroto, M. (2010). The chick somitogenesis oscillator is arrested before all paraxial mesoderm is segmented into somites. *BMC Dev Biol* **10**, 24.

Tzouanacou, E., Wegener, A., Wymeersch, F. J., Wilson, V. and Nicolas, J. F. (2009). Redefining the progression of lineage segregations during mammalian embryogenesis by clonal analysis. *Dev Cell* **17**, 365-376.

van Helden, J. (2003). Regulatory sequence analysis tools. *Nucleic Acids Res* **31**, 3593-3596.

Voiculescu, O., Bertocchini, F., Wolpert, L., Keller, R. E. and Stern, C. D. (2007). The amniote primitive streak is defined by epithelial cell intercalation before gastrulation. *Nature* **449**, 1049-1052.

Voiculescu, O., Papanayotou, C. and Stern, C. D. (2008). Spatially and temporally controlled electroporation of early chick embryos. *Nat Protoc* **3**, 419-426.

Waddington, C. H. (1932). III. Experiments on the development of chick and duck embryos, cultivated in vitro. *Philosophical Transactions of the Royal Society of London. Series B, Containing Papers of a Biological Character* **221**, 179-230.

Wei, Y. and Mikawa, T. (2000). Formation of the avian primitive streak from spatially restricted blastoderm: evidence for polarized cell division in the elongating streak. *Development* **127**, 87-96.

Xiong, F., Ma, W., Benazeraf, B., Mahadevan, L. and Pourquie, O. (2020). Mechanical Coupling Coordinates the Co-elongation of Axial and Paraxial Tissues in Avian Embryos. *Dev Cell* **55**, 354-366 e355.

Yamamoto, A., Amacher, S. L., Kim, S.-H., Geissert, D., Kimmel, C. B. and De Robertis, E. (1998). Zebrafish paraxial protocadherin is a downstream target of spadetail involved in morphogenesis of gastrula mesoderm. *Development* **125**, 3389-3397.

Yamanaka, Y., Tamplin, O. J., Beckers, A., Gossler, A. and Rossant, J. (2007). Live imaging and genetic analysis of mouse notochord formation reveals regional morphogenetic mechanisms. *Dev Cell* **13**, 884-896.

Yang, E., van Nimwegen, E., Zavolan, M., Rajewsky, N., Schroeder, M., Magnasco, M. and Darnell, J. E., Jr. (2003). Decay rates of human mRNAs: correlation with functional characteristics and sequence attributes. *Genome Res* **13**, 1863-1872.

Supplementary material

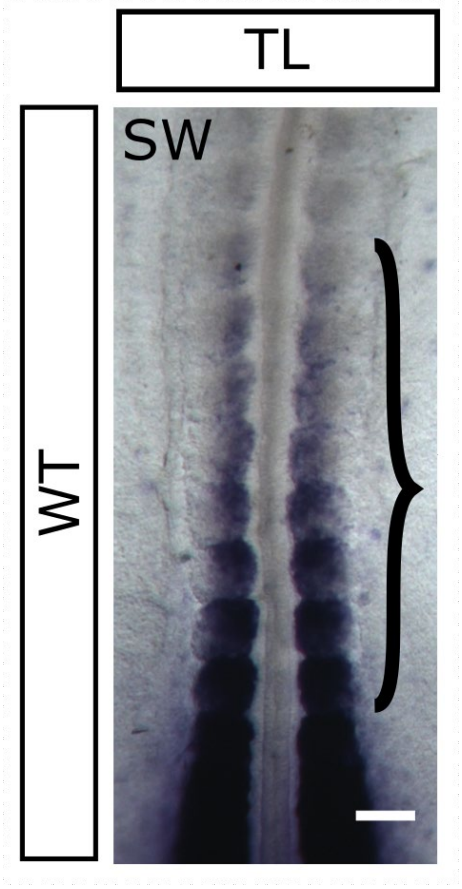

Supplementary figure 3.1 TBX6L expression extends to the 7-8 most recently formed somites. HH10+ wild type chick embryo showing somite expression of TBX6L with longer stain development revealing previously undescribed TBX6L expression in somites I-VIII (curved bracket).

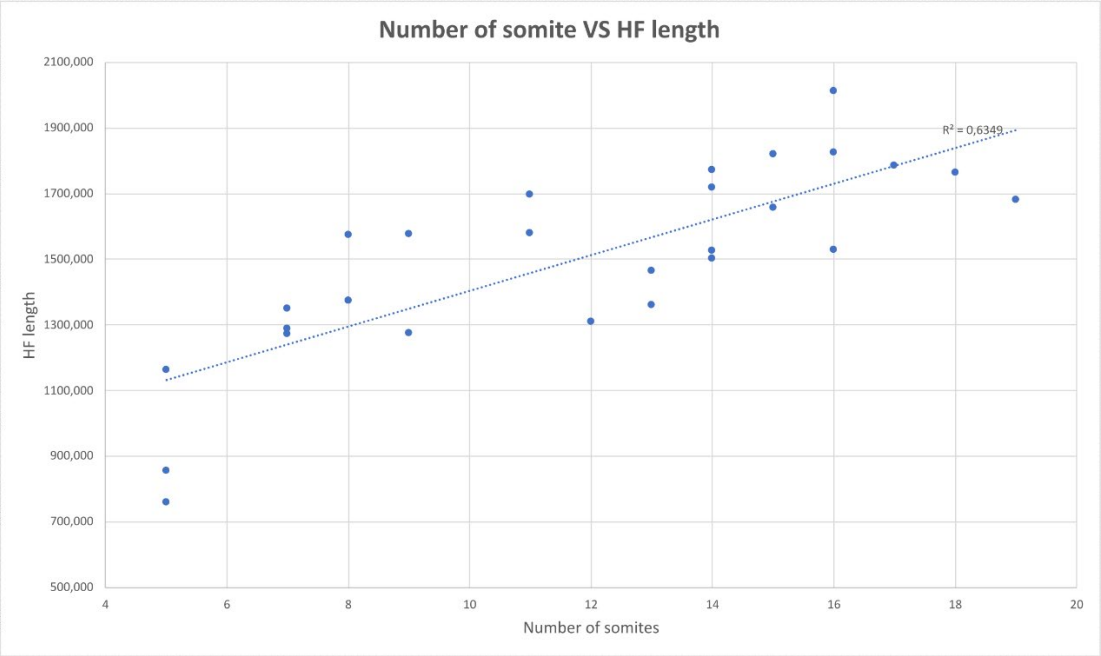

Supplementary figure 3.2 HF length of pCAT-empty electroporated embryos shows a growth trend with stage increase

The HF length measurement values of pCAT-empty electroporated embryos with fluorescence imaged at more and less than 400ms are plotted against the number of somites of the corresponding embryos. The linear trend and its R2 value are both shown.

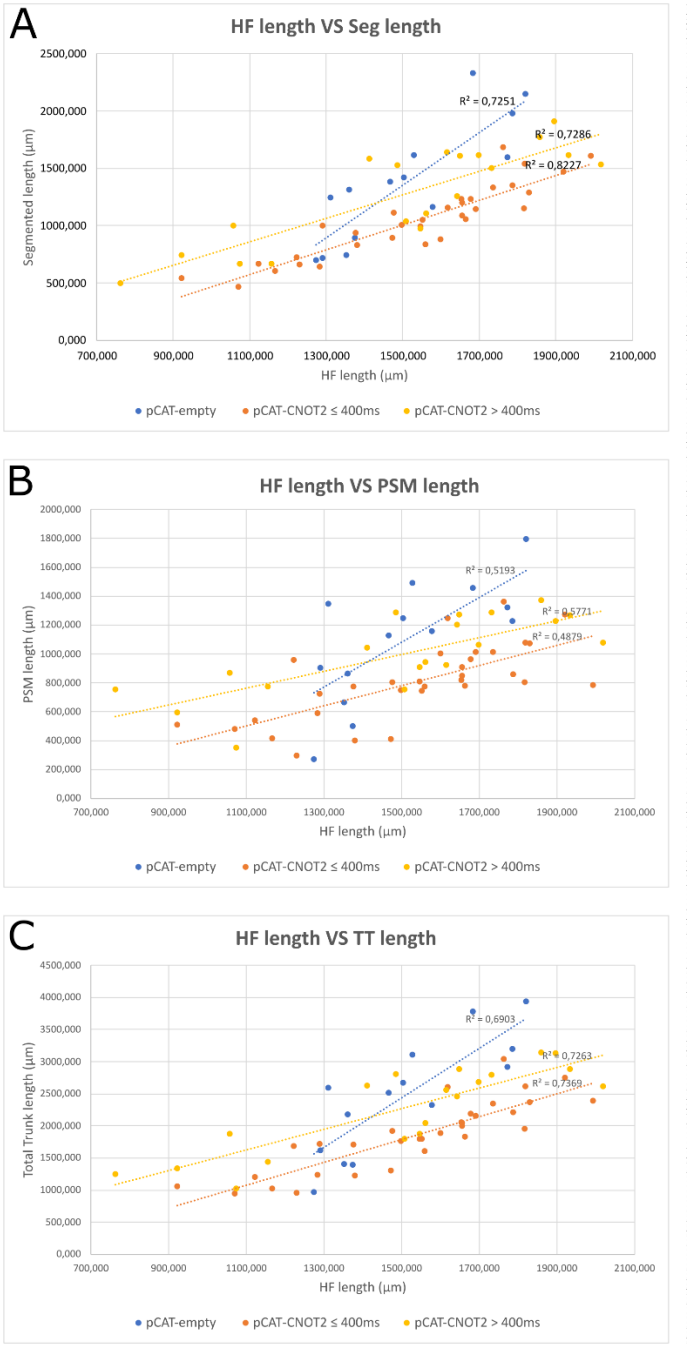

Supplementary figure 3.3 pCAT-CNOT2 electroporated embryos, that showed less fluorescence show the same elongation dynamics for Seg, PSM and TT portions of the embryo as embryos with more fluorescence.

(A-C) The length measurement values of the Seg, PSM and TT (A, B and C, respectively) portions of the embryo are plotted against the length measurement values of the HF for pCAT-empty and both pCAT-CNOT2 electroporated embryos that showed fluorescence imaged at more and less more than 400ms. Both groups of pCAT-CNOT2 electroporated embryos showed very similar elongation rates, although with proportionally higher length values for embryos that showed less fluorescence. The linear trend and its R2 value are both shown for all groups.

Supplementary movies 3.1-3.4 CNOT2 represses TBX6L in its low expression areas
(3.1-3.2) Morph merge of figures 3.13 B1-B3 and respective close-up showing reduction of TBX6L in the CNOT2 electroporated in the 5 most recently formed somites
(3.1-3.2) Morph of images of the embryo in figure 3.13 C and of figures 3.13 C1'-C3' (of the same embryo) showing reduction of TBX6L in the CNOT2 electroporated axial/paraxial progenitor region

Chapter IV – A morphometric characterization of early chicken embryo elongation

And now for something completely different (Anonymous news host)

In *Monty Python's Flying Circus (1969-1974)*

Size matters not. Look at me. Judge me by my size, do you ? (Master Yoda)

In *Star Wars: The Empire strikes back (1980)*

matters

The posterior limit of the *area pellucida* (pPL) as a reliable proxy for the end of the primitive streak in chick elongation studies

Ana C Maia-Fernandes, Tomas Pais de Azevedo, Ana Marreiros, Isabel Palmeirim, Raquel P Andrade

Centre for Biomedical Research - CBMR, University of Algarve, Algarve Biomedical Center, University of Algarve; Centre for Biomedical Research - CBMR, University of Algarve, Algarve Biomedical Center , University of Algarve; Centre for Biomedical Research - CBMR, University of Algarve, Algarve Biomedical Center, University of Algarve, Department of Medicine and Biomedical Sciences, University of Algarve; Centre for Biomedical Research - CBMR, University of Algarve, Algarve Biomedical Center , University of Algarve, Department of Medicine and Biomedical Sciences, University of Algarve; Center for Biomedical Research - CBMR, University of Algarve, Algarve Biomedical Center , University of Algarve, Department of Medicine and Biomedical Sciences, University of Algarve

Correspondence
rgandrade@ualg.pt

Disciplines
Developmental Biology

Keywords
Embryo Elongation
Morpholgical Landmarks
Chicken Embryo

Type of Observation
Standalone

Type of Link
Standard Data

Submitted Mar 22, 2019
Published Apr 5, 2019

Triple Blind Peer Review
The handling editor, the reviewers, and the authors are all blinded during the review process.

Full Open Access
Supported by the Velux Foundation, the University of Zurich, and the EPFL School of Life Sciences.

Abstract

Early embryo elongation involves coordinated cellular and tissue behaviors that are readily observable in the chick embryo vertebrate model system. Easily identifiable morphological landmarks are crucial to obtain reliable morphometric data, particularly when assessing tissue elongation over time. The posterior end of the primitive streak marks the caudal end of the chick embryonic tissue. However, the identification of its precise location is ambiguous, especially to the untrained eye. Herein, we assessed if the posterior limit of the *area pellucida* (pPL), which is readily recognizable due to the optical contrast with the *area opaca*, is a valid proxy for the caudal limit of the primitive streak. Measurements of total embryo length were performed in multiple images of chick embryos over time using both caudal landmarks. We found that the pPL offered greater precision and a higher degree of inter-user reproducibility, when compared to the end of the primitive streak. Importantly, our work uncovers a quantitative proportionality between embryo length measurements using the end of the primitive streak and the pPL as caudal landmarks. We have thus validated the pPL as a reliable morphological proxy for the end of the primitive streak in chick embryo elongation studies.

Introduction

Vertebrate embryo body elongation requires the orchestrated growth of multiple tissues, involving cell proliferation, migration and rearrangements along the anterior-posterior axis [1]. During early development, the embryo body elongates as epiblast cells, migrate through the primitive streak and are specified into multiple tissues. Live-imaging studies have been used with great success to characterize the dynamics of these processes, as well as to evaluate the impact of different culture conditions or drug exposure on embryo elongation [1]. The chick embryo is an ideal model for such experimental approaches, due to the availability of *in ovo* and *ex-ovo* culture systems amenable to live imaging approaches, and also because it presents striking morphological similarities to human development in early stages [2].

The choice of specific morphological landmarks is a critical step when characterizing embryo elongation. These should be easily and reproducibly identifiable throughout the whole course of the experiment, and also among distinct users. When studying net embryo elongation at the expense of the epiblast tissue, it is useful to measure embryo length until the end of the primitive streak. However, it is not trivial to pinpoint this morphological landmark in a reproducible manner, even when analyzing the same embryo over time. This introduces a degree of inaccuracy to the measurements performed, and strongly hinders automated image recognition and analysis. The posterior limit of the *area pellucida* (henceforth designated pPL) is located immediately caudal to the end of the primitive streak. The pPL is readily recognizable due to the optical contrast between the *area pellucida* and the *area opaca*, and has been used to characterize embryo elongation rates in several studies [3] [4] [5] [6]. However, to what extent the pPL can be used as a reliable proxy for the end of the primitive streak has not yet been assessed.

Objective

The objective of this work was to validate the easily identifiable posterior limit of the *area pellucida* (pPL) as a reliable proxy for the end of the primitive streak for chick embryo elongation studies.

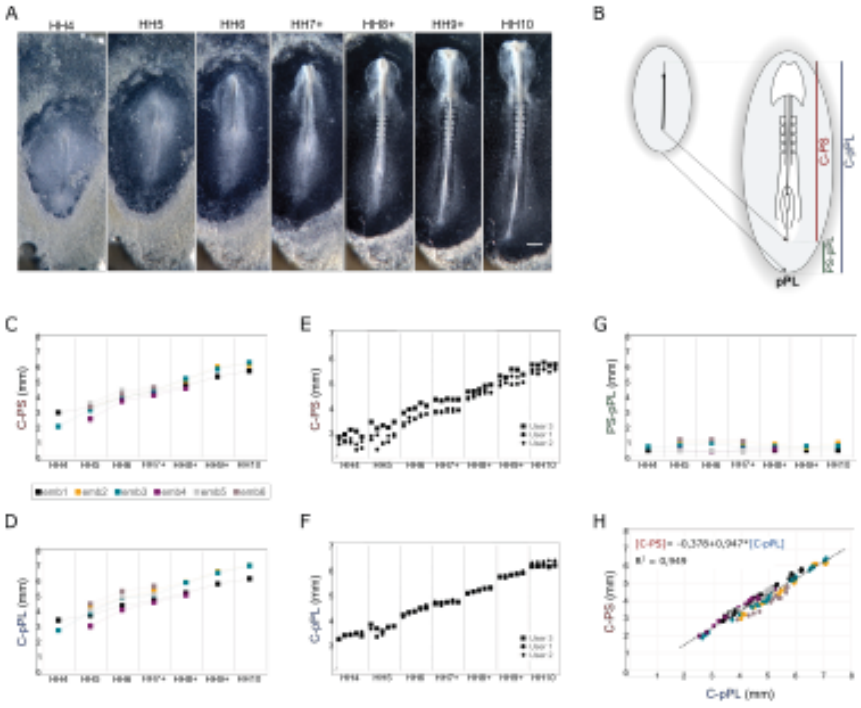

Figure Legend

Figure 1. The posterior limit of the *area pellucida* (pPL) is a valid and reproducible landmark for chick embryo elongation studies.

(A) Representative images of the developmental stages analyzed, obtained from a single embryo over time. Scale bar: 0.5 mm.

(B) Illustration of the measurements performed. C-PS: distance from the crown to the caudal end of the primitive streak (red line); C-pPL: distance from the crown to the pPL (blue line); PS-pPL: distance from the caudal end of the primitive streak to the pPL (green line).

(C) Measured C-PS length per developmental stage. Colored symbols represent different embryos (emb; n=6).

(D) Measured C-pPL length per developmental stage. Colored symbols represent different embryos (emb; n=6).

(E) C-PS length of multiple images of a single embryo per developmental stage (n=5), independently measured by 3 different users.

(F) C-pPL length of multiple images of a single embryo per developmental stage (n=5), independently measured by 3 different users.

(G) Measured distance between the end of the primitive streak and the pPL (PS-pPL) per developmental stage. Colored symbols represent different embryos (emb; n=6).

(H) C-PS measures plotted against respective C-pPL lengths. Colored symbols represent different embryos (emb; n=6).

Results & Discussion

We performed time-lapse imaging of chick embryos cultured in New [7] or EC [8] systems (n=3 each) from early gastrulation to somitogenesis stages (HH4 to HH10 [9]) (Fig. 1A). Embryo length was measured from the crown to the end of the primitive streak (C-PS; Fig. 1B, C) and to the pPL (C-pPL; Fig. 1B, D). Measurements were performed in multiple independent frames per developmental stage (n=5 each) for each embryo (total n=6). We found that embryo growth over time displays a similar trend independently of the morphological landmark used (Fig. 1C, D). In fact, both C-PS and C-pPL measurements increase steadily in the embryonic stages analyzed.

To test the reproducibility of the results when the measurements are performed using each landmark, C-PS and C-pPL were measured in a single embryo over time by 3 operators with different years of experience with the chick embryo model (Fig. 1E, F). Figure 1E evidences significant variability in C-PS length measured by distinct users, which can differ up to 0.84 mm (HH5; 2.81 mm average length). This stems from differences in where each operator positions the end of the primitive streak. Importantly, the variability of the C-pPL measurement performed by the independent users is almost negligible (Fig. 1F). This highlights that the contrast between the posterior border of the *area pellucida* and the *area opaca* is an easily recognizable landmark for both experienced and inexperienced experimentalists. The pPL landmark thus allows for high precision measurements for embryo length studies.

For pPL to be a valid proxy for the end of the primitive streak, the distance between the two landmarks (PS-pPL) should be approximately constant over time; i.e., any variation in C-pPL length should be exclusively due to a respective variation in C-PS. We found that this is the case, since the natural variations observed in PS-pPL distances over time (Fig. 1G) were neglectable when compared to the progressive increase in C-pPL length (Fig. 1D). These findings evidence that C-pPL variation over time reliably represents C-PS dynamics, thus validating the use of the pPL as a precise and reliable morphological landmark for chick embryo elongation studies.

Finally, when C-PS values were plotted against their respective C-pPL, for all embryos and developmental stages analyzed, a direct proportionality was found represented by the equation [C-PS] = -0.378 + 0.947[C-pPL] with $R2 = 0.949$ (mean error of estimated C-PS = 0.206±0.132). This means that the absolute value of C-PS length can be directly calculated from C-pPL measurement.

Conclusions

Altogether, our results evidence that the posterior limit of the area pellucida (pPL) is a reliable morphological proxy for the end of the primitive streak. The pPL landmark provides higher precision measurements and minimizes inter-user variability. Importantly, we describe a novel quantitative relationship between C-PS and C-pPL, which represents a powerful tool to directly infer C-PS from experimentally-measured C-pPL.

Limitations

This study was performed in HH4-HH10 [9] embryonic stages, thus the pPL landmark was only validated for this developmental time window. Although the findings are con-

sistent in both New and EC culture systems, the sample size is limited and may not reflect the variability that could be found with a larger population set.

Alternative Explanations

Conjectures

With the recent technological developments, there is an increased usage of live-imaging approaches to study embryo elongation and elucidate the mechanisms underlying this highly coordinated event. This may involve experimentally challenging the system by altering gene expression, signaling pathway modulation, microsurgical approaches, among others. As such, a thorough and precise characterization of chick embryo elongation in control conditions is more relevant than ever. The pPL herein validated is a powerful landmark for such studies, as it provides greater precision and inter-user reproducibility in embryo length measurements. Finally, the clear optical contrast between the *area pellucida* and *area opaca* may allow the precise identification of the pPL landmark by automated image recognition and analysis tools.

Additional Information

Methods

Chicken embryos and culture

Fertilized chicken (Gallus gallus) eggs were provided by commercial sources and incubated in a humidified atmosphere and controlled temperature (38°C). HH4-5 [9] embryos were cultured in either New [7]or EC [8] culture systems for up to 24 h at 38°C in a humidified atmosphere.

Image acquisition and analysis

Time-lapse movies were performed using a Zeiss SteREOLumarV12 Stereomicroscope coupled with a Zeiss Axiocam MRc camera. Measurements were performed in 5 independent frames per developmental stage for each embryo analyzed (150 images in total), using Axiovision Se 64 Rel 4.9.1 (Carl Zeiss) or FIJI [10] software. Data analysis was performed using Excel and SPSS software.

Funding Statement

This work was supported by FCT, Portugal (grant PTDC/BEX-BID/5410/2014) and Research Center Grant UID/BIM/04773/2013 CBMR 1334. The Light Microscopy Unit was partially funded by PPBI-POCI-01-0145-FEDER-022122. TPA and ACMF were supported by FCT fellowships SFRH/BD/84825/2012 and PTDC/BEX-BID/5410/2014, respectively.

Acknowledgements

We thank Gil Carraco for help in time-lapse imaging and Ana P. Martins-Jesus for performing measurements as an independent user. We thank Gil Carraco, Ana P. Martins-Jesus, Isabel Duarte, Ramiro Magno and Paulo Martel for helpful discussions. We acknowledge the staff of the Light Microscopy Unit of CBMR-UAlg for technical support. ACMF thanks José and Ana Paula Fernandes for their constant support in her growth.

Ethics Statement

Not Applicable.

Citations

[1] Bertrand Bénazéraf. "Dynamics and mechanisms of posterior axis elongation in the vertebrate embryo". In: *Cellular and Molecular Life Sciences* 76.1 (2019), pp. 89–98. DOI: 10.1007/s00018-018-2927-4. URL: https://doi.org/10.1007/s00018-018-2927-4.

[2] Claudio Stern. "The chick model system: a distinguished past and a great future". In: *The International Journal of Developmental Biology* 62.1-2-3 (2018), pp. 1–4. DOI: 10.1387/ijdb.170270cs. URL: https://doi.org/10.1387/ijdb.170270cs.

[3] Ruth Bellairs, D. R. Bromham, and C. C. Wylie. "The influence of the area opaca on the development of the young chick embryo". In: *Journal of Embryology and Experimental Morphology* 17 (1967), pp. 195–212.

[4] Claudio D. Stern and Ruth Bellairs. "The roles of node regression and elongation of the area pellucida in the formation of somites in avian embryos". In: *Journal of Experimental Morphology* 81 (1984), pp. 75–92.

[5] Kaichiro Sawada and Hirohiko Aoyama. "Fate maps of the primitive streak in chick and quail embryo: ingression timing of progenitor cells of each rostro-caudal axial level of somites." In: *The International Journal of Developmental Biology* 43 (1999), pp. 809–815.

[6] Chompunut Lumanglkul et al. "Characterizing early embryonic development of Brown Tsaiya Ducks (Anas platyrhynchos) in comparison with Taiwan Country Chicken (Gallus gallus domestics)". In: *PLOS ONE* 13.5 (2018), e0196973. DOI: 10.1371/journal.pone.0196973. URL: https://doi.org/10.1371/journal.pone.0196973.

[7] D. A. T. New. "A New Technique for the Cultivation of the Chick Embryo in vitro". In: *Journal of Embryology and Experimental Morphology* 3 (1955), pp. 320–331.

[8] Susan C. Chapman et al. "Improved method for chick whole-embryo culture using a filter paper carrier". In: *Developmental Dynamics* 220.3 (2001), pp. 284–289. DOI: 10.1002/1097-0177(20010301)220:3<284::aid-dvdy1102>3.3.co;2-x. URL: https://doi.org/10.1002/1097-0177(20010301)220:3%3C284::aid-dvdy1102%3E3.3.co;2-x.

[9] Viktor Hamburger and Howard L. Hamilton. "A series of normal stages in the development of the chick embryo". In: *Journal of Morphology* 88.1 (1951), pp. 49–92. DOI: 10.1002/jmor.1050880104. URL: https://doi.org/10.1002/jmor.1050880104.

[10] Johannes Schindelin et al. "Fiji: an open-source platform for biological-image analysis". In: *Nature Methods* 9.7 (2012), pp. 676–682. DOI: 10.1038/nmeth.2019. URL: https://doi.org/10.1038/nmeth.2019.

A MORPHOMETRIC CHARACTERIZATION OF EARLY CHICK EMBRYO ELONGATION

Maia-Fernandes, A.C.[1,2*], Pais de Azevedo, T. [1,2,3*], Ramalhete, S.[1,2], Martins, G.[3¥], Palmeirim, I.[1,2,4], Duarte, I.[2,5], , Martel, P.[5,6], Marreiros, A.[1,2], Andrade, R.P.[1,2,4§]

[1]ABC-RI, Algarve Biomedical Center Research Institute, Faro, Portugal

[2]Faculdade de Medicina e Ciências Biomédicas (FMCB), Universidade do Algarve, Campus de Gambelas, 8005-139 Faro, Portugal

[3]Departamento de Biologia Animal, Centro de Ecologia, Evolução e Alterações Ambientais, Faculdade de Ciências, Universidade de Lisboa, 1749-016 Lisbon, Portugal

[4]Champalimaud Research Program, Champalimaud Center for the Unknown, Lisbon, Portugal

[5]Center for Health Technology and Services Research (CINTESIS), Polo da Universidade do Algarve, 8005-139 Faro, Portugal

[6]Faculdade de Ciências e Tecnologia (FCT), Universidade do Algarve, Campus de Gambelas, 8005-139 Faro, Portugal

[¥]Current address: Advanced imaging unit – IGC, Lisbon, Portugal

*equal contribution

[§]Corresponding author (rgandrade@ualg.pt)

The work that follows is the manuscript of an article in preparation for submission

Introduction

Vertebrate embryo elongation requires a high level of coordination of several tissues in time and space. This process starts very early in development, after the first cell divisions and the establishment of the blastoderm. At this time, the primitive streak (PS), a thickening of the caudal portion of the epiblast that extends anteriorly is formed and establishes the anteroposterior (AP) axis of the embryo. After the PS has fully extended, it starts to regress and shorten, as epiblast cells migrate inwardly through it and move anteriorly and laterally, originating the three germ layers, through the process known as gastrulation. As the cells are laid down, they start to organize themselves forming structures such as the notochord, neural tube and presomitic mesoderm (PSM). This originates an AP gradient of differentiation with the formation of the head structures anteriorly, segmentation of the PSM in the middle and gastrulation still occurring posteriorly. Cell migration and structure formation in this fashion leads to the elongation of the AP axis of the embryo (Benazeraf and Pourquie, 2013; Hamburger and Hamilton, 1951). As this is such a crucial period in embryo development, it is no surprise many congenital diseases may have their origin in problems arising during these first stages, making them highly relevant in biomedical research. The study of gastrulation in human embryos, however, is limited by ethical regulations such as the 14-day rule, which limits experiments done in human embryos (Hyun, 2016) to the first 14 days of development. It is in this period that gastrulation starts and, as such, the use of model organisms becomes vital. With more than 2000 years of history of usage, one such organism is the chicken embryo (Stern, 2004; Stern, 2018). Its many advantages in relation to other models include its availability throughout the year, its relative cheap cost, the accessibility to the embryo without the need to sacrifice any adults, the possibility of culture through numerous techniques, both in ovo and ex-ovo reviewed in (Stern and Bachvarova, 1997), and the ability to perform chimeric studies in conjunction with quail embryos. But the chick embryo is not only a very good model for morphological studies, as with the advent of molecular biology, several techniques were devised, allowing for manipulation of gene expression studies. These include the possibility of changing gene expression through use of morpholinos (Norris and Streit, 2014) or *in ovo* or *ex ovo* electroporation (Momose et al., 1999) and even the development of transgenic lines (Chapman et al., 2005; Huss et al., 2015; Sato and Lansford, 2013; Serralbo et al., 2020). But the most interesting advantage of the chick embryo as a model regarding biomedical research is its similarity

to the human embryo. It is in fact the most similar model when it comes to the tridimensional organization of the embryo during gastrulation, making it the ideal candidate to study this very important process. Attesting to this fact and to the ongoing relevance of the chick embryo is its contribution to a recent milestone of human development research. Specifically, human stem cells were treated with Wnt and Activin were transplanted to gastrulating chick embryos where they were able to induce a new axis of development, establishing the "organizer" capacity of these cells (Martyn et al., 2018). As such, a thorough knowledge and characterization of gastrulation in chick embryos is of great relevance.

The use of the chick embryo as a developmental model has been greatly facilitated by the key work of Hamburger and Hamilton published in 1951 (Hamburger and Hamilton, 1951). The objective of this work was to characterize and establish stages for the entire chick embryo development, based on external morphological characters. Since embryos with the same time of incubation show different morphological features, the independence of the developmental time of this method represented a huge advantage. Besides this, the authors added photographs, illustrations and small descriptions of each stage. Because of this, the HH staging tables have become the gold standard and have been widely used since 1951. However, Hamburguer and Hamilton's work was not without its limitations, as stated by the authors themselves. One is the fact that one embryo may show characteristics of different stages, making the staging process more uncertain. Also, the figures shown represent only discrete transient stages, which does not inform on the relative change of different structures and the rate at which they do so. With the advent of live imaging, it is now possible to provide more complete data by continuously analyzing different stages of the same embryo. Besides that, while the illustrations remain remarkable in detail, the photomicrographs shown do not stand up to current microscopy standards, as better equipment with much higher resolution is now available.

Nevertheless, with the framework developed by Hamburger and Hamilton, many studies on the mechanics of chick elongation have been performed. These have uncovered the role of different mechanisms on the elongation of the different embryonic structures. The PS for instance, elongates through a combination of cell divisions oriented over the AP axis (Wei and Mikawa, 2000) and convergent extension (Lawson and Schoenwolf, 2001; Voiculescu et al., 2007), that is, mediolateral cell or tissue intercalation movements (Keller et al., 2008). As for the axial structures, while the notochord extends through three

different processes, cell accretion (addition of cells from Hensen's node), cell rearrangements and oriented cell division (Sausedo and Schoenwolf, 1993; Sausedo and Schoenwolf, 1994), the neural tube mainly elongates through oriented cell division and convergent extension (Sausedo et al., 1997; Schoenwolf et al., 1989). Alternatively, the PSM was shown to elongate through different mechanisms (Benazeraf et al., 2010). Throughout the AP length of the PSM, there is both a gradient of cell motility under the control of the FGF gradient (cells moving with a higher rate in the posterior, when compared to the anterior), and an opposing gradient of cell density. These opposing gradients create a bias in the directionality of movement of PSM cells to the posterior end, contributing to elongation over short time scales. However, over larger periods of time, the increase in PSM cell number due to proliferation and addition of new cells add on to the directional cell movement, resulting in elongation without severe change in PSM width (Benazeraf et al., 2017). The mechanisms of whole embryo elongation on the other hand, have not yet been fully uncovered, although recent studies have highlighted the importance of specific tissues. The PSM, for instance, has been proposed to be a driving force of posterior axis elongation. In ablation experiments of different embryo portions, the removal of the PSM was shown to have the strongest effect on elongation speed (Benazeraf et al., 2010). This effect is also seen when its gradient of cell motility is impaired by changes in FGF signalling or by use of cell movement inhibitors. Another region of the embryo that could contribute to the elongation of its axis is the Axial-Paraxial Hinge (APH), which corresponds to a combination of cells from the rostral portion of the node and from anterior portion of the PS, which are closely connected (Charrier et al., 1999). When this region is ablated (Charrier et al., 1999) or the connection between the two regions broken by a physical barrier (Thibert et al., 2003), this results in truncated embryos posterior to the forelimbs in 4-day old embryos reviewed in (Charrier et al., 2005).

Still the exact contributions of each structure, region or mechanism remains to be determined and it is possible that it is a combinatory action of different forces that results in the elongation of the early chicken embryo (reviewed by (Bénazéraf, 2019). In this sense, there is a need for studies and tools to help quantify these variables. The development of a transgenic quail system (Huss et al., 2015), for example, allowed for a thorough characterization of the chick embryo elongation from stage HH10+ (Benazeraf et al., 2017). This work described the different tissue coupling and uncoupling dynamics,

uncovering extensive tissue sliding, which may be underlying elongation in these stages. However, in early somitogenesis stages, such a characterization has not yet been performed.

In this work we set out to produce a thorough description of early chick embryo using high temporal and spatial resolution. For that, we performed high quality time-lapse imaging of chicken embryos from HH4 to HH10 and measured the distances between multiple morphological landmarks over time. With this data, we were able to assess elongation rates of the whole embryo and its composing portions, uncovering the relative contribution of each tissue for overall A-P growth. Using this characterization, we assembled a novel morphometric tool which provides detailed information regarding early chick embryo elongation over time, being able to blindly discriminate different stages using only the measurements here determined. This tool can thus be used to detect and quantify deviations to normal parameters of tissue length upon experimental manipulation, even if transient.

Materials and Methods

Eggs and embryos - Fertilized chicken (gallus gallus) eggs were acquired from commercial sources and incubated in humidified temperature at 37-38 ºC. Embryo staging was performed according to the Hamburger and Hamilton classification (Hamburger and Hamilton, 1951). Embryos in stages HH3-5 were incubated ex-ovo in EC (Chapman et al., 2001) and New culture (New, 1955)up to 27 hours.

Live-imaging - Live imaging of embryos cultured ventrally in EC culture (Chapman et al., 2001) and New culture (New, 1955) was performed in an incubation chamber (UNO Stage Top Incubator, Okolab) and a homemade chamber, respectively, with humidified-saturated atmosphere and controlled temperature at 38ºC using steREO Lumar V12 (Zeiss) for up to 27 hours with frames acquired each 3-6 minutes.

Analysis - Length measurements were performed in selected images (representing 1h time intervals) using Axiovision Se64 Rel 4.9.1 (Carl Zeiss) or Zen 2.5 (blue edition, Carl Zeiss). The last frame in stage HH4 and the first frame in HH8 were used as reference to perform the time alignment, where time 0 corresponds to the last frame in HH4. Only when average calculations were performed, was the alignment adjusted, and all time points were rounded to the nearest whole value. A somitic cleft was considered completely formed only when it was clearly visible from its axial to lateral limits. Data analysis was performed using Excel and SPSS software. The complete dataset will be made freely available upon publication.

ICETEA tool

ICETEA was constructed using Google Colaboratory. The tool and all underlying program scripts will be made freely available upon publication.

Results and Discussion

Characterization of chicken embryo tissue elongation from early gastrulation (HH4) to 10-somite stage (HH10)

In order to characterize the chicken embryo elongation dynamics, we performed time-lapse imaging on cultured embryos at stages ranging from HH4 to HH10 (Hamburger and Hamilton, 1951) (Figure 4.1 A; Supplementary movie 4.1). Length measurements were performed for the whole embryo axis, as well as for different portions using multiple landmarks as reference points (Figure 1B): from the crown to the posterior limit of the head fold (C-HF); crown to the middle of the second somite. (C-Seg); crown to the node (C-N); crown to the posterior limit of the PS (C-PS); crown to the posterior limit of the *area pellucida* (pPL) (C-pPL); middle of the second somite to the posterior border of the last formed somite (SEG); anterior limit of the PSM to the node (PSM); node to the posterior margin of the PS (N-PS) and from the node to the pPL (N-pPL). For all these measurements, the length values were plotted against time (Figure 4.1 C) and the rates of elongation were calculated (Figure 4.1 D, Supplementary figure 4.1 A).

The total length of the embryo was assessed by the C-pPL and C-PS measurements (Figure 4.1 A). Our results evidenced that the embryo elongates gradually over time (Figure 4.1 C, C-pPL, C-PS), despite major changes in embryo morphology that take place from full length primitive streak stage (HH4) until the formation of 10 somites (HH10). C-pPL and C-PS measurements showed similar dynamics and elongation rates of 0.159 ± 0.038 mm/min and 0.139 ± 0.038 mm/min, respectively (Figure 4.1 D, Supplementary figure 4.1 A). This further confirms that C-pPL can be used as a user-friendly proxy for total embryo length assessment, as previously described (Maia-Fernandes et al., 2019). Elongation in the embryonic stages studied depends on gastrulation occurring at the posterior end, with concomitant node regression. Accordingly, the C-N measurement shows a linear growth over time (Figure 4.1 C, C-N), with an elongation rate of 0.202 ± 0.052 mm/min (Figure 4.1 D, Supplementary figure 4.1 A). The three measurements described encompass multiple portions of the embryo. We next studied the elongation dynamics of these individual sections in relationship to each other and to the whole embryo. The PSM (Figure 4.1 C, PSM) shows a slight increase in its length over time (0.072 ± 0.023 mm/min; (Figure 4.1 D). SEG and C-HF

show strikingly consistent sizes per time point in all embryos analysed (Figure 4.1 C, SEG, C-HF). These tissues elongate linearly and at similar rates (SEG: 0.107 ± 0.015 mm/min; C-HF: 0.106 ± 0.015 mm/min) (Figure 4.1 D, Supplementary figure 4.1 A). The C-Seg measure is not significantly altered over time (Figure 4.1 C, C-Seg), meaning that once somites are formed, the anterior-most portion of the embryo does not elongate further. The headfold, however, continues to grow in a parallel embryonic plane. This explains why the C-HF measurement displays a different behaviour. Finally, two measurements showed a negative elongation rate, N-pPL and PS (Figure 4.1 C, N-pPL, PS; Figure 4.1 D), meaning that their lengths are actually decreasing over time. This is consistent with gastrulation taking place at the posterior-most region of the embryo, with progressive depletion of epiblast-like cells and shortening of the PS (Spratt Jr, 1947).

Interestingly, we found that the SEG and PSM are the individual portions that most contribute to overall embryonic elongation (Figure 4.1 E). This is in accordance with previously published results, where a random cell motility gradient on the PSM was described as controlling axial elongation Benazeraf2010 (Benazeraf et al., 2010) and where the PSM was discovered to be the tissue with higher volumetric expansion and proliferation speed (Benazeraf et al., 2017). While the length of the SEG region is known to increase over time, as new somites are being formed, the behaviour of the PSM is less intuitive. In this region of the embryo, cells are periodically being removed as somites appear, while new cells are entering through the continuation of gastrulation. The observed elongation of the PSM means that the net result between these two events is positive, indicating that the rate of ingression of new cells in the posterior PSM overrides the rate of PSM shortening due to somite formation. An overall growth of the PSM tissue during early somitogenesis was previously reported by Gomez et al. (2008).

As described above, several embryo portions elongate linearly with time. This is the case of C-PS (total embryo length), C-N, SEG and C-HF (Supplementary figure 4.1 A). We next analysed the intrinsic variation of each measurement, to identify which would provide high potential for discriminating developmental time, i.e., measurements with significant percentual length increments per time unit (Figure 4.1 F). All measures above – C-PS, C-N, SEG and C-HF - show high percentual change in their lengths. Importantly, C-N, SEG and C-HF show less variability among embryos (as evidenced by smaller dispersion of the data), making them suitable candidates for proxies of time.

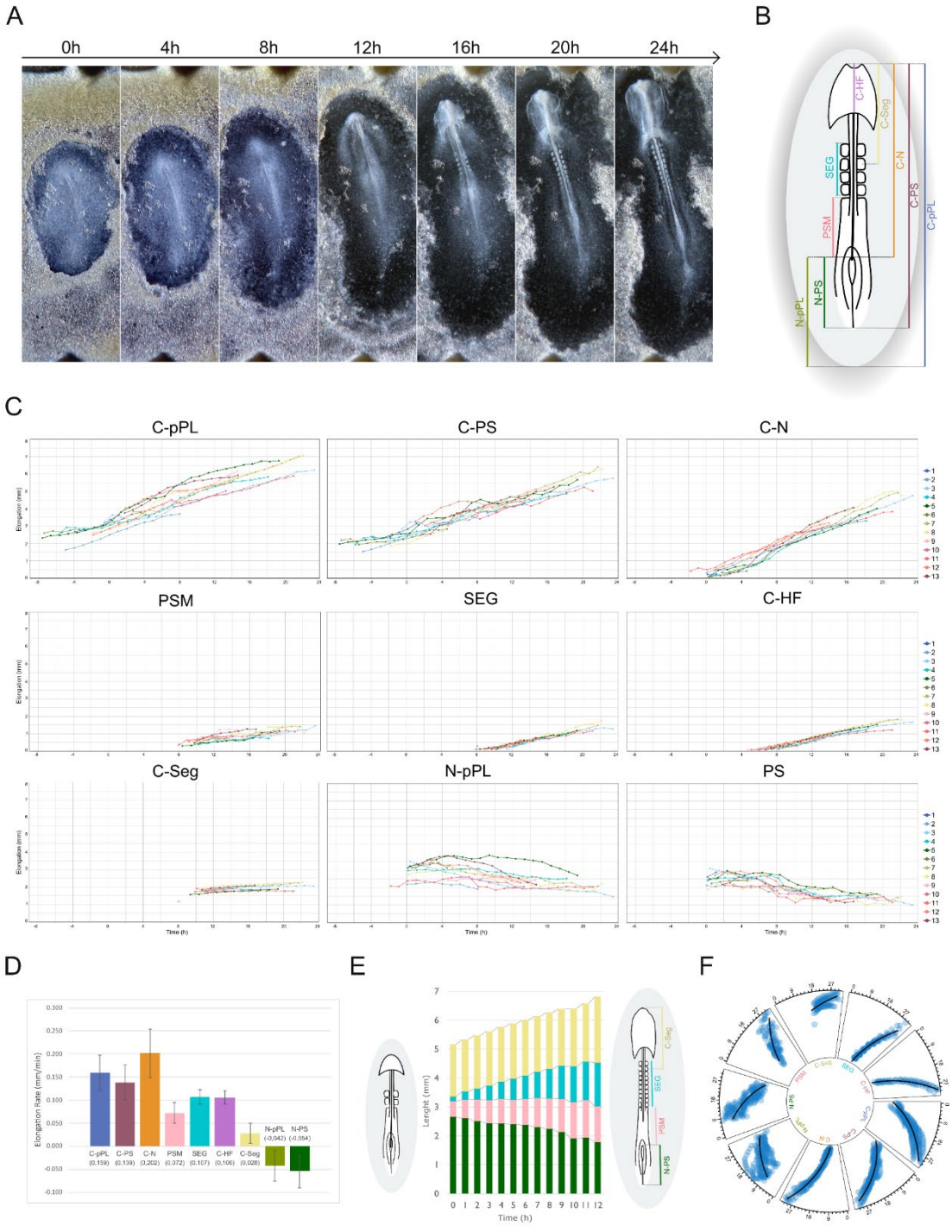
A
0h
4h
8h
12h
16h
20h
24h
B
C-HF
C-Seg
C-N
C-PS
C-pPL
SEG
PSM
N-PS
N-pPL
C
C-pPL
C-PS
C-N
PSM
SEG
C-HF
C-Seg
N-pPL
PS
Elongation (mm)
Time (h)
D
Elongation Rate (mm/min)
C-pPL (0.159)
C-PS (0.139)
C-N (0.202)
PSM (0.072)
SEG (0.107)
C-HF (0.106)
C-Seg (0.028)
N-pPL (-0.042)
N-PS (-0.054)
E
Lenght (mm)
Time (h)
F

Figure 4.1. Realtime characterization of chicken embryo elongation over a 24h-time period. **(A)** Representative images of a time-lapse acquisition of chicken embryo growth *ex vivo* during 24h. **(B)** Identification of the morphological landmarks used for the measurements performed. **(C)** Visualization of the length measurements obtained for each embryo portion over time. Time 0 min corresponds to the last frame classified as HH4. Each colour represents an individual embryo (embryos 1 – 13). **(D)** Graphical representation of the elongation rates of each embryo portion analysed. **(E)** Zymograph of the relative contribution of different embryo portions to overall elongation. **(F)** Percentual variation in length of each measurement performed over time. Yy axis: relative length (0 – 1). Xx axis: Time (h). Circles represent individual measurements. C-HF, crown to posterior limit of the head fold. C-Seg, crown to the middle of the second somite. C-N, crown to node. C-PS, crown to posterior limit of the PS. C-pPL, crown to posterior limit of the area pellucida. SEG, middle of the second somite to posterior border of the last somite. PSM, anterior limit of the PSM to node. N-PS, node to posterior limit of the PS. N-pPL, node to posterior limit of the *area pellucida*.

Length measurements allow for the discrimination of Hamburger and Hamilton (HH) stages of development

Having identified the elongation dynamics of the different portions of the embryo, we wished to study how these measurements relate to developmental time, specifically to the progression of the embryo through the embryonic stages HH4-10 as defined by (Hamburger and Hamilton, 1951). To do so, we started by determining the duration of each stage in hours. To this end, we classified the HH stage of each acquired frame per embryo and then calculated the time difference between the first and last frame of each HH stage. The mean duration time per stage (Figure 4.2 A) and the distribution of the HH stages over 24 hours of development (Figure 4.2 B) are presented. Globally, we observed that gastrulation stages prior to the formation of the first somite (HH4 and HH5) have longer duration (6 – 6.3 hours) than early somitogenesis stages (HH7-9; 2.6 – 4.7 hours on average). HH6 had the shortest duration, in line with the already described transitory nature of this developmental stage (Hamburger and Hamilton, 1951). HH stages progress sequentially with some degree of overlap. This is in line with what is already described (Hamburger and Hamilton, 1951), validating our stage alignment, while at the same time establishing a baseline to which compare our measurements.

We then plotted the measurements for each of the embryonic portions against the corresponding HH stage (Figure 4.2 C). The whole embryo length, corresponding to measurements C-pPL and C-PS, shows a clear HH stage progression with a very similar pattern as when a time scale is used (Figure 4.2 B). When the remaining measurements are considered, they are also able to recapitulate HH stage advancement, albeit reflecting the dynamics of each different embryonic portion and showing different levels of overlap.

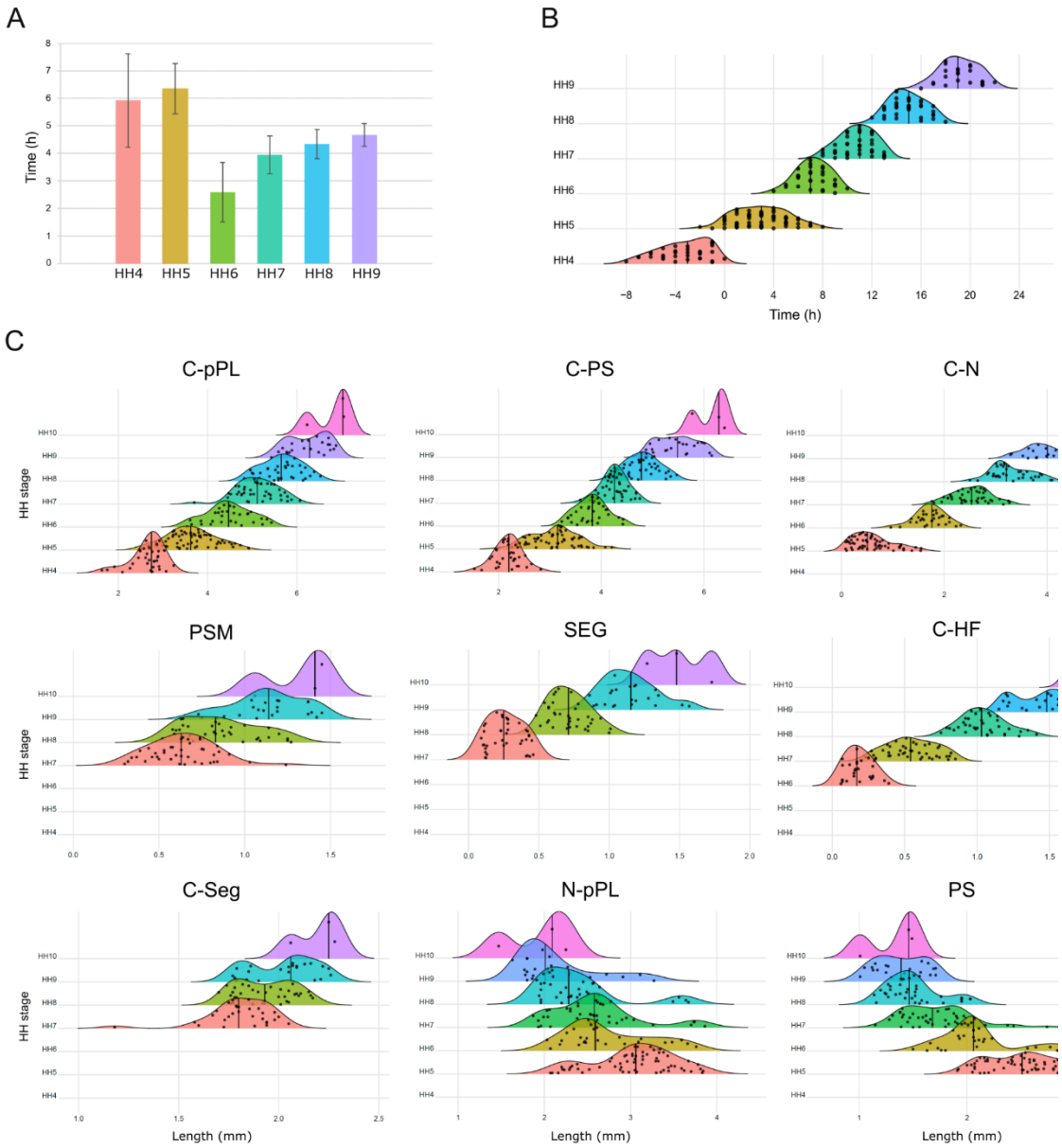

D

C-HF (mm)		Observations per HH stage (%)						
Min	Max	HH4	HH5	HH6	HH7	HH8	HH9	HH10
a	0,3	0,0	0,0	89,3	10,7	0,0	0,0	0,0
0,3	0,87	0,0	0,0	4,5	86,4	9,1	0,0	0,0
0,87	1,15	0,0	0,0	0,0	0,0	100,0	0,0	0,0
1,15	1,43	0,0	0,0	0,0	0,0	47,1	52,9	0,0
1,43	a	0,0	0,0	0,0	0,0	0,0	81,3	18,8

E

C-N (mm)		Observations per HH stage (%					
Min	Max	HH4	HH5	HH6	HH7	HH8	HH9
a	0,96	0,0	100,0	0,0	0,0	0,0	0,0
0,96	1,57	0,0	63,2	36,8	0,0	0,0	0,0
1,57	2,34	0,0	0,0	67,6	32,4	0,0	0,0
2,34	2,95	0,0	0,0	0,0	86,7	13,3	0,0
2,95	3,29	0,0	0,0	0,0	20,0	80,0	0,0
3,29	4,13	0,0	0,0	0,0	0,0	55,6	44,4
4,13	a	0,0	0,0	0,0	0,0	0,0	76,9

Figure 4.2. Characterization and discrimination of Hamilton and Hamburger stages using length measurements.
(A) Graphical representation of the duration of early HH developmental stages. **(B)** Temporal distribution of HH stages. **(C)** Ridge plot visualization of the length measurements of each embryo portion per HH stage. **(D,E)** HH stage classification tables based on C-HF **(D)** and C-N **(E)** measurements. Shaded boxes indicate the percentage of embryos in each stage with the corresponding portion length. C-HF, crown to posterior limit of the head fold. C-Seg, crown to the middle of the second somite. C-N, crown to node. C-PS, crown to posterior limit of the PS. C-pPL, crown to posterior limit of the *area pellucida*. SEG, middle of the second somite to posterior border of the last somite. PSM, anterior limit of the PSM to node. N-PS, node to posterior limit of the PS. N-pPL, node to posterior limit of the *area pellucida*.

Three embryo portions, C-N, SEG and C-HF elongate progressively as HH stages progress (Figure 4.2 C). N-pPL and PS (Figure 4.2 C) reflect their length reduction nature and, together with C-Seg and PSM, show the highest overlap between different stages.

One of our objectives was the formulation of a quantitative staging system based upon the length of specific embryonic portions. For that, one or more of the different measurements performed could be used as a proxy for developmental time. As stated earlier, three of them, C-N, SEG and C-HF best resembled the HH stage progression dynamics when a time scale was used (Figure 4.2 B). The classical staging system (HH) is based on morphological landmarks and the number of somites defines somitogenesis HH stages. Since our objective is an alternate staging system, we assessed the possibility that C-N and C-HF could be used for correctly staging HH4-10 embryos. For that, we applied an optimal binning algorithm to the data, which produced stage classification tables that allow to discriminate HH stage based on C-HF (Figure 4.2 D) or C-N (Figure 4.2 E) measurements. In tables obtained, each length value measured is positioned in a category between a minimum and maximum value. For each category, the probability of a specific embryo being in the corresponding stage is presented. For example, if the measurement of the C-HF of a certain embryo is between 0.3 and 0.87 mm, there is an 86.4% probability that it is in stage HH7 (Figure 4.2 D). While this approach lacked in precision, it further evidenced that using a quantitative value, specifically AP axis length measurements, it is possible to discern different HH stages, i.e., length can be used as a proxy of developmental time.

Interdependent elongation of different embryonic tissues

Having described overall embryo elongation of embryos HH4-10 and showing its relationship with the time of development, we next sought to identify possible

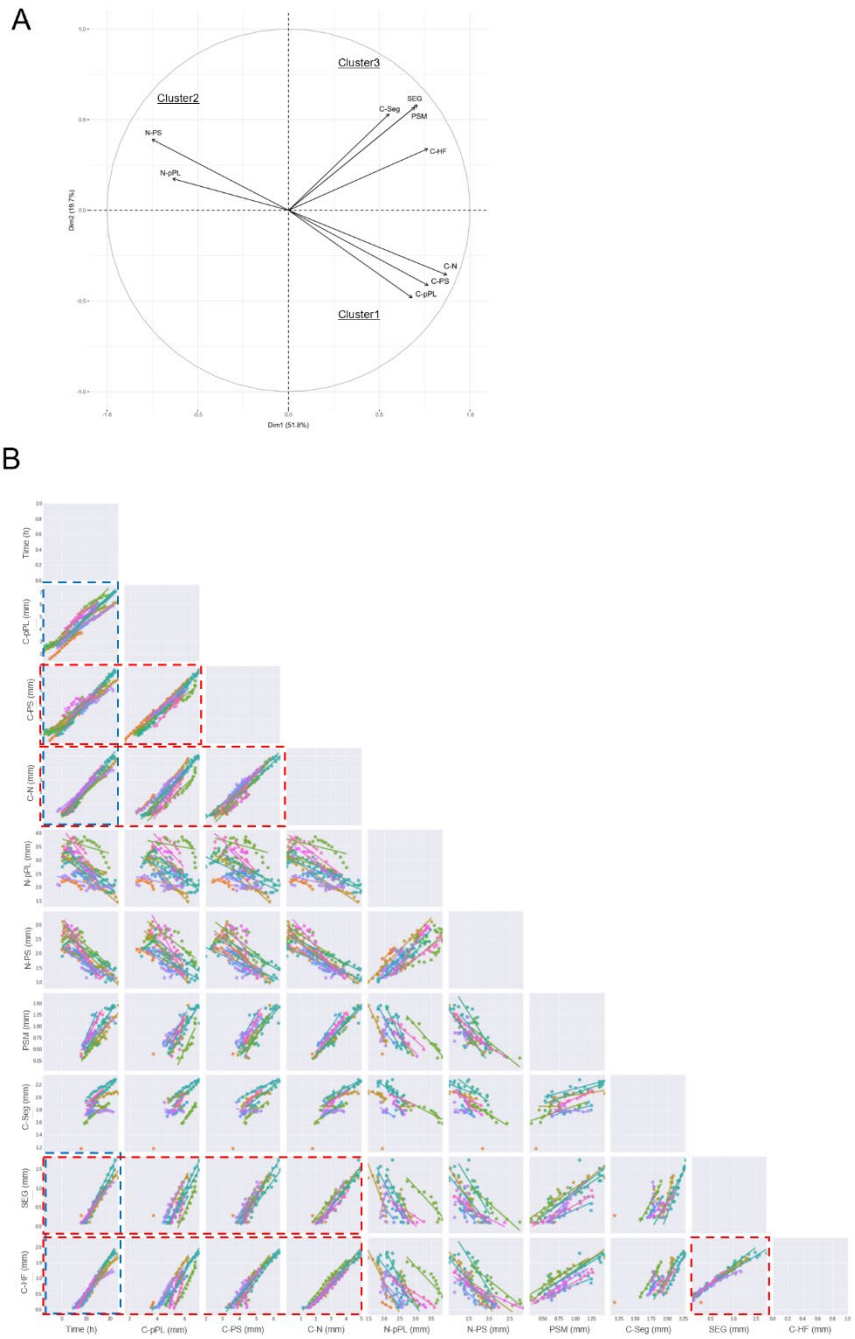

Figure 4.3. Correlation between the elongation of multiple tissues and developmental time
(A) Principal component analysis of the embryonic measurements performed. **(B)** Pair plot analysis of the relationship between all measurements performed and incubation time. Colours represent individual embryos and lines correspond to the linear regression of the data per embryo. Dashed boxes highlight strong correlation among length measurements (red) or with incubation time (blue). C-HF, crown to posterior limit of the head fold. C-Seg, crown to the middle of the second somite. C-N, crown to node. C-PS, crown to posterior limit of the PS. C-pPL, crown to posterior limit of the *area pellucida*. SEG, middle of the second somite to posterior border of the last somite. PSM, anterior limit of the PSM to node. N-PS, node to posterior limit of the PS. N-pPL, node to posterior limit of the *area pellucida*.

relationships between the elongation dynamics of different embryonic portions. For that, we performed a PCA analysis (Figure 4.3 A) that would blindly unveil which measurements are related to one another. We found that the 9 measurements are organized in three clusters of high correlation. The total embryo measurements C-pPL and C-PS belong to the same cluster as C-N (Cluster 1), suggesting that their behaviour is highly similar. Cluster 2 is formed by the measurements that have their values reduced over time, N-pPL and PS. This cluster is in a directly antagonistic quadrant in relation to cluster 1, indicating that their behaviours are compensatory. The final cluster (Cluster 3) includes the remaining segments of the embryo proper, C-Seg, C-HF, SEG and PSM.

Our analysis hinted at possible correlations between different measurements. To confirm and better describe these relationships, we plotted each measurement with the remaining 9 (Figure 4.3 B). We have previously shown that elongation of the embryo proper (C-PS) is directly correlated and can be fully described by the C-pPL measurement (Maia-Fernandes, Pais-de-Azevedo et al., 2019). Here, we found that the length of partial portions of the embryo are also strongly correlated with C-PS, namely C-HF, SEG and C-N (Figure 4.3 B, red boxes). Hence, measuring the length from the embryo crown to the posterior limit of the headfold (C-HF), for example, can be used to inform on the total length of the embryo. Unveiling these correlations can be very useful in experimental situations when a specific tissue is manipulated and we want to assess the impact on the elongation of the other embryo portions, or even when only a portion of the embryo is visible, and inferences need to be made regarding the entire AP axis.

Inferring Time from Space: a novel morphometric tool for embryo elongation dynamics analysis

The results presented in Figure 3B evidence that C-PS, C-HF, SEG and C-N strongly correlate with time (Figure 4.3 B, blue boxes). Importantly, this finding allows the temporal alignment of different embryos using length measurements alone. This is particularly relevant because it is not possible to attribute an absolute developmental time to chicken embryos, since their development initiates while still inside the hen. Comparison of embryos within the same HH stage lacks temporal precision, as evidenced by the significant time window each HH stage encompasses (Figure 2A). Moreover, many

experimental manipulations perturb key morphological landmarks used for HH classification, thus concealing the impact on the rate of development. Since length allows for reliable time-inference, it is now possible to experimentally challenge the molecular mechanisms in control of the rate of development and measure the output on length, as a proxy for time.

We developed an open-source computational tool appropriately named ICETEA (Interactive Chick Embryo Tool for Elongation Analysis) (Figures 4.4 and 4.5) with the purpose of allowing the free access and easy analysis of the quantitative data acquired throughout this work to the scientific community. These include a total of 1445 data entries, concerning 9 different measurements performed on 13 embryos at 1-hour intervals, up to 27 hours of incubation (226 images). The ICETEA user is presented with multiple options for graphical visualization and analysis of the raw data (Figure 4.4). These include visualization of all, or individual measurements (in the yy axis) plotted against time or any of the time-proxy lengths, C-N or C-HF (xx Axis). Linear regression analysis can be performed with different confidence intervals (Figure 4.4 A) or data can be discriminated per embryo (Figure 4.4 B). Residual plot visualization is also available (Figure 4.4 C). Another very important functionality of ICETEA is the ability to analyse new experimental data by contracting it to our solid reference set (Figure 4.5). Measurements performed in a single time point (Figure 4.5 A) or over a period of time (Figure 4.5 B) (uploaded from file of inserted manually) be compared to the reference dataset as long as the same morphological landmarks are used for length measurements. Once again, proper alignment for comparison of these new data with our dataset is performed using C-N or C-HFR as a proxy for time. Alterations to the reference can thus be interpreted as time displacements, i.e., if an experimental manipulation results in shortening of the C-N region of the embryo, one can be informed on how much time this tissue is delayed in development in comparison with the wildtype conditions (Figure 4.5 A).

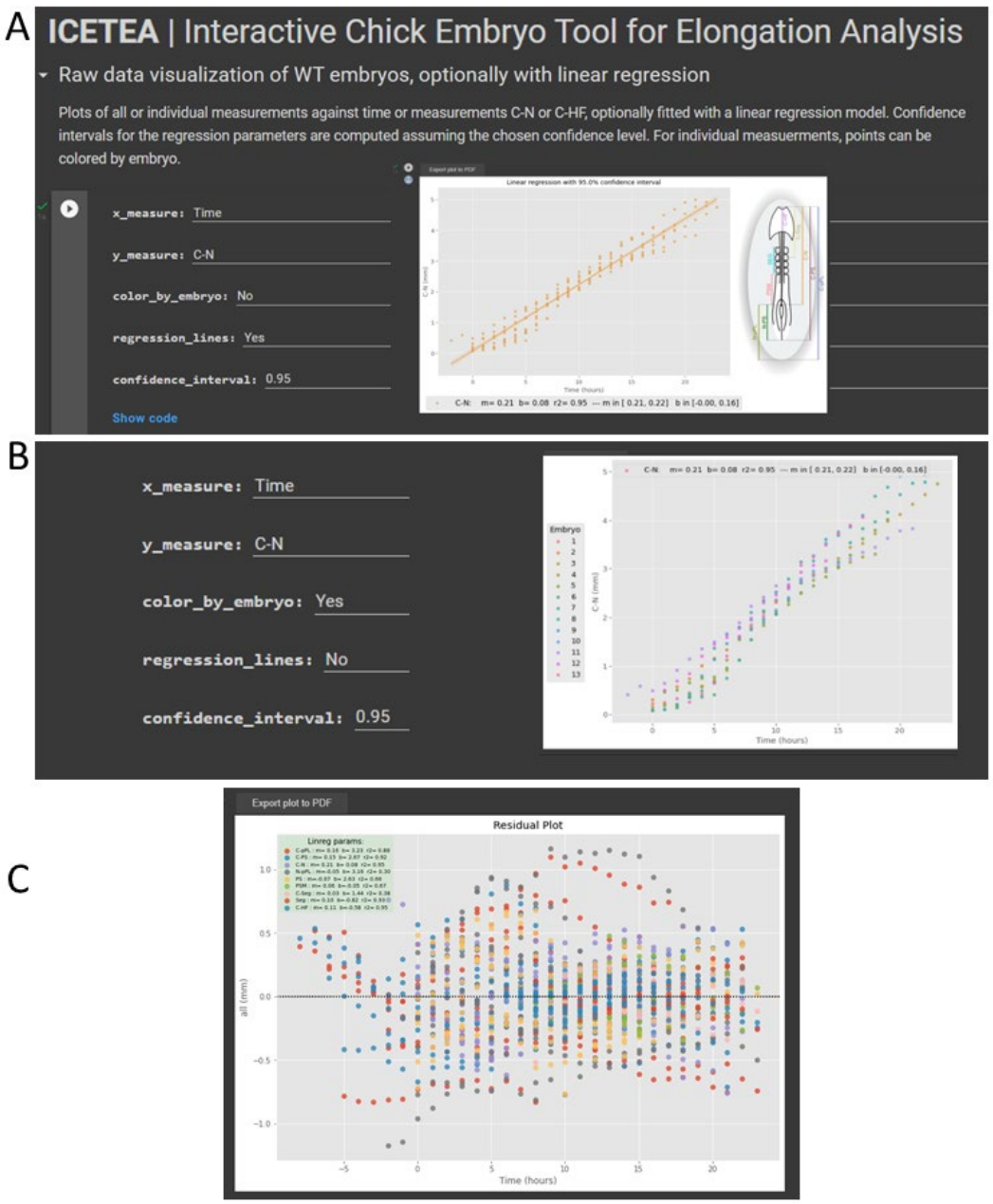

Figure 4.4. Exploring chick elongation data using ICETEA (Interactive Chick Embryo Tool for Elongation Analysis)
Visualization of the reference dataset is provided with multiple options, exemplified in panels **(A)** C-N vs Time, with linear regression, and **(B)** C-N vs Time discriminated per embryo. **(C)** Regression plot presented for all measurements vs Time. Multiple options are available to user.

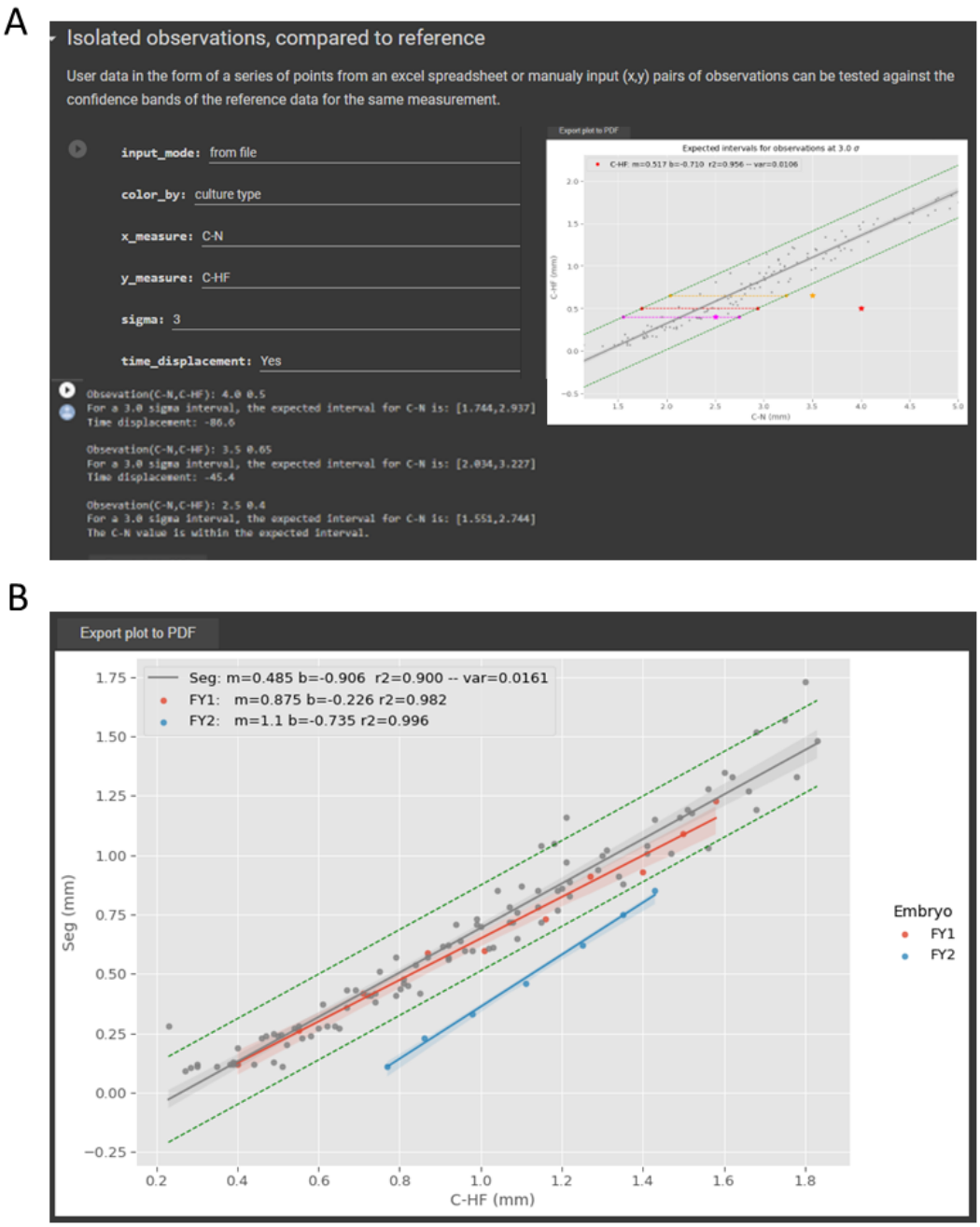

Figure 4.5. Using ICETEA to compare new experimental data with the reference database. Novel measurements performed **(A)** at a single time point or **(B)** over time are compared to the reference dataset. Alignment with reference is accomplished through C-N or C-HF. Information on data temporal displacement is available.

Conclusions

We report a detailed morphometric characterization of chick embryo elongation from HH4 to HH10. The correlation between elongation of the whole embryo with different embryo portions was evidenced and the PSM and segmented regions of the embryo were found to contribute the most for total AP elongation. Time was linearly correlated with total embryo growth, as well as with the elongation of the notochord (C-N) and with the distance between the crown and the posterior limit of the headfold (C-HF), hence length can be used as a proxy for time. These two measurements were found to be independent, which allows one to be used as reference when the other is experimentally manipulated. We provide a morphometric characterization of HH stages and report a new computational tool available to the chick embryo community – ICETEA - which allows the analysis of the effect of experimental manipulations on embryo tissue elongation, by direct comparison with our new reference dataset. With our work we hope to 1) provide knowledge on the elongation dynamics of early chick embryo, 2) offer an alternative staging system, based on quantitative classification data, thus increasing precision and reproducibility, 3) provide freely accessible high-quality morphometric data and 4) reveal a novel morphometric tool for the community to explore. This data will, hopefully, help answer some of the lingering questions on vertebrate embryo elongation, as well as address quantitatively the impact of different embryo manipulations to overall development.

References

Bénazéraf, B. (2019). Dynamics and mechanisms of posterior axis elongation in the vertebrate embryo. *Cellular and Molecular Life Sciences* **76**, 89-98.

Benazeraf, B., Beaupeux, M., Tchernookov, M., Wallingford, A., Salisbury, T., Shirtz, A., Shirtz, A., Huss, D., Pourquie, O., Francois, P., et al. (2017). Multi-scale quantification of tissue behavior during amniote embryo axis elongation. *Development* **144**, 4462-4472.

Benazeraf, B., Francois, P., Baker, R. E., Denans, N., Little, C. D. and Pourquie, O. (2010). A random cell motility gradient downstream of FGF controls elongation of an amniote embryo. *Nature* **466**, 248-252.

Benazeraf, B. and Pourquie, O. (2013). Formation and segmentation of the vertebrate body axis. *Annu Rev Cell Dev Biol* **29**, 1-26.

Chapman, S. C., Collignon, J., Schoenwolf, G. C. and Lumsden, A. (2001). Improved method for chick whole-embryo culture using a filter paper carrier. *Developmental dynamics: an official publication of the American Association of Anatomists* **220**, 284-289.

Chapman, S. C., Lawson, A., Macarthur, W. C., Wiese, R. J., Loechel, R. H., Burgos-Trinidad, M., Wakefield, J. K., Ramabhadran, R., Mauch, T. J. and Schoenwolf, G. C. (2005). Ubiquitous GFP expression in transgenic chickens using a lentiviral vector. *Development* **132**, 935-940.

Charrier, J. B., Catala, M., Lapointe, F., Le-Douarin, N. and Teillet, M. A. (2005). Cellular dynamics and molecular control of the development of organizer-derived cells in quail-chick chimeras. *Int J Dev Biol* **49**, 181-191.

Charrier, J. B., Teillet, M. A., Lapointe, F. and Le Douarin, N. M. (1999). Defining subregions of Hensen's node essential for caudalward movement, midline development and cell survival. *Development* **126**, 4771-4783.

Hamburger, V. and Hamilton, H. L. (1951). A series of normal stages in the development of the chick embryo. *J Morphol* **88**, 49-92.

Huss, D., Benazeraf, B., Wallingford, A., Filla, M., Yang, J., Fraser, S. E. and Lansford, R. (2015). A transgenic quail model that enables dynamic imaging of amniote embryogenesis. *Development* **142**, 2850-2859.

Hyun, I. (2016). The 14-Day Rule: Historical and Ethical Underpinnings. *The Ethics of Early Embryo Research & the Future of the 14-Day Rule, The Petrie-Flom Center for Health Law Policy, Biotechnology, and Bioethics at Harvard Law School*.

Keller, R., Shook, D. and Skoglund, P. (2008). The forces that shape embryos: physical aspects of convergent extension by cell intercalation. *Phys Biol* **5**, 015007.

Lawson, A. and Schoenwolf, G. C. (2001). Cell populations and morphogenetic movements underlying formation of the avian primitive streak and organizer. *Genesis* **29**, 188-195.

Maia-Fernandes, A., Pais de Azevedo, T., Marreiros, A., Palmeirim, I. and Andrade, R. (2019). The posterior limit of the area pellucida (pPL) as a reliable proxy for the end of the primitive streak in chick elongation studies. *Matters*.

Martyn, I., Kanno, T., Ruzo, A., Siggia, E. and Brivanlou, A. (2018). Self-organization of a human organizer by combined Wnt and Nodal signalling. *Nature* **558**, 132-135.

Momose, T., Tonegawa, A., Takeuchi, J., Ogawa, H., Umesono, K. and Yasuda, K. (1999). Efficient targeting of gene expression in chick embryos by microelectroporation. *Development, growth & differentiation* **41**, 335-344.

New, D. (1955). A new technique for the cultivation of the chick embryo in vitro.

Norris, A. and Streit, A. (2014). Morpholinos: studying gene function in the chick. *Methods* **66**, 454-465.

Sato, Y. and Lansford, R. (2013). Transgenesis and imaging in birds, and available transgenic reporter lines. *Development, growth & differentiation* **55**, 406-421.

Sausedo, R. A. and Schoenwolf, G. C. (1993). Cell behaviors underlying notochord formation and extension in avian embryos: quantitative and immunocytochemical studies. *The Anatomical Record* **237**, 58-70.

Sausedo, R. A. and Schoenwolf, G. C. (1994). Quantitative analyses of cell behaviors underlying notochord formation and extension in mouse embryos. *The Anatomical Record* **239**, 103-112.

Sausedo, R. A., Smith, J. L. and Schoenwolf, G. C. (1997). Role of nonrandomly oriented cell division in shaping and bending of the neural plate. *Journal of Comparative Neurology* **381**, 473-488.

Schoenwolf, G. C., Bortier, H. and Vakaet, L. (1989). Fate mapping the avian neural plate with quail/chick chimeras: origin of prospective median wedge cells. *Journal of Experimental Zoology* **249**, 271-278.

Serralbo, O., Salgado, D., Véron, N., Cooper, C., Dejardin, M.-J., Doran, T., Gros, J. and Marcelle, C. (2020). Transgenesis and web resources in quail. *Elife* **9**, e56312.

Spratt Jr, N. T. (1947). Regression and shortening of the primitive streak in the explanted chick blastoderm. *Journal of Experimental Zoology* **104**, 69-100.

Stern, C. D. (2004). The chick embryo--past, present and future as a model system in developmental biology. *Mech Dev* **121**, 1011-1013.

Stern, C. D. (2018). The chick model system: a distinguished past and a great future. *International Journal of Developmental Biology* **62**.

Stern, C. D. and Bachvarova, R. (1997). Early chick embryos in vitro. *Int J Dev Biol* **41**, 379-387.

Thibert, C., Teillet, M.-A., Lapointe, F., Mazelin, L., Le Douarin, N. M. and Mehlen, P. (2003). Inhibition of neuroepithelial patched-induced apoptosis by sonic hedgehog. *Science* **301**, 843-846.

Voiculescu, O., Bertocchini, F., Wolpert, L., Keller, R. E. and Stern, C. D. (2007). The amniote primitive streak is defined by epithelial cell intercalation before gastrulation. *Nature* **449**, 1049-1052.

Wei, Y. and Mikawa, T. (2000). Formation of the avian primitive streak from spatially restricted blastoderm: evidence for polarized cell division in the elongating streak. *Development* **127**, 87-96.

Supplementary material

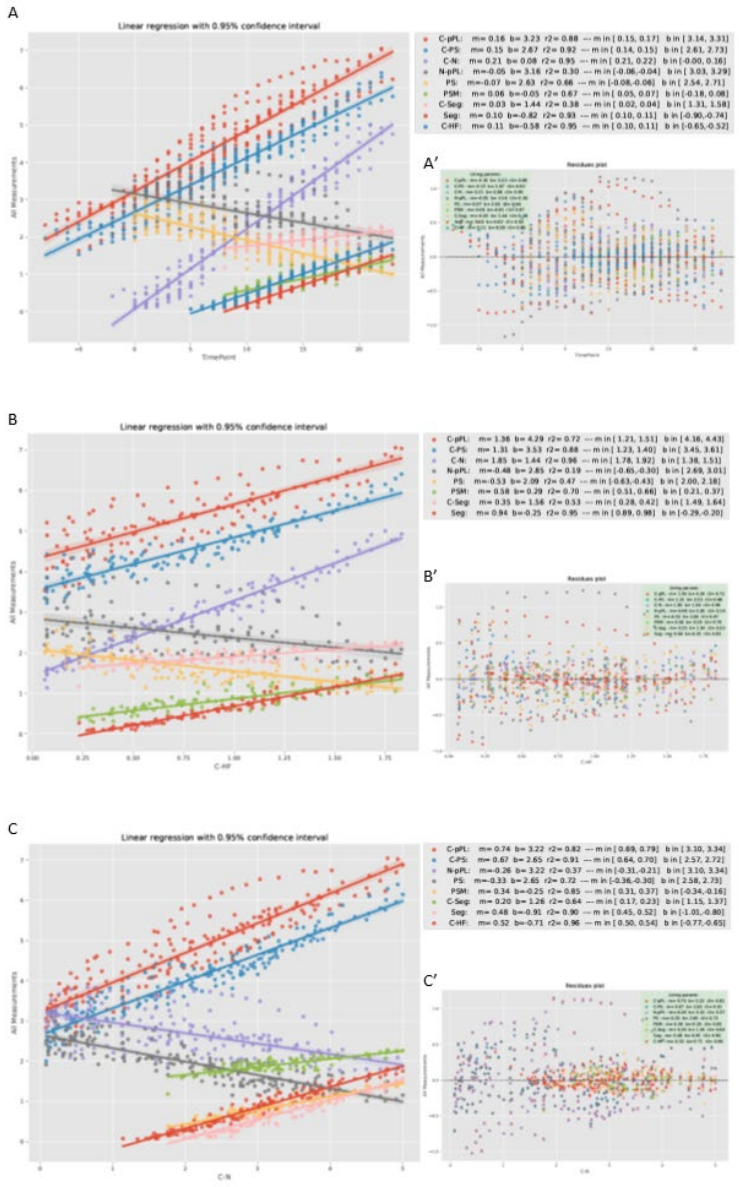

Supplementary Figure 4.1. Regression curves for all measurements as a function of (A) Time, (B) C-HF and (C) C-N length.
The respective residual plots are shown **(A'-C')**. Linear regression curves (r2>0.90) are highlighted by a red rectangle.

Supplementary Movie 4.1. Time-lapse of embryo elongation from stage HH4 to HH11^{-} with 24h duration

Chapter V – General Discussion

You have to let it all go, neo. Fear, doubt, and disbelief. Free Your Mind! (Morpheus)

In *The Matrix (1999)*

You must unlearn what you have learned (Master Yoda)

In *Star Wars: The Empire strikes back (1980)*

General Discussion

When this thesis was started, we set out a path to clarify the role of the notochord in the formation of the vertebral body, the nature of the segmented signal and its shift between zebrafish and chick, and the possible reasons for it.

Along that path, due to some fortunate (as well as some unfortunate !) events, but mostly due to sheer scientific curiosity and drive to increase the boundaries of knowledge, we found a new direction with a very related but slightly different story. This is, as I am told by everyone around me that has completed a PhD, a normal thing. We ended up with a story about a sometimes-forgotten structure that had its very important role in the past diminishing throughout time, but still has a word to say in the present.

1 The notochord, a shifting structure during evolution

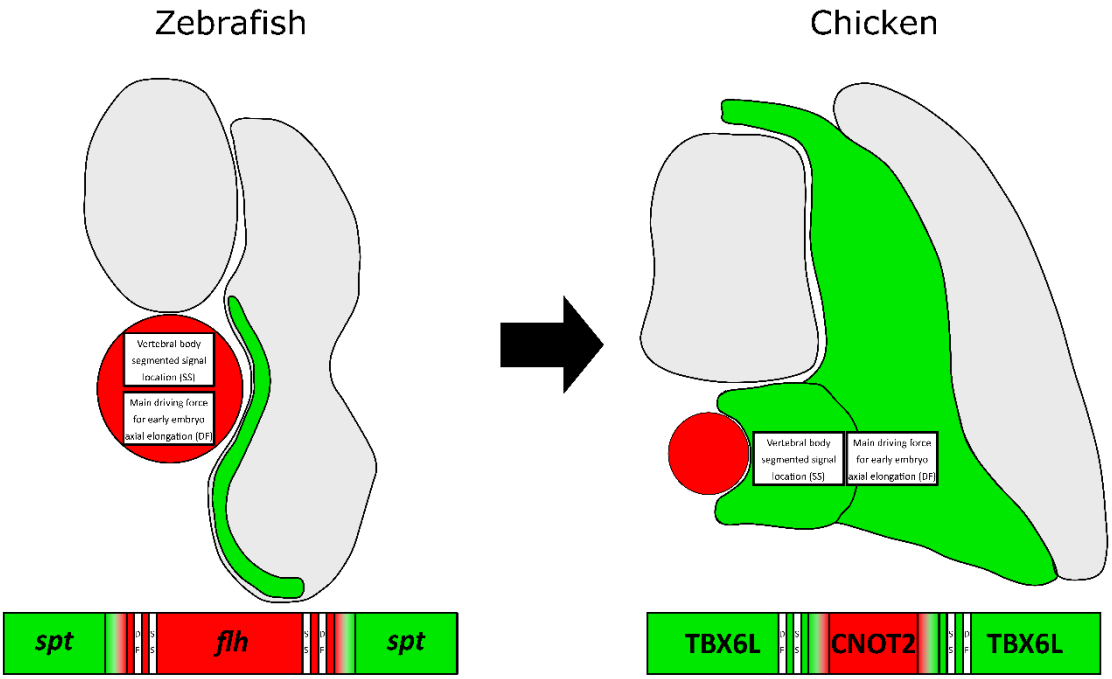

Figure 5.1. The shifting size and role of the notochord during evolution is due to changes in axial/paraxial mesoderm progenitor gene expression territories.
Transverse sections of zebrafish and chicken embryos of mature somite stages are represented showing the notochord in red and the sclerotome in green. The relative size differences of these structures between both species (not in scale) are depicted. Also shown is which structure is the main driving force for early embryo elongation (DF) and segmented vertebral body formation. Bellow the image of each embryo is a schematic representation of the expression territories of *flh*/CNOT2 on *spt*/TBX6L in their respective species.

The notochord is a very important structure in development (Corallo et al., 2015; Stemple, 2005), both physically and molecularly, fulfilling various roles, as a support structure, a driver of morphological movements or a signaling center. However, throughout evolution, its role is suffering a clear shift in several of its aspects, some of them covered in this thesis (Figure 5.1).

1.1 The shifting notochord size and structural functions

The first difference that we can observe in the notochord, while comparing different species of the animal kingdom is in its size in relation to the rest of the embryo. In anamniotes like the zebrafish and *Xenopus*, the notochord is much larger, when comparing to amniotes like the chicken and the mouse (Scott and Stemple, 2005). In terms of general mechanical function, the notochord acts as a hydrostatic skeleton (Long et al., 2002) in all chordate embryos (Annona et al., 2015), where it functions as the first axial skeleton during its initial stages of development. However in the adult, the maintenance of this function depends on the group of animals we consider. In non-vertebrate chordates such as the amphioxus, and in vertebrates that include agnathans (jawless fish) like lampreys or hagfish, or some actinopterygians (ray-finned fishes) like the sturgeon, the notochord persists in the adult (Annona et al., 2015). Contrarily, in the majority of the remaining vertebrates, the adult axial skeleton function is assumed by the vertebral column. In many of these animals the notochord does not persist in the adult, giving rise instead to the *nucleus pulposus* of the intervertebral disc. This shift in size and function is usually described as occurring concomitantly to the migration from a water-based environment such as the sea to a land-based one. In these new conditions, the notochord as an axial structure is no longer sufficient to withstand the pressure of gravity and the absence of the support provided by water. Thus, a different kind of skeleton was developed during evolution through a transition of function from the notochord to the vertebral column. This can indeed be observed in the evolutionary tree of life as the reduction in size of the notochord is accompanied by an increase in size of the new type of tissue appearing in vertebrates, the sclerotome (Figure 5.1). While in teleosts like the zebrafish the sclerotome is only a thin row of cells, in tetrapods like the chicken it takes up more than half of the size of the mature somite. Curiously, not only is the notochord reducing its size, as the sclerotome is increasing it, but the muscle components of the somite, the dermomyotome and myotome, are also suffering this reduction.

1.2 The shifting role of the notochord in the formation of the vertebral bodies

As described above, throughout evolution the vertebral column is gradually assuming the role of the axial skeleton that had belonged to the notochord. However, the notochord did not completely lose this role, as it is still important for the formation of one of vertebrae components, the vertebral body. The formation of segmented vertebral bodies is a process that is achieved through different ways in animals such as the zebrafish or the chicken (Bagnat and Gray, 2020; Pais de Azevedo et al., 2012), with a clear shifting role of the notochord. The zebrafish, as other teleosts start the production of segmented vertebral bodies through the mineralization of the notochordal sheath (Bensimon-Brito et al., 2012; Fleming et al., 2004; Grotmol et al., 2003; Lleras Forero et al., 2018). As such, it is in the notochord that the signal for segmented vertebral body formation is located, more specifically in the cells located at the periphery of the notochord, the chordoblasts. As for amniotes like the chicken embryo, the segmented signal is positioned in the most medially located sclerotome cells that will give rise to the vertebral body (Christ et al., 2004; Christ et al., 2007a; Christ et al., 2007b; Scaal, 2016; Senthinathan et al., 2012). However, since several previous studies showed that notochord ablation leads to the formation of unsegmented vertebral bodies (Strudel, 1955; Watterson et al., 1954), this led us to consider if the role previously located on the notochord had completely shifted to the medial sclerotome. The results present in chapter II of this thesis, along with other ones published in a recent paper (Ward et al., 2018) also investigating the role of the notochord confirmed two ideas: 1) the segmented signal for vertebral body formation is indeed initially provided by the sclerotome cells, as Von Ebner's fissure, the first morphological landmark of segmented vertebrae does not disappear when the notochord is ablated (our results); and 2) the notochord is nevertheless still important for maintenance of the signal needed for segmented vertebral bodies to form (Ward et al., 2018). Together, these results are another example of a shifting role of the notochord through the animal tree of life that, nevertheless, has not yet fully concluded.

The knowledge of vertebral body development in animals such as the zebrafish and the chicken leads to an interesting idea: Could the vertebral bodies and arches constitute two separate developmental modules, with the first one being under the control of the notochord and the medial sclerotome (Pais de Azevedo et al., 2012) ? Indeed

several lines of evidence lead to that assumption: Firstly, as we have seen, the segmented vertebral body is formed by the mineralization of the notochordal sheath by the chordoblasts in animals such as the zebrafish and by the cooperation of the medial sclerotome and notochord in animals, such as the chicken. In these last cases, the two structures cooperate to such a degree that the extracellular matrix that allows for the migration of the sclerotome cells to the perinotochordal space is produced by both structures and not just one (Scaal, 2016; Smits and Lefebvre, 2003). Secondly, several experimental works point to an uncoupling of vertebral bodies and arches (Fleming et al., 2015; Pais de Azevedo et al., 2012), of which we will point some: 1) in farmed Atlantic salmons, animals can show fusion of vertebrae, with only the vertebral body being fused and not the arches. 2) in chicken embryos where the notochord is ablated (Strudel, 1955; Watterson et al., 1954), the vertebral bodies appear fused, but not the arches. 3) in the *fused somites* mutant zebrafish, the vertebral bodies appear normal, while the arches are shown to be fused (van Eeden et al., 1996). Thirdly, study of the fossil record (Fleming et al., 2015) shows that vertebral bodies and arches appear at different times.

1.3 The shifting role of the notochord in axial elongation

As the notochord is the first axial skeleton of the embryo of all chordates, it was logical for it to be considered as a major contributor for the mechanics of AP axis elongation. Reinforcing this point is the extraordinary capacity for the notochord to straighten, stiffen and elongate due to hydraulic pressure by the swelling in its vacuolated cells (Adams et al., 1990; Koehl et al., 2000). This elongation capacity was also shown to be autonomous (Keller et al., 2003), at least in zebrafish embryos: Experiments where the epiboly of the YSL and EL was blocked, the notochord was able to extend beyond the point where the epiboly stopped (Baumann and Sander, 1984); In another set of experiments, but this time with epiboly of the deep cells halted, the notochord was once again shown to be able to elongate (Kane et al., 1996). In a very recent study (McLaren and Steventon, 2021), the authors studied the role of the notochord in zebrafish embryo axis elongation through notochord ablation. Their results led them to propose a very interesting model: The notochord cells vacuolate in an anterior to posterior gradient, leading to expansion. However, this expansion is resisted by the posterior notochord cells that are still unvacuolated, which are being added from the posteriorly located progenitor region, causing physical stress. Since these cells are coupled with the flanking somitic

ones, the generated stress is transmitted to the segmented portion anterior to the coupled area, translating into elongation of the paraxial section of the embryo. The depletion of notochord progenitors from the progenitor allows for stress to be transmitted to more posterior positions, continuing elongation.

In amniotes, the necessary forces for the elongation of the embryo were also investigated. Very elegant ablation experiments where most of the blastoderm of early gastrulation embryos was removed (Spratt Jr, 1947; Waddington, 1957) showed the formation of an elongated structure very similar to the embryo axis, with neural tube, notochord, and somites. This showed that the forces necessary for elongation would have to derive from these structures. In this author's Masters thesis, the results of these experiments were confirmed and the specific role of the notochord in elongation was investigated through ablation of different AP segments along the axis of the embryo (Pais De Azevedo, 2009). These results showed that the notochord could not be the main driving force for elongation, as the operated embryos were non-significantly shorter. However, a notochord role could not be ruled out as there was a trend of stronger effect, the higher length of notochord was removed. Later works (Benazeraf et al., 2010) set out to explore the origin of axial elongation forces in the chicken embryo: Through a series of ablation experiments of different structures and tissues, they found that PSM absence had a higher effect in axial elongation and that a random posterior-to-anterior gradient of cell motility was its main driving force. The chicken embryo early elongation dynamics description present in chapter IV of this thesis is in accordance with these discoveries: We show that among the four individual regions of the embryo (C-Seg, Seg, PSM and N-PS), Seg and PSM are the ones with a higher contribution to the overall embryonic axis elongation. Further experiments led to a fascinating model (Xiong et al., 2020), comparable to a combustion engine, as the authors describe: The expansion of PSM due to the random mobility gradient causes a compression on the axially located tissues, the neural tube, and the notochord, leading them to elongate. This, in turn, pushes the progenitor cells out of the progenitor region, supplying the PSM with new cells that will contribute to the motility gradient, restarting the cycle.

When we compare the two models for zebrafish and chicken elongation, we immediately observe one similarity and one difference. The similarity is that, in both systems extension of the AP axis relies on elongation of the axial tissues, one of them being the notochord. And while, in both models, elongation of the axial tissues is an

important component of the mechanical system, the difference lies precisely on the level of importance: On the zebrafish model, the main driving force for whole axis elongation stems from the elongation of the notochord (McLaren and Steventon, 2021), while in the chicken model, the equivalent main force is the PSM expansion due to the gradient of cell motility (Xiong et al., 2020).

Through all this knowledge, we once again envision an evolutionary situation where the notochord has shifted from being a main driving force for axial elongation, to having this role transferred to the PSM/somites, while at the same time maintaining an important role.

There is, however, another similarity between the models describing the elongation on the zebrafish and chicken embryos, which is the importance of an area of axial and paraxial mesoderm progenitor cells. And it is in this region that lies the key for the explanation between the possible biological processes by which the notochord shift observed throughout evolution.

1.4 The role of progenitor cells and genes in underlying these evolutionary shifts

What then could be behind the shifts we just described ? During evolution, what could have made one structure become smaller or lose cells and another correspondingly bigger or increase its cell number ? On the other hand, what could be the reason for the notochord to change the preponderance of its role in early embryo elongation and in conferring the signal for segmented vertebral body formation ?

When we think of the possible biological mechanisms underlying these shifts, we take to the teachings of the science of Evo-Devo and go look in development for the reasons for evolutionary difference. As we have seen before, it is possible for whole structures to be converted into other completely different ones, by simple changes in the expression of key genes (Carroll, 2005). As such, in solving this riddle, we searched for genes that were important on the decision between axial (notochord) and paraxial (PSM/somites) mesoderm. To cite (Halpern et al., 1995): (…) thresholds of growth factors may be important in specifying different types of mesoderm (…). In our search, we found *flh*/CNOT2 (Stein et al., 1996a; Talbot et al., 1995), a transcription factor with a huge role in this decision.

We thus conducted experiments where we investigated the role of CNOT2 in the decision between axial and paraxial mesoderm in the chicken embryo. Our chapter III results showed that, in the chicken embryo, CNOT2 upregulation leads to a decrease in paraxial mesoderm cells, a reduction of somite size, an enlargement of axial mesoderm structures and repression of TBX6L in specific areas of the embryo. This leads us to propose that, in chicken axial/paraxial progenitor cells, the cell fate decision to the axial mesoderm path is made by the expression of CNOT2 that leads to repression of TBX6L and the paraxial mesoderm fate.

Taking all the previous information into account a very interesting hypothesis is placed before us: During evolution of the chordates/vertebrates, the cells that once belonged to the notochord in more basal groups of animals, now belong to the most medial portion of PSM/somite/sclerotome in the so-called higher vertebrates, while maintaining the functions they had previously (Figure 5.1). As to why this has happened, we propose that it was the result of shifts in the territory of expression of *flh*/CNOT2 and *spt*/TBX6L (Figure 5.1). More specifically, the axial/paraxial progenitor region cells progressively lost *flh*/CNOT2 capacity for repressing *spt*/TBX6L, leading to increasingly more cells changing their fate from axial to paraxial mesoderm. Two factors make this a very plausible scenario: 1) in the chicken embryo, the notochord and medial somite progenitor cells are located in very close regions with a small overlapping zone (Selleck and Stern, 1991), acting as a progenitor stem-cell niche (Solovieva et al., 2022). In our chapter III results, we show that this corresponds to the small overlap in CNOT2/TBX6L expression territories. The proximity of notochord and somite progenitor cells also occurs in other vertebrate species (Wymeersch et al., 2021); 2) as we also observed in chapter III, the promotor region of both *spt* and TBX6L contains Not gene family binding motifs, but with chicken TBX6L containing half of zebrafish *spt*, possibly resulting in lessened repressing activity by *flh*/CNOT2. As such, is thus reasonable to think that the loss of repressing activity of *flh*/CNOT2 on *spt*/TBX6L during evolution allowed notochord progenitor cells on the overlap region to shift to a paraxial mesoderm fate, thus leading to the differences observed.

To summarize our model (Figure 5.1): During evolution there is an ongoing shift in the territories of expression of *flh*/CNOT2 and *spt*/TBX6L due to loss of repressing capability of *flh*/CNOT2, coming from loss of Not binding motifs. This causes a shift of cells that would normally integrate the notochord into originating somite instead. As these

cells still maintain their original functions and roles in development, these roles are progressively being transferred from the notochord to the PSM/somite/sclerotome.

Going back to the initial question of this thesis, on finding the reason for a change in the signal for segmented vertebral body formation, our model provides a very interesting explanation. However, one can ask if it would truly answer our initial question. A very recent work in the zebrafish mutant *spondo* (Peskin et al., 2020) seems to point in that direction. In this mutant, the normal molecular notochord segmentation does not occur, and vertebral bodies and intervertebral discs do not form. Instead, these animals show the presence of vertebral elements formed by the arches, reminiscent of ancestral teleost fishes, in which the notochord persisted unmineralized, with the formation of somite-derived arches. They found that, in *spondo*, as well as in another mutant *calymmin*, the notochordal sheath is deficiently formed and that the migration pattern of sclerotome-derived osteoblasts is altered. Normally, these would migrate to notochord specific areas, following the segmented pattern established by the mineralization of the notochordal sheath. In *spondo* mutants, these cells instead migrate to the areas where arches are normally forming, presumably retaining the original somite patterning. This is a fascinating example of how changes in gene expression can alter the signal source of the segmented pattern from one structure to another, supporting our model for explaining the differences in the formation of segmented vertebrae in different species.

2 Biomedical relevance of this thesis

Finally, as I am performing a PhD in Biomedical Sciences at the Faculty of Medicine of the University of Algarve, there are a few relevant considerations about the biomedical value of our findings and discussions. As we all know, it is based on the discoveries of fundamental sciences that applied science can improve medicine and welfare of the population. The discovery of the genetic causes of several human malformations is one of the areas where developmental biology can contribute greatly (Nobrega et al., 2021), as:1) it is during development that congenital malformations occur; 2) most of the genetical toolkit is underlying the development of humans and model organisms is very similar or even the same, and 3) the congenital malformations referred occur usually due to defects on the genes of the referred toolkit.

Some categories of congenital malformations that particularly related to the topic of this thesis are the Spondylocostal Dysostosis (SCDO) (Sparrow et al., 2011) and the Congenital Scoliosis (CS) (Sparrow et al., 2012). SCDO is characterized by multiple defects in the vertebrae and ribs, including fusions and deletions, often affecting the entire spine. CS is more specifically as a lateral curvature of the spine, exceeding 10 degrees, also caused by defects in vertebrae. In terms of frequency, SCDO occurs in 1 per 40,000 births (Andrade et al., 2007; Nobrega et al., 2021), while CS is more frequent, at 1 in 1000 births (Hedequist and Emans, 2007). Many of the malformations associated with these two conditions have already been proven to be directly related to several developmental genes, including the segmentation clock genes (Andrade et al., 2007; Nobrega et al., 2021).

More specifically, the orthologs of two of the genes analyzed in this thesis are known to be important for biomedical research. The human TBX6, for example, is a known gene, in which mutations associated with it have been linked to cases of SCDO and other congenital spine defects (Chen et al., 2016; Sparrow et al., 2013). This human gene is a member of Tbx6/16 subfamily (Ahn et al., 2012; Griffin et al., 1998; Lardelli, 2003; Windner et al., 2012), from which TBX6L, one of the genes analyzed in this thesis is also a family member. The mammalian *Noto* is also a very important gene for biomedical research, in this case in the study of degeneration of the intervertebral disc (McCann and Seguin, 2016). *Noto* has been used to trace notochord derived cells that form the *nucleus pulposus* of the intervertebral disc (McCann et al., 2012). As such, a *NOTO-eGFP* reporter system is now being used to derive *nucleus pulposus* cells from human pluripotent stem cells. These cells are now being successfully used in transplantation studies in attenuating injury induced intervertebral disc degeneration (Zhang et al., 2020). *Noto* is a member of the Not gene family (Abdelkhalek et al., 2004; Plouhinec et al., 2004; Stein et al., 1996b), the same family from which another of the genes focused on this work, the chicken CNOT2, also is a member of.

Finally, the most severe phenotype of CNOT2 electroporated embryos, in which both halves of the neural tube have been separated by a mass of axial mesoderm cells are reminiscent of the medical condition Diastematomyelia (M. Catala2021, personal communication October 18, 2021). Patients with this condition show a separation of the spinal cord into two halves by a medially located septum, which can be rigid or fibrous in nature (Cheng et al., 2012).

3 How different biological subjects all come together through Evo-Devo.

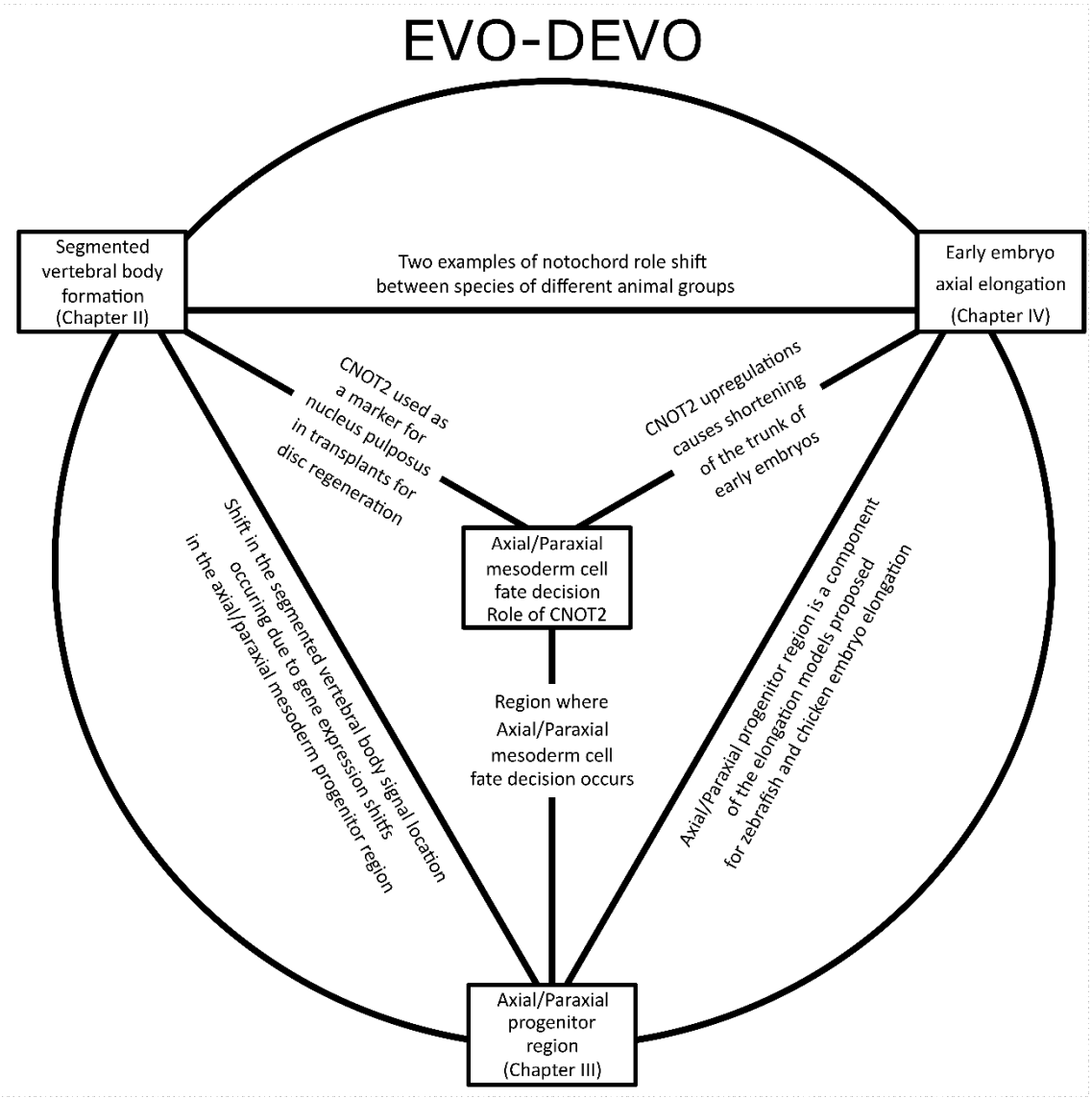

Figure 5.2. The relationships between the different topics covered in the chapters of this thesis. Diagram representing the several topics covered in the chapters of this thesis, and the connective links between them. All the topics and links are subjects covered by evolutionary and developmental biology.

As we have seen during this section, this thesis has covered at least three different biological topics, one on each chapter: 1) formation of segmented vertebral bodies (Chapter 2); 2) elongation of the AP axis of early embryos (Chapter 4); and 3) the axial/paraxial mesoderm progenitor region (Chapter 3). Interestingly, there was a fourth topic that represented the key component that unites all of them: The genetics of axial/paraxial progenitor cell fate as the possible evolutionary reason for the developmental differences and similarities between different groups of animals. In this

case, specifically, the role of CNOT2 (Figure 5.2). The relationship between such different subjects and the connection between them proves, once again, the importance and beauty of evolutionary and developmental biology (Gilbert, 2017; Wallingford, 2019).

References

Abdelkhalek, H. B., Beckers, A., Schuster-Gossler, K., Pavlova, M. N., Burkhardt, H., Lickert, H., Rossant, J., Reinhardt, R., Schalkwyk, L. C., Muller, I., et al. (2004). The mouse homeobox gene Not is required for caudal notochord development and affected by the truncate mutation. *Genes Dev* **18**, 1725-1736.

Adams, D. S., Keller, R. and Koehl, M. A. (1990). The mechanics of notochord elongation, straightening and stiffening in the embryo of Xenopus laevis. *Development* **110**, 115-130.

Ahn, D., You, K. H. and Kim, C. H. (2012). Evolution of the tbx6/16 subfamily genes in vertebrates: insights from zebrafish. *Mol Biol Evol* **29**, 3959-3983.

Andrade, R. P., Palmeirim, I. and Bajanca, F. (2007). Molecular clocks underlying vertebrate embryo segmentation: A 10-year-old hairy-go-round. *Birth Defects Res C Embryo Today* **81**, 65-83.

Annona, G., Holland, N. D. and D'Aniello, S. (2015). Evolution of the notochord. *Evodevo* **6**, 30.

Bagnat, M. and Gray, R. S. (2020). Development of a straight vertebrate body axis. *Development* **147**.

Baumann, M. and Sander, K. (1984). Bipartite axiation follows incomplete epiboly in zebrafish embryos treated with chemical teratogens. *Journal of Experimental Zoology* **230**, 363-376.

Benazeraf, B., Francois, P., Baker, R. E., Denans, N., Little, C. D. and Pourquie, O. (2010). A random cell motility gradient downstream of FGF controls elongation of an amniote embryo. *Nature* **466**, 248-252.

Bensimon-Brito, A., Cancela, M. L., Huysseune, A. and Witten, P. E. (2012). Vestiges, rudiments and fusion events: the zebrafish caudal fin endoskeleton in an evo-devo perspective. *Evol Dev* **14**, 116-127.

Carroll, S. B. (2005). *Endless forms most beautiful: The new science of evo devo and the making of the animal kingdom*: WW Norton & Company.

Chen, W., Liu, J., Yuan, D., Zuo, Y., Liu, Z., Liu, S., Zhu, Q., Qiu, G., Huang, S. and Giampietro, P. F. (2016). Progress and perspective of TBX6 gene in congenital vertebral malformations. *Oncotarget* **7**, 57430.

Cheng, B., Li, F. T. and Lin, L. (2012). Diastematomyelia: a retrospective review of 138 patients. *J Bone Joint Surg Br* **94**, 365-372.

Christ, B., Huang, R. and Scaal, M. (2004). Formation and differentiation of the avian sclerotome. *Anat Embryol (Berl)* **208**, 333-350.

Christ, B., Huang, R. and Scaal, M. (2007a). Amniote somite derivatives. *Developmental dynamics: an official publication of the American Association of Anatomists* **236**, 2382-2396.

Corallo, D., Trapani, V. and Bonaldo, P. (2015). The notochord: structure and functions. *Cell Mol Life Sci* **72**, 2989-3008.

Fleming, A., Keynes, R. and Tannahill, D. (2004). A central role for the notochord in vertebral patterning. *Development* **131**, 873-880.

Fleming, A., Kishida, M. G., Kimmel, C. B. and Keynes, R. J. (2015). Building the backbone: the development and evolution of vertebral patterning. *Development* **142**, 1733-1744.

Gilbert, S. F. (2017). Developmental biology, the stem cell of biological disciplines. *PLoS Biol* **15**, e2003691.

Griffin, K. J., Amacher, S. L., Kimmel, C. B. and Kimelman, D. (1998). Molecular identification of spadetail: regulation of zebrafish trunk and tail mesoderm formation by T-box genes. *Development* **125**, 3379-3388.

Grotmol, S., Kryvi, H., Nordvik, K. and Totland, G. K. (2003). Notochord segmentation may lay down the pathway for the development of the vertebral bodies in the Atlantic salmon. *Anat Embryol (Berl)* **207**, 263-272.

Halpern, M. E., Thisse, C., Ho, R. K., Thisse, B., Riggleman, B., Trevarrow, B., Weinberg, E. S., Postlethwait, J. H. and Kimmel, C. B. (1995). Cell-autonomous shift from axial to paraxial mesodermal development in zebrafish floating head mutants. *Development* **121**, 4257-4264.

Hedequist, D. and Emans, J. (2007). Congenital scoliosis: a review and update. *Journal of Pediatric Orthopaedics* **27**, 106-116.

Kane, D. A., Hammerschmidt, M., Mullins, M. C., Maischein, H.-M., Brand, M., van Eeden, F., Furutani-Seiki, M., Granato, M., Haffter, P. and Heisenberg, C.-P. (1996). The zebrafish epiboly mutants. *Development* **123**, 47-55.

Keller, R., Davidson, L. A. and Shook, D. R. (2003). How we are shaped: the biomechanics of gastrulation. *Differentiation: ORIGINAL ARTICLE* **71**, 171-205.

Koehl, M., Quillin, K. J. and Pell, C. A. (2000). Mechanical design of fiber-wound hydraulic skeletons: the stiffening and straightening of embryonic notochords. *American Zoologist* **40**, 28-041.

Lardelli, M. (2003). The evolutionary relationships of zebrafish genes tbx6, tbx16/spadetail and mga. *Dev Genes Evol* **213**, 519-522.

Lleras Forero, L., Narayanan, R., Huitema, L. F., VanBergen, M., Apschner, A., Peterson-Maduro, J., Logister, I., Valentin, G., Morelli, L. G., Oates, A. C., et al. (2018). Segmentation of the zebrafish axial skeleton relies on notochord sheath cells and not on the segmentation clock. *Elife* **7**.

Long, J. H., Jr., Koob-Emunds, M., Sinwell, B. and Koob, T. J. (2002). The notochord of hagfish Myxine glutinosa: visco-elastic properties and mechanical functions during steady swimming. *J Exp Biol* **205**, 3819-3831.

McCann, M. R. and Seguin, C. A. (2016). Notochord Cells in Intervertebral Disc Development and Degeneration. *J Dev Biol* **4**.

McCann, M. R., Tamplin, O. J., Rossant, J. and Seguin, C. A. (2012). Tracing notochord-derived cells using a Noto-cre mouse: implications for intervertebral disc development. *Dis Model Mech* **5**, 73-82.

McLaren, S. B. P. and Steventon, B. J. (2021). Anterior expansion and posterior addition to the notochord mechanically coordinate zebrafish embryo axis elongation. *Development* **148**.

Nobrega, A., Maia-Fernandes, A. C. and Andrade, R. P. (2021). Altered Cogs of the Clock: Insights into the Embryonic Etiology of Spondylocostal Dysostosis. *J Dev Biol* **9**.

Pais De Azevedo, T. (2009). Dynamics of embryo axis elongation in amniotes vs. anamniotes: The role of the notochord. In *Faculty of Sciences*. Lisbon, Portugal: University of Lisbon.

Pais de Azevedo, T. P., Witten, P. E., Huysseune, A., Bensimon-Brito, A., Winkler, C., To, T. T. and Palmeirim, I. (2012). Interrelationship and modularity of notochord and somites: a comparative view on zebrafish and chicken vertebral body development. *Journal of Applied Ichthyology* **28**, 316-319.

Peskin, B., Henke, K., Cumplido, N., Treaster, S., Harris, M. P., Bagnat, M. and Arratia, G. (2020). Notochordal Signals Establish Phylogenetic Identity of the Teleost Spine. *Curr Biol* **30**, 2805-2814 e2803.

Plouhinec, J. L., Granier, C., Le Mentec, C., Lawson, K. A., Saberan-Djoneidi, D., Aghion, J., Shi, D. L., Collignon, J. and Mazan, S. (2004). Identification of the mammalian Not gene via a phylogenomic approach. *Gene Expr Patterns* **5**, 11-22.

Scaal, M. (2016). Early development of the vertebral column. *Semin Cell Dev Biol* **49**, 83-91.

Scott, A. and Stemple, D. L. (2005). Zebrafish notochordal basement membrane: signaling and structure. *Curr Top Dev Biol* **65**, 229-253.

Selleck, M. A. and Stern, C. D. (1991). Fate mapping and cell lineage analysis of Hensen's node in the chick embryo. *Development* **112**, 615-626.

Senthinathan, B., Sousa, C., Tannahill, D. and Keynes, R. (2012). The generation of vertebral segmental patterning in the chick embryo. *J Anat* **220**, 591-602.

Smits, P. and Lefebvre, V. (2003). Sox5 and Sox6 are required for notochord extracellular matrix sheath formation, notochord cell survival and development of the nucleus pulposus of intervertebral discs. *Development* **130**, 1135-1148.

Solovieva, T., Lu, H. C., Moverley, A., Plachta, N. and Stern, C. D. (2022). The embryonic node behaves as an instructive stem cell niche for axial elongation. *Proc Natl Acad Sci U S A* **119**.

Sparrow, D. B., Chapman, G. and Dunwoodie, S. L. (2011). The mouse notches up another success: understanding the causes of human vertebral malformation. *Mamm Genome* **22**, 362-376.

Sparrow, D. B., Chapman, G., Smith, A. J., Mattar, M. Z., Major, J. A., O'Reilly, V. C., Saga, Y., Zackai, E. H., Dormans, J. P., Alman, B. A., et al. (2012). A mechanism for gene-environment interaction in the etiology of congenital scoliosis. *Cell* **149**, 295-306.

Sparrow, D. B., McInerney-Leo, A., Gucev, Z. S., Gardiner, B., Marshall, M., Leo, P. J., Chapman, D. L., Tasic, V., Shishko, A. and Brown, M. A. (2013). Autosomal dominant spondylocostal dysostosis is caused by mutation in TBX6. *Human molecular genetics* **22**, 1625-1631.

Spratt Jr, N. T. (1947). Regression and shortening of the primitive streak in the explanted chick blastoderm. *Journal of Experimental Zoology* **104**, 69-100.

Stein, S., Fritsch, R., Lemaire, L. and Kessel, M. (1996a). Checklist: vertebrate homeobox genes. *Mech Dev* **55**, 91-108.

Stein, S., Niss, K. and Kessel, M. (1996b). Differential activation of the clustered homeobox genes CNOT2 and CNOT1 during notogenesis in the chick. *Dev Biol* **180**, 519-533.

Stemple, D. L. (2005). Structure and function of the notochord: an essential organ for chordate development. *Development* **132**, 2503-2512.

Strudel, G. (1955). LINFLUENCE MORPHOGENE DU TUBE NERVEUX ET DE LA CORDE SUR LA DIFFERENCIATION DE LA COLONNE VERTEBRALE ET DE SA MUSCULATURE CHEZ LEMBRYON DE POULET. *COMPTES RENDUS DES SEANCES DE LA SOCIETE DE BIOLOGIE ET DE SES FILIALES* **149**, 188-190.

Talbot, W. S., Trevarrow, B., Halpern, M. E., Melby, A. E., Farr, G., Postlethwait, J. H., Jowett, T., Kimmel, C. B. and Kimelman, D. (1995). A homeobox gene essential for zebrafish notochord development. *Nature* **378**, 150-157.

van Eeden, F. J., Granato, M., Schach, U., Brand, M., Furutani-Seiki, M., Haffter, P., Hammerschmidt, M., Heisenberg, C. P., Jiang, Y. J., Kane, D. A., et al. (1996). Mutations affecting somite formation and patterning in the zebrafish, Danio rerio. *Development* **123**, 153-164.

Waddington, C. H. (1957). *The strategy of the genes*: Allen &Unwin, London.
Wallingford, J. B. (2019). We Are All Developmental Biologists. *Dev Cell* **50**, 132-137.
Ward, L., Pang, A. S. W., Evans, S. E. and Stern, C. D. (2018). The role of the notochord in amniote vertebral column segmentation. *Dev Biol* **439**, 3-18.
Watterson, R. L., Fowler, I. and Fowler, B. J. (1954). The role of the neural tube and notochord in development of the axial skeleton of the chick. *Am J Anat* **95**, 337-399.
Windner, S. E., Bird, N. C., Patterson, S. E., Doris, R. A. and Devoto, S. H. (2012). Fss/Tbx6 is required for central dermomyotome cell fate in zebrafish. *Biol Open* **1**, 806-814.
Wymeersch, F. J., Wilson, V. and Tsakiridis, A. (2021). Understanding axial progenitor biology in vivo and in vitro. *Development* **148**.
Xiong, F., Ma, W., Benazeraf, B., Mahadevan, L. and Pourquie, O. (2020). Mechanical Coupling Coordinates the Co-elongation of Axial and Paraxial Tissues in Avian Embryos. *Dev Cell* **55**, 354-366 e355.
Zhang, Y., Zhang, Z., Chen, P., Ma, C. Y., Li, C., Au, T. Y. K., Tam, V., Peng, Y., Wu, R., Cheung, K. M. C., et al. (2020). Directed Differentiation of Notochord-like and Nucleus Pulposus-like Cells Using Human Pluripotent Stem Cells. *Cell Rep* **30**, 2791-2806 e2795.